From Knowledge to Wisdom

ISSN 1934-7359 (Print)
ISSN 1934-7367 (Online)
DOI:10.17265/1934-7359

Journal of Civil Engineering and Architecture

Volume 10, Number 1, January 2016

David Publishing Company
www.davidpublisher.com

Journal of Civil Engineering and Architecture

Volume 10, Number 1, January 2016 (Serial Number 98)

David Publishing Company
www.davidpublisher.com

Publication Information:
Journal of Civil Engineering and Architecture is published monthly in hard copy (ISSN 1934-7359) and online (ISSN 1934-7367) by David Publishing Company located at 616 Corporate Way, Suite 2-4876, Valley Cottage, NY 10989, USA.

Aims and Scope:
Journal of Civil Engineering and Architecture, a monthly professional academic journal, covers all sorts of researches on structural engineering, geotechnical engineering, underground engineering, engineering management, etc. as well as other issues.

Manuscripts can be submitted via Web Submission, or e-mailed to civil@davidpublishing.com or civil@davidpublishing.org. Submission guidelines and Web Submission System are available at http://www.davidpublisher.com.

Editorial Office:
616 Corporate Way, Suite 2-4876, Valley Cottage, NY 10989, USA
Tel: 1-323-984-7526, 323-410-1082 Fax: 1-323-984-7374, 323-908-0457
E-mail: civil@davidpublishing.com; civil@davidpublishing.org; shelly@davidpublishing.com

Abstracted/Indexed in:
Cambridge Science Abstracts (CSA)
Ulrich's Periodicals Directory
Chinese Database of CEPS, Airiti Inc. & OCLC
Summon Serials Solutions, USA
China National Knowledge Infrastructure (CNKI)
Turkish Education Index
Google Scholar
ProQuest, USA
J-Gate

Subscription Information:
$720/year (print)

David Publishing Company
616 Corporate Way, Suite 2-4876, Valley Cottage, NY 10989, USA
Tel: 1-323-984-7526, 323-410-1082 Fax: 1-323-984-7374, 323-908-0457
E-mail: civil@davidpublishing.com; civil@davidpublishing.org; shelly@davidpublishing.com
Digital Cooperative Company: www.bookan.com.cn

DAVID PUBLISHING

David Publishing Company
www.davidpublisher.com

Journal of Civil Engineering and Architecture

Volume 10, Number 1, January 2016 (Serial Number 98)

Contents

Journal of Civil Engineering and Architecture 10 (2016) 1-12
doi: 10.17265/1934-7359/2016.01.001

Building Maintenance Supported on Virtual Reality Environments: Roofs and Walls

Alcínia Zita Sampaio
Department of Civil Engineering and Architecture, Technical University of Lisbon (IST/ICIST), Lisbon 1049-001, Portugal

Abstract: The paper presents the description of a research work that has its main objective as the development of a technological tool for supporting building maintenance with resort to new information and visualization technologies. Three main components of the building were analyzed: roof, facades and interior walls. The ceramic tile roof covering constitutes a component of the building envelope and fulfils an important function in its performance, namely in its protection against the permeation of moisture and rain water. Facade coating plays a significant role in the durability of buildings, since it constitutes the exterior layer that ensures wall protection against aggressive actions of physical, chemical or biological nature. The paint coating, applied to interior walls while improving their aesthetic character, performs an important function of protection against deterioration agents related to building use. A survey was conducted of the main anomalies that occur in these components, their respective causes and the adequate interventions, in order to plan maintenance strategies. The collected information serves as a basis for the implementation of applications using interactive visualization technologies to support the planning of building maintenance. During this work, the basic knowledge related to the materials, the techniques of rehabilitation and conservation and the planning of maintenance is outlined and discussed. In addition, methods of interconnecting this knowledge with the virtual applications were explored. The implemented prototypes were tested in real cases. This research work provides an innovative contribution to the field of maintenance, supported by emergent virtual reality technology.

Key words: Construction, maintenance, inspections, interaction, virtual reality.

1. Introduction

The main aim of a research project PTDC/ECM 67748/2006 [1] concerns the development of virtual models as tools to support decision-making in the planning of construction maintenance. VR (virtual reality) technology can support the management of data throughout the lifecycle of a building, allowing interaction and data visualization. For Kim [2], VR technology is defined as an advanced interface for computer applications, which allows the user to navigate and interact in real time with a computer, generated 3D environments, using multi-sensory devices. Currently, this technology is applied in a vast and diverse number of areas, ranging from medicine to entertainment, to simulators for commercial or military use, and engineering or architecture areas.

During their service lives, buildings deteriorate and become obsolete. As soon as they are built, the process of decay begins, as well as the deterioration of the fabric and services. The inevitable process of decay can be controlled, and physical life of the building can be extended if they are properly maintained. The degradation of buildings is influenced by several factors, such as the fabric of the material, the environment and the period of usage. If a building is not well maintained, it will affect the user's quality and productivity [3]. So, maintenance has impacted on the efficiency and overall budget of facilities in a building. Today, building maintenance offices are using computer programs toward the control of the maintenance activity. Computer maintenance programs are required for keeping buildings in efficient condition during their lifecycle. They are used as tools to decide upon what, when and

Corresponding author: Alcínia Zita Sampaio, Ph.D., assistant professor, research fields: BIM (building information modeling), maintenance, engineering education and virtual reality.

how much is a maintenance need of a building [4]. According to Therivel [5] and Nita et al. [6], the building maintenance is defined as the diversity of associated activities, as well as the involved interests. The main purpose, on the financial resources use, should be the building preservation. The diagnostic methodology of the deterioration process identifies the defect with the implementation of restrain measures, finding the most important causes, identifying a solution, controlling the outcome and preventing the effects recurrence.

The coating materials can be ceramic tiles in roofs, stones in facades and painted surfaces in interior walls. Factors, such as the constant exposure to the weather, pollutants and the normal actions of housing use, linked to its natural ageing, give rise to its deterioration. So, some irregularities can appear, which can negatively affect the aesthetic aspect and the performance of the element coating [7]. The kind of building material that composes the roofs, facades and the interior wall has a continuous lifestyle, so it requires the study of preventive maintenance (the planning of periodical local inspections) and of corrective maintenance with repair activity analysis. Technical inspections must be drawn by competent assessors to evaluate the physical state of building elements and services and to assess the maintenance needs of the facility. The literature suggests that, ideally, a technical inspection must be performed annually because the longer the period between inspections is, the more accurate and extensive the inspection becomes [8].

A building or its components should perform to the desired level in order to maintain healthy environment. A building's roof covering of ceramic tiles constitutes a component of its surrounding and possesses an important function in the performance of a building, namely in its protection against the permeation of moisture and rain water. The weather significantly influences the state of use of peripheral walls of the building once the humidity through the wall thickness causes anomalies in the inner surface of the wall. According to Flores-Colen and Freitas [8], in normal conditions of habitation use and when correctly applied, a paint coating can remain unaltered for about five years. Since these building components are exposed to bad atmospheric conditions and natural use of the house, the materials frequently show an evident degree of deterioration, requiring maintenance interventions. To perform maintenance activities, a survey of failures in the building must be conducted in order to arrive at the best solution for repair and maintenance. Establishing suitable maintenance strategies for this type of coating is based on the knowledge of the most frequent irregularities, the analysis of the respective causes and the study of the most adequate repair methodologies. Currently, the management of information related to the maintenance of buildings is based on the planning of action to be taken and on the log of completed work. The capacity to visualize the process can be added through the use of 3D models, which facilitate the interpretation and understanding of target elements of maintenance and, furthermore, the possibility of interaction with the geometric models can be provided through the use of VR technology. The developed VR models can be considered as useful computer tool with advanced visualization capacities in the maintenance field. Westerdahl et al. [9] presented a VR visual model of building showing degradation over time. The VR system in maintenance was found to improve communication between managers and workers and helped to decrease the initial time schedules in repair works.

The VR models of maintenance facilitate the visual and interactive access to results, supporting the definition of inspection reports, whether in new constructions or those needing rehabilitation. The 3D model of the building linked to a database concerning maintenance produces a collaborative virtual environment, that is, one that can be manipulated by partners is interested in consulting, creating, transforming and analyzing data in order to obtain results and to make decisions. Namely, inspection reports can be defined and consulted by different collaborators. The process of developing the interface of each application considers these purposes. In addition, these applications can be easily transported to any building place in order to obtain adequate anomaly surveillance and a consequent methodology of rehabilitation, supported on the database. The interaction and the data visualization allowed by the models turn these applications simple and direct to be worked with. The VR applications aimed to promote the use of computerized tools to facilitate and expedite the conduct of inspections. With this tool, the user can perform an inspection that contains all the useful information and also automatically displays the most provable pathologies causes. In addition, the maintenance specialist has access to the history of inspections carried out. So, the rehabilitation expert can do the evaluation of the degradation of the building more effectively and establish an adequate strategy to the repair works.

2. Interactive Applications

The implemented prototypes, concerning three building components, roofs [10], facades [11] and interior walls [12], incorporate interactive techniques and input devices to perform visual exploration tasks. To support each system, a database was created which included a bibliographic research support, made in regard to the closure materials used in the roof, and interior and exterior walls of a building, anomalies concerning different kinds of covering material and corrective maintenance. Currently, the study of anomalies is a complex process due to increasing demands by users, development of methods for diagnosis and employed different construction solutions. Thus, the existence of a collection of synthesized and computerized data, enabling the exchange of information between those involved in construction, is an important aid in this process. Repair activities were also studied. The consulted bibliography concerning diverse material usually applied as building components covering allowed the creating of lists of recommendations and repair methodologies. Based in this research, a database of methodologies was carried out. However, this information intends to present just a suggestion of repair work. The maintenance specialist must evaluate the degree of the anomalies and the real characteristic of the building component covering, in order to establish the most adequate strategy for the irregularity observed in the place. In addition, the database can be updated with new information concerning other irregularities, repair methodologies or even new material. The VR applications intend to be a support tool to the maintenance activity.

The programming skills of those involved in the project had to be enhanced so that they could achieve the integration of the different kinds of databases needed in the creation of the interactive model. The interactive applications support on-site inspections and the on-going analysis of the evolution of the degree of deterioration of the coating materials. A set of computational systems were used in their development and the scheme of links between software is presented in Fig. 1:

- The AutoCAD was used in the creation of the 3D model of the building, based on drawings presented in Fig. 2;
- The VR system, EON Studio, was applied to program the interactive actions linked with the geometric elements of the 3D model (Fig. 3 shows the main interface);
- The Visual Basic software was used in the creation of all the windows of the application and in the establishment of links between components;
- The Microsoft Access application was applied on the definition of a relational database.

2.1 VR (Virtual Reality) Model of Roofs

The roof covering is the most effective element of a building's surrounding in its edification performance and as such must be efficient in the face of mechanical, thermal, solar radiation and water action [13]. The functional requirements to be fulfilled are essentially defined in terms of habitability, safety, durability and economics. Although several covering materials can

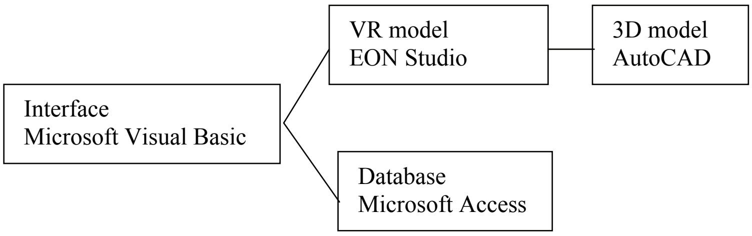

Fig. 1 Scheme of links between software.

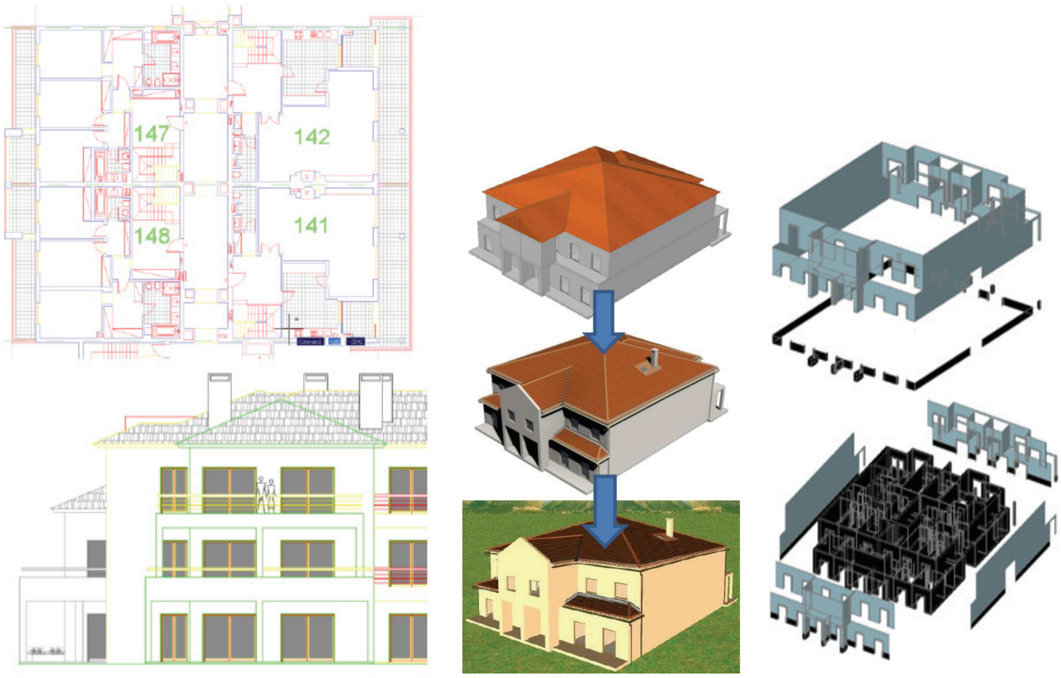

Fig. 2 Technical drawings and the 3D model of the building.

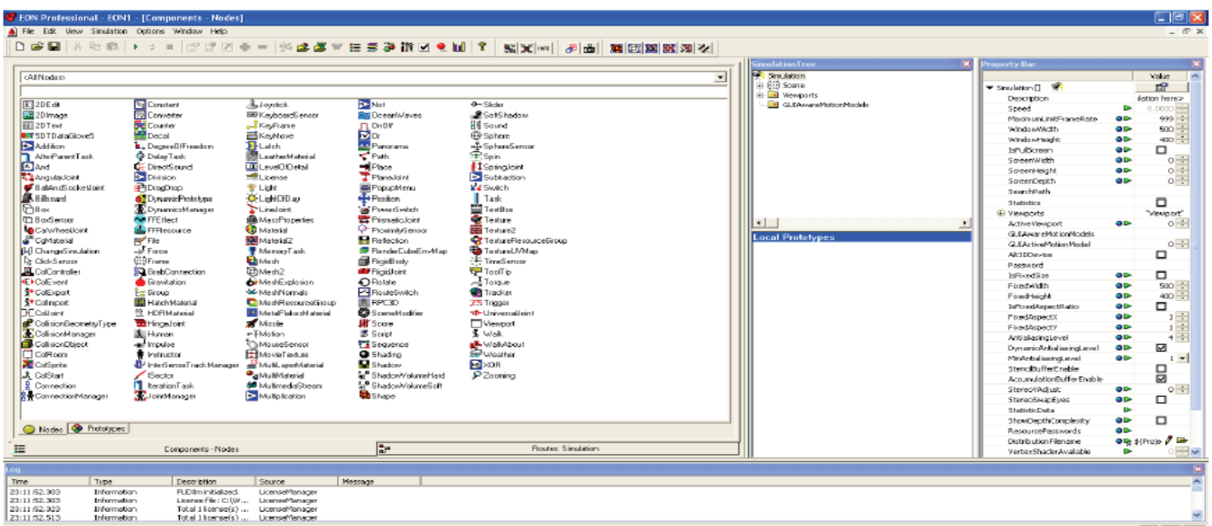

Fig. 3 The EON Studio interface.

be applied in the execution of pitched roofs, the most frequently applied covering in Portugal is the ceramic tile. The tile covering ensures the continuity of the architectural tradition, allows the creation of visual effects through the variety of shapes and ancillary parts, offers a good performance in the face of atmospheric agents and a high durability and is, furthermore, an ecological product, for it is non-toxic, renewable and biodegradable [14]. As the covering performs a predominant role in the protection of buildings, namely against moisture permeation, it requires a greater attention in regards to the analysis of its deterioration process.

The developed VR application supports the inspection activity [10]. Concerning the pathology analyses and the maintenance planning as a way to optimize the inspection process and the diagnosis of anomalies associated with the roof covering, it was necessary to create a classification system that encapsulated the information collected on this theme. Therefore, four categories on the elements typology were considered:

- the elements that compose the covering support structure;
- the ones that constitute the current surface of the covering;
- the elements considered as singular covering points;
- the ones that form the rainwater draining system.

An in-depth study on the anomalies that might occur and the most likely causes associated with the different elements of the roof are contained within the database. To each anomaly, one or more probable causes in its occurrence are specified, as it is the recommended intervention as a way to eliminate it. To maintain the ease in structuring the database, the causes and the intervention are both linked to the anomaly. Table 1 illustrates two examples of anomalies associated to the type of element (current surface and singular covering points), respective provable causes and recommended interventions. Meetings for all information regarding the described anomalies were prepared tables containing the anomaly, their specifications, as well as the repair solutions and methodologies. This process is then implemented in the program to support the maintenance of buildings. Additionally, a survey of images for each anomaly was conducted.

The implemented interface (Fig. 4) allows the user to perform, intuitively, an inspection to an inclined roof. The first step in using the application is, naturally, to identify the building to be analyzed and the respective roofing characteristics.

Upon opening the selected file, it is possible to manipulate the model through functions that allow the moving of a camera around it and by the selection of covering elements to be identified and monitored. Each element to be monitored must be identified so as to be included in the application's database (Fig. 4). During this process, the camera must be focused on the element so the coordinates of position and orientation to be associated to it are accurate, thus being available for use in subsequent interactions (selection and visualization of an identified element), as shown in Fig. 4.

Table 1 Anomalies associated to respective causes and recommended repair methodology.

Element type	Anomaly	Causes	Repair methodology
Current surface	Cracking of coating element 	• Laying the support structure; • Lack of walkways on roofs; • Placing heavy equipment on roof	Replacement of damage elements
Singular covering points	Insufficient size of the trim 	Deficient execution	Element removal and placement of new trim with higher heights

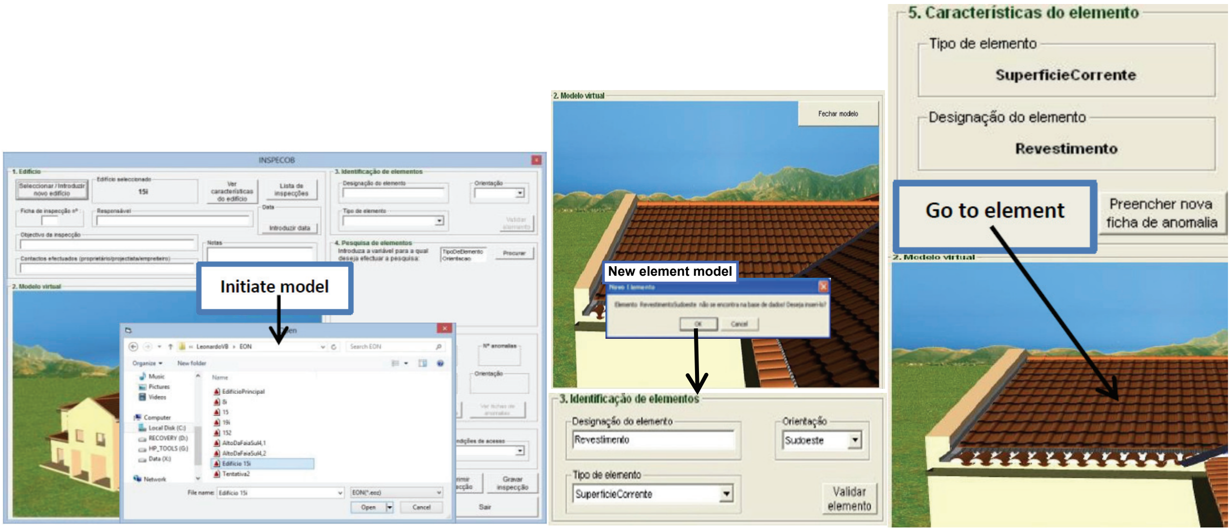

Fig. 4 The VR model of roofs interface.

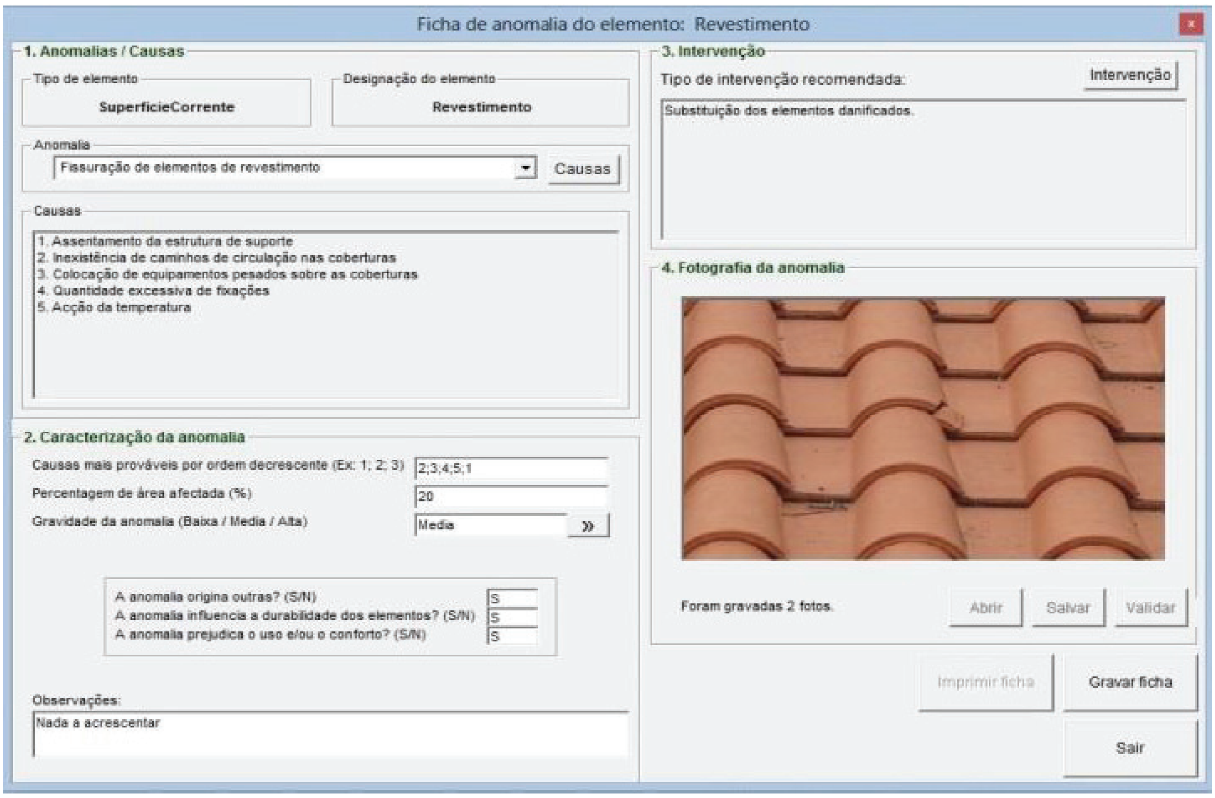

Fig. 5 The anomaly chart interface.

The filling out of a new anomaly chart (Fig. 5) or the viewing of existing charts' data is made available through the interface anomaly chart accessed by the main interface. In the anomaly chart, the scroll-down menu referring to the anomaly field shows the anomalies that have been registered in the database in association with each of the types of elements. So, for example, in relation to the covering element, belonging to the current surface group, the associated anomalies are shown in the scroll-down menu. The causes and intervention modes were equally associated to the anomalies and, therefore, by selecting the respective control buttons, the probable causes and recommended "intervention" fields are filled-out with the database records connected to the selected anomaly.

The severity of the anomaly can be characterized according to three parameters (low, medium and high), reflecting the previously realized study. The value shown in this field is then used in the element's color change in the virtual model, through the emission of information to EON, altering itself according to the severity of the anomaly, green for low, yellow for medium and red for high (Fig. 6).

The inspection chart interface also comprises a photo insertion zone, thus it is possible to add photographs taken in the inspection location or other images related to the element being analyzed, forming a considerably relevant complementary information for the subsequent study of repair/maintenance relative to the observed severity.

The user of this application can conduct inspections at any time, access the registered information and the virtual model and, thus, be supported by the historical, define adequate plan for the roof maintenance or reparation work. Such work will only be possible by storing all the information inserted into the application, as well as the changes made to the building's virtual model in a previous inspection allowed by the application. Since the application is based on clear and systematized information, there can be a reduction in inspection subjectivity, and it may be used by different technicians. Thus, the information collected by technicians becomes clear and objective, which permits an easier analysis of the inspection data.

2.2 VR (Virtual Reality) Model of Facades

The facades VR model allows interaction with the 3D geometric model of a building, visualizing components for each construction [11]. It is linked to a database (Table 2) of the corresponding technical information concerned with the maintenance of the materials used as exterior closures. The aim of the survey of conditions in facades is to create a database of support software which is meant to be implemented and to support planning of inspections and maintenance strategies in buildings DG449 [7]. The database contains the identification of anomalies that can be observed in different types of finish mentioned above. Each anomaly is called by type of anomaly, which is subdivided into groups designated by the specifications of anomalies. Each specification corresponds to one or more causes of their occurrence. For each specification, there are equated anomaly repair solutions appropriate to their method of repair. The repair techniques included in the database are mainly focused on the treatment of the coating finishing, not considering other layers that make up a facade but often require repair to eliminate all causes.

The visualization of the pathology data of these exterior closure materials requires an understanding of their characteristics [15]:

- types of material, painted surfaces, natural stone panels and ceramic wall tiles;
- application processes, stones (panel, support devices or adherent products), ceramic tiles (fixing mechanism or procedures), painted surfaces (types of paint products, prime and paint scheme surface, exterior emulsion paints or application processes);
- anomalies, dust and dirt, lasting lotus leaf effect,

Fig. 6 The color alteration of elements.

Table 2 Anomalies in facades and associated repair solutions and methodologies.

Anomaly	Specification of the anomaly	Repair solution	Repair methodology
Detachment 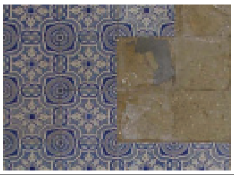	Fall in areas with deterioration of support	Replacement of the coat (with use of a repair stand as necessary)	(1) Removal of the tiles by cutting grinder with the aid of a hammer and chisel; (2) Timely repair of the support in areas where the detachment includes material constituent with it; (3) Digitizing layer of settlement; (4) Re-settlement layer and the tiles
Cracking/fracturing 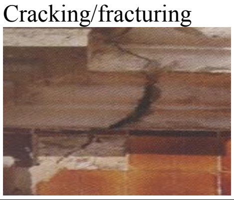	Failure of the support (wide cracks with well-defined orientation)	Replacement of the coat (with repair of cracks in the support)	(1) Removal of the tiles by cutting grinder; (2) Removal of material adjustment in the environment and along the joint; (3) Repair of cracks, clogging with adhesive material (mastic); (4) Settlement layer made with cement in two layers interspersed with glass fibre; (5) Re-settlement layer and the tiles

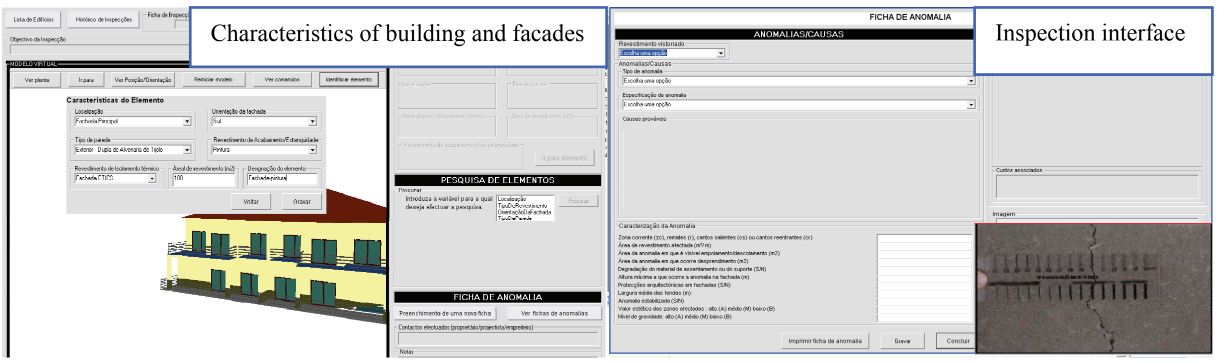

Fig. 7 The main and inspection interfaces of the VR application.

covering power, insufficient resistance to air permeability or weatherproof isolation, damaged stones or ceramic tiles, alkali and smear effect, efflorescence, fractures and fissures;

- repair works, surface cleaning, wire truss reinforcing, cleaning and pointing of stonework joints, removing and replacement of ceramic wall tiles, removing damaged paint and paint surface, preparing and refinishing stone panels.

The VR model interface is composed of a display window allowing users to interact with the virtual model and a set of buttons for inputting data and displaying results (Fig. 7). For each new building to be monitored, the characteristics of the environment (exposure to rain and sea) and the identification of each element of the facades must be defined (facade orientation, double or single exterior wall and area and type of coating).

Once each monitored element has been characterized, several inspection reports can be defined and recorded and thereafter consulted when needed. An inspection sheet (Fig. 7) is accessed by the main interface. Using the drop-down menus of the interface, the user can associate the characteristics of the observed anomaly to a facade element, the type of anomaly, the specification, details and the probable cause of the anomaly, an adequate repair solution and pictures taken in the building. After completing all fields relating to an anomaly, the user can present the report as a PDF (portable document format) file.

The developed software is easy to handle and transport for on-site inspections and comprises information of the causes, solutions and methods for repairing. As the 3D model is linked to a database in an interactive environment and has a friendly interface to deal with this knowledge, it allows a collaborative system. With this application, the user may fully interact with the program referring to the virtual model at any stage of the maintenance process and analyze the best solution for repair work. It can also support the planning of maintenance strategies.

2.3 VR (Virtual Reality) Model of Painted Walls

The material most frequently used in the coating of ordinary interior walls of buildings is paint. The durability of the painted coating depends on the environment in which it is used and on the surface it is applied to, as well as the rate of deterioration of the binder in the paint. Irregularities manifest themselves in various ways and in different degrees of severity. According to Coias [16], in normal conditions of exposure and when correctly applied, a paint coating can remain unaltered for about five years. Based on the study made of the causes of the anomalies, specific methodologies for their resolution were established.

The developed VR application supports on-site inspections and the on-going analysis of the evolution of the degree of deterioration of the coating [12]. The VR model identifies each interior wall surface in each of the rooms of the house, as independent elements. The application is supported by a database, composed by the most common irregularities (Fig. 8), their probable causes and suitable repair processes, which facilitate the inspection process (Table 3).

In addition, the model assigns a color to each of the coating elements and the colors defined by the time variable so that the evolution of the deterioration of the coating material is clearly shown through the alteration in color. The main interface of the application gives access to the inspection and maintenance modules (Fig. 9). On an on-site inspection

(a) (b) (c) (d)

Fig. 8 Common defects in painted interior walls: (a) swelling; (b) efflorescence; (c) cracking; (d) blistering.

Table 3 Anomalies and associated repair methodology.

Classification	Anomalies	Repair methodology
Alteration in colour	Yellowing	Cleaning the surface and repainting with a finish both compatible with the existing coat and resistant to the prevailing conditions of exposure in its environment
	Bronzing	
	Fading	
	Spotting	
	Loss of gloss	
	Loss of hiding power	
Deposits	Dirt pick-up and retention	Cleaning the surface
	Viscosity	
Changes in texture	Efflorescence	• Removal by brushing scraping or washing; • Repainting the surface; • When necessary apply sealer before repainting
	Sweating	
	Cracking	
	Chalking	
	Saponification	
Reduction in adhesion	Peeling	• Proceed by totally or partially removing the coat of paint; • Check the condition of the base and proceed with its repair where necessary; • Prepare the base of the paint work
	Flaking	
	Swelling	

visit, the element to be analyzed is selected interactively on the virtual model, and using the inspection interface, the specialist can select the irregularity included in the list of the database, which corresponds to the observed defect, and can select also the probable cause and the prescribed repair methodology (Fig. 9). The inspection data are recorded and associated to each monitored element, allowing subsequently the planning of repair works, thus providing a tool for the definition of a rehabilitation strategy.

The VR application allows the user to monitor the evolution of wear and tear on the paint coating in a house. For this technical information relative to the reference for the paint used, its durability and the date of its most recent application must be added to each element through the maintenance interface (also accessed from the main interface, as shown in Fig. 9).

The period of time between the date indicated to examine the building and the date when the paint was applied is compared to the duration advised for repainting. The value given for this comparison is associated to the RGB (red, green, blue) parameters which define the color used for wall in the virtual model, from pale green (color referring to the date of painting) to red (indicates that the date the model was consulted coincides with that advised for repainting, Fig. 10).

3. General Procedure and Benefits

The implemented VR applications support buildings inspections. The geometric models of houses to be inspected are created using geometric modeling systems, based on drawings of the architectural design. Each VR application was implemented to support the inspection of a building component types: roofs, facades and interior walls.

The ability of interaction is added to the geometric models using the selected VR software—the EON Studio. At the inspection building place, the expert must have in his notebook the geometric model inserted in the VR application. On site, the engineer identifies in the model each building component to be monitored. Then, the engineer performs the inspection process by observing the real anomalies. The professional must select the corresponding element in

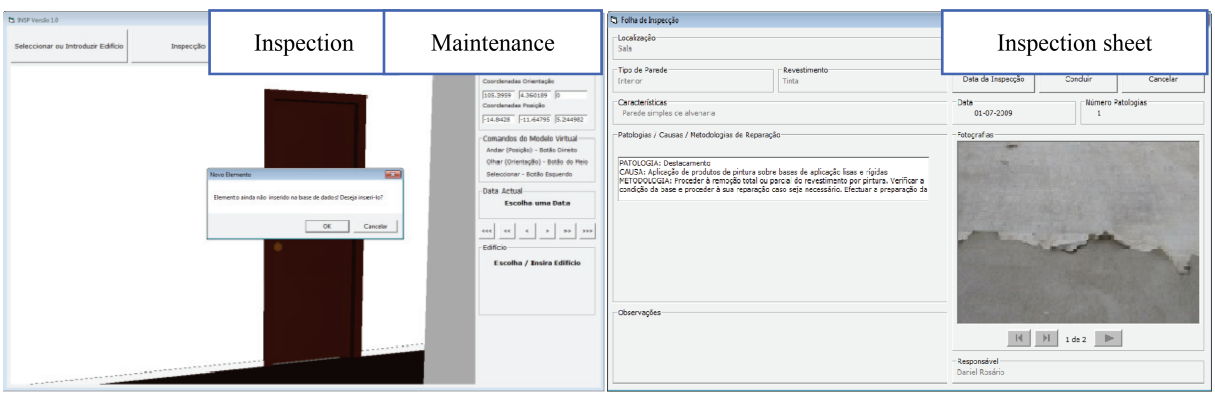

Fig. 9 The main interface of the virtual application and an inspection sheet.

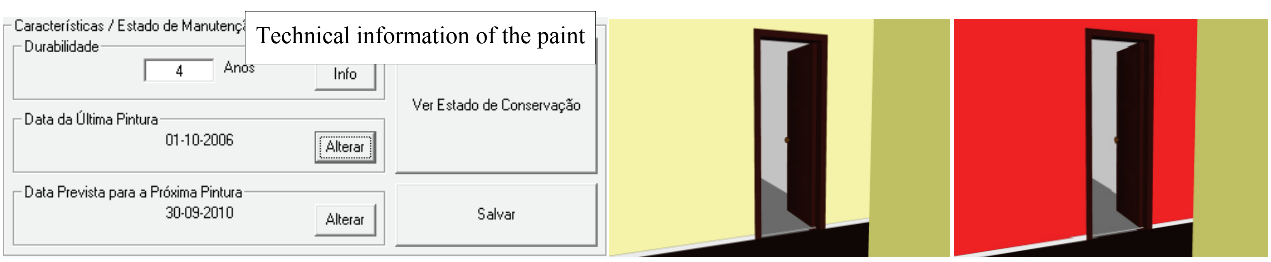

Fig. 10 Coating chromatic alteration according to deterioration state of the paint.

the model and open an interactive inspection sheet. Based on the observation of the real anomaly, the engineer fills in the set fields of the inspection sheet and adds one or two photos of the observed irregularity. The inspection process should cover all the elements on which the specialist observes an anomaly. Later, the expert examines the set of registered anomalies and establishes a plan of maintenance or repair to the building.

The benefits in use of interactive models which support the buildings inspection, are demonstrated through the facility, as the virtual model of the building can be associated to the irregularities observed on site. And also, after inspection, the engineer can analyze more easily the set of the observed problems and define a global planning with a greater knowledge of the type of anomalies and their extension. The building geometric models, when associated with the result of the inspection, provide a suitable technical communication with the customer or owner of the building.

4. Conclusions

The presented VR applications support the inspection activity of roofs, facades and painted interior walls and promote the use of information technology tools with advanced graphic and interactive capabilities, in order to facilitate and expedite the maintenance process. The VR capacity of chromatic alteration was applied in two of the models allowing users to see, in the virtual environment, the state of gravity of anomalies or conservation of the coating materials.

The information about pathologies, causes and repair methods, collected from a specialized bibliography, has been organized in such a way as to establish each model database to be used as a base for the drawing up of a tool to support building maintenance. The main aim of the applications is to facilitate maintenance enabling the rapid and easy identification of irregularities, as well as the possible prediction of their occurrence through the available inspection record. This analysis has been shown as playing an important role in conservation and in the reduction of costs related to the wear and tear of buildings and contributes to the better management of buildings where maintenance is concerned.

With the proposed applications, it is intended that the user at a later stage inspection and assessment of the building may fully interact with the programs, referring to the virtual model at the stage the engineer wants and recreating the best steps to take in the methods of repair by viewing the details of construction and costs and comparing alternatives. The VR software tools are easy to handle and transport to the site inspection comprising information on the causes, solutions and methods for repairing, storing data and information obtained by crossing, including the procedures for inspections and allowing the inspector to view previous inspections both during the inspection and at a later stage of analysis and determination of actions. In this way, the developed tools support maintenance of buildings, using VR interactive technology.

A VR application has some technical limitations regarding the handling of the virtual model. The user must be familiarized with the walking through capacity within a virtual environment. The user must know how to select an element of the model, how to link information and how to consult it. Another limitation concerns the narrow range of components that were studied until now. Other components, like floors, windows and doors, water supply and air conditioning systems, can be also implemented as VR applications for maintenance propose.

Acknowledgments

The authors gratefully acknowledge the financial support of the Foundation for Science and Technology, a governmental organization for the research project PTDC/ECM 67748/2006 [1].

References

[1] Sampaio, A. Z., and Gomes, A. M. 2011. *Virtual Reality Technology Applied as a Support Tool to the Planning of Construction Maintenance.* Research Project PTDC/ECM/ 67748/2006, FCT (Foundation for Science and Technology), Lisbon, Portugal.

[2] Kim, J. J. 2011. *Virtual Reality*. Rijeka: InTech. ISBN 978-953-307-518-1.

[3] Korka, J., Oloufa, A., and Thomas, H. 1997. "Facilities Computerized Maintenance Management Systems." *J. Archit. Eng.* 3 (3): 118-23. doi: 10.1061/(ASCE)1076-0431(1997)3:3(118).

[4] Horner, R. M. W., El'Haram, M. A., and Munns, A. K. 1997. "Building Maintenance Strategy: A New Management Approach." *Journal of Quality in Maintenance Engineering* 3 (4): 273-80. doi: 10.1108/13552519710176881.

[5] Therivel, R. 1993. "Systems of Strategic Environmental Assessment." *Environmental Impact Assessment Review* 13 (3): 145-68. doi: 10.1016/0195-9255(93)90029-B.

[6] Nita, A. K., Sun, M., Petley, G., and Barrett, P. 2002. "Improving the Business Process of Reactive Maintenance Projects." *Facilities* 20 (7/8): 251-61. doi: 10.1108/02632770210435161.

[7] Murray, M., Pryke, S., and Yates, T. 2000. *Cleaning Exterior Masonry, Part 1 Developing and Implementing a Strategy, Part 2 Methods and Materials.* London: BRE (Building Research Establishment) Press.

[8] Flores-Colen, I., and Freitas, V. P. 2008. "Stains in Facades' Rendering—Diagnosis and Maintenance Techniques' Classification." *Construction and Building Materials* 22 (3): 211-21. doi: 10.1016/j.conbuildmat.2006.08.023.

[9] Westerdahl, B., Suneson, K., Wernemyr, C., Roupé, M., Johansson, M., and Allwood, C. M. 2006. "Users' Evaluation of a Virtual Reality Architectural Model Compared with the Experience of the Completed Building." *Automation in Construction* 15 (2): 150-65. doi: 10.1016/j.autcon.2005.02.010.

[10] Afonso, L. P. 2013. "Virtual Reality Technology Applied to the Maintenance of Roofs." M.Sc. thesis, Technical University of Lisbon, Lisbon, Portugal. (in Portuguese)

[11] Gomes, A. R. 2010. "Virtual Reality Technology Applied to the Maintenance of Facades." M.Sc. thesis, Technical University of Lisbon, Lisbon, Portugal. (in Portuguese)

[12] Rosario, D. P. 2011. "Virtual Reality Technology Applied to the Maintenance of Painted Interior Walls." M.Sc. thesis, Technical University of Lisbon, Lisbon, Portugal. (in Portuguese)

[13] Harrison, H. W., Trotman, P. M., and Saunders, G. K. 2009. *Roofs and Roofing—Performance, Diagnosis, Maintenance, Repair and the Avoidance of Defects.* 3rd ed. London: BRE (Building Research Establishment) Press. Accessed July 14, 2015. http://www.brebookshop.com/samples/139437.pdf.

[14] Garcez, N., Lopes, N., and Silvestre, J. 2012. "System of Inspection, Diagnosis and Repair of External Claddings of Pitched Roofs." *Construction and Building Materials* 35: 1034-44. doi: 10.1016/j.conbuildmat.2012.06.047.

[15] Gomes, A. M., and Pinto, A. P. 2009. *Construction Materials.* Didactic Text. Lisbon: IST Student Association, Technical University of Lisbon.

[16] Coias, V. 2009. *Inspections and Essays on Rehabilitation of Buildings.* 2nd ed. Lisbon: IST Press, 448. ISBN: 978-972-8469-53-5. Accessed July 14, 2015. http://istpress.tecnico.ulisboa.pt/node/285. (in Portuguese)

Journal of Civil Engineering and Architecture 10 (2016) 13-21
doi: 10.17265/1934-7359/2016.01.002

Leveraging Publicly Available Building Energy Data as a Design Firm in the United States

Stephen D. Ray[1, 2], Luke Leung[2], Arathi Gowda[2] and Niancen Miao[2]

1. Department of Physics and Engineering, North Park University, Chicago IL 60625, USA

2. Skidmore, Owings and Merrill LLP, Chicago IL 60604, USA

Abstract: Publicly available building energy data are exploding—thirteen American cities and 14 states now require them by law. This emergence of data nudges building owners and tenants to reduce energy consumption by comparing their usage to that of similar buildings. However, vast untapped energy reductions and deeper physical understandings can still be extracted from these data. This paper extends the energy saving impact and provides key insight into building performance through publicly-disclosed data by describing three initiatives at a large design firm. An internal high performance design reporting program compares projects from around the world and across offices. A case study of 706 buildings in New York City illustrates the value of tracking large-scale patterns to a design firm. Per capita energy and carbon usage is correlated to life expectancy to better inform neighborhood and city design. As more data freely flow out into the public, engineers must strategically engage it.

Key words: High performance buildings, tall buildings, big data, life expectancy.

1. Introduction

June 1, 2014 marked the first compliance deadline of the *Chicago Building Energy Use Benchmarking Ordinance*. As of July 2015, Chicago joins 13 other US cities that require certain commercial buildings to report building energy usage data in hopes of reducing energy consumption. Benchmarking data along with other large datasets of measured building energy use, such as the CBECS (Commercial Buildings Energy Consumption Survey) and the DOE (Department of Energy's) Buildings Performance Database, offer overwhelming amounts of information on actual building performance. These data on their own are akin to tombs of notes awaiting a musician's interpretation and performing. This paper describes a few ways where a large design firm makes music out of the vast, publicly available datasets through internal high performance design goals, informing tall building design with data from New York City, and considering a city's impact on life expectancies.

Corresponding author: Stephen D. Ray, Ph.D., P.E., research fields: building energy, natural ventilation, computational fluid dynamics, thermal comfort and indoor air quality.

2. Internal High Performance

2.1 Design Goals

Publicly available data provide insight to large-scale trends in building energy use, which are discussed in subsequent sections. These data also have been used to inform key decision makers on individual projects within the firm. As part of a firm-wide initiative to compare every project to measure performance of similar buildings, internal HPD (high performance design) goals are tracked on each project, as shown in Fig. 1. The projects are compared to the 2003 CBECS results through the EPA (Environmental Protection Agency's) Target Finder as part of their ENERGY STAR® program [1, 2]. Each project is compared to buildings of similar climate, gross floor area and building function within the 5,215 building CBECS database to generate an energy savings relative to CBECS. International project locations are first assigned a corresponding United States climate that can then be used for comparison with the CBECS data.

These relative energy savings provide some measure of a normalized energy performance metric for projects around the world.

More importantly, the use of publicly available building energy data provides a standard measure of comparison between various offices within the firm. This comparison has motivated engineers and energy modelers within each of the offices to dive even further into the details of energy modeling best practices as they attempt to outperform their peers. The comparison also informs general modeling practices at various stages of the project phase. Should projects that only last through schematic design be treated differently than projects that last through construction documents? As shown in Fig. 1, projects in CD (construction documents) phase tended to perform best across all offices. One might argue much of the uncertainty which has been removed from the model by the time CD is reached, but such explanation does not explain the subsequent drop in performance for buildings in CA (contract administration) phase. Furthermore, the energy model is not always updated at every stage of design, so the increase in performance may simply be explained by the particular buildings in CD during the considered year. Ongoing comparisons across multiple years are needed for a more thorough analysis. The comparison, perhaps most importantly, provides bragging rights to directors and partners across the firm and raises awareness of energy performance for key decision makers. Moving forward, the firm believes this internal competition should be encouraged to better integrate engineering and architectural design using performance metrics and the forms they inspire.

Limitations to this methodology shown in Fig. 1 inform how broadly results are applied. One of the biggest limitations comes from the energy model used to simulate the energy consumption of each project. Increasing levels of detail are used in the energy model as a project progresses and not all projects go through the same phase. A more general issue with energy models also affects results: modeling variability. Each modeler works slightly differently, which adds to the uncertainty of the simulated results. More standardized energy modeling practices and the development of more sophisticated energy models that track uncertainties, such as the ongoing work at Argonne National Labs, will help reduce skewed comparisons between projects that may be influenced by modeling

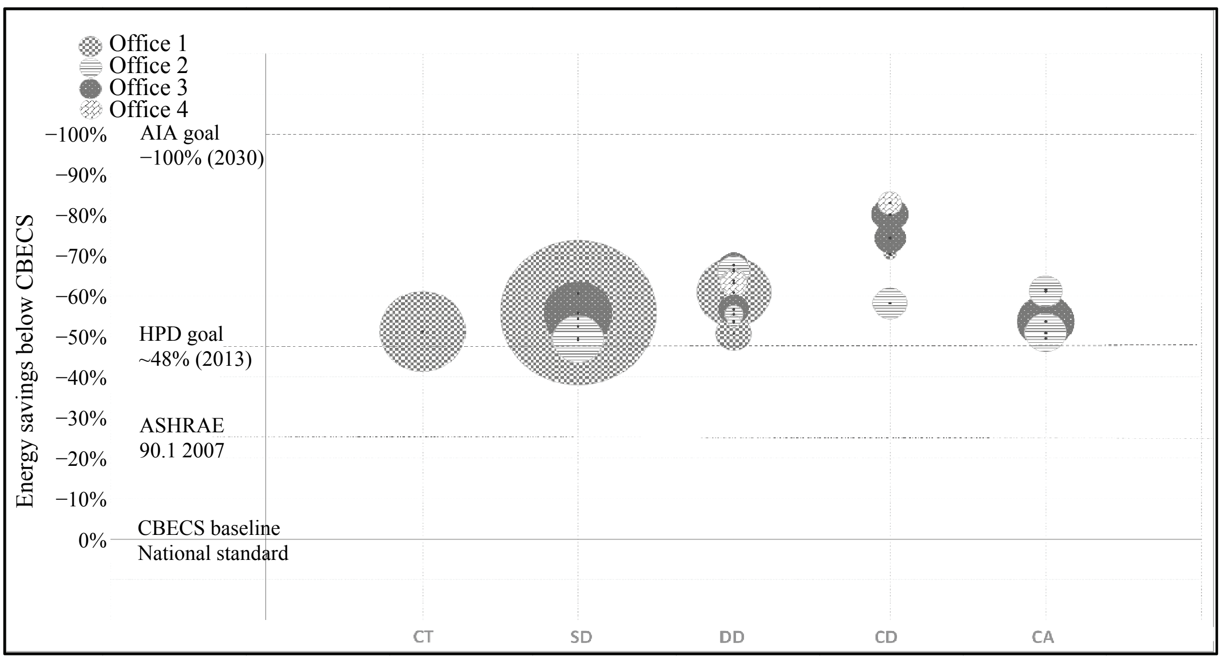

Fig. 1 Plot of project energy savings below similar buildings in CBECS across four offices of a large design firm. Project phase is plotted on the horizontal axis and bubble size corresponds to project gross floor area.

practices more than actual design [3].

Other limitations arise from using CBECS data. Of the 5,215 buildings in CBECS, 95% have a gross floor area of 50,000 ft^2 or less and 90% are two-story or one-story buildings [2]. No buildings over 1,000,000 ft^2 are included [2]. Given the scale of projects at a large architecture firm, a database that includes larger buildings could broaden the application of such standardized comparisons. An additional limitation of this methodology is its use in international projects. For instance, comparable data are not available for projects in China which is problematic given that 38% of global floor space growth is being projected in China from 2015 to 2035 [4]. Even though climate information is used to correlate international projects to buildings in similar American climates through CBECS, other factors that may vary with country and affect energy consumption are not controlled. Factors, like code requirements, comfort norms, construction practices and occupancy patterns, all affect building energy consumption and can vary from nation to nation. All of these factors complicate the firm's initial efforts to compare EUI (energy usage intensity) in various geographic markets, while helping to prioritize the need for energy modeling and benchmarking as the global engineering community continues to develop its understanding of building energy performance.

2.2 New York City Data in Tall Building Design

2.2.1 Tall Building Energy Usage

In 2009, New York City was the first city in the United States to require large buildings to publicly release energy consumption data by passing *New York City Local Law 84*. Although the city analyzes these data annually and releases various reports, the particular comparisons and analyses most useful to the firm were not considered—particularly the performance of tall and super tall buildings. Exploring the data internally not only strengthened internal frameworks on the energy usage of tall buildings, but also provided insight into a rating system commonly pursued by clients.

The analyzed data were collected by the City of New York in 2012 and released in September 2013 [5]. Unfortunately, the city does not release any direct measure of building height in their energy benchmarking data, but the Department of City Planning does through the PLUTO (Primary Land Use Tax Lot Output) [6]. The PLUTO data used in this study were collected between February and May 2013 [6].

The data have been cleaned to remove any building with incomplete data or large outliers, which likely resulted from poor data collection. While numerous confounding factors impact building energy consumption, some care is taken to eliminate as many factors as possible. Since all of the data are collected in New York City over the same year, the same weather conditions applied to all the buildings. Only office buildings with at least 80% of their gross floor area used as office space are considered to minimize the confounding factor of building use. The total number of buildings that meet all these criteria and are used in this study is 706. Energy usage is measured using site EUI in the units of $kBtu/ft^2/yr$, which is calculated by dividing the entire building site energy in one year by the total floor area.

These measured data are considered alongside predicted EUI values from the DOE's ENERGY STAR program. Using the same 2003 CBECS data, they have performed various regressions to identify the six strongest predictors of building energy use, which include gross floor area, cooling degree days and heating degree days [7]. Despite the ENERGY STAR program's reporting source EUI, it converts the site EUI inputted into portfolio manager using constant source-site ratios across the country [7]. Electricity purchased from the grid and natural gas use ratios of 3.14 and 1.05, respectively [7]. Site energy intensity is also preferred because it allows for a better comparison between building characteristics, which is more aligned with the goals of this paper than source energy considerations. Climate data from New York City and San Francisco are used to generate a predicted EUI versus gross floor area curve.

As shown in Fig. 2, shorter buildings consume less energy per unit area on average than taller buildings. While the EUI of buildings from 0 to 29 floors steadily increases with elevation, a distinct jump is observed at 30~39 floors, after which a plateau is reached for taller buildings. The average EUI of buildings with 10~19 floors increases by 33% as compared to buildings with 30~39 floors. An increase in 20 floors leads to 33% more energy consumption. With the same increase of 20 floors from 30 to 39 to more than 50 floors, the average EUI actually slightly decreases by 3% after reaching the plateau at 30~39 floors. The predicted EUI from the DOE's correlation also predicts a plateau for larger buildings. Although their correlation does not include a direct measure of building height, the gross floor area serves as a reasonable proxy.

This plateau is consistent with a firm-wide internal framework for tall building energy usage. Above 30~40 floors, much of the lost chilled-water efficiency from introducing a heat exchanger in a pressure break is already incurred. Sky view factors will also typically not increase with elevation past 30~39 floors, since most buildings of that height are already exposed to a large sky. Wind speeds also do not increase as rapidly at higher elevations. According to ASHRAE (American Society of Heating, Refrigeration and Air Conditioning Engineers), a local wind speed of 5.5 m/s at 40 m (approximately the 10th floor) increases by 27%

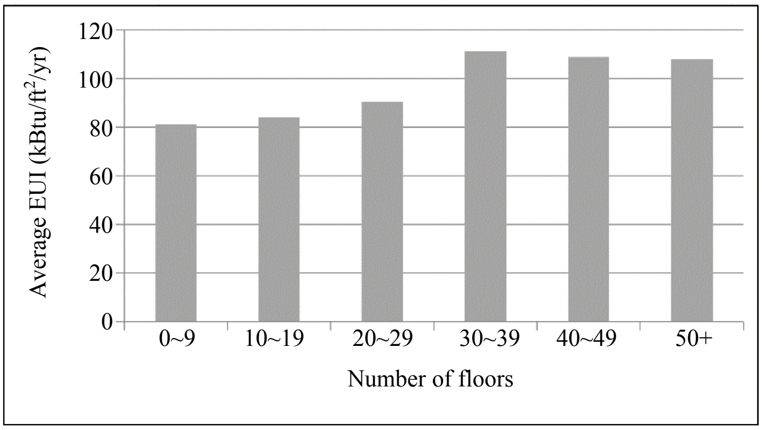

(a)

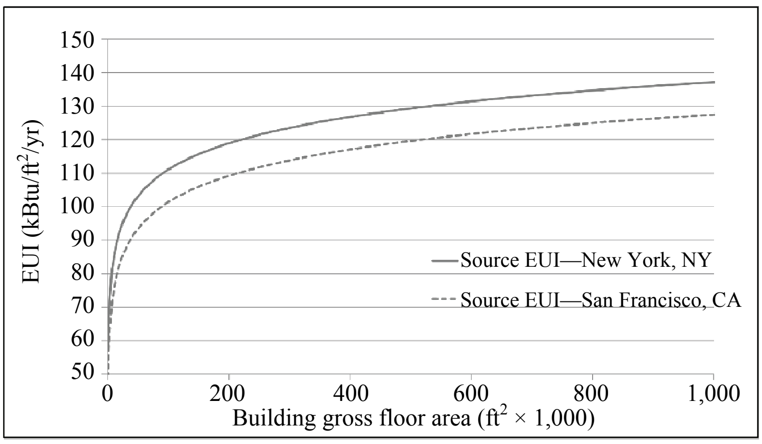

(b)

Fig. 2 Comparison between building characteristics: (a) average site EUI (units in kBtu/ft^2/yr) of New York office buildings reported by the City of New York as a function of total number of floors; (b) predicted site EUI (units in kBtu/ft^2/yr) as a function of building gross floor area from the DOE.

to 7.0 m/s at 120 m (the 30th floor), while the 7.0 m/s local speed at 120 m only increases by 12% to 7.8 m/s at 200 m (the 50th floor) [8]. Aerosol levels and moisture content similarly vary less at higher elevations, as they are further away from the pollutant and moisture sources at ground level.

While these factors alone do not fully account for the observed trend, they contribute to an explanation. Another factor that may lead to higher EUIs in taller buildings is the fact that many financial institutions with energy dense trading floors and even onsite data centers typically occupy tall buildings. The 55-story Bank of America Tower is a well-known example of how financial institutions can require large plug loads that significantly impact the total building energy use [9]. Further investigation is required to confirm how systematic these large plug loads are in financial institutions and if the financial institutions in New York City occupy tall buildings. This issue relates to a larger conversation about building energy use: productivity. Rather than solely focus on the inputs to a building, should we not also consider the outputs to calculate some type of overall efficiency? An attempt to quantify this efficiency has been made by the building economic energy coefficient, but further development and dialog are needed to sufficiently vet the metric [10].

The 2013 report released by New York City shows newer office buildings consume more energy than older ones [11]. This same trend is reproduced in this study for office buildings lower than 25 floors, as shown in Fig. 3. However, buildings taller than 25 floors do not follow this trend, and those constructed after 1970 have actually, on average, been consuming less energy than those constructed between 1930 and 1970. Additionally, the difference between buildings taller and shorter than 25 floors has been decreasing over the decades. Renovations impact these numbers and are discussed in another paper [12].

These results have also helped reinforce internal frameworks for understanding the energy consumption of tall buildings. A more detailed explanation of this framework is presented elsewhere [12]. The framework considers unique features of tall buildings that lead to higher EUIs. For example, in taller buildings: elevators travel further distances at faster speeds; multiple pressure breaks in chilled and hot water lines increase pumping energy and reduce temperature differences of the water; infiltration can increase based on the stack effect and higher wind velocities; increased exposure to solar gains, because fewer surrounding buildings provide shading, can also increase cooling loads; larger internal loads from intense computing clusters require more electricity and cooling to offset heat gains. This framework provides a general understanding of tall buildings that has been

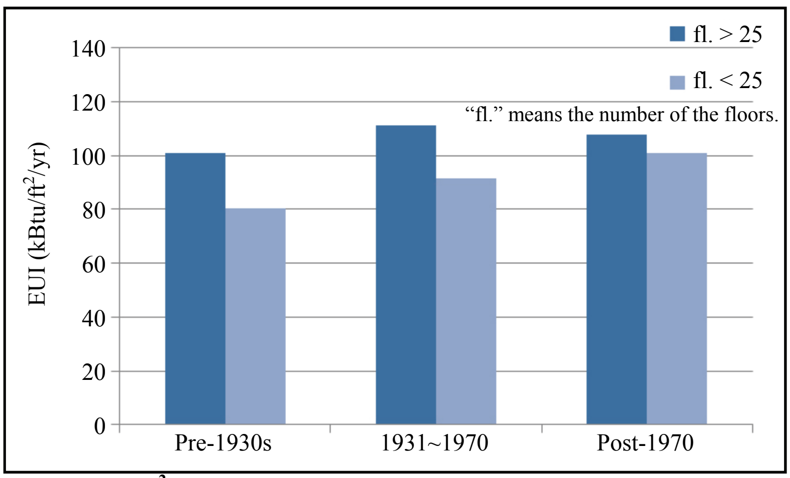

Fig. 3 Average EUI (units in kBtu/ft^2/yr) of all office buildings with 80% or more official area as a function of various construction eras in New York subdivided by buildings below and above 25 floors.

illustrated with both energy simulations and measured energy data. After surviving these vetting processes, the framework informs the foundation of tall building design used at the firm.

2.2.2 Informing Rating System Use

In addition to helping validate an internal tall building energy framework, these data from New York City can help inform the use of the ENERGY STAR rating system. Plotting the EUI as a function of ENERGY STAR rating, as shown in Fig. 4, shows a desirable trend for the EPA: Higher ENERGY STAR ratings are correlated with lower EUIs in New York City office buildings. The program benchmarks the energy efficiency of a specific building against other similar buildings and rates the building on a scale from 1 to 100, with 100 indicating a high level of comparable energy efficiency. In addition to suggesting that higher ratings are, on average, identifying more energy efficient buildings, a linear regression suggests a difference between taller and low-rise buildings. Each subsequently taller bin has a higher average EUI for the same rating. Each bin follows this trend except buildings with 30~39 floors, which deserves further investigation. Another noteworthy characteristic is the similar slope of every linear regression except two bins, 30~39 and greater than 50 floors. These similar slopes suggest that the average decrease in EUI with ENERGY STAR rating is fairly uniform across most building heights. One plausible explanation for the divergence from these similar slopes for taller buildings is the lack of benchmarking data for large buildings, which is discussed in a later section. Although more data and further investigation will illuminate stronger conclusions, the current trend in New York City helps the firm better inform clients in tall or low-rise buildings, who are seeking an ENERGY STAR rating.

3 National Data for Perspective Beyond Buildings

Publicly available building energy data impact more than the design of single buildings. It also can help inform the design of neighborhoods and cities. A growing body of research suggests that large cities not only use resources more efficiently than smaller ones, but also lead to higher productivity [13, 14]. This

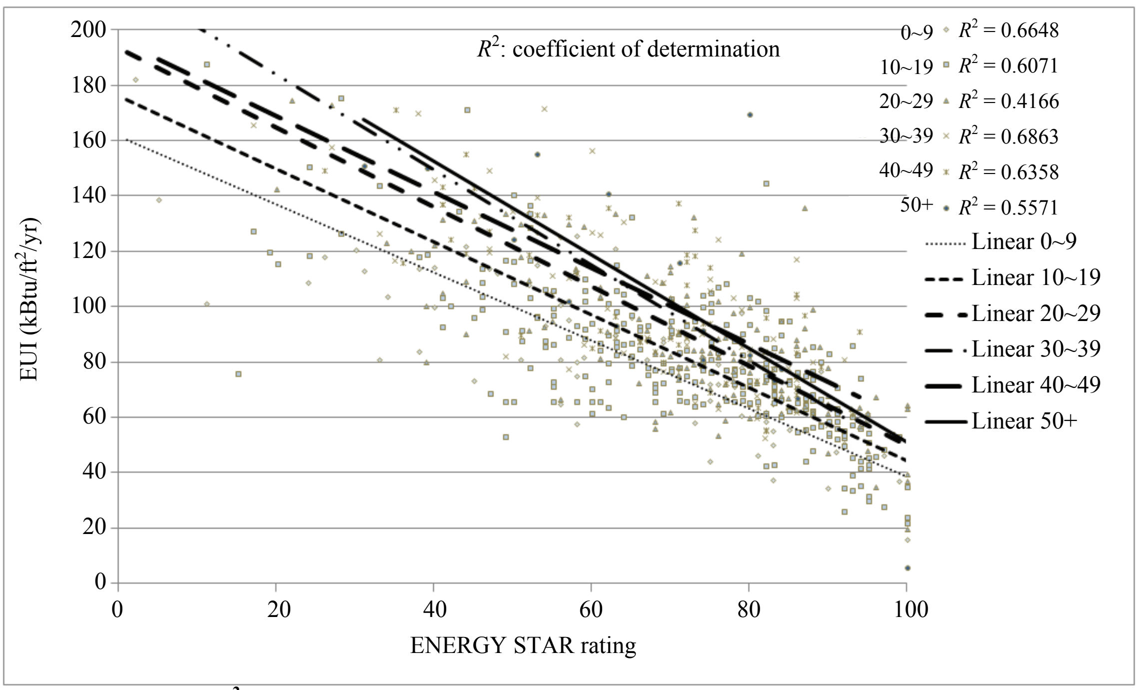

Fig. 4 EUI (units in kBtu/ft^2/yr) plotted as a function of ENERGY STAR rating for various building heights with linear regressions fitted to each bin of heights.

phenomenon has been quantified around the world, while in the absence of binding global climate change policies, cities are adapting to perform better than nations in per capita greenhouse gas emissions. Per capita emissions in New York City are only 29.7% of those in the United States as a whole [15]; Those in Rio de Janeiro are only 28.0% of those of Brazil as a whole [16]; And those in Barcelona are only 33.9% of those of Spain as a whole [17]. To add to this research from a slightly varied perspective, the firm uses publicly available data to investigate the impact of cities on quality of life.

Life expectancy is a well-documented and relatively consistent metric of quality of life. In this study, life expectancy data are collected from the Institute for Health Metrics and Evaluation from 2009 and made accessible through the measure of America organization [18]. It is used to correlate life expectancy to various developmental and environmental parameters: mean income per capita, education index and carbon emissions per capita. Mean income per capita data are expressed as 2010 US dollars and were collected between 2005 and 2009 by the US Census Bureau [19]. Education index is based on two indicators: school enrollment of children, which is weighted by a factor of one-third, and educational degree attainment of people 25 years and older, which is weighted by a factor of two-thirds [18]. Carbon use per capita data account for the carbon emissions associated with residential and transportation sectors in 100 largest US cities [20, 21]. A rigorous methodology is used to collect, analyze and normalize the carbon emissions data that originate with actual energy sold by all utilities for residential energy and vehicle-miles traveled as reported by the HPMS (Highway Performance Monitoring System) maintained by the Federal Highway Administration [20, 21].

Life expectancy depends on too many factors to fully explore in this paper. Moreover, these other factors are not all properly controlled in the obtained data. Nonetheless, correlations between life expectancy and the considered developmental and environmental parameters can still provide insightful relationships. Income and education are commonly known to impact life expectancy, thus the coefficient of determination R^2 between these two factors and life expectancy should provide a baseline correlation, to which other factors can be compared. A city's per capita carbon footprint provides the strongest linear correlation to life expectancy with an R^2 of 0.34, as shown in Fig. 5, which beats out other factors like education index and income that have an R^2 of 0.22 and 0.30, respectively. While causality is not considered in this study, the connectivity of cities may impact their inhabitants' life span. Increased physical activity and greater concentrations of world-class medical care may extend the lives of city dwellers who tend to have smaller carbon footprints.

This type of research adds to the body of work used by the firm to inform the design of cities and neighborhoods. Although the dataset is restricted to the US and provides a limited view to the myriad factors impacting life expectancy, it adds another piece to the larger body of work used to help shape firm values.

4. Conclusions

Publicly available data are continuing to grow but provide little value on its own. This paper presents some of the ways a large design firm which engages this data to inform design practices through a very select number of applications. A more exhaustive list is outside the scope of this paper, which has focused on using publicly available data to inform design practices.

An internal high performance design reporting program leverages CBECS data to compare projects around the world and spark best-practice conversations throughout the firm.

Benchmarking data from New York City help validate an internal tall building energy framework, particularly how tall buildings tend to have higher EUIs until they reach 30 stories, at which point an EUI plateau

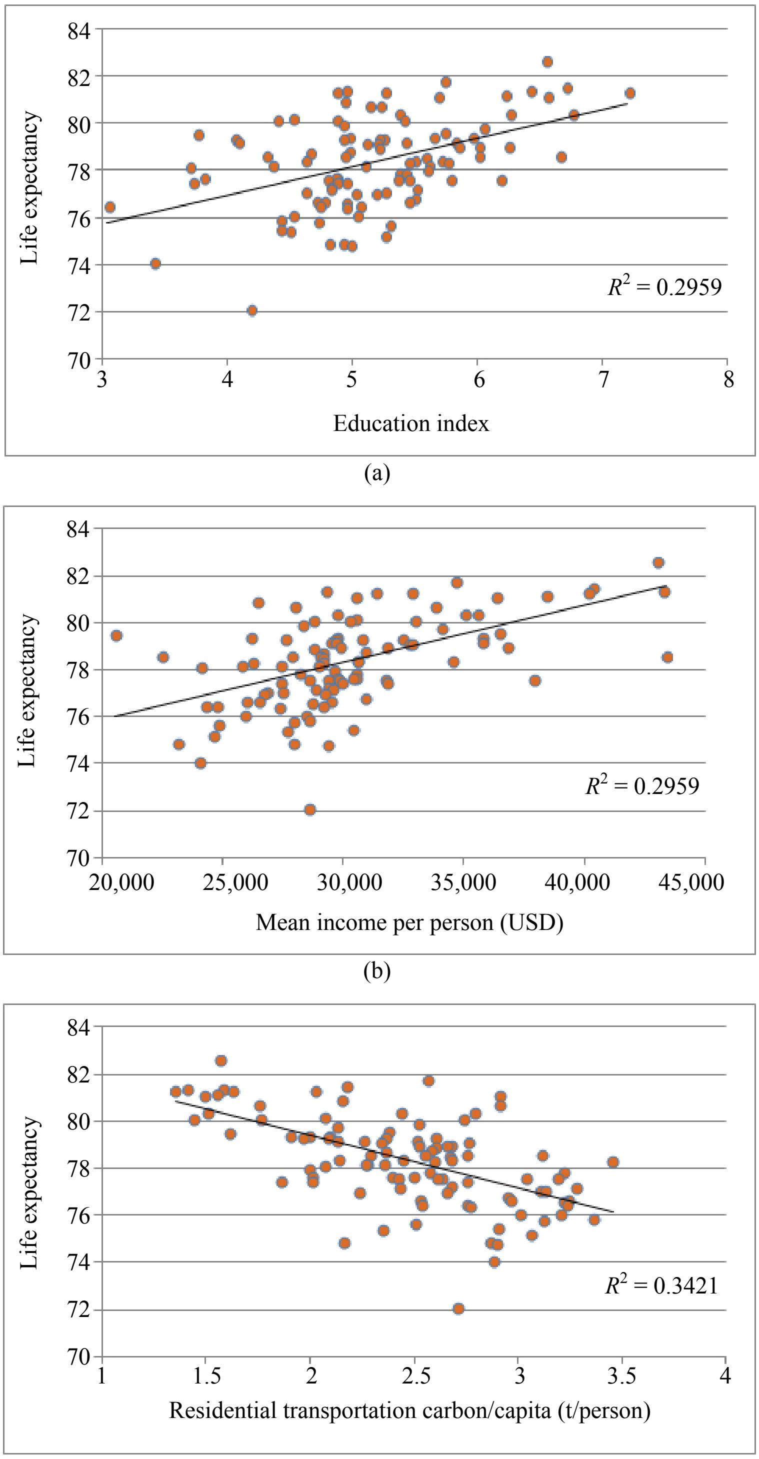

(c)

Fig. 5 Average EUI (units in kBtu/ft^2/yr) of all New York office buildings reported by the City of New York as a function of total number of floors: (a) educational index; (b) mean income per person; (c) residential/transportation carbon/capita.

is reached. The New York City data also provide key insights into relevant trends in the ENERGY STAR program: Taller buildings obtain higher ENERGY STAR ratings in New York City for a given EUI than shorter buildings, which may stem from the sparse large-building data in the CBECS dataset.

Lastly, per capita energy usage data are used in conjunction with life expectancy, mean income and education data to add to the body of work that informs neighborhood and city design.

These examples demonstrate a few simple ways that publicly available data can inform design at a large architecture firm.

References

[1] ENERGY STAR. 2014. "US Environmental Protection Agency and US Department of Energy." ENERGY STAR. Accessed December 15, 2014. http://www.energystar.gov.

[2] US EIA (United States Energy Information Administration). 2003. *CBECS (Commercial Buildings Energy Consumption Survey)*. Washington, D.C.: US Department of Energy.

[3] CCHRB (Chicago Committee on High Rise Buildings). 2014. *Existing High-Rise Buildings—Refurbish, Repurpose or Replace?*. Chicago: CCHRB.

[4] Dobbs, R., Remes, J., Manyika, J., Roxburgh, C., Smit, S., and Schaer, F. 2012. *Urban World: Cities and the Rise of the Consuming Class*. Washington, D.C.: McKinsey Global Institute.

[5] The City of New York. 2013. "Green Buildings and Energy Efficiency: Benchmarking Scores and Reports." The City of New York. Accessed September 26, 2013. http://www.nyc.gov/html/gbee/html/plan/ll84_scores.shtml.

[6] NYCDCP (New York City Department of City Planning). 2013. "Bytes of the Big Apple™." Accessed September 26, 2013. http://www.nyc.gov/html/dcp/html/bytes/applbyte.shtml.

[7] ENERGY STAR. 2013. *Portfolio Manager® Technical Reference*. Washington, D.C.: US Environmental Protection Agency and US Department of Energy.

[8] ASHRAE (American Society of Heating, Refrigeration and Air Conditioning Engineers). 2009. *ASHRAE Fundamentals*. Atlanta: ASHRAE.

[9] Calhoun, K., and Torbert, R. 2013. *The Bank of America Tower—What Is and What Could Have Been*. New York: Rocky Mountain Institute.

[10] Baumgartner, S., Coleman, J., and Aboff, A. 2013. "Linking NYC Energy Database to Tenant Contribution to Economy." Presented at 2013 Greenbuild International Conference and Expo (Greenbuild 2013), Philadelphia, USA.

[11] New York City. 2013. *A Greener, Greater New York*. New York City Local Law 84 Benchmarking Report September 2013, New York City.

[12] Leung, L., and Ray, S. D. 2013, "Low-Energy Tall Buildings? Room for Improvement as Demonstrated by New York City Energy Benchmarking Data." *International Journal of High-Rise Buildings* 2 (4): 285-91.

[13] West, G. B., Brown, J. H., and Enquist, B. J. 1997. "A General Model for the Origin of Allometric Scaling Laws in Biology." *Science* 276 (5309): 122-6.

[14] West, G. B., Brown, J. H., and Enquist, B. J. 2001. "A General Model for Ontogenetic Growth." *Nature* 413 (6856): 628-31.

[15] New York City PlaNYC. 2007. *Inventory of New York City Greenhouse Gas Emissions*. New York: Mayor's Office of Operations, New York City.

[16] Dubeux, C., La Rovere, E. 2007. "Local Perspectives in the Control of Greenhouse Gas Emissions—The Case of Rio de Janeiro." *Cities* 24 (5): 353-64.

[17] Baldasano, J., Soriano, C., and Boada, L. 1999. "Emission Inventory for Greenhouse Gases in the City of Barcelona, 1987~1996." *Atmospheric Environment* 3: 3765-75.

[18] Social Science Research Council. 2011. "Mapping the Measure of America. 2010-2011 Dataset." Social Science Research Council. Accessed December 2, 2013. http://www.measureofamerica.org.

[19] US Census Bureau. 2009. *American Community Survey 2005~2009, Table B20017*. Washington, D.C.: US Census Bureau.

[20] Brown, M. A., and Logan, E. 2008. *The Residential Energy and Carbon Footprints of the 100 Largest U.S. Metropolitan Areas*. Working Paper No. 39, Georgia Tech Ivan Allen College, School of Public Policy Working Paper Series.

[21] Southworth, F., Sonnenberg, A., and Brown, M. A. 2008. *The Transportation Energy and Carbon Footprints of the 100 Largest US Metropolitan Areas*. Working Paper No. 37, Georgia Tech Ivan Allen College School of Public Policy Working Paper Series.

Journal of Civil Engineering and Architecture 10 (2016) 22-36
doi: 10.17265/1934-7359/2016.01.003

Sensibility Analysis of the Brazilian Standards for Energy Efficiency Regarding the Variation of Internal Load Density in Office Buildings in Brazilian Bioclimatic Zones 1 and 7

Mariane Pinto Brandalise, Eduardo Grala da Cunha and Larissa Cristina de Oliveira

Laboratory of Comfort and Energy Efficiency, Architecture and Urbanism, Federal University of Pelotas, Pelotas 96010-020, Brazil

Abstract: The RTQ-C (*Technical Requirements of Quality for the Energy Performance Level of Commercial Buildings*) publication classified the buildings in five efficiency levels. In RTQ-C, the evaluation can be done with two methods: a prescriptive method and a simulation one. This paper aims to identify the sensibility of the prescriptive method RTQ-C regarding the variation of equipment internal load density in office buildings in bioclimatic Zones 1 and 7 of the Brazilian bioclimatic zoning. The research results show that the building with walls and roof configured to meet specific prerequisites for energy efficiency Levels B and C had a lower consumption than buildings that meet the prerequisites to Level A. The study also showed that buildings with high internal load density of equipment, maximum shape factor and high, with walls and roofs with higher thermal transmittance, have lower power consumption than constructions with an envelope with greater thermal resistance. The increase in internal load density causes an increase in the internal heat generated by the large amount of equipment. In buildings with higher thermal insulation (Level A), the internal heat is maintained in the environment, causing overheating and the need for an air conditioning system.

Key words: RTQ-C, internal load density, office buildings, energy modeling, energy efficiency in buildings.

1. Introduction

In Brazil, the first governmental programs and specific legislations that aimed at energy efficiency appeared in the 1980s, with the creation of PBE (Brazilian Labeling Program) and PROCEL (National Program for Electric Energy Conservation). The PBE has the objective of informing consumers about the performance of products, regarding conditions such as energy efficiency and noise, for example. The PROCEL has the objective of promoting rationalization of electricity consumption to combat waste and reduce costs and sector investments, increasing energy efficiency.

In 2001, Brazil faced a crisis in the energy sector and public attention turned to this problem. At that time, the government had to look for more effective measures related to the rationalization of electricity consumption. The first step was the publication of *Law 10295*, on October 17, 2001 [1], which determined that the energy-using equipment produced domestically or imported, as well as the buildings constructed in the country, should meet the minimum energy efficiency requirements. In December of that same year, Decree No. 4059, regulating *Law No. 10295*, was published, and the creation of the working group on buildings was also established, which presented a way to regulate the buildings constructed in Brazil to encourage rational use of electricity in the country [2].

After some years of discussion and work, the INMETRO (National Institute for Metrology, Quality and Technology) published the first version of the RTQ-C (*Technical Quality Requirements for Energy Efficiency Level in Commercial, Public and Service*

Corresponding author: Eduardo Grala da Cunha, Dr., research field: energy efficiency.

Buildings) in 2007, having its final version published in 2009. Soon after, in 2010, the RTQ-R (*Quality Technical Standards for Energy Efficiency Level in Residential Buildings*) was published, too.

The RTQ-C aims to develop conditions for the labeling of the energy efficiency level of commercial, services and public buildings, discriminating the technical requirements to be assessed and methods for classification of buildings regarding energy efficiency, to obtain the ENCE (National Energy Conservation Label). To classify the building energy efficiency level, the RTQ-C assesses three individual systems: envelope, lighting system and air conditioning system, considering weights of 30%, 30% and 40%, respectively. A partial (envelope, envelope and lighting, envelope and air conditioning) or general label can be conceded to the building, in which the three systems were evaluated, resulting in a final classification. The classification always ranges from A (most efficient) to E (less efficient).

The project assessment is realized through two methods: the prescriptive method, which is a simplified method, and the simulation method. The prescriptive method was developed using the statistical method of multiple linear regression.

In the prescriptive method, the numerical equivalents for the envelope, lighting and air conditioning are calculated, considering artificial conditioned environments for areas of prolonged permanence. The envelopes consume indicator (IC_{env}) is found by equations determined according to the bioclimatic zone, in which the project is settled. For each bioclimatic zone, there are two different equations, one for buildings with a projected area (A_{pe}) smaller than 500 m^2 and another for buildings with a projected area bigger than 500 m^2.

The RTQ-C presents maximum limits of thermal transmittance for walls and roofs according to the energy efficiency level and the bioclimatic zone in which the building is located. Those limits, however, do not take into consideration the possibility for occupation and heat generation. The regulation makes observations regarding the ILD (internal load density) only for an artificial lighting scenario.

It is common sense that as higher the wall thermal resistance as better is the thermal energy performance of the building. However, some works show that, for office buildings, this analysis depends on other variables, like the climate and the internal load density of the building. According to Westphal [3], for an office-building model in Curitiba City, with the internal load density about 20 W/m^2, low external thermal absorbance, and occupancy pattern about 8 h/day, the increase of thermal transmittance increases the air conditioning energy consumption. However, in the same building with internal load density of 50 W/m^2, a energy consumption decrease is observed, considering the HVAC when the envelope has higher thermal transmittance. Melo [4] showed that the internal load density increases, and the impact of the HVAC energy consumption increases, too. However, if the thermal transmittance of the walls is increased, the internal heat dissipations is easy. As a result, we have lower consumption observing the Curitiba and Florianópolis climate in Brazil.

Chvatal [5] held a study that aimed to analyze the impact of the envelope thermal insulation of the buildings in the thermal performance, observing the tropical climates. It was observed that the heat losses in the building for the insulated envelop become difficult and the internal temperature increases. In this study, it was possible to observe that the thermal discomfort in summer is high due to the high internal load of equipment and occupancy occurs during the same period of the maximal solar gains.

Considering the importance of those researches and the limitation of the Brazilian Energy Efficiency Regulation (RTQ-C, prescriptive method) that uses only 25 W/m^2 as internal load density to the developing of the linear regression equations, it was decided to analyze the sensibility of the RTQ-C to the internal load density variation. Two Brazilian bioclimatic zones were chosen to analyze the sensibility of the prescriptive method of RTQ-C, Zones 1 and 7. Zone 1 is the coldest one of the country. The average temperatures are under 20 °C, and the annual thermal amplitude is between 9 °C and 13 °C. Bioclimatic Zone 7 is characterized by tropical and wet climate, presenting concentrated rains period since October until April. Between May and September, the dry air mass over the center of the country minimizes the rainy formation. The maximum temperatures can reach 40 °C in the warmer months, and in the coldest, the average of the minimal is 16.6 °C.

2. Method

The method employed to reach the objective of this paper is divided into five stages, which are presented as follows: analysis models definition; ILD assessment, to be used in the configuration of the analysis models; determination of analysis models envelopes according to RTQ-C, energy consumption determination on the evaluated models; comparison of consumption in buildings with envelopes Level A, Level B or Level C, with different equipment internal load density.

2.1 Determination of the Analysis Models

For this study, five different analysis models were defined. The first analyzed model was defined based on the study developed by Carlo [6]. The author, through a photographic survey in five Brazilian cities, was able to observe typical volumetries, more frequent in the urban landscape, destined to some commercial activities. Through the survey, it was possible to generate a representative model for each activity. The first defined model was identified by the author with the "big offices" name and characterized as a vertical edification, with floor area smaller than 500 m^2, having five floors, rectangular shape, with dimensions of 27-m length, 7.8-m width and 15-m height. Fig. 1 illustrates the "big offices" model.

The other analyzed models were determined with basis on the equations from RTQ-C, which defines limits for a minimal shape factor and a maximum shape factor. The shape factor is determined by the ratio between the envelope area and the total volume of the building. The RTQ-C establishes for bioclimatic Zones 1 and 7, with a minimal shape factor of 0.17 for buildings with a projected area bigger than 500 m^2 and the maximum shape factor of 0.60 for buildings with a projected area smaller than 500 m^2. For each shape factor (minimal and maximal), two models were defined with the intention of assessing the differences between a larger roof area against a larger wall area. Thus, Models 1 and 2 (Figs. 2 and 3), with the minimal shape factor, show 10 and 2 floors, respectively. The Models 3 and 4 (Figs. 4 and 5), with maximal shape factor, possess 10 and 1 floors, respectively. The volumetric characteristics for each model can be observed in Table 1, as follows.

2.2 Characterization of the Internal Load Density to Be Used in the Configuration of the Analysis Models

The ILD is defined by the sum total of the three main internal sources of heat: lighting, electrical appliances and human beings. The lighting system of the models was configured with the lighting potency density of 10 W/m^2. RTQ-C classifies the lighting system for office buildings as Level A, with a limit potency of 9.7 W/m^2.

Fig. 1 The "big offices" model.

Fig. 2 Model 1.

Fig. 4 Model 3.

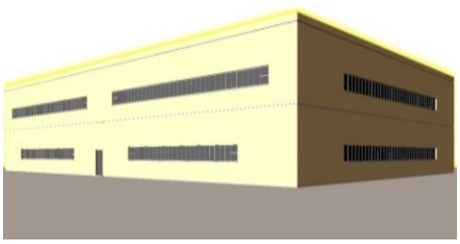

Fig. 3 Model 2.

Fig. 5 Model 4.

Table 1 Volumetric characteristics of models based on RTQ-C.

Variables	Minimal shape factor		Maximal shape factor	
	Model 1	Model 2	Model 3	Model 4
Dimensions	35 m × 25 m	70 m × 45 m	10 m × 6m	27 m × 7.5 m
Height	30 m	10 m	30 m	4 m
Floor area	875 m^2	3,150 m^2	60 m	211 m^2
Total area	8,750 m^2	6,300 m^2	600 m^2	211 m^2
Shape factor	0.17	0.17	0.60	0.60
Height factor	0.10	0.50	0.10	1.00
Number of floors	10.00	2.00	10.00	1.00

However, the DesignBuilder software allows only for the use of round numbers, this being the reason the value was rounded up to 10 W/m^2. The air conditioning system of the models was considered as a split type, with a COP (performance coefficient) of 3.21, considered Level A in the RTQ-C.

The ASHRAE Fundamentals [7] standard classifies the offices in four types of appliances internal load density. In this paper, only two types of density were observed: medium and high. Table 2 characterizes the adopted values according to the ASHRAE Fundamentals [7] standards for appliances internal load density, NBR 16.401—Part 3 [8] person density and RTQ-C [9] for lighting potency density.

Table 2 Characterization of the internal load densities used in the analysis models.

Office type	ILD appliances (W/m^2)	Person density (person/m^2)	Lighting potency density (W/m^2)
Medium density	11	0.14	10
High density	21	0.20	10

Table 3 Envelope prerequisites for bioclimatic Zone 1.

Envelope prerequisites	Level A	Level B	Level C
Thermal transmittance roof	0.5 W/m^2·K	1.0 W/m^2·K	2.0 W/m^2·K
Thermal transmittance external wall	1.0 W/m^2·K	2.0 W/m^2·K	3.7 W/m^2·K
Roof absorptance	0.20	0.20	0.20
External wall absorptance	0.20	0.20	0.20

Table 4 Envelope prerequisites for bioclimatic Zone 7.

Prerequisite	Wall	Roof	Absorptance
Level A	W1: U = 2.50 W/m^2·K and maxCT = 80 KJ/m^2·K	U = 1.00 W/m^2·K	Roof: α < 0.50
	W2: U = 3.7 W/m^2·K and CT > 80 KJ/m^2·K	-	Wall: α < 0.50
Level B	W1: U = 2.50 W/m^2·K and maxCT = 80 KJ/m^2·K	U = 1.50 W/m^2·K	Roof: α < 0.50
	W2: U = 3.7 W/m^2·K and CT > 80 KJ/m^2·K	-	Wall: without prerequisite
Level C	W1: U = 2.50 W/m^2·K and maxCT = 80 KJ/m^2·K	U = 2.00 W/m^2·K	Roof: without prerequisite
	W2: U = 3.7 W/m^2·K and CT > 80 KJ/m^2·K	-	Wall: without prerequisite

W1 means Wall 1; W2 means Wall 2.

Table 5 Parameters used in the analysis models.

Parameters	Adopted values
Use pattern (h/day) (occupancy, appliance and lighting) (Saturdays and Sundays were not considered as occupancy periods)	From 08:00 a.m. to 12:00 a.m.—100% From 12:00 a.m. to 02:00 p.m.—10% 02:00 p.m. to 06:00 p.m.—100%
Air conditioning system's performance coefficient (W/W)	3.21 W/W for heating and cooling
Heating setpoint (°C)	18
Cooling setpoint (°C)	24
Orientation of major frontage	North/south

2.3 Determination of the Building Envelope Characteristics

RTQ-C determines that the thermal transmittance of external walls and roofs and their absorptance, are specific prerequisites of the envelope. These prerequisites have limits established for each bioclimatic zone, regarding the level of intended energy efficiency. In this paper, models walls and roofs were configured with the thermal characteristics according to the prerequisites for bioclimatic Zones 1 and 7, as shown on Tables 3 and 4, respectively. The absorptance was considered constant at 0.20 in both analyzed bioclimatic zones. Bioclimatic Zone 7 allows for two different wall configurations, so each model was configured two times, one with each wall type.

2.4 Determination of Energy Consumption in Models with Characteristics According to Different RTQ-C Levels for Energy Efficiency

In order to obtain the energy consumption from buildings with characteristics according to the different energy efficiency levels proposed on RTQ-C, simulation were made through the DesignBuilder software, version 3.0.0.15. First, the "PR_Curitiba.epw" weather file was configured for the city of Curitiba, bioclimatic Zone 1, and the "MT_Cuiaba.epw" file was configured for the city of Cuiaba, bioclimatic Zone 7. After modeling the buildings in the software, the parameters used in the energy modeling were informed, as visible in Table 5.

2.5 Comparison between Consumption in Buildings with Levels A, B and C and Envelopes with Different Appliances Internal Load Densities

Through the energy modeling, the yearly energy consumption rate for each model was obtained. These data made it possible to assess and compare the energy performance for the different envelope configurations according to the RTQ-C. The Level A model presents a limit for the frontage's opening percentage lower to that on the Levels B and C models, therefore, a comparison was made between the Level A model with maximum WWR (window to wall ratio) of 0.15 with Model 2, with maximum WWR of 0.10. On the other WWRs, the analysis between Levels B and C models was made. Results are shown as comparative analysis of the diverse simulations made in a table form.

3. Results Analysis

The results analysis is divided in two parts: The first part shows results for bioclimatic Zone 1 and the second part shows the results for bioclimatic Zone 7.

3.1 Bioclimatic Zone 1

In Table 6, the results found for bioclimatic Zone 1 can be observed, after which there would be the analysis of the results.

3.1.1 "Big Offices" Model

In the equipment ILD, it was possible to observe the buildings envelope, meeting the prerequisites for Level A presented as a higher energy consumption by comparison with the others, mainly due to the fact that this envelope is more insulated, preventing the heat exchange from the inside with the outside. As for the

Table 6 Results for bioclimatic Zone 1.

Energy modeling results for bioclimatic Zone 1														
Energy efficiency			Medium ILD					High ILD					Influence of internal load density in the envelope of energy performance according to the levels of energy efficiency	
			WWR					WWR						
			0.05	0.10	0.15	0.20	0.25	0.05	0.10	0.15	0.20	0.25	Model A	Model C
Model "big office"	✚	⇧	B	B	B	C	C	C	C	C	C	C	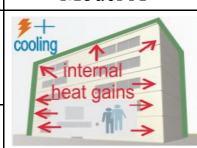	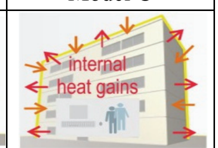
	▬	⬇	A	A	A	B	B	A	A	A	B	B		
Model 1	✚	⇧	C	C	C	C	C	C	C	C	C	C	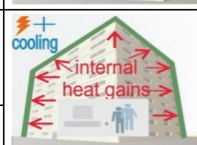	
	▬	⬇	A	A	A	B	B	A	A	A	B	B		
Model 2	✚	⇧	C	C	C	C	C	C	C	C	C	C	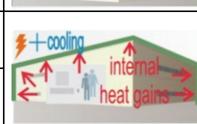	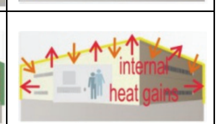
	▬	⬇	A	A	A	B	B	A	A	A	B	B		
Model 3	✚	⇧	B	B	B	C	C	C	C	C	C	C	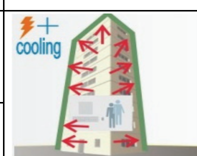	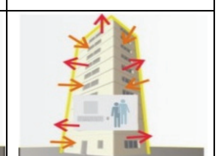
	▬	⬇	C	A	A	B	B	A	A	A	B	B		
Model 4	✚	⇧	A	A	-	-	-	B	B	-	-	-		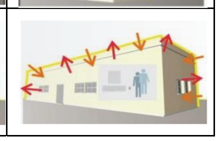
	▬	⬇	C	C	-	-	-	C	A	-	-	-		

✚⇧: More energy efficient model;

▬⬇: Less energy efficient model.

Level B model, the smallest energy consumption is showed until the WWR = 0.15. Observing the results of the heat exchanges between components of the building, it can be concluded that Level C has shown the largest heat losses in walls, covertures and roofs, while in Level B, the same occurred trough glasses, ground floor and infiltration. Starting from WWR = 0.20, the Level C presents smaller energy consumption by a small difference (67 kWh). Both Levels B and C models decreased their heating consumption from WWR 0.20 to WWR 0.15, and have increased their cooling. Level C, however, by having a higher thermal transmittance, allows a bigger exchange with the outside environment, thus needing a smaller energy consumption for cooling, therefore, showing a smaller overall energy consumption.

As for the influence of ILD in the results, it can be assessed that, with the increase in ILD, Level C showed the smallest energy consumption amongst all WWRs. With the increase in internal heat, the better insulated buildings (Levels A and B) need a higher use of an air conditioning system for cooling, since they do not make it difficult for the internal heat to dissipate to the outside environment.

3.1.2 Model 1

In Model 1, with minimal shape factor and 10 floors, models that presented a higher thermal insulation (Level A) in its envelope showed a higher energy consumption when compared with the models of higher thermal transmittance (Levels B and C). One can observe that the models with the envelope meeting the Level C prerequisites have obtained the best energy performance on both analyzed ILDs. Assessing the thermal gains in buildings, it is possible to assess that the models configured for Level C show bigger heat losses through walls, roofs and ground. Therefore, Level C models show higher energy consumption for heating, while the Levels A and B models need higher energy consumption for cooling, thus bringing the higher overall energy consumption rate.

3.1.3 Model 2

In Model 2, with minimal shape factor and two floors, it was possible to observe that in both equipment densities analyzed (11 W/m^2 and 21 W/m^2), the ones presenting a higher thermal insulation in its envelops (Level A) have showed higher energy consumption compared to those buildings with higher thermal transmittance (Levels B and C). As seen before in the other models, this fact occurs due to overheating in the inside of the building, caused by the thermal insulation not allowing for internal heat to dissipate in the outside environment. Therefore, the Level C model presenting the higher thermal transmittance value showed the best thermal performance.

It was possible to observe that in both models with shape factor (Models 1 and 2) that presented area bigger than 500 m^2, the increase of the internal load density did not change the simulation results. It was possible to realize that even in the medium ILD, the Level A model already presented overheating, occurring the biggest energy consumption regards to energy Levels A and B.

3.1.4 Model 3

In Model 3, with maximum shape factor and 10 floors, average ILD of equipments (11 W/m^2), it could be observed that, as the opening percent of the frontage changed, the results were also modified. In WWR = 0.05, Level C model presented the higher energy consumption and a difference of 459 kWh from the Level A model. The Level C model, having the biggest heat losses through envelopment (roof and walls), needing a higher energy consumption for heating, thus consuming more energy than the other level models. Starting with WWR = 0.10, with the increase in heat gains through radiation, the Level A models start to consume more energy. This happens due to overheating caused by the envelope’s insulation, which prevents heat from dissipating to the outside of the building. Therefore, Level A models showed higher energy consumption for cooling, and as a consequence, they consume more energy than the remaining

Levels B and C. As for the Level B models, they are the ones that showed the best energy performance for WWR up to 0.15, due to their capacity to keep milder internal temperatures, not needing much energy neither for heating or cooling. From WWR = 0.20 onward, when the radiation heat gains increase, the Level B models need higher energy consumption for cooling, which brings a higher energy consumption when compared with Level C models.

With the increase in ILD, the Level C models presented the best energy performance. As previously noted, the Level C models, showing a higher thermal transmittance, allow for a larger heat exchange with the outside environment, thus allowing the heat generated by the increase in equipments to dissipate outside, needing a smaller energy consumption for cooling. As for the more insulated models (Levels A and B), they end up generating overheat in the inside of the building, which brings a higher use of the cooling system and by consequence a higher energy consumption.

3.1.5 Model 4

In Model 4, with maximum shape factor and one floor and with average equipment ILD (11 W/m^2), buildings with the envelope meeting the prerequisites for Level A showed the lowest energy consumption. It was possible to observe that the Level A models had a larger heat loss through glass, ground floor and infiltration. As for the Level C models, the heat loss was through walls and roof, as expected, due to these buildings having higher thermal transmittance in those elements. Therefore, by allowing a larger heat exchange with the outside environment, the Level C models showed the higher energy consumption both for cooling and heating, thus bringing the larger energy consumption when compared with other levels.

Analyzing the same model with a high ILD (21 W/m^2), the found results are different. In the model with WWR = 0.05, Level C model presented the higher energy consumption, while the Level B model had the lowest one. This is because Level C model presents a higher energy consumption for heating, once it presents higher heat losses through walls and roof in comparison with other levels models. Level A model, in turn, presents a higher consumption for cooling, since it presents the lowest heat losses through walls and roof, keeping the ambience overheated. Therefore, Level B model, less insulated than the Level A one, presented the best result, since it needs lower energy consumption for cooling and heating.

As for WWR = 0.10, Level A model presented the highest energy consumption. With the opening increase, the radiation heat gains also increased, which when added to the internal heat generated by equipment and brought the increase in overheating. Therefore, the model needed higher energy consumption for cooling, thus consuming more energy than Level C model.

3.2 Bioclimatic Zone 7 Results

In Table 7, the results for bioclimatic Zone 7 can be found. Next, there is the results analysis.

3.2.1 "Big Offices" Models

In the medium equipment ILD energy modeling, it can be observed in Wall 1 (W1) that the envelope meeting the Level A prerequisites presented a higher energy consumption comparing to the others. This is justified by the higher energy consumption needed for cooling, due to the presence of a more thermal insulated envelope than that in the remaining models (Levels B and C). The Level C envelope presented the lowest energy consumption; The Level B model needs higher energy consumption for cooling the Level C model. In the results found with the high equipment ILD, Level A model also presented the highest energy consumption. As for the Level C models, they present the lowest consumption up to WWR = 0.10. After that, Level B models are the ones presenting the lowest energy consumption. With the increase in LID causing increase in internal heat, the Level C models, having higher thermal transmittance, allow for a larger heat loss when comparing with other models. However, with WWR = 0.10 and onward, the Level C models need

Table 7 Bioclimatic Zone 7 results.

Energy modeling results for bioclimatic Zone 7													
Models	Wall	Energy efficiency		Medium ILD					High ILD				
				WWR					WWR				
				0.05	0.10	0.15	0.20	0.25	0.05	0.10	0.15	0.20	0.25
Model "big offices" 	W1	+	⇧	C	C	C	C	C	C	C	B	B	B
		−	⬇	A	A	A	B	B	A	A	A	C	C
	W2	+	⇧	C	B	B	B	B	C	B	B	B	B
		−	⬇	A	A	C	C	C	A	A	C	C	C
Model 1 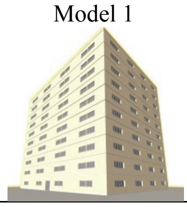	W1	+	⇧	C	C	C	C	C	C	C	C	C	C
		−	⬇	A	A	A	B	B	A	A	A	B	B
	W2	+	⇧	C	C	C	C	C	C	C	C	C	C
		−	⬇	A	A	A	B	B	A	A	A	B	B
Model 2 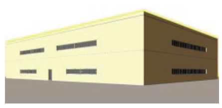	W1	+	⇧	C	C	C	C	C	C	C	C	C	C
		−	⬇	A	A	A	B	B	A	A	A	B	B
	W2	+	⇧	C	C	C	C	C	C	C	C	C	C
		−	⬇	A	A	A	B	B	A	A	A	B	B
Model 3 	W1	+	⇧	C	C	C	C	C	C	C	C	C	C
		−	⬇	A	A	A	B	B	A	A	A	B	B
	W2	+	⇧	C	C	C	C	C	C	C	C	C	C
		−	⬇	A	A	A	B	B	A	A	A	B	B
Model 4 	W1	+	⇧	A	B	-	-	-	B	C	-	-	-
		−	⬇	C	C	-	-	-	C	A	-	-	-
	W2	+	⇧	B	C	-	-	-	C	C	-	-	-
		−	⬇	A	A	-	-	-	A	A	-	-	-

W1—Wall 1: $U = 2.5$ W/ m^2·K, *CT* is maximum about 80 KJ/m^2·K;
W1—Wall 1: $U = 3.7$ W/ m^2·K, $CT > 80$ KJ/m^2·K;

+ ⇧: More energy efficient model;

− ⬇: Less energy efficient model.

a higher energy consumption for cooling and heating when compared to the Level B model.

In the office model, with Wall 2 (W2) ($U = 3.7$ W/m^2·K, $CT > 80$ KJ/m^2·K), the results were a little different from those with Wall 1 (W1). The Level A model presented the highest energy consumption with WWR up to 0.10, value after which the Level C model showed the highest energy consumption. As for the Level B model, it presented the lowest energy consumption amongst all analyzed WWRs, with the exception of WWR = 0.05, with which the Level C model presented the best energy consumption level. These results were equal to the ones for the other two analyzed ILDs. Observing the results for WWRs = 0.05, the Level C model presents the higher heat loss through envelope, therefore, presenting a lower energy consumption for cooling than the models Levels A and B. From WWR = 0.10 onwards, the Level B model presents the higher heat losses through envelope. It also presents lower energy consumption than that of Level C model (56 kWh). With high ILD, the same fact occurs for Level C model, which presents the highest heat loss through envelope only for WWR = 0.05, therefore, needing a lower energy consumption for cooling. In the subsequent WWRs, the Level B model presents the higher heat loss through envelope. Level C models, starting from WWR = 0.15, because they increase their radiation gains and present a higher thermal transmittance in the roof, begin to need a higher consumption for cooling and heating, thus presenting the higher energy consumption.

Assessing the behavior of wall, with medium ILD, Wall 2 (W2) presented the higher energy consumption with WWR = 0.05 for all levels (Levels A, B and C) when compared to Wall 1 (W1). With the increase in WWR, Wall 1 (W1) needs a higher energy consumption for cooling, which causes higher energy consumption in comparison with Wall 2 (W2). With WWR = 0.05, the envelope configured with Wall 1 (W1) shows higher heat losses than the envelope configured with Wall 2 (W2). Therefore, the model with Wall 2 needs a higher consumption for cooling if compared with Wall 1 (W1), and consequently, they present higher energy consumption. With the increase of the radiation gains, the internal heat also increases and, since Wall 2 (W2) presents higher thermal transmittance, it allows for the heat to dissipate in the external environment, needing less consumption for cooling and presenting lower energy consumption than Wall 1 (W1). With the increase in ILD, and the increase in internal heat, Wall 2 (W2) shows the lower consumption precisely because it needs a lower consumption for cooling.

3.2.2 Model 1

In Model 1, with minimum shape factor and 10 floors, the models that presented higher insulation in its coverings (Level A) showed a higher energy consumption compared to the models with higher thermal transmittance in its coverings (Levels B and C) on both analyzed ILD (11 W/m^2 and 21 W/m^2). The Level A models presented the higher heat losses through glass and walls, however, they still presented a large amount of heat stored in their insides, due to thermal insulation of the covering. This way, the need for cooling was higher when compared to other energy efficiency levels. As for the Level C models, they presented the higher heat losses through roof, coverture and floor, and they also presented the lower energy consumption for cooling. Bioclimatic Zone 7 presents high temperatures, so there was no need for heating in any of the models assessed. This way, the Level C models showed lower energy consumption. The increase in ILD did not influence the results, once, since the medium ILD, the Level A models presented high temperatures, needing a higher consumption for cooling. However, in high ILD (21 W/m^2), the difference in results between the energy efficiency levels was higher. In medium ILD (11 W/m^2), WWR = 0.15, the Level A model presented 1,870 kWh/year more than the Level C model, as for the high ILD (21 W/m^2), the yearly difference was 2,330 kWh.

In Model 1, with Wall 2 (W2) (U = 3.7 W/m^2·K, CT > 80 KJ/m^2·K), the results were the same as the ones for Wall 1 (W1). Level A presented the highest energy consumption and Level C presented the lowest. The models with Wall 1 (W1) (U = 2.50 W/m^2·K, CT is maximum about 80 KJ/m^2·K), however, presented higher energy consumption than those with Wall 2 (W2). With medium ILD for Level A model, WWR = 0.015, presenting the largest difference in yearly consumption: 6,760 kWh. This result was influenced by the fact that Wall 2 (W2) presented a higher heat loss through walls and, therefore, needed lower energy consumption for cooling, thus presenting lower energy consumption. In high ILD, the differences in consumption between Wall 1 (W1) and

Wall 2 (W2) were higher, the highest one with Level A models and with WWR = 0.15, in which Wall 1 (W1) presented energy consumption 10.330 kWh higher than Wall 2 (W2). This happens due to the increase in internal heat, Wall 1 (W1) presenting lower thermal transmittance than Wall 2 (W2).

3.2.3 Model 2

In Model 2, with minimum shape factor and two floors, it was possible to observe on both equipments ILDs (11 W/m^2 and 21W/m^2), as well as in both analyzed walls that the models presenting higher thermal insulation in their envelope (Level A), presented higher energy consumption when compared to the models with higher thermal transmittance (Levels B and C). Model 2 presents a large area of coverture (3.150 m^2), this way, even in the models with medium ILD, they presented need for energy consumption for cooling, specially the Level A model. Said model presents overheating due to having a more insulated roof, therefore, needing higher consumption for cooling when compared to models from other levels. This justifies why the ILD did not influence the results. Although having no influence in the results, the increase in ILD brought a higher difference in energy consumption between Levels A, B and C. In Wall 1 (W1), WWR = 0.15, medium ILD, the Level A model presented 4.860 kWh more than the Level C model, which presented the lowest energy consumption. As for high ILD, this difference changes to 16.880 kWh.

Regarding the difference between walls, with medium ILD (11 W/m^2), Wall 1 (W1) (U = 2.50 W/m^2·K, CT is maximum about 80 KJ/m^2·K) presents lower energy consumption, while with high ILD, Wall 2 (W2) (U = 3.7 W/m^2·K, CT > 80 KJ/m^2·K) presents lower energy consumption. On both analyzed ILDs, Wall 2 (W2) loses more heat than Wall 1 (W1), because it presents higher thermal transmittance, which allows for a larger heat exchange with the environment. However, in medium ILD, analyzing all the elements (glass, walls, roof, floors and infiltration), models with Wall 1 (W1) lose more heat than models with Wall 2 (W2), therefore, models with Wall 2 (W2) need a higher consumption for cooling and thus consume more energy. As for high ILD, the difference in heat loss through walls results increases, this way, models configured with Wall 2 (W2) need lower energy consumption for cooling and consequently consume less energy. In this ILD, the larger difference in loss heat between Walls 1 and 2 was 16.160 kWh with WWR = 0.15, Level A.

3.2.4 Model 3, Bioclimatic Zone 7

In Model 3, with maximum shape factor and 10 floors, ILD did not influence the results. In both analyzed ILDs (11 W/m^2 and 21 W/m^2), Level A model presented higher energy consumption and Level C model presented the best energy performance, with all WWRs analyzed. And this result was equal on both analyzed walls. This result can be explained by the same fact that occurred in Model 2, an overheating in Level A models, creating the need for cooling. As an example, in medium ILD, WWR = 0.15, Level A model presented energy consumption 43 kWh and 104 kWh higher than models Levels B and C, respectively, and 51 kWh and 123 kWh in high ILD for the same WWR. Bioclimatic Zone 7 presents elevated temperatures, this way, the Level A model, presenting more insulated roof that causes overheating inside the building, which can be observed since medium ILD as well. In high ILD, with the increase in internal heat, the overheating in Level A models becomes more noticeable, presenting higher difference in energy consumption when compared to other levels models (Levels B and C).

Regarding the energy efficiency of walls, it was possible to observe that Wall 1 (W1) presented higher energy consumption, lower only for models with medium ILD, WWR = 0.05, for all levels studied (Levels A, B and C). With increase in the frontage opening percentage, Wall 2 (W2) presents the best performance, as well as in models with high ILD. Wall 1 (W1), presenting lower thermal transmittance, exchanges less internal heat with the outside environment and with the increase in openings, which increase the radiation gains, Wall 1 (W1) needs higher energy consumption for cooling, when compared to Wall 2 (W2). With high ILD, which increases internal heat, Wall 2 (W2) presents higher thermal transmittance allowing for a larger exchange with the outside and, once again, presents a smaller need for cooling, thus presenting lower energy consumption than Wall 1 (W1).

3.2.5 Model 4

In Model 4, with maximum shape factor and one floor, with medium equipment ILD (11 W/m^2), the models with envelopes meeting the prerequisites for Level C presented the higher consumption level for Wall 1 (W1). This is due to the fact that the Level C model is losing less heat than models from other levels (Levels A and B), the difference being greater than 807 kWh with WWR 0.10 when compared to Level A. It was also possible to observe that the Level C model presents a higher heat loss through roof, although it loses less heat through walls when compared with the Levels A and B models. This way, the Level C model presented the highest energy consumption for heating and cooling due to presenting a higher thermal transmittance and allowing a larger heat exchange with the outside environment. Level A presented the lower consumption with WWR = 0.05, as for WWR = 0.10, Level B presented the lower consumption. This difference is due to the fact that with the increase in openings the models gain more heat through radiation, which brings an increase in energy consumption for cooling, while the Level A model, presenting more insulated roof, kept more internal heat, needing higher energy consumption when compared to Level B model.

With the increase in ILD (21 W/m^2), the results presented a small difference. Level B presented the lowest energy consumption with WWR = 0.05 and Level C did the same with WWR = 0.10. Level C presented the highest energy consumption with WWR = 0.05, and Level A did the same with WWR = 0.10. With WWR = 0.05, Level C presents higher energy consumption for heating and cooling, when compared to other levels (Levels A and B). This is due to the fact that the roof presents higher thermal transmittance. As for WWR = 0.10, with the increase in solar radiation gains, the level C model presents the lowest energy consumption for cooling, and Level A presents the highest, due to presenting more insulated roof, keeping internal heat. It should be noted that the differences between levels were small. Level A presented energy consumption of 16.554 kWh/year, Level B had 16.520 kWh/year and Level C 16.514 kWh/year.

Regarding the walls, it can be observed that they influenced the results. In Wall 2 (W2), the Level A models presented the highest energy consumption on both analyzed ILDs (11 W/m^2 and 21 W/m^2), and Level C presented the lowest energy consumption, with the sole exception of WWR = 0.05, medium ILD, in which Level B presented the best energy performance. It was possible to observe that, with WWR = 0.05, Wall 2 (W2), presenting a higher transmittance gained much more heat when compared with Wall 1 (W1), the difference being 2.889 kWh. This way, the Level A model of Wall 2 (W2) consumes more energy for cooling. In the models with Wall 2 (W2), Level A presents higher energy consumption, because Wall 2 (W2) has bigger thermal transmittance value than Wall 1 (W1). This way, heat enters into the building with Level A roof, and building with a higher insulation compared to other levels (Levels B and C), needs higher consumption for cooling. As for Wall 1 (W1), in which the transmittance is lower, the Level C model, because it presents higher transmittance in its roof, presents the higher energy consumption, needing cooling and heating for the edification. However, with high ILD and WWR = 0.10, Level A model presents the highest consumption. In this case, the internal heat gains added to the increase in gains through radiation increased the need for cooling, and Level A model, showing the more insulated roof, presented the worst performance. Since this model is a one floor only model, the roof has a higher influence over results than in the remaining models.

4. Conclusions

This paper has shown that buildings with high ILD and a higher thermal insulation envelope may obtain higher energy consumption. It was observed that for bioclimatic Zone 1, the building with walls and roof configured to meet the prerequisites for Level C (walls and roof thermal transmittance) presents lower consumption when compared with the envelope meeting Level A requirements.

It was also possible to observe that in both models with minimum shape factor and area larger than 500 m^2, the increase in ILD did not alter the results. It can be observed that even with medium ILD, the Level A model already presents overheating, creating higher energy consumption when compared to models from other levels (Levels B and C). As for the models with area smaller than 500 m^2, the increase in ILD did influence the results.

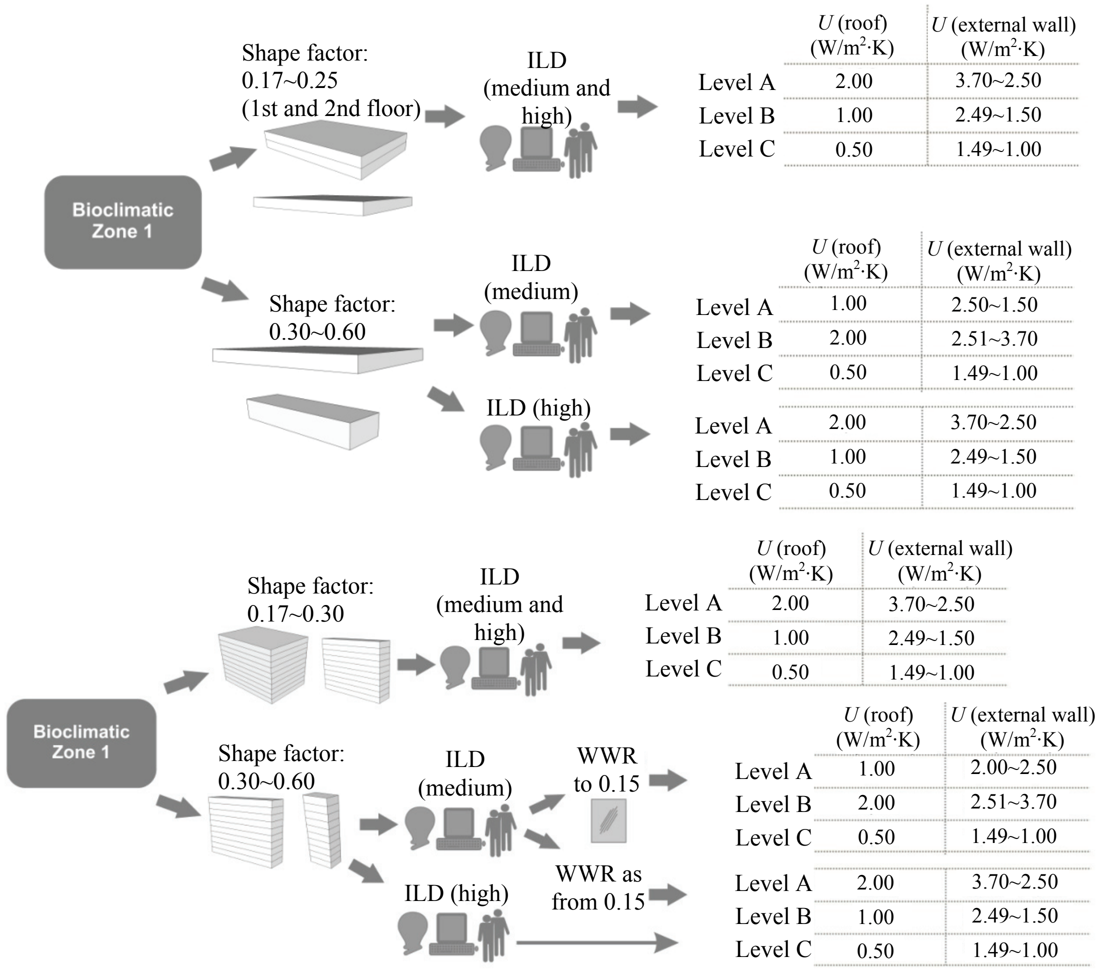

Fig. 6 Bioclimatic Zone 1 results.

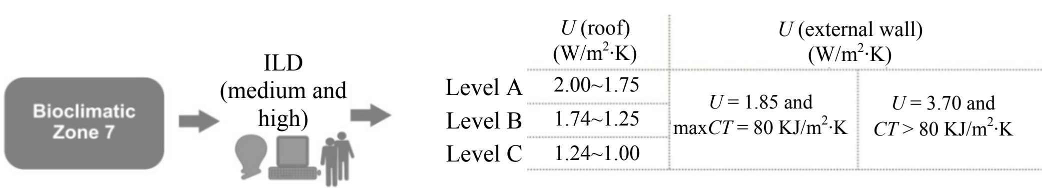

Fig. 7 Bioclimatic Zone 7 results.

In bioclimatic Zone 7, the ILD influenced two models only: the offices building and Model 2. Since, for bioclimatic Zone 7, the only factor considered is the roof insulation, the changes in ILD did not influence much. However, it was possible to observe that both models configured for Level A presented higher energy consumption, because they present overheating even in medium ILD, the same happening in bioclimatic Zone 1.

Regarding the employed walls, in bioclimatic Zone 7, it was possible to verify that Wall 2 (W2) (U = 3.7 W/m^2·K, CT > 80 KJ/m^2·K) presents better performance in high ILDs, since it needs less energy consumption for cooling, because it presents higher thermal transmittance and allows the internal heat to dissipate outside. As for Wall 1 (W1) (U = 2.50 W/m^2·K, CT is maximum about 80 KJ/m^2·K), it presents the best performance for medium ILD, WWR = 0.05 and in buildings of one or two floors. With WWR = 0.05, Wall 2 (W2) needs higher consumption for cooling when compared with Wall 1 (W1). As for Model 2, with minimal shape factor and two floors, Wall 1 (W1) presented the best performance since it needs less energy consumption for cooling.

The work done emphasizes the importance of the analysis of the internal load density variation observing other building variables, as it was shown in another presented researches. Pino et al. [10] developed a work where the results defined that for the Santiago do Chile climate with low cloudiness during the spring, and in the summer, it can happen overheating in office buildings. This phenomenon occurs in the most of the buildings with large WWR in facades and without solar protection [10]. In the realized work by Melo [4], the results showed that high buildings with high ILD (70 W/m^2) combined with lower solar absorptance of external surfaces the increase of the thermal transmittance of the walls results a decrease of the energy consumption observing the Brazilian cities of Florianópolis, Curitiba e São Luis [4].

According to the results obtained from different configurations, observing the specifics requirements of the RTQ-C, thermal transmittance values of walls and roofs were indicated, considering also different ILD and bioclimatic zones. These values are presented in Figs. 6 and 7. The work contribution is defined by the classification of the thermal transmittance for the different levels of energy efficiency considering WWR, ILD and shape factor.

References

[1] Official Gazette. 2001. *Law No. 10295 of 17 October 2001: About the National Policy for Conservation and Rational Use of Energy*. Brasilia: Official Gazette. (in Portuguese)

[2] Official Gazette. 2001. *Decree No. 4059 of 19 December 2001*. Brasilia: Official Gazette. (in Portuguese)

[3] Westphal, F. 2007. "Analysis of the Uncertainty and Sensitivity Applied to the Simulation of Energy Performance of Commercial Buildings." M.Sc. thesis, Postgraduate Program in Civil Engineering, Federal University of Santa Catarina, Florianopolis. (in Portuguese)

[4] Melo, A. P. 2007. "Analysis of the Influence of Thermal Transmittance Coefficient in Energy Consumption of Commercial Buildings." M.Sc. thesis, Postgraduate Program in Civil Engineering, Federal University of Santa Catarina, Florianopolis. (in Portuguese)

[5] Chvatal, K. 2007. "Relationship between Thermal Insulation Level of the Surroundings of Buildings and Potential Overheating in Summer." Ph.D. thesis, Engineering Sciences Department, University of Porto. (in Portuguese)

[6] Carlo, J. 2008. "Development of Energy Efficiency Assessment Methodology for Envelopes of Nonresidential Buildings." Ph.D. thesis, Graduate Program in Civil Engineering, Federal University of Santa Catarina, Florianópolis. (in Portuguese)

[7] ASHRAE (American Society of Heating, Refrigerating and Airconditioning Engineers). 2009. *ASHRAE Handbook—Fundamentals*. Atlanta: ASHRAE, 9-19.

[8] ABNT (Brazilian Association of Technical Standards). 2008. *NBR 16.401: Installation of Air Conditioning—Central and Unitary Systems. Part 3: Indoor Air Quality*. Rio de Janeiro: ABNT. (in Portuguese)

[9] INMETRO (National Institute of Metrology, Standardization and Industrial Quality). 2013. *Quality Technical Standards for Energy Efficiency Level in*

Commercial and Public Services Buildings. Brasília: Eletrobras. (in Portuguese)

[10] Pino, A.. Bustamante, W., Escobar, R., and Pino, F. 2012. "Thermal and Lighting Behavior of Office Buildings in Santiago of Chile." *Energy and Buildings, Elsevier* 47: 441-9. Accessed November 1, 2013. http://www.sciencedirect.com/science/article/pii/S0378778811006268.

Journal of Civil Engineering and Architecture 10 (2016) 37-43
doi: 10.17265/1934-7359/2016.01.004

DAVID PUBLISHING

Control of Pavement-Surface Temperature-Rise Using Recycled Materials

Satoru Ishiguro[1] and Masayoshi Yamanaka[2]

1. Graduate School of Bioresources, Mie University, Tsu 514-8507, Mie, Japan

2. Asahidoboku Co. Ltd., Yokkaichi 510 -0033, Mie, Japan

Abstract: High temperatures of the asphalt concrete pavements in summer contribute to the heat island phenomenon in the urban areas. The effective cool-pavement technologies are sought to mitigate the pavement environment. In this paper, developed heat-reflective pavements are constructed from open-graded asphalt concrete, in which voids in the upper part of the pavement are filled with a cement mortar, containing recycled materials as a fine aggregate. The recycled materials used in this study are: crushed oyster shells, roof tile debris, pottery debris, glass cullet, crushed escallops and coral sand. The temperature reduction of the pavement surfaces at an open site is measured in the summer. The results show that the maximum surface temperature of the pavements falls by approximately 8~10 °C compared to the asphalt concrete pavement. Furthermore, it is found that the temperature reduction is mainly due to the increased solar radiation reflectance of the pavement surface.

Key words: Heat-reflecting pavement, asphalt concrete pavement, filling mortar, oyster shell, recycled materials.

1. Introduction

Asphalt concrete pavements generally tend to absorb solar radiation heat because they are black, and the temperature can rise to a maximum of 60 °C or above at the surface in daylight in summer. This high temperature of the asphalt concrete pavement can cause rutting, asphalt aging, heat island phenomenon and fire accidents [1]. In particular, asphalt aging can reduce the ductility and increase the risk of cracking in the pavements [1]. Cracking can be crucial in the asphalt concrete pavements of the reinforced concrete bridge decks, in which it can accelerate the rebar corrosion process and reduce the durability and the service life of the structure [2].

In order to control the pavement surface temperature rise, cool-pavement technologies, such as solar heat-blocking pavement and water-retaining pavement, have been developed [3, 4]. In the former pavement, a reflective paint with a high reflection rate in a near-infrared wavelength band is used on the pavement surface. Cool pavements can also be created with existing paving techniques of asphalt and concrete, as well as new techniques, such as the use of coatings [5, 6]. Among the wide variety of existing materials, concrete is a suitable cool pavement material since it can create high reflective surfaces with the use of lighter cements and aggregates [7]. A high reflective concrete surface can be also achieved by using a cement replacement, such as ground granulated blast furnace slag which is a waste product from the steel industry [8, 9].

Nowadays, there is increasing interest in the utilization of waste materials. In the case of the construction industry, a growing trend exists towards the recycling of waste or by-products as supplementary construction materials [10, 11]. In the area of Mie Prefecture, Japan, for example, oyster farming constitutes a major fisheries activity and produces a large quantity of oyster shells. Some of the shells are pulverized in a factory after removing salt and later utilized as oyster shell lime. However, most oyster shells end up as industrial waste materials without being reused. Fig. 1 shows piles of oyster shells

Corresponding author: Satoru Ishiguro, professor, research field: concrete technology.

gathered at a factory site of Toba Kakigara Center, Toba City, Mie Prefecture, Japan. The factory produces 6,000 t of oyster shell lime, annually.

In a previous study, the authors reported that heat-reflecting pavements using oyster shell lime reduce surface temperatures by up to approximately 12 °C compared with new dense-graded asphalt pavements [12]. Crushed escallop and coral sand were also demonstrated to be useful as a fine aggregate for the filling mortar of heat-reflecting pavements [13]. In a recent study, it was found that mortars made by the oyster shell aggregate and ground granulated blast furnace slag could be effectively utilized as a filler mortar of the heat-reflecting pavement [14].

In this study, heat-reflecting pavements using recycled materials, such as crushed pottery debris, glass cullet and roof tile debris, have been investigated and compared with the pavement using oyster shells. All of the recycled materials were produced at factories located in Mie Prefecture. The reduction in the pavement-surface temperature-rise is evaluated by both field experiments and laboratory tests.

2. Experimental Program

2.1 Sample Preparation

A cross section of the pavement tested in this study is shown in Fig. 2. The heat-reflecting pavement is an open-graded asphalt concrete, in which voids in the upper part of the pavement are filled with a cement mortar, containing recycled materials. The pavements have 50-mm thickness and were placed on a 100-mm-thick crushed stone bed. A maximum aggregate size of 13 mm or 20 mm is used for the open-graded asphalt concrete pavement. The top 10 mm to 15 mm of the open graded asphalt pavement is filled with mortars by using a vibrator. The pavement surfaces treated by grinding after hardening of the filling mortar. Fig. 3 presents the grinded surface of the pavement filled with oyster shell mortar.

Fig. 4 shows the materials utilized as a fine aggregate for mortars. Different types of recycled materials are used for the filling mortar. Oyster shells, a waste product from oyster farming, are pulverized into a fine powder with a particle size of less than 2 mm to form the lime used as a fine aggregate for the filling mortar in this study. Other recycled materials, such as roof tile debris, pottery debris and glass cullet, are also pulverized as fine aggregates with a particle size of less than 3 mm. Natural river sand is employed as a control

Fig. 1 Oyster shell piles gathered at a factory site located in Toba City, Mie Prefecture.

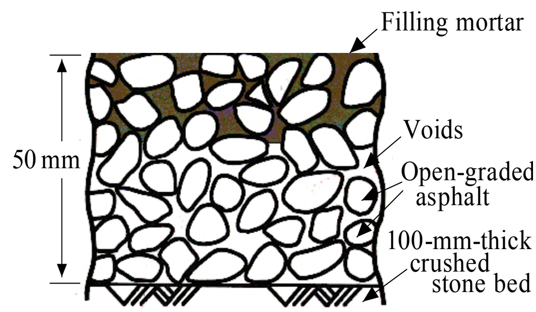

Fig. 2 Cross section of the pavement.

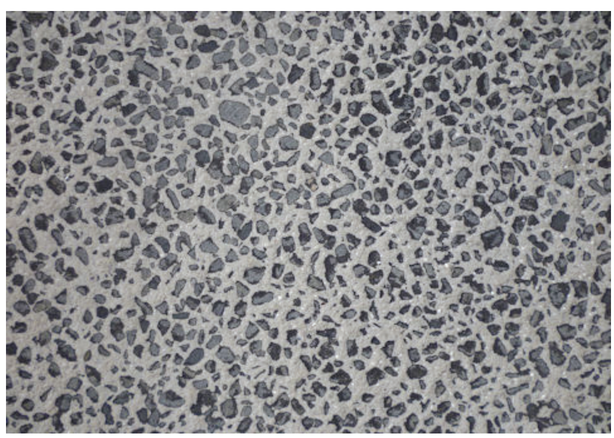

Fig. 3 Grinded Surface of the pavement filled with oyster shell mortar.

Fig. 4 Materials used as fine aggregate for mortar.

in this study. In the filling mortar mixture, ordinary Portland cement and the recycled materials are used as the binder and fine aggregate, respectively. Table 1 shows the properties of the filling mortars with different aggregates. The aggregate-to-cement ratio of 2:1 was used for mixtures. Different water-to-cement ratios (*W*/*C*) were used to make the filling mortar so that the mixtures had similar workability. Chemical admixtures, such as super plasticizers, were not used in the mixture design. The compressive strength of mortars was measured at the age of 7 days that the pavement surfaces were subjected to grinding treatments. The results showed that the mortars with oyster shell and escallop aggregates have high water-to-cement ratios (*W*/*C*) and the compressive strengths were lower than those of the other mortars.

2.2 Test Procedure

Fields experiments were performed to evaluate the surface heat reduction of asphalt concrete pavements in the summer. The pavements were constructed at the Mie University testing site located in Tsu City, Mie Prefecture, as shown in Figs. 5 and 6, to monitor the surface temperature in summer. In this experiment, Section A is the open-graded asphalt concrete pavement with a maximum aggregate size of 13 mm, and the other sections (Sections B-F, H and I) had maximum aggregate size of 20 mm. The dense-graded asphalt pavement (Section G), with a maximum aggregate size of 20 mm, was utilized as a control one. The oyster shell sections (Sections A and B), the escallop section (Section H), and the coral sand section (Section I) were filled with mortar in June 2011. These sections had an area of 1.5 m × 1.5 m. The heat-reflecting pavements (Sections C-F), made with a cement mortar, containing various recycled materials, were filled in June 2012. This section had an area of 0.75 m × 0.75 m. The temperature measurements were conducted in late July 2012, via thermocouples attached to the pavement surfaces; A data logger recorded the temperature at 1 min intervals. The air temperature and solar radiation intensity were monitored at the same time.

Brightness and color tests for the pavement surfaces were performed with a digital color reader (CR-13, Konica Minolta Optics Inc.) by the direction of the instrument manufacturer. The average values in different points on every pavement surface are calculated and evaluated using the parameters of an L^*, a^* and b^* color space [15].

Spectral reflectance was determined by a spectral reflectometer of UV-3100PC and MPC-3100 for the dense-graded asphalt and the hardened and dried mortars.

Table 1 Properties of mortar with different aggregates.

Aggregate type	Maximum particle size (mm)	*W*/*C* (%)	Aggregate cement ratio	7-day compressive strength (MPa)
Oyster shell	2	110	2:1	6.97
Roof tile debris	3	95	2:1	16.1
Pottery debris	3	83	2:1	17.0
Glass cullet	2.5	55	2:1	24.3
Escallop	2	110	2:1	9.39
Coral sand	2.5	58	2:1	27.1
River sand	5	50	2:1	32.9

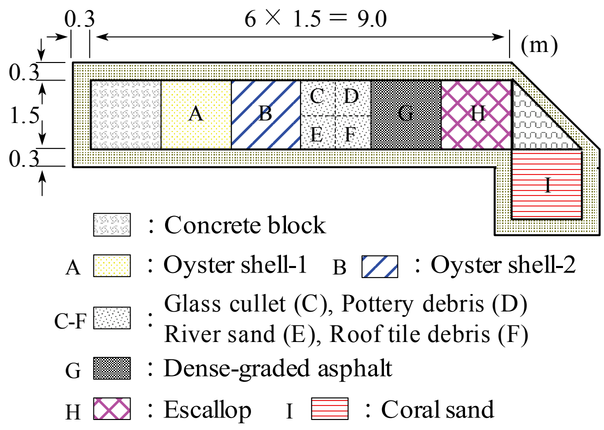

Fig. 5 Plan view of the pavement Sections A-I.

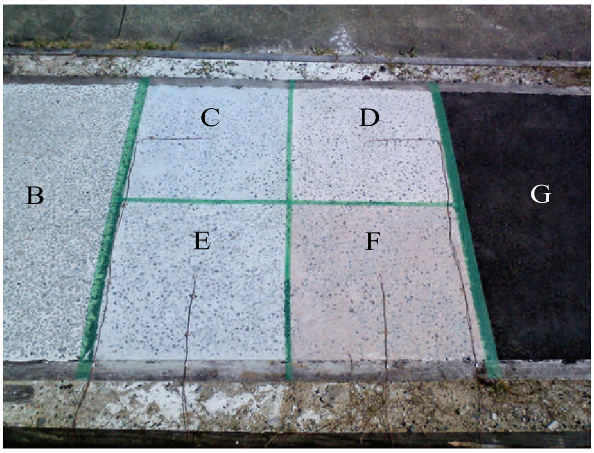

Fig. 6 View of the pavement Sections B-G.

The specimens were 30 mm × 30 mm × 20 mm in size. Wavelength for this test was 380~2,600 nm.

The skid resistances of the pavements were tested in accordance with ASTME303 (standard test method for measuring surface frictional properties using the British pendulum tester).

Wheel-tracking tests were performed under defined standards of Japan Road Association. The specimens with a maximum aggregate size of 20 mm, which was filled with the oyster shell mortar, were prepared and tested.

3. Results and Discussions

3.1 Surface Temperature

The surface temperature changes of pavements Sections B-G, air temperature and solar radiation are shown in Fig. 7. There was no rainfall during the measurement period.

The surface temperature of the black dense-graded asphalt reached a maximum of 63.1 °C on July 26, whereas the surface temperature of the heat-reflecting pavements did not exceed 54.3 °C. The heat-reflecting pavements were up to approximately 9 °C lower than that of the dense-graded pavement on a fine day. This temperature reduction is as a result of the higher solar reflectance due to the lighter colored mortar.

The maximum surface temperatures of the pavements in the three consecutive days from July 26 to July 28 are indicated in Fig. 8. The numerical values represent the average of the three consecutive days. The maximum measured daily temperatures of the heat-reflecting pavements fell by approximately 8~10 °C compared with that of the dense-graded asphalt. The pavement filled with the escallop mortar exhibited the lowest surface temperature. The maximum temperature of the pavement using the pottery debris was slightly lower than that using the other recycled materials. The variations in the temperature difference are partly due to variations in the

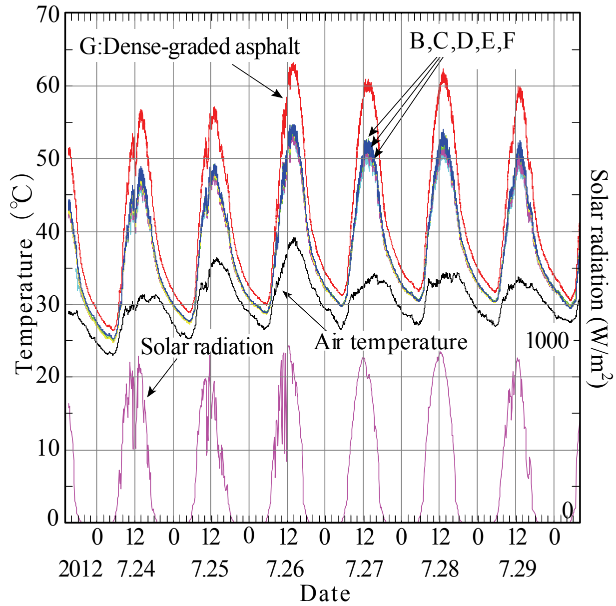

Fig. 7 Surface temperature changes on the pavements Sections B-G, air temperature and solar radiation of test period.

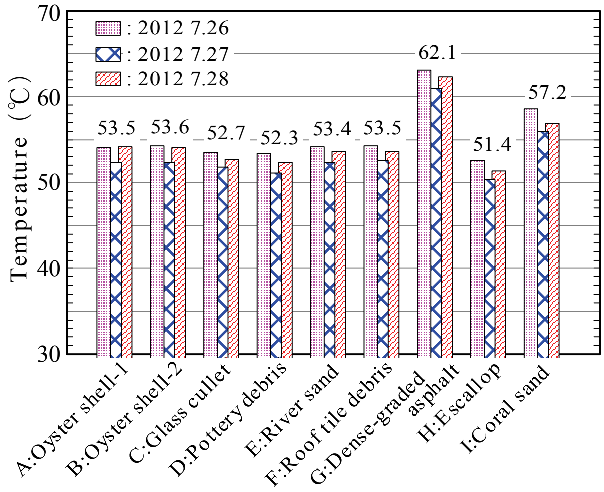

Fig. 8 Maximum surface temperatures of pavements.

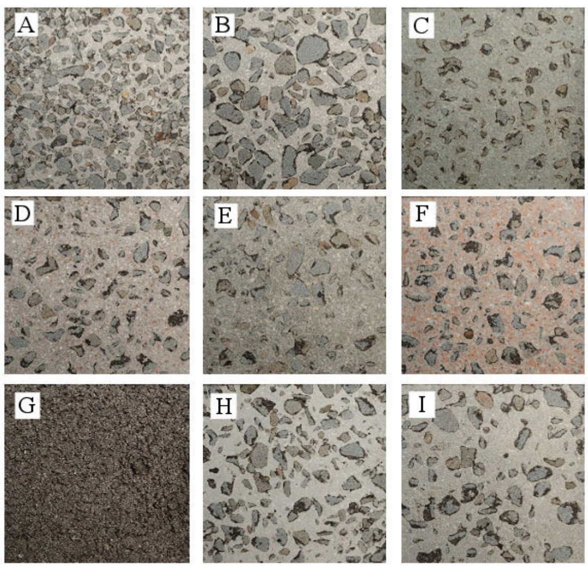

Fig. 9 Surface patterns and colors of pavements.

Table 2 Brightness and color values of pavement surface.

Pavement section		Brightness L^*	Color a^*	b^*
A	Oyster shell-1	61.7	0.5	4.3
B	Oyster shell-2	62.3	0.4	4.5
C	Glass cullet	58.8	-0.4	4.9
D	Pottery debris	63.8	2.1	5.3
E	River sand	60.8	0.1	5.4
F	Roof tile debris	60.6	4.8	7.7
G	Dense-graded asphalt	31.1	1.4	3.6
H	Escallop	68.1	0.2	3.7
I	Coral sand	61.1	0.4	5.3

surface colors of each pavement. It was found that the heat-reflecting pavement using natural river sand was effective in keeping the pavement cool in summer. The results of the field experiments reveal that the surface temperatures of the heat-reflecting pavements under summer sunlight irradiation decrease during the days and nights. Therefore, it can increase the durability of the pavement and reduce the urban heat island effect.

3.2 Brightness and Color

Fig. 9 shows the surface patterns and colors in the area of 15 cm × 15 cm on pavements Sections A-I. The average values of the brightness and colors in 20 different points on every pavement surface are listed in Table 2. Brightness value (L^*) is expressed in the range from 0 (black) to 100 (white). The a^* value presents from green ($-a^*$) to red ($+a^*$) and the b^* value from blue ($-b^*$) to yellow ($+b^*$). The results show that the brightness of the pavement surface filled with the pottery debris and escallop mortars are rather higher than the other heat-reflecting pavements, and the dense-graded asphalt has the lowest (L^*).

3.3 Spectral Reflectance

Fig. 10 presents the spectral reflectance of the dense-graded asphalt and the mortars with different aggregates. The spectral reflectance in the near-infrared region is 5~10% for the dense-graded asphalt. On the other hand, the spectral reflectance of mortars is significantly different from that of the dense-graded asphalt. The reflectance value of the

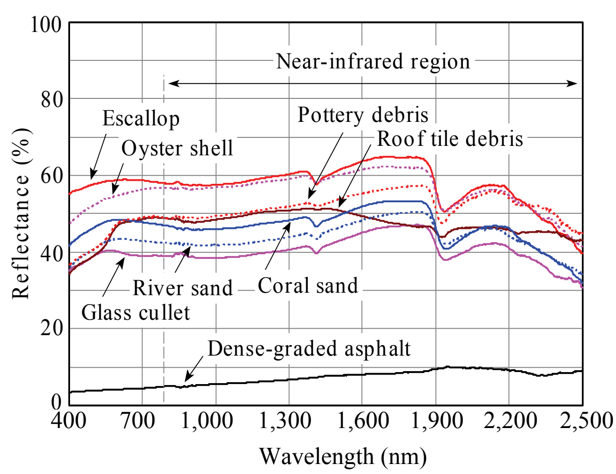

Fig. 10 Spectral reflectance of dense-graded asphalt and mortars with different aggregates.

Table 3 BPN (British pendulum number) of the pavements obtained by skid resistance test.

Section	A	B	C	D	E	F	G	H	I
BPN	80	79	77	77	80	73	88	74	80

(a)

(b)

Fig. 11 Pavements constructed by the top-filling of oyster shell mortar: (a) parking lot; (b) sidewalk.

mortar with escallop or oyster shell aggregate is relatively higher than the other mortars. The results confirm that the dense-graded asphalt is darker in color and has a lower reflectance compared with the cement mortars with recycled aggregate. The results also demonstrate that the top-filling of mortars can increase the spectral reflectance or solar reflection of pavement surfaces.

3.4 Skid Resistance

The results of a skid resistance test in a wet condition are summarized in Table 3. The test results show that the BPN (British pendulum number) values of the heat-reflecting pavements are higher than the value of 40 required for pedestrian roads [16].

3.5 Dynamic Stability

The average value of the dynamic stability was 21,000 times per millimeter under the test temperature of 60 °C. The durability of pavement against rutting was considerably improved by top-filling of the oyster shell mortar.

4. Case Study

Figs. 11a and 11b show the heat-reflecting pavements constructed by top-filling of the oyster shell mortar in a parking lot and a sidewalk, which are located in Yokkaichi City and Ise City, Mie Prefecture. These pavements have been constructed by a road-paving company under the supervision of authors. A maximum aggregate size of 13 mm and 20 mm are used for the open-graded asphalt concrete pavement. The surface pattern of the pavement in the parking lot with a maximum aggregate size of 13 mm is shown in Fig. 3. In constructing of the parking lot, in order to get the enough workability for the mortar, a super plasticizer was used in the mixture.

The temperature reduction of the pavement surfaces at the parking area was evaluated experimentally by taking measurements for a week in early August. The results revealed that the maximum surface temperature of the pavement fell by approximately 8~10 °C compared with that of an asphalt concrete pavement set up at a testing site.

Pavements made with top-filling of mortars may cost up to two times more due to the filling and grinding treatment. However, it offers several key advantages, including an improvement in durability and the creation of beautiful surface-patterns.

5. Conclusions

Heat-reflecting pavements using recycled materials have been developed, and the temperature reduction effect was evaluated by field experiments and laboratory tests. The results of this study are summarized as follows:

(1) The surface temperatures of the heat-reflecting pavements are approximately 8~10 °C lower than that of the dense-graded asphalt pavement. This is mainly due to the increase in the solar radiation reflectance;

(2) The heat-reflecting pavement filled with mortar containing crushed shell or pottery debris is lighter in color and has a higher solar reflectance compared with those of other recycled materials;

(3) Beautiful patterns were produced by grinding the pavement surface after hardening the filling mortar;

(4) The heat-reflecting pavements using recycled materials are environmentally friendly and contribute to promoting the effective use of waste products.

Acknowledgments

The authors wish to express their gratitude for the financial support of the Japan Society for the Promotion of Science.

References

[1] Chen, M. Z., Wei, W., and Wu, S. P. 2009. "On Cold Materials of Pavement and High-Temperature Performance of Asphalt Concrete." *Materials Science Forum* 620-622: 379-82.

[2] Sajedi, S., and Huang, Q. 2015. "Probabilistic Prediction Model for Average Bond Strength at Steel-Concrete Interface Considering Corrosion Effect." *Engineering Structures* 99 (15): 120-31.

[3] Japan Road Association. 2009. *The Guidebook about the Pavement Technology which Considered Environment.* Tokyo: Japan Road Association, 99-109. (in Japanese).

[4] Society of Road-Surface Temperature-Rise Control. 2015. "Solar Heat-Blocking Pavement." Society of Road-Surface Temperature-Rise Control. Accessed May 25, 2015. http://www.coolhosouken.com/. (in Japanese)

[5] United States Environmental Protection Agency. 2015. "Cool Pavements." United States Environmental Protection Agency. Accessed August 5, 2015. http://www.epa.gov/heatisld/mitigation/pavements.htm.

[6] Pomerantz, M., Akbari, H., Chen, A., Taha, H., and Rosenfeld, A. H. 1997. *Paving Materials for Heat Island Mitigation.* Lawrence Berkeley National Laboratory Report LBL-38074.

[7] Levinson, R., and Akbari, H. 2001. *Effects of Composition and Exposure on the Solar Reflectance of Portland Cement Concrete.* Lawrence Berkeley National Laboratory Report LBNL-48334.

[8] Marceau, M. L., and Vangeem, M. G. 2008. "Solar Reflectance Values for Concrete." In *Proceedings of Concrete International,* 52-8.

[9] Seymour, P., O'Flynn, D., and O'Connor, C. 2009. "GGBS and Reducing Global Warming—The Albedo Effect." *World Cement* 40 (12): 46-52.

[10] Sargin, S., Saltan, M., Morova, N., Serin, S., and Terzi, S. 2013. "Evaluation of Rice Husk Ash as Filler in Hot Mix Asphalt Concrete." *Construction and Building Materials* 48: 390-7.

[11] De Brito, J., and Saikia, N. 2013. *Recycled Aggregate in Concrete, Use of Industrial, Construction and Demolition Waste.* London: Springer.

[12] Ishiguro, S., and Yamanaka, M. 2010. "Research on Heat Reflection Pavement Using Cement Mortar Containing Crushed Oyster Shell." In *Proceedings of the Japan Concrete Institute,* 1367-72. (in Japanese)

[13] Ishiguro, S., and Yamanaka, M. 2012. "Heat Control of Asphalt Concrete Pavement Using Filling Mortar." In *Proceedings of the Japan Concrete Institute,* 1384-9. (in Japanese)

[14] Islam, M. R., Ishiguro, S., and Yamanaka, M. 2015. "Surface Heat Reduction of Asphalt Concrete by Top Filling with Mortar Prepared by Oyster Shell Aggregate and Ground Granulated Blast Furnace Slag and Their Strength in Different Curing Condition." *IDRE Journal* 296: 1-7.

[15] Konica Minolta Measuring Instruments. 2015. "Color Spaces." Konica Minolta Measuring Instruments. Accessed March 5, 2015. http://sensing.konicaminolta.asia/learning-center/color-measurement/color-spaces/.

[16] Japan Road Association. 1996. *Manual for Asphalt Pavement.* Tokyo: Japan Road Association, 172-3. (in Japanese)

Journal of Civil Engineering and Architecture 10 (2016) 44-52
doi: 10.17265/1934-7359/2016.01.005

Numerical Analysis of the Influence of Geometry of Ceramic Units (Blocks) on Structural Walls

Gihad Mohamad[1], Eduardo Rizzatti[1], Humberto Roman[2], Gerson M. S. Alva[3] and André Lubeck[4]

1. Structural and Building Construction Department, Federal University of Santa Maria, Santa Maria 97105-900, Brazil

2. Building Construction Department, Federal University of Santa Catarina, Santa Maria 97105-900, Brazil

3. Civil Engineering College, Federal University of Uberlandia, Uberlândia 38414-172, Brazil

4. Civil Engineering College, Federal University of Pampa, Alegrete 97546-550, RS, Brazil

Abstract: This paper presents finite element results of ceramic masonry prisms and walls under concentric compression. Four different hole geometries of ceramic units were studied (called Types A, B, C and D). The A-type unit had two rectangular hollows, B-type and C-type units have two rounded hollows and different net areas, and the D-type unit had two rectangular hollows and a double central web. This study analyzed units, prisms and structural walls joined by bedding mortar. The objective was to verify the stress distribution in units and mortars. The results showed that the distribution of compressive stress along the length and width of those units was uniform, but lateral tensile stress along the length was distinct for different geometries. In addition, this study observed that hollow shapes have an important influence in stress distribution. The D-type unit was the one that showed more uniform tension distribution, without peaks of stress concentration. This indicates that a D-type unit is the most efficient unit for use in masonry structures.

Key words: Ceramic units, structural masonry, geometry.

1. Introduction

Nowadays, one of the most disseminated construction techniques in Brazil is structural masonry. Because of its simplicity of execution, availability in different regions of the country and low cost, it has received great relevance in the construction environment. Thus, the interaction between research centers and companies that produce units (blocks) has grown in the last decades, resulting in the development of different types of units and mortars.

The knowledge of the influence of unit geometry on the phenomena that results in masonry failure or how geometry influences internal stress and strain distribution is important for a complete understanding of this technique and for a safe and economic design.

On the other hand, numerical analysis is a fast and low-cost way to evaluate the behavior of structures, and there is some accessible software adapted to masonry analysis.

In this context, the numerical study of the influence of unit's geometry on masonry resistance can contribute to improve this technique.

2. Masonry Strength

Refs. [1-5] pointed out some aspects with great influence on masonry strength.

2.1 Block Strength

Compressive strength of units is one of the most important aspects in masonry strength. However, increasing masonry strength is not linearly proportional to increasing unit strength.

2.2 Unit Geometry

In Brazilian practice hollows blocks are used without infill. So, the presence of hollows can result in stress concentration during load application. Fig. 1

Corresponding author: Gihad Mohamad, Dr., research fields: masonry structures and structural analysis.

shows the different geometries of blocks proposed in the Brazilian standard NBR 15270-2 [6].

Studies by Ganesan and Ramamurthy [7] evaluated the influence of different unit geometries and mortar properties over concrete masonry using the finite elements method. Stack bond prisms with three units high were simulated using a heterogeneous elastic-linear model.

Three different unit geometries were tested: (1) units with three hollows; (2) units with two hollows and standard dimensions; (3) units with two hollows and a double center. Different mortar properties were simulated using four different elasticity modulus ratios (E_b/E_m): 1.0, 1.5, 2.0 and 2.8, with a constant E_b. The elasticity modulus ratio is important to analyze the influence of mortar on the failure mode and strength of masonry. The ratio between net and gross areas was kept constant.

Even being constant, the relation between net and gross area were higher in units with three hollows. When compared to units with two hollows, the ones with a simple central web showed higher stress levels than the ones with double central web units. Therefore, unit's geometry influences the level and distribution of stress in masonry and masonry efficiency varies by changing geometry and type of layer.

Ganesan and Ramamurthy [7] commented about studies conducted in the Building Technology Laboratory in India, where three different unit geometries were tested. So, a face shell bedding was used for the block Type A, and a full mortar bedding was used for the others two types of units. The studied types of units, strengths and efficiency ratio are shown in Fig. 2.

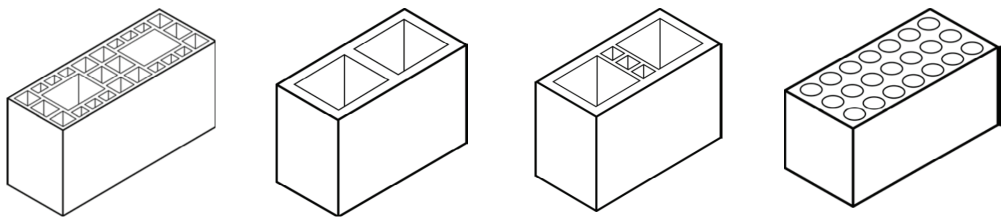

Fig. 1 Ceramic blocks—defined by NBR 15270-2 [6].

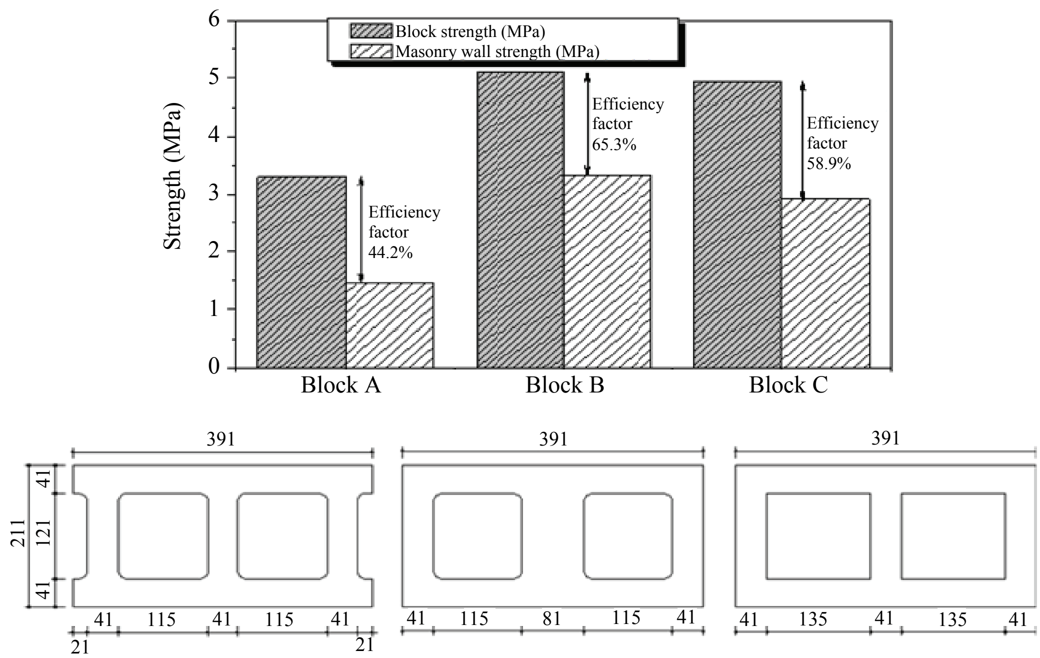

Fig. 2 Geometric shape of concrete units tested at Building Technology Laboratory (units in mm) [7].

The researchers also pointed out the relevance of studying unit geometry to achieve a high efficiency of structural walls.

3. Materials and Components of Masonry

The main component used when manufacturing ceramic units is red clay. It contains silica, aluminum silicate and ferrous oxides. These components with an average grain size of 0.005 mm result in a plastic material when moist, although it becomes stiff when dry. Another important feature of moist clay is cohesion, to keep the mold's shape before and during the drying process.

During the manufacturing process, clay is dosed (formulated) to correct any faults or to amplify a specific feature, such as unit's compressive strength or fire resistance. In Brazil, the compressive strength of the available units varies from 3 MPa (low strength) to 100 MPa (high strength).

Brazilian standards [6, 8, 9] require control of the physical properties of units used in structural masonry. The NBR 15270-2 [6] limits the acceptance of units to the control of dimensions, square, flatness and water absorption. The limits for these properties are shown in Table 1.

The same standards also limit the minimum dimensions of walls used in structural masonry. For hollow wall units, the central web must have a minimum thickness of 7 mm and side webs of at least 8 mm. The minimum web thickness of solid web ceramic units must be 20 mm, and the central web may present hollows, as its total thickness is greater than or equal to 30 mm, with 8 mm as the minimum thickness of any cross web. Fig. 3 shows the minimum web dimensions for ceramic units.

4. Analytical Program

The analytical program aims to evaluate the influence of the geometry of red clay ceramic units on the compressive strength of masonry prisms with three units high. Four different geometries were tested, named A, B, C and D. These four different geometries are shown in Fig. 4.

Fig. 5 shows the dimensions of each one of these unit geometries. The A-type unit is a two-rectangular hollow. B-type and C-type have two circular hollows. The difference between them is their net area, which is larger for Unit B. The D-type has two rectangular

Table 1 Dimensional tolerances for ceramic units—NBR 15270-2 [6].

Dimension	Dimensional tolerances relative to individual measurements (mm)	Dimensional tolerances relative to the average (mm)
Width (*W*)	±5	±3
Height (*H*)	±5	±3
Length (*L*)	±5	±3
Deviation relative to square (*D*)	3	
Flatness of faces or deflection (*F*)	3	
Water absorption (*wa*)	8% ≤ *wa* ≤ 22%	

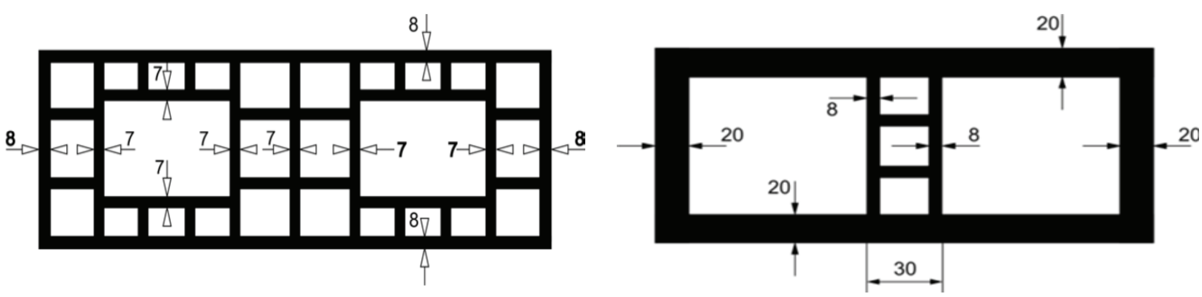

Fig. 3 Dimensions in mm of face shells and ceramic unit's webs—NBR 15270-2 [6].

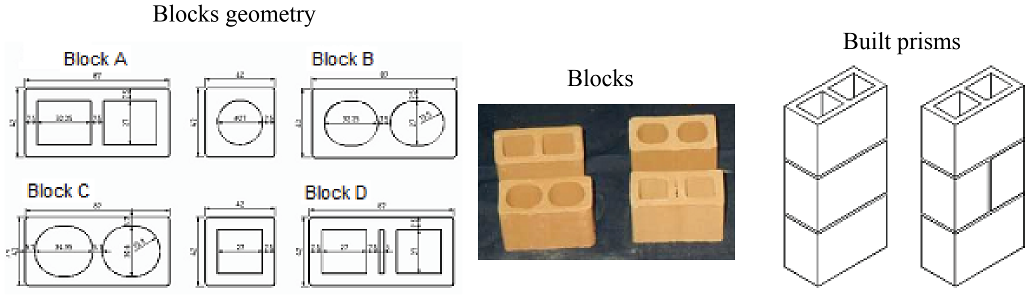

Fig. 4 Geometrical shapes of ceramic units and three units high prisms.

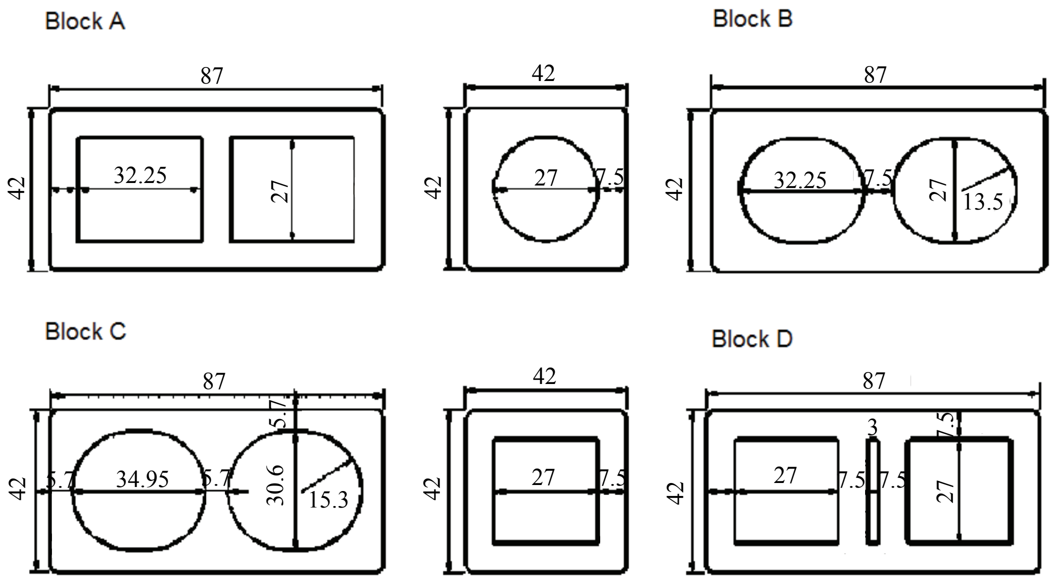

Fig. 5 Geometry types of the tested units (units in mm).

hollows but its cross web has a double thickness.

More information about the analytical program and analysis results can be seen in Ref. [10].

5. Numerical Analysis

The numerical analysis was performed using a computer program CASTEM 2000. This is an analysis software based on finite element method. This simulation used solid elements with eight nodes. These elements fit well because of the regular shape of units, prisms and walls.

The units, prisms and walls were discretized into meshes, as shown in Fig. 6. For B-type and C-type units with circular hollows, meshes of tetrahedral elements with six nodes in transition zones were used.

A linear elastic isotropic model was adopted for numerical simulation of units and mortar. A preliminary analysis using elastic modulus and Poisson's ratio of materials (unit and mortar) was performed to obtain a stress-strain behavior. After that, the prisms were simulated, considering the same load condition and axial concentric compression, corresponding to mean values previously obtained on preliminary computation results and varying only the elastic modulus of the unit. A mortar with a constant modulus of elasticity of 6 GPa was used. Values for elastic modulus and Poisson's ratios of all materials simulated are shown in Table 2. The displacements along Directions X and Y (transversal), on prism's upper and lower surface, were restricted to simulate real test confinement conditions caused by friction between the press plate and the prism. On the lower

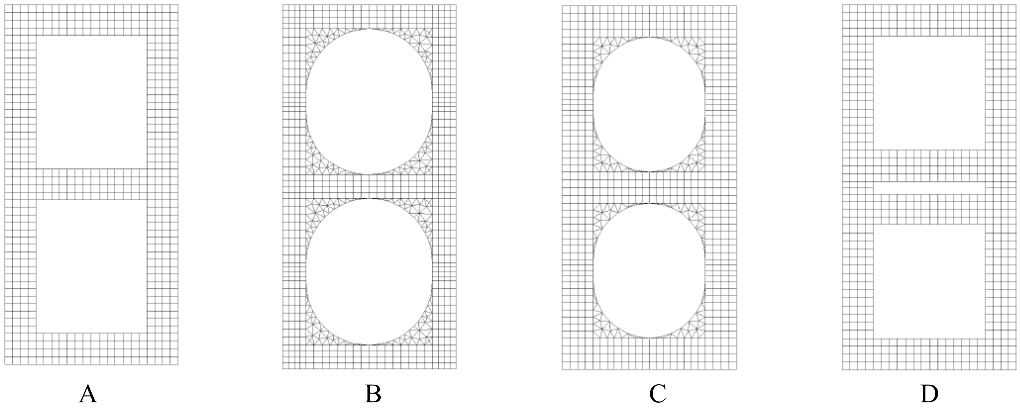

Fig. 6 Mesh used in numerical simulations of different units and walls with mortar joint.

Table 2 Young's modulus and Poisson's ratio of units and the mortar.

Item	Unit	Mortar
Young's modulus (MPa)	28,000	6,000
Poisson's ratio	0.07	0.20

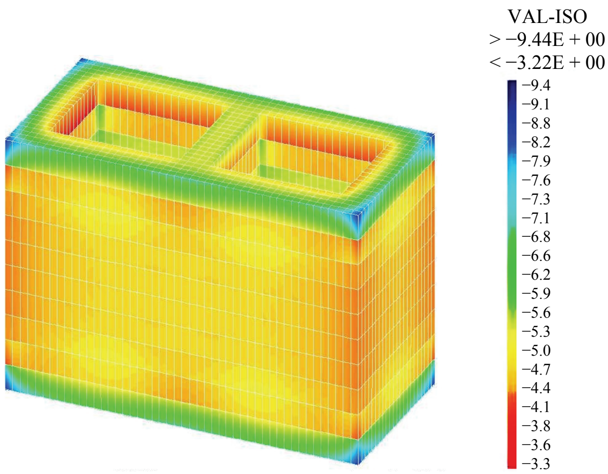

Fig. 7 Distribution of main stress on a unit (A-type).

surface, the displacements along Direction Z (axial direction) were also restricted. The load was applied by imposition of increments of compression axial force.

Fig. 7 shows the main stress distribution along the length and width of the unit obtained in the linear elastic isotropic numerical model. Figs. 8 and 9 show the tensile and compressive stress along Lines 1 and 2, which represent unit's length and width, respectively.

Fig. 8 shows that the distribution of stress compression is uniform along unit's length (Line 1) and width (Line 2). There is a little variation from lateral surfaces (Region "a") to the unit's center (Region "c").

It is perceptible in Fig. 9 that distribution of tensile stress along the length (Line 1) varies with unit's geometry. Small levels of compressive stress were observed next to the central web of the D-type unit. B-type and C-type units have developed low levels of compression stress in Region "c" of Fig. 9. A concentration of tensile stress was observed in Region

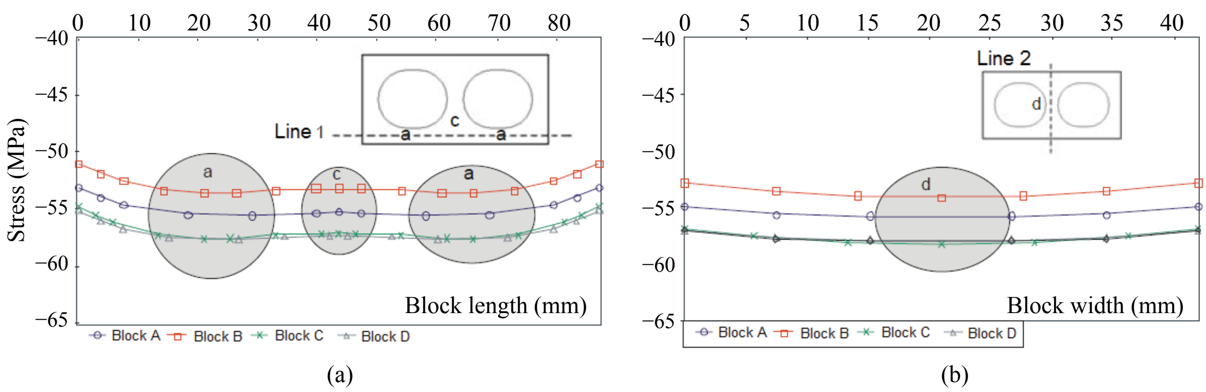

Fig. 8 Distribution of compressive stress on a unit along its length and width: (a) Line 1; (b) Line 2.

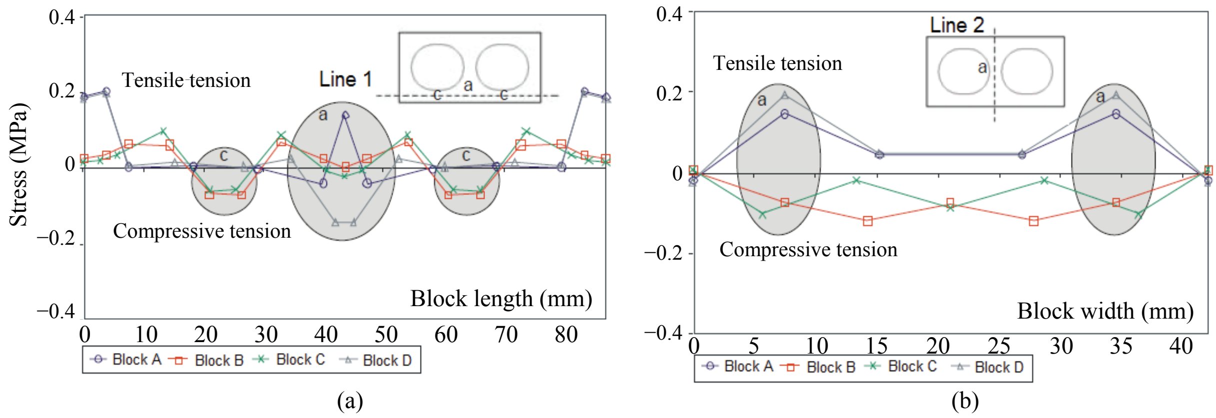

Fig. 9 Distribution of tensile stress along the length and width: (a) Line 1; (b) Line 2.

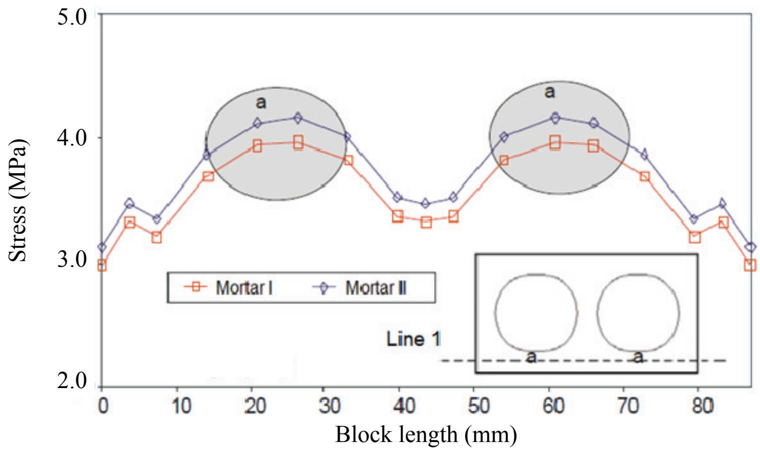

Fig. 10 Distribution of compressive stress in a prism for different mortars.

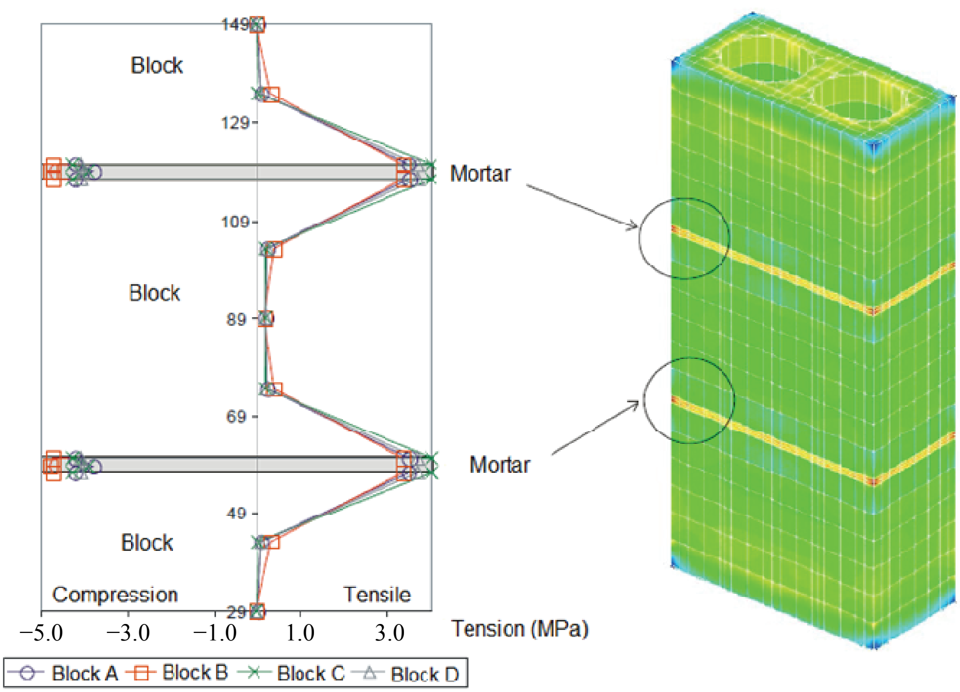

Fig. 11 Distribution of tensile and compressive stress along the prism's height.

"a" of A-type units. When stress distribution is analyzed along Line 2 (width), geometry Types B and C had a different behavior from Types A and D, as shown in Region "a" of Fig. 9. For Types B and C, the stress in Region "a" was compression, and it was tension for Types A and D. The distribution of tensile stress in Region "a" along Line 2 of A-type and D-type units was uniform.

To evaluate the influence of mortar's elastic modulus over the level of main stress compression developed at prism's mortar joints, a simulation changing the values of mortar's elastic modulus was conducted. Two values of mortar's elastic modulus were tested, 4.5 GPa and 6 GPa. A small variation of stress distribution was observed between these two values of elastic modulus. The highest value was in the middle of the core's face shell, highlighted in Region "a" of Fig. 10.

By comparing stress distribution in the unit and in the mortar, compressive stress was induced to the mortar and tensile stress to the unit. Fig. 11 presents the maximum main stress in prisms along a vertical line beginning at the center of the lower unit and ending at the center of the upper unit. These numerical results showed that lateral confinement stress level in the mortar was approximately 4.5 MPa. This indicates that mortar works under tri-axial compression and unit works under biaxial tension-compression, as shown in Fig. 11.

On walls, stress under compression load in the two central layers was analyzed for each unit's type. Fig. 12 shows stress distribution for the C-type unit. Figs. 13 and 14 show stress results along the length (Line 1) and width (Line 2) for geometry Types A, B,

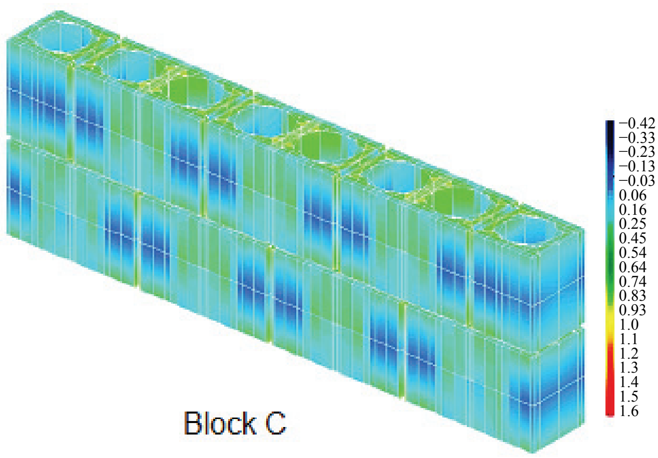

Fig. 12 Distribution of tensile and compressive stress on the intermediary layers of masonry.

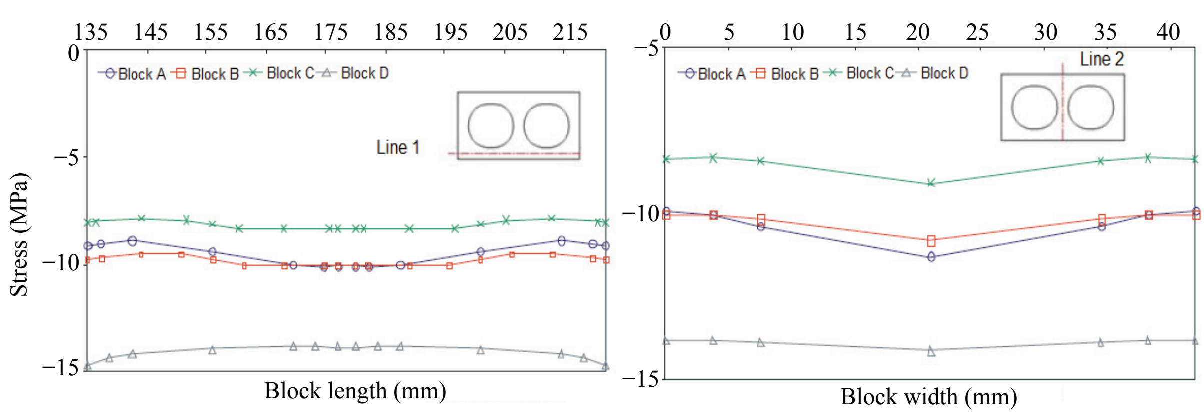

(a) (b)

Fig. 13 Distribution of compressive stress on the intermediary wall's layer: (a) Line 1; (b) Line 2.

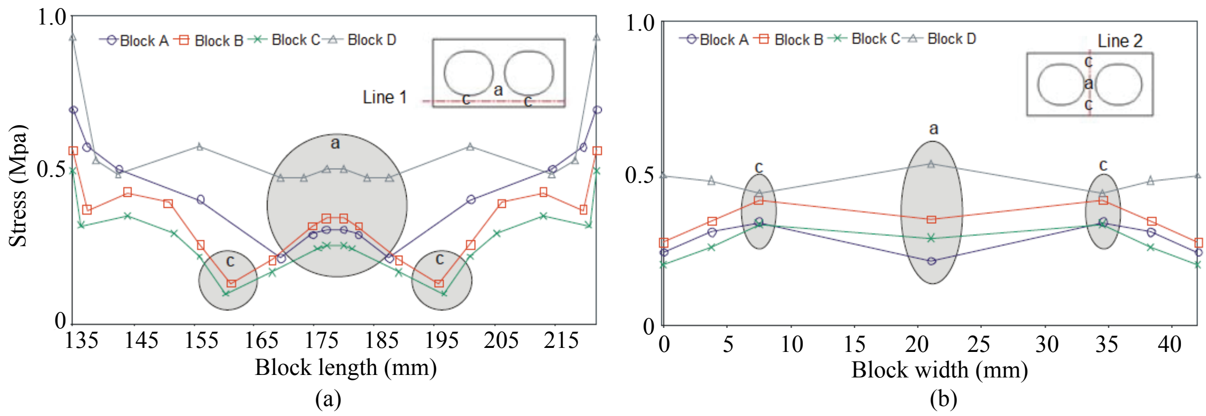

Fig. 14 Distribution of tensile stress on the intermediary wall's layer: (a) Line 1; (b) Line 2.

C and D.

In wall's analysis, the stress distribution in eight mortars' interfaces was evaluated. The stress distribution along the width and length of different unit's geometries are shown in Figs. 13 and 14. Dashed lines over a unit represent points of stress evaluation, changing between compressive and tensile behavior along the block length, as indicated by Lines 1 and 2 in Figs. 13 and 14.

Evaluating compressive stress distribution on walls resulted in no significant variations along Lines 1 and 2. In addition, the distribution of tensile stress has a significant difference along unit's length and width, depending on its geometric shape. D-type units induced a more uniform distribution of tensile stress in central region (Region "a"), probably based on the presence of a double central web that provides an alignment of unit's lateral faces. In Region "c", Types B and C along Line 1 showed the lowest tensile stress level, due to the rounded shape of their hollows, reducing the amount of stress. By analyzing stress along the cross-web direction (Line 2), it is perceptible that, in the middle of cross-webs, units have a different behavior relative to geometry, as shown in Region "a" and not in Region "c".

6. Conclusions

This numerical analysis of ceramic unit masonry under compression supports these conclusions:

- The difference in stiffness between units and mortar results in an inversion of stress distribution in prisms. Units were under biaxial tension-compression and mortar was under tri-axial compression;
- No significant variation was found in the compressive stress distribution on walls;
- By analyzing the tensile stress distribution on the wall, a significant difference in stress levels along the unit's length and width was observed, depending on its geometrical shape;
- A more uniform tensile stress distribution in the unit's central region (Region "a") was observed in D-type units, probably related to the presence of a double central web that provides an alignment of unit's lateral faces;
- B-type and C-type units, along Line 1 and in the region called "c", showed the lowest tensile stress level. The rounded-shape hollows in the encounter between face shells and cross-webs were effective to reduce stress magnitude.

References

[1] Atkinson, R. H., Noland, J. L., and Abrams, D. P. 1985. "A Deformation Failure Theory for Stack-Bond Brick Masonry Prism in Compression." In *Proceedings of 7th International Brick Masonry Conference*, 577-92.

[2] Hamid, A. A., and Drysdale, R. G. 1976. "Behavior of Concrete Block Masonry under Axial Compression." *American Concrete Institute Journal* 76 (6): 707-21.

[3] Hegemeir, G. A., Krishnamoorthy, G., Numm, R. O., and Moorthy, T. V. 1978. "Prism Tests for the Compressive Strength of Concrete Masonry." In *Proceedings of North American Masonry Conference,*

181-7.

[4] Hilsdorf, H. K. 1969. *Investigation into the Failure Mechanism of Brick Masonry Loaded in Axial Compression.* Houston: Gulf Publishing Company.

[5] Khoo, C. L. 1972. "A Failure Criterion for Brickwork in Axial Compression." Ph.D. thesis, University of Edinburgh, Scotland.

[6] Brazilian Standard. 2005. *Blockwork Clay Masonry Blocks. NBR 15270-2.* Rio de Janeiro: Brazilian Standard.

[7] Ganesan, T. P., and Ramamurthy, K. 1992. "Behavior of Concrete Hollow-Block Masonry Prisms under Axial Compression." *Journal of Structural Engineering* 118: 1751-69.

[8] Brazilian Standard. 1985. *Masonry Structures—Method of Test. NBR 8949.* Rio de Janeiro: Brazilian Standard.

[9] Brazilian Standard. 1995. *Mortar—Compressive Strength. NBR 13279.* Rio de Janeiro: Brazilian Standard.

[10] Rizzatti, E. 2003. "Block Geometry Influence on the Mechanical Strength on Masonry Structures." Ph.D. thesis, UFSC (Federal University of Santa Catarina), Florianópolis. (in Portuguese)

Journal of Civil Engineering and Architecture 10 (2016) 53-63
doi: 10.17265/1934-7359/2016.01.006

Behavior of Reinforced Concrete Columns under Combined Axial Load and Bending in Accordance with a Nonlinear Numerical Model

Carlos Eduardo Luna de Melo[1] and Guilherme Sales Soares de Azevedo Melo[2]

1. Department of Technology, Faculty of Architecture and Urbanism, University of Brasília , Brasília 70910-900, Brazil

2. Department of Civil Engineering and Environmental, Faculty of Technology, University of Brasília , Brasília 70910-900, Brazil

Abstract: A nonlinear numerical model was developed to analyze reinforced concrete columns under combined axial load and bending up to failure. Results of reinforced concrete columns under eccentric compression tested to failure are presented and compared to results from a numerical nonlinear model. The tests involved 10 columns with cross-section of 250 mm × 120 mm, geometrical reinforcement ratio of 1.57% and concrete with compression strength around 40 MPa, with 3,000 mm in length. The main variable was the load eccentricity in the direction of the smaller dimension of cross-section. Experimental results of ultimate load and of the evolution of transverse displacements and concrete strains are compared with the numerical results. The estimated results obtained by the numerical model are close to the experimental ones, being suitable for use in verification of elements under combined axial load and bending.

Key words: Columns, reinforced concrete, combined axial load and bending, numerical analysis.

1. Introduction

Reinforced concrete columns are important structural elements, which, in a standard structure of building, have main function of supporting horizontal and vertical loads, transmitting these loads to foundations.

With the advent of the computers and high performance concretes, concrete structures became slenderer, with better use of concrete and reinforcement strength. Among the consequences of that technological advance, there is great likeliness to reach a limit state of instability of the columns.

The complexity of study of reinforced concrete elements under axial load and bending is due to its nonlinear behavior. The physical nonlinearity due to reinforced concrete and reinforcement constitutive nonlinear equations, the geometrical nonlinearity due to iteration between internal forces and displacements due to load, lead to simplified or iterative solutions.

Knowing the behavior of columns under combined axial load and bending during loads steps until failure is very important, mainly in slender columns, where the second order effects are significant. Experimental studies are difficult to be done, and it is necessary to resort a cross section reduction of the column in order to avoid costs with frame tests and equipment, and consequently becoming a medium proportion test.

Having a numerical model to analyze reinforced concrete columns under combined axial load and bending is important to predict, to analyze test results and to design columns.

A nonlinear numerical model was developed based on work presented by Nagato [1], which considers compression field theory given by Vecchio and Collins [2]. The developed numerical model, called “FLECO2C”, considers physical and geometrical nonlinearities.

Corresponding author: Carlos Eduardo Luna de Melo, Ph.D., professor, research fields: structural engineering, numerical and experimental tests, reinforced and prestressed concrete structures.

2. Experimental Program

Ten reinforced concrete columns with 250 mm × 120 mm in cross section (area of cross section A_c equals to 300 cm^2) and concrete compression strength around 40 MPa with 3,000 mm in length were tested.

The longitudinal reinforcement consisted of six 10-mm diameter bars (where A_s is the area of six bars). The longitudinal steel ratio ρ_s is equal to 1.57 and the slenderness λ is equal to 90.9. The transversal reinforcement consisted of 5-mm diameter rectangle stirrups, with 5 mm of diameter and 100 mm of spacing. Near to column ends the stirrups were 50 mm spaced. All these data were based on Refs. [3-6].

Geometry details of columns ends were used to measure rotations of columns ends and provide application of the eccentric load.

The main variable of tests was load eccentricity. Fig. 1 shows the columns sizes used in present work in mm.

The columns were identified by the following notation: *PFN e-L*, where, *PFN* = column under axial load and bending, *e* = load eccentricity in direction of less dimension of cross section (mm) and *L* = column length (m). Table 1 shows a summary of characteristics of columns. Further details about test data can be found in Refs. [3, 4, 7].

Each longitudinal bar and concrete compressed

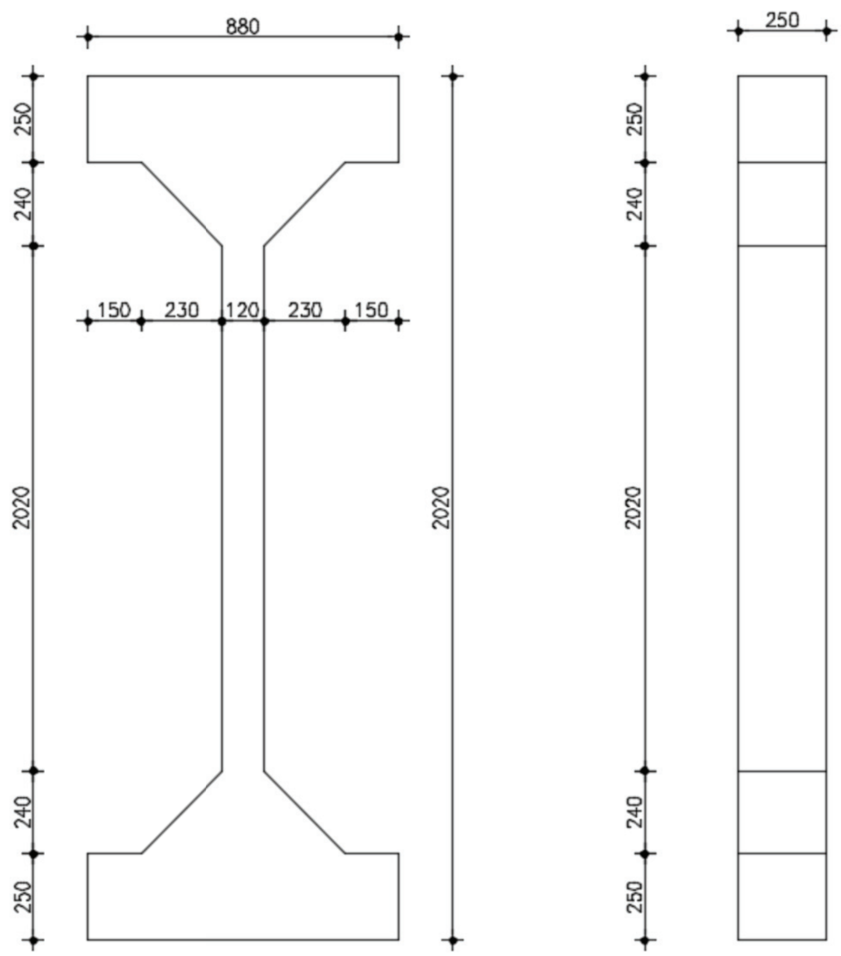

Front view

Side view

Fig. 1 Geometry details of concrete columns (units in mm).

Table 1 Data for tested columns.

Column	e (mm)	λ^*	L (mm)	A_c (cm^2)	A_s (cm^2)	ρ_s (%)
PFN 0-3	0					
PFN 6-3	6					
PFN 12-3	12					
PFN 15-3	15					
PFN 18-3	18	90.9	3,000	300	4.71	1.57
PFN 24-3	24					
PFN 30-3	30					
PFN 40-3	40					
PFN 50-3	50					
PFN 60-3	60					

*Considered 3,140 mm between pins.

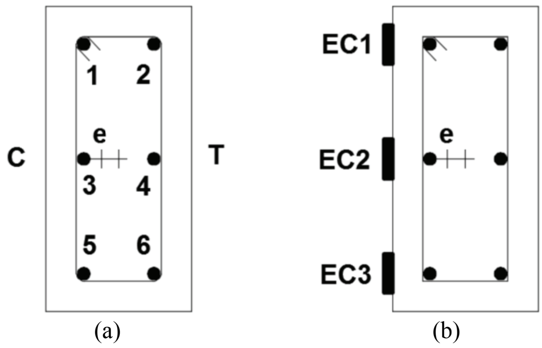

Fig. 2 Placement of strain gauges on: (a) reinforcement; (b) concrete surface.

surface were monitored at mid-height using strain gauges. The compressed surface is called C-face and the least compressed surface (or tensioned face) is called T-face. Fig. 2 shows the placement of strain gauges on reinforcement and concrete surface at middle height.

The columns were tested using a steel reaction frame, where the load was applied using a jack until column failure and measured using a load cell. The load eccentricity was applied moving the center of the plates from each column axe. Fig. 3 shows the test setup used with positioning of load cell, jack, rollers, column and electric deflections gauges (D1 to D7).

3. Materials Tests

Concrete compression strength was obtained by compression test, and tensile strength was obtained from the indirect tensile test (Brazilian test). The elastic modulus was obtained by tests of specimens, and in some cases, recommendations by Ref. [8] were used. Reinforcement strength was obtained by pull-out test. The concrete cylinder strength varied from 33.9 MPa to 39.7 MPa. Table 2 shows experimental results of concrete and steel.

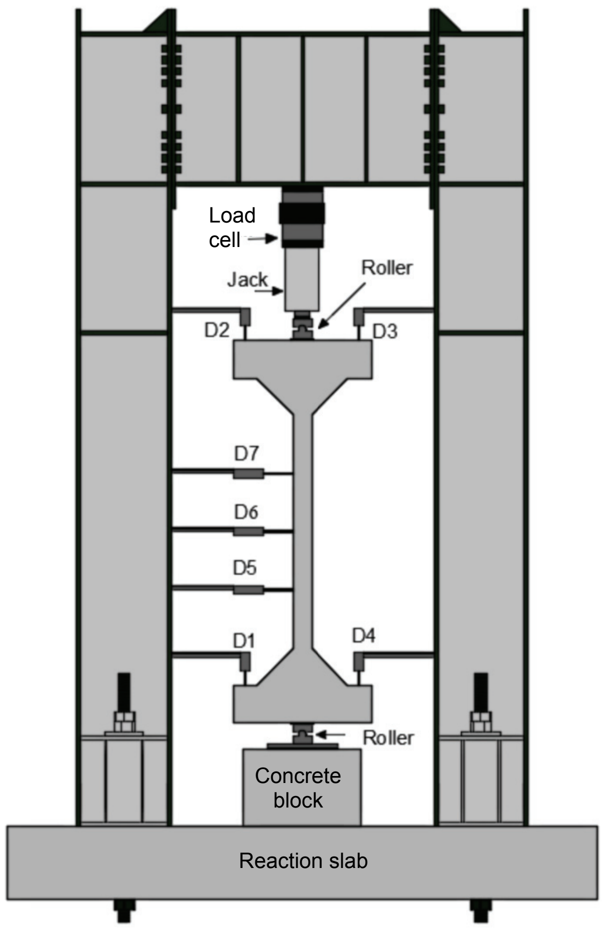

Fig. 3 Test setup for reinforced concrete columns under compression.

Table 2 Experimental results of concrete and steel.

Column	f_c (MPa)	f_{ct} (MPa)	E_c (GPa)	f_y^* (MPa)	f_u^* (MPa)	E_s^* (GPa)
PFN 0-3	35.8	3.1	28.7			
PFN 6-3	39.6	2.5	32.1			
PFN 12-3	39.6	2.5	32.1			
PFN 15-3	35.8	3.1	28.7			
PFN 18-3	39.7	2.4	30.6	595	705	190
PFN 24-3	39.7	2.4	30.6			
PFN 30-3	33.9	3.3	31.5			
PFN 40-3	33.9	3.3	31.5			
PFN 50-3	37.6	3.1	31.1			
PFN 60-3	37.6	3.1	31.1			

*tests results of same lot of material;
f_c is the highest compressed concrete stress;
f_{ct} is the highest tensile concrete stress;
f_y is the tensile yield steel strength;
f_u is the ultimate tensile steel strength;
E_s is the steel modulus of elasticity;
E_c is the concrete modulus of elasticity.

4. Numerical Model

In order to simulate the columns behavior subjected to combine axial load and bending, a computing program was used, which was developed using Fortran compiler. The numerical model, called FLECO2C, simulates the same tests conditions, applying load in steps until failure. FLECO2C is divided in two parts: a nonlinear physical model, which considers the physical nonlinearities of concrete and reinforcement, and a nonlinear geometric model, which uses the results obtained on nonlinear physical model to calculate the horizontal displacements.

4.1 Consideration of Physical Nonlinearity

The consideration of physical nonlinearity of numerical model was presented by Nagato and Regis [9] and the program was called CACODI. The CACODI program was made using Fortran 77 compiler and the aim was the study of shear resistance of reinforced concrete elements under axial load and bending with different longitudinal reinforcement ratios.

The model is based on compression field theory by Vecchio and Collins [2], which developed a computing program that applies the theory called SMAL (shear and moment under axial load).

For the compressed concrete behavior, the stress-strain law proposed by Carreira and Chu [10] was adopted:

$$\sigma_c = \frac{f_c \beta \left(\varepsilon_c / \varepsilon_0\right)}{\beta - \left(\varepsilon_c / \varepsilon_0\right)^{\beta}} \qquad (1)$$

$$\beta = \frac{1}{1 - \dfrac{f_c}{E_c \varepsilon_0}} \qquad (2)$$

where, σ_c is the compressed concrete stress; f_c is the highest compressed concrete stress; β is the material parameter; ε_c is the compressed concrete strain; ε_0 is the strain corresponding to the highest compressed concrete strain; E_0 is the initial elasticity modulus of concrete.

The variable *CT* (concrete type) was used in main program to choose the concrete behavior with descendent line or without descendent line (Fig. 4). This law is valid to $\varepsilon_u \leq \varepsilon_c \leq 0$ to concrete with descendent line ($CT = 1$), or $\varepsilon_0 \leq \varepsilon_c \leq 0$ to concrete without descendent line ($CT = 2$), which $\sigma_c = f_c$, $\varepsilon_u \leq \varepsilon_c \leq 0$ (Fig. 4). All analyses were done using concrete with descendent line ($CT = 1$), and the concrete without descendent line was disposed for design purposes.

For the tensioned concrete behavior, a similar law used by Maia [11] was adopted, but the tension strength of concrete used was defined by Vecchio and Collins [2] (Fig. 5):

$$\sigma_{ct} = E_0\varepsilon_t \text{ for } \varepsilon_t \leq \varepsilon_{cr} \tag{3}$$

$$\sigma_{ct} = f_{cr}\left(\frac{\varepsilon_{ut}-\varepsilon_t}{\varepsilon_{ut}-\varepsilon_{cr}}\right)^2 \text{ for } \varepsilon_{cr} < \varepsilon_t \leq \varepsilon_{ut} \tag{4}$$

$$\sigma_{ct} = 0 \text{ for } \varepsilon_t \geq \varepsilon_{ut} \tag{5}$$

$$f_{cr} = 0.33\sqrt{f_c} \quad \text{(MPa)} \tag{6}$$

$$\varepsilon_{cr} = f_{cr}/E_0 \tag{7}$$

where, σ_{ct} is the tensile concrete stress; f_{cr} is the cracking tensile concrete stress; ε is the tensile concrete strain; ε_{ut} is the highest tensile concrete strain; ε_{cr} is the strain corresponding to the highest tensile concrete strain; E_0 is the initial elasticity modulus of concrete.

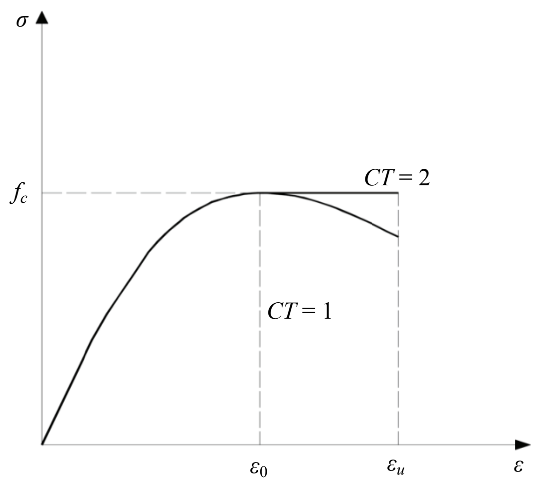

Fig. 4 Stress-strain diagram of compressed concrete.

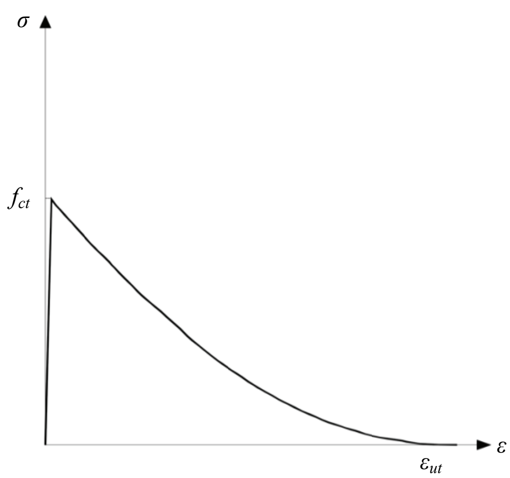

Fig. 5 Stress-strain diagram of tensile concrete.

The highest tensile concrete strain $\varepsilon_{ut} = 5 \times 10^{-3}$ on CACODI program was adopted because it leads to adjust results with experimental results presented by Vecchio [12].

A bilinear behavior was adopted to longitudinal steel bars (Fig. 6), assuming that stress-strain diagram is valid to compression and tension.

The reinforcement stress was obtained by:

$$\sigma_s = E_s\varepsilon_s \text{ when } \varepsilon_y < \varepsilon_s < \varepsilon_y \tag{8}$$

$$\sigma_s = \pm f_y \text{ when } \varepsilon_y \geq \varepsilon_s \geq \varepsilon_y \tag{9}$$

where, σ_s is the steel stress; E_s is the steel modulus of elasticity; ε_s is the steel strain; f_y is the tensile yield steel strength; ε_y is the is the yield tensile steel strain and ε_{su} is the highest tensile steel strain.

4.2 Calculation Process

The rectangular cross section, given by b and h, was discretized in "m" concrete layers and "n" reinforced layers, where each concrete layer has width b_i, height h_i and position in relation to the highest cross section compressed fiber (y_{ci}), and each reinforced layer has the area of longitudinal steel (A_{slj}) and position in relation to the highest cross section compressed fiber (y_{slj}) (Fig. 7).

After changing the neutral axis deep and curvature, it was possible to determine in each concrete layer strain (ε_{cli}), stress (σ_{cli}), concrete load (F_{cli}), transversal loads

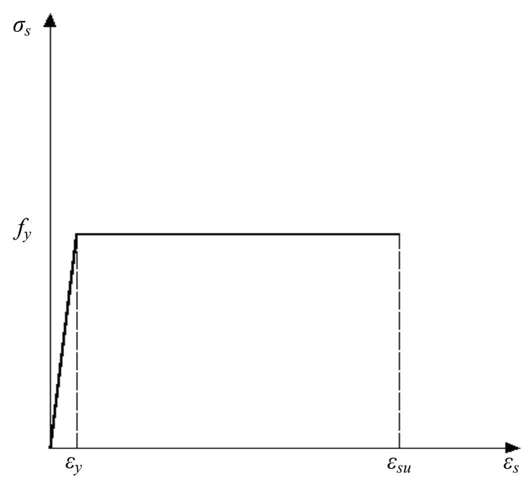

Fig. 6 Stress-strain diagram of longitudinal bars (CA-50).

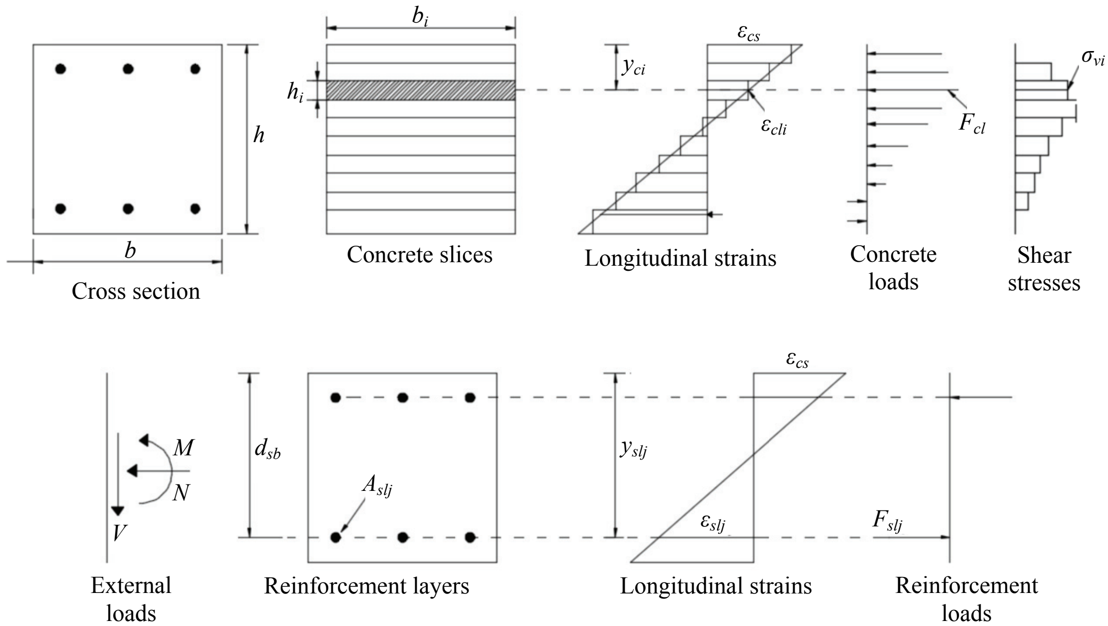

Fig. 7 Cross section discretization.

(σ_{vi}) and in each reinforced layer strain (ε_{slj}), stress (σ_{slj}) and reinforced load (F_{slj}).

The following hypotheses were considered on CACODI program:

- Bernoulli hypothesis that means the plane sections remain plane until failure;
- equilibrium condition that means the internal forces balance external forces.

Given these hypotheses, it is possible to reach the cross section equilibrium by the following equations:

$$N = \sum_{i=1}^{m} \sigma_{cli} b_i h_i + \sum_{j=1}^{n} \sigma_{slj} A_{slj} \quad (10)$$

$$M = \sum_{i=1}^{m} \sigma_{cli} b_i h_i (y_{ci} - h) + \sum_{j=1}^{n} \sigma_{sli} A_{sli} (y_{sj} - h) \quad (11)$$

$$V = \sum_{i=1}^{m} \tau_{vi} b_i h_i \quad (12)$$

where, N is the axial force, M is the bending moment and V is the shear force.

The first summation of Eq. (10) determines the internal concrete resultant (*RC*) and the second one determines the internal reinforcement resultant (*RS*). In Eq. (11), the first and the second summations determine the internal bending moment related to internal concrete resultant (*MC*) and related to internal reinforcement resultant (*MS*), respectively. In Eq. (12), the summation determines the internal concrete resultant by the compression field theory.

The curvature of the cross section is determined by neutral axis variation until equilibrium of internal forces is satisfied. The calculus is processed by iteration.

It is important to emphasize that it is possible to ignore the shear load in the program, and in this work, the shear load was ignored.

4.3 Consideration of Geometric Nonlinearity

The CACODI program analyses an isolated cross section under axial load, shear load and bending, and it does not apply directly to second order effects, which occur in columns under axial load and bending, yet these results can be used to do that analysis.

In order to determine the second order effects in a column under axial load and bending, a subroutine, called SECORDER, was developed, using the moment-area theorem.

Half of the column was divided in cross sections (s), and in each load step the main program analyses each cross section (s) subjected to axial load (N) and bending (M), given by the following Eq. (13):

$$M_s = N \cdot (e + \delta_{(i-1,\, s)}) \tag{13}$$

where, e is the initial eccentricity, $\delta_{(i-1,\, s)}$ is the column horizontal displacement of section (s) determined on the previous iteration ($i - 1$).

The main program determines the curvature for each section (*PHI*) and the SECORDER subroutine converts these curvatures into displacements, using the moment-area theorem (Fig. 8). The new displacements are used to calculate the new bending moments, which are introduced in the main program again until they reach an established tolerance given by the user.

5. Comparison of Test Data with Numerical Model Results

On this topic, the results obtained on tests are compared with FLECO2C estimates. Initially, concrete strain and horizontal displacements at mid-height of columns are presented, during load steps until failure and finally the ultimate loads of columns.

5.1 Concrete Strains

Concrete average strains at a more compressed surface located at mid-height of columns during the load steps until failure are presented and compared with numerical program results (Fig. 9).

It can be noticed that the concrete strains predicted by the numerical model presents close results of concrete strains for nearly all cases. The seen-far behaviors were given by *PFN* 12-3, *PFN* 18-3 and *PFN* 24-3 columns, probably due to high geometric imperfections or due to incorrect load eccentricity.

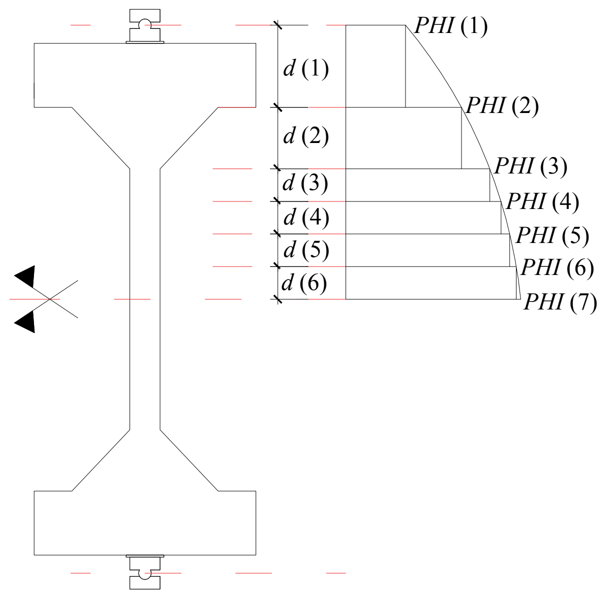

Fig. 8 Column discretization.

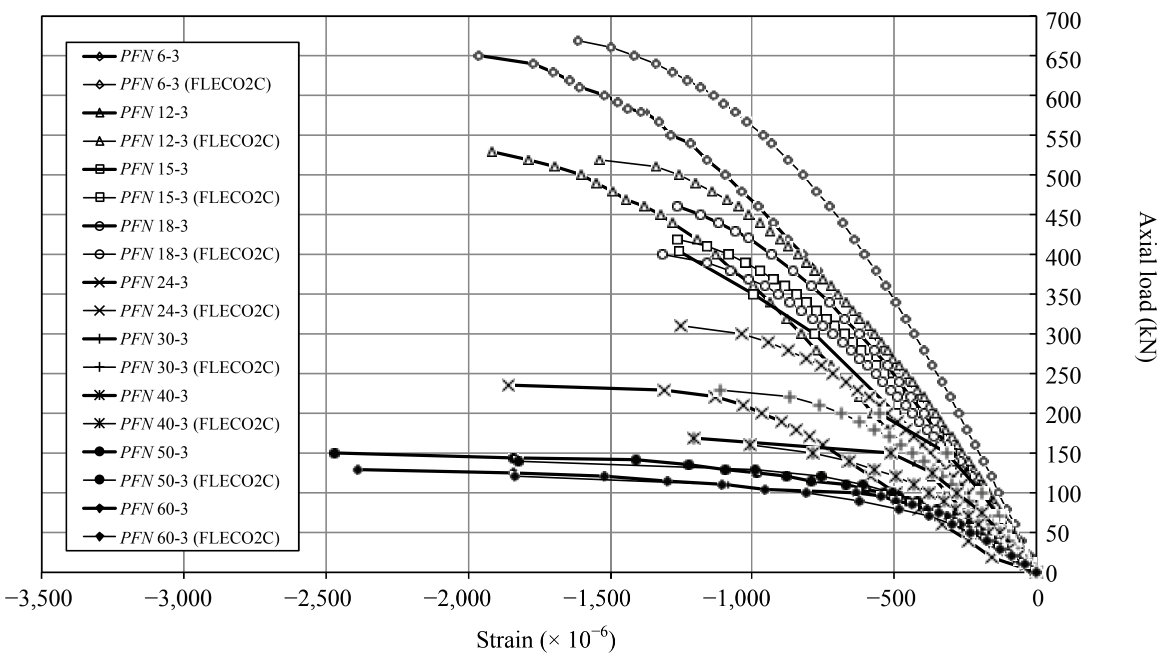

Fig. 9 Concrete strains at mid-height.

5.2 Horizontal Displacements

Horizontal displacements at mid-height of columns during the load steps until failure are presented and compared with numerical model results (Fig. 10).

It can be seen that the horizontal displacements predicted by the numerical model presents close results of horizontal displacements for almost all cases. Column *PFN* 24-3 presented far results, probably due to high geometric imperfections or due to incorrect load eccentricity. It was necessary to retest *PFN* 24-3 column to validate the results.

5.3 Ultimate Loads

With FLECO2C, it was possible to estimate the ultimate load of each column. The horizontal displacements were incremented in each load step until the column failure.

The ultimate load was determined when it was not possible to balance the external load with the cross section internal load. Table 3 shows a comparison between numerical loads and ultimate loads with statistic results, and Fig. 11 shows F_u/F_{num} plotted against relative eccentricity e/h.

As shown in Table 3 and Fig. 11, the ultimate loads predicted by the numerical model presents close results for nearly all cases, except for *PFN* 18-3, *PFN* 24-3 and *PFN* 30-3.

6. Analysis of Numerical Results

On this topic, an analysis is presented between results obtained on a numerical model and obtained on tests. The whole analysis was done using applied load eccentricity, considered at cross section center of gravity, and geometric imperfections were not considered.

An accurate concrete strain estimate and horizontal displacements on *PFN* 6-3 column results can be seen in Figs. 9 and 10, when compared with FLECO2C results. The displacement curve estimated by FLECO2C presented an adequate approximation when compared with test results, presenting greater stiffness and ultimate load 4% greater than the test result. Probably, the real eccentricity of column was greater than the one used on the numerical model.

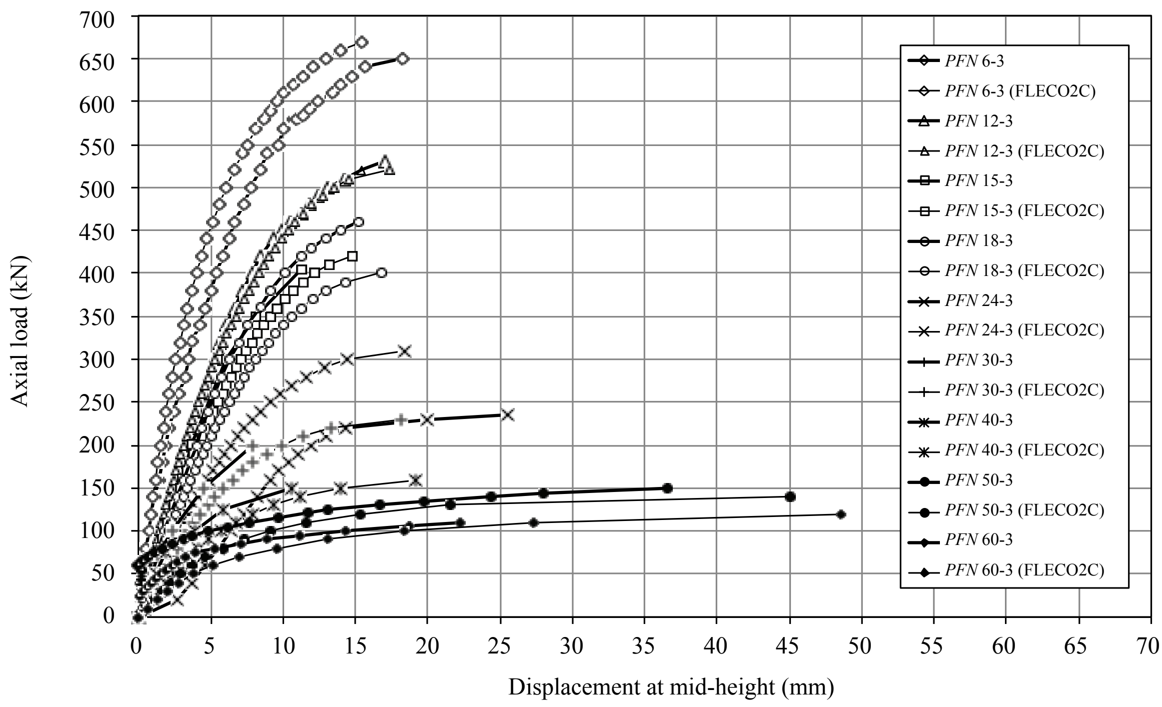

Fig. 10 Horizontal displacements at mid-height.

Table 3 Ultimate loads versus numerical loads.

Column	F_u (kN)	F_{num} (kN)	F_u/F_{num}	Mean	Standard deviation	Coefficient of variation (%)
PFN 0-3	1,053.0	980.0	1.07	1.01	0.10	10.2
PFN 6-3	652.0	680.0	0.96			
PFN 12-3	535.0	530.0	1.01			
PFN 15-3	446.5	430.0	1.04			
PFN 18-3	460.5	410.0	1.12			
PFN 24-3	241.0	320.0	0.75			
PFN 30-3	254.8	230.0	1.11			
PFN 40-3	170.2	170.0	1.00			
PFN 50-3	155.0	150.0	1.03			
PFN 60-3	131.0	130.0	1.01			

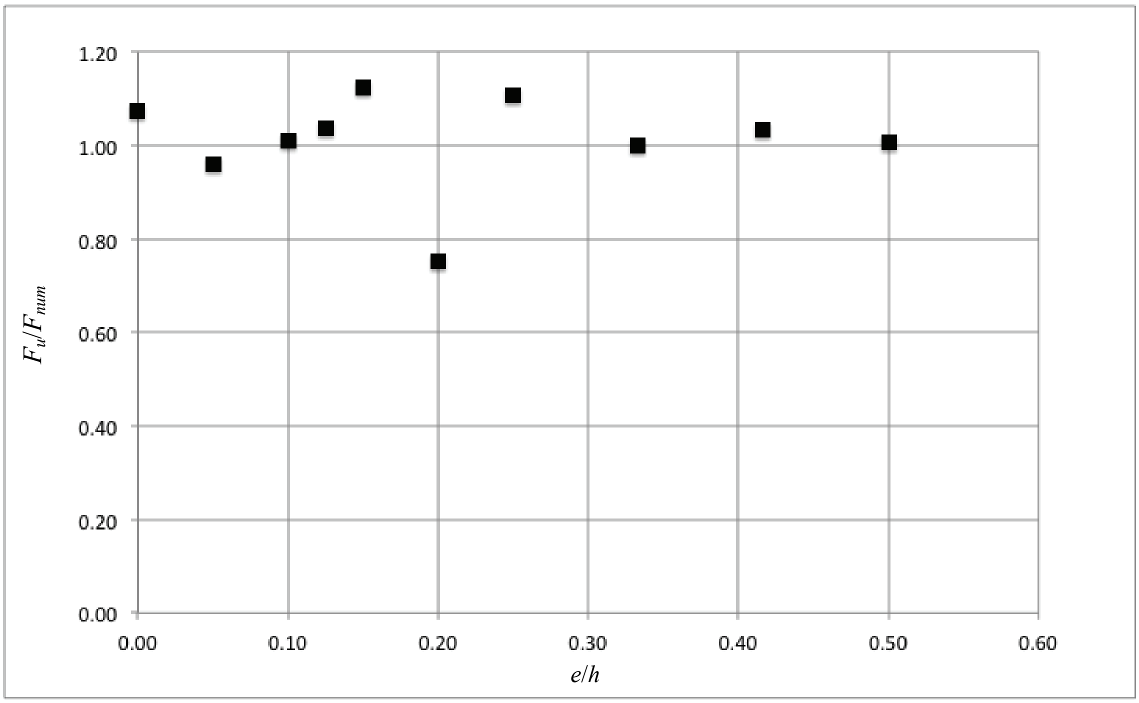

Fig. 11 F_u/F_{num} plotted against relative eccentricity e/h.

It is possible to see a fragile behavior of columns with eccentricity less or equal to 18 mm, given by *PFN* 6-3, *PFN* 12-3, *PFN* 15-3 and *PFN* 18-3. All the others presented an asymptotic tendency of curve and were more frequently verified in columns with high eccentricity, on *PFN* 50-3 and *PFN* 60-3, as expected and obtained on numerical results.

The *PFN* 12-3 column presented a close behavior of horizontal displacements and ultimate load prediction, as can be seen in Fig. 10 and Table 3, respectively. The concrete strain obtained on the numerical model presented far results from the test of *PFN* 12-3 column, probably due to problems on strain gauges, as can be seen in Fig. 9.

The *PFN* 15-3 column presented adequate predicted results of concrete strain and horizontal behavior, in comparison with test results, as can be seen in Figs. 9 and 10. Better results could be given reducing the load step on test.

Figs. 9 and 10 point out far results of horizontal displacements and concrete strains on *PFN* 18-3 and *PFN* 24-3 column compared to FLECO2C results. The displacement curve estimated by FLECO2C presented lower stiffness on *PFN* 18-3 results and higher stiffness on *PFN* 24-3 results. Results of ultimate loads given by the numerical model presented 12% less than *PFN* 18-3 ultimate load and 15% greater than *PFN* 24-3 ultimate load. Probably, the real eccentricity of column was different than the one used on the numerical model or geometric imperfections affected those results. It is necessary to retest PFN 24-3 column to best validate the results.

Numerical results from *PFN* 30-3, *PFN* 40-3, *PFN* 50-3 and *PFN* 60-3 presented close concrete strain results and horizontal displacements when compared with test results, as can be seen in Figs. 9 and 10, evidencing a preponderance of bending moments on columns and presenting an asymptotic curve with tendency of instability of columns. Ultimate loads were very close with numerical loads predictions, except for *PFN* 30-3 that presented ultimate load, given by the numerical model, 11% less than the test result.

7. Conclusions

The aim of this work was the development for a numerical study of reinforced concrete columns subjected to axial load and bending. The following conclusions are presented and about 10 columns are tested.

The FLECO2C program presented adequate results of ultimate loads, concrete strains and horizontal displacements in comparison with test results, presenting coherent results and close to the test results with a few exceptions.

All columns presented ratios of F_u/F_{num} close to 1.00, with exception to *PFN* 18-3, *PFN* 24-3 and *PFN* 30-3, which probably had problems on geometric of columns or load eccentricity.

The best results were achieved in columns with relative eccentricity e/h higher or equal to 0.25 ($e \geq 30$ mm), evidencing difficulties in applying eccentricities lower than 30 mm.

It is noteworthy that, at ultimate load, it is hard to obtain horizontal displacements and concrete strains because, at this moment, in some cases, the values increase indefinitely. Therefore, the test behavior is valid at close of ultimate load, mainly for columns with high eccentricity.

Factors, such as bonding of strain gauges, geometric imperfections of cross sections, test setup and handling of columns, may have affected some results.

Acknowledgments

The authors are grateful to Structures Laboratory of University of Brasilia and to the CNPq (National Council for Science and Technological Development) as Brazilian research development agencies.

References

[1] Nagato, Y. 1987. "Strength of Reinforced Concrete Members with Circular Cross-Section under the Combined Action of Shear, Axial, Compression and Bending Moment." Ph.D. thesis, Federal University of Rio de Janeiro, Rio de Janeiro.

[2] Vecchio, F. J., and Collins, M. P. 1982. "The Response of Reinforced Concrete to In-plane Shear and Normal Stresses." Publication No. 82-03, University of Toronto, Canada.

[3] Dantas, A. B. 2006. "Reinforced Concrete Columns Tested under Axial Load and Bending." Master thesis, University of Brasília. (in Portuguese)

[4] Santos, G. S. 2009. "Numerical and Experimental Analysis of Reinforced Concrete Columns Subjected to Axial Load and Bending." Master thesis, University of Brasília. (in Portuguese)

[5] Araújo, L. M. B. 2004. "Theoretical and Experimental Analysis of Reinforced Concrete Columns Subjected to Axial Load and Bending." Master thesis, Civil Engineering School, Federal University of Goiás. (in Portuguese)

[6] Adorno, A. L. C. 2004. "Theoretical and Experimental Analysis of Unreinforced and Reinforced Columns Subjected to Axial Load and Bending." Ph.D. thesis, University of Brasília. (in Portuguese)

[7] Melo, C. E. L. 2009. "Experimental and Numerical Analysis of Pin-Ended Reinforced Concrete Columns Subjected to Axial Load and Bending." Ph.D. thesis, University of Brasilia, 2009.

[8] Comite Euro-International du Beton. 1993. *CEB-FIP Model Code 1990—Design Code.* London: Comite Euro-International du Beton, 1993.

[9] Nagato, Y., and Regis, P. A. 1997. "Shear in Reinforced Concrete Members of Circular Sections: CACODI E SACCOL Programs." In *Proceedings of XVIII CILAMCE—Ibero-Latin American Congress on Computational Methods in Engineering,* 569-76. (in

Portuguese)

[10] Carreira, D. J., and Chu, K. H. 1985. “Stress-Strain Relationship for Plain Concrete in Compression.” *Journal of the American Concrete Institute* 82: 797-804.

[11] Maia, A. C. F. 1979. “Nonlinear Analysis of Reinforced and Prestressed Concrete Frames in View of the Rheological Behavior of Concrete.” Ph.D. thesis, University Pierre et Marie Currie.

[12] Vecchio, F. 1981. “Response of Reinforced Concrete Subjected to In-plane Shear and Normal Stresses.” Ph.D. thesis, Universityof Toronto.

Journal of Civil Engineering and Architecture 10 (2016) 64-71
doi: 10.17265/1934-7359/2016.01.007

Characterization of Stabilized Earth Blocks with Incorporation of Cement Expanded Polystyrene for Use in Buildings

Malahimi Anjorin, Chakirou Akanho Toukourou, Aristide Comlan Houngan, Christophe Awanto and Largum Madougou

Laboratory of Applied Mechanics and Energetics (LEMA), Polytechnic School of Abomey Calavi, Cotonou 01 BP 2009, Benin

Abstract: This work focuses on the development of local building materials in Benin for their efficient use in buildings. It aims to make mud bricks lightened with good mechanical, thermal and sound properties and enhance the waste polystyrene. This article is the result of experimental work on a broad field of applied sciences: building mechanics. The study is focused on BTS (blocks of stabilized earth) chosen as reference materials to which we linked polystyrene. The percentage of polystyrene varies from 0% to 100% starting from a constant volume of each reference material. The results showed that the increase in polystyrene percentage lowers mechanical properties. These results also showed that the gradual addition of polystyrene to the laterite-cement mixture has a significant influence on the density and mechanical resistances of the final composite material.

Key words: Characterization, bocks of compressed earth, polystyrene, mechanical resistances.

Nomenclature

B	Width (m)
E	Thickness (m)
F_f	Breaking load bending (N)
F_c	Breaking load compressive (N)
L	Length (m)
M	Weight (kg)
R_f	Flexural strength (MPa)
R_c	Compressive strength (MPa)
S	Area (m^2)
V	Volume (m^3)
P	Density ($kg \cdot m^3$)
BTS	Stabilized earth blocks

1. Introduction

To partially address concerns, such as reducing electricity consumption in buildings, reducing the emission of gases through the greenhouse effect due to large air conditioning facilities and extra protection environment by recycling polystyrene waste [1-3], we conducted an experimental study on the behavior of BTS with added polystyrene. This is a study conducted in the LEMA (Laboratory of Applied Mechanics and Energetics), on the thermomechanical properties of BTS alleviated. According to our surveys, the addition of polystyrene in mortars and concrete help to achieve good thermal insulation of the envelope [4-6]. The main objective of this study is to experimentally characterize the mechanical behavior of BTS. One of the objectives is to find earth blocks acceptable mechanical properties to erect walls or fences and buildings that will be easy to implement as stipulated by the French and Belgian standards [7]. A weight ratio of laterite-cement constant equal to 9 was adopted for all compositions. Then, the main concern was to adjust to the amount of introduced polystyrene. Some preliminary tests have indeed shown that the workability of the mortar and the density of the blocks are affected by the introduction of polystyrene. The influence of the percentage of polystyrene on the bulk density has also been shown in this study, on the compressive strength of the cubic form of test

Corresponding author: Chakirou Akanho Toukourou, Dr., research fields: mechanic and materials.

specimens and the tensile strength of the samples.

2. Sample Preparation

2.1 Used Materials

All materials used in this work are of local origin. For making blocks, the used materials are: Cement CPJ 35, laterite or earth Bakhita bar, water and polystyrene. The latter component is also the only variable parameter.

2.1.1 Laterite or Earth Bar

Laterite used for making the blocks is a soil taken from Bakhita in Abomey Calavi, in the suburb of Cotonou in the Republic of Bénin. After drying the ground, it was sieved with two sieves (2 mm) for making test pieces to be cooked, taking into account the finer particle size clay. Fig. 1 shows the appearance of the used size.

2.1.2 Cement

The cement used for making blocks is CPJ-35 kind from the League of SCB Lafarge (Lafarge Cement of Benin). Fig. 2 shows the package of cement used for making cement blocks stabilized.

2.1.3 Polystyrene

The used expanded polystyrene beads are suitable for incorporation into the blocks. They have varying diameters. Its bulk density is about 17.5 kg/m^3, which is at least 60 times smaller than the densities of the clay and the earth bar. Fig. 3 shows photos of PES (polystyrene) waste and obtained ground product.

In this study, three granular classes were determined. Fig. 4 shows the appearances of the different classes. Only the granular class whose ball diameters are less than or equal to 2 mm was used.

Diameter $\Phi < 5$ mm

Fig. 1 Different sizes of used laterite.

Fig. 2 Photo of the used cement.

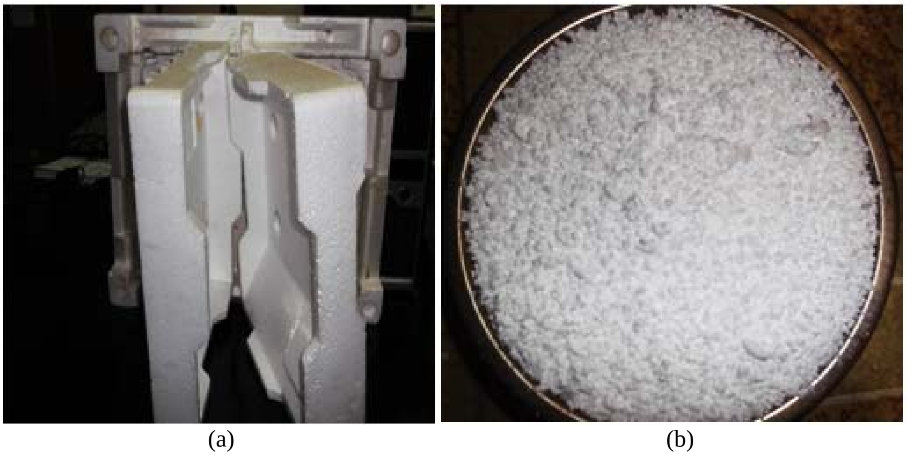

(a) (b)

Fig. 3 Photos of the used polystyrene: (a) PES waste; (b) ground product.

(a) (b) (c)

Fig. 4 Different granular classes PES: (a) $\Phi \leq 2$ mm; (b) $2 < \Phi \leq 4$ mm; (c) $\Phi > 4$ mm.

(a) (b) (c) (d)

Fig. 5 Photos of some used materials: (a) Mold 4 × 4 × 16; (b) Mold 10 × 10 × 3; (c) graduated container; (d) balance.

2.1.4 Dampening Water

Dampening water is distributed by the drinking water supply network of the University Campus of Abomey.

2.1.5 Materials

For making blocks, many current materials and supplies (scales, containers, trowels, molds, formwork oil, etc.) are used. Fig. 5 shows the pictures of some used materials.

2.2 Procedures

All samples were prepared manually; The mortar mixture is made using a trowel, and the blocks were molded by hand (hand molding). Standard prismatic tests French standard (NF P 18-400, NA 2600) of dimensions 4 cm × 4 cm × 16 cm have been used for the determination of flexural strengths three points. These same samples were used to determine the weight loss. Equivalent cubic specimens (4 cm × 4 cm × 16 cm) were obtained by crushing the resulting equivalent cubic test half-prisms.

The samples were first a course of 28 days, that is to say, they are protected from the sun and wind in a high relative humidity for 28 days to allow the cement to reach its maximum strength [8]. After curing, the blocks were always dried out of direct sunlight (avoid too rapid withdrawal) to allow evaporation of water and the removal of the clay fraction.

All tests were made with a temperature in an oven of 105 °C. For each type of test, the number of specimens is 3 and test body is 4 cm × 4 cm × 16 cm for mechanical testing and measurements of bulk densities.

For mechanical testing, testing in three flexure dots and those in compression on the half blocks from the flexural strength were performed.

2.3 Formulation

2.3.1 Dosage

The following percentages were studied:

- polystyrene: 10%, 20%, 30%, 40%, 50%, 60%, 70%, 80%, 90% and 100% of the soil volume measured in accordance with the dosages adopted by Chafi [5] to properly highlight the influence of this by-product in low dosages;
- cement: 10% and 90% laterite.

Of course, for each characteristic of interest, the results were compared with a reference block (control) performed according to the same methods of implementation and earth assays, cement and water.

The only parameter changing from one to the other is

Table 1 Notations adopted for the different samples.

No.	Designation	Rating
1	Control block	F
2	Block reinforced with 10% polystyrene	F1
3	Block reinforced with 20% polystyrene	F2
4	Block reinforced with 30% polystyrene	F3
5	Block reinforced with 40% polystyrene	F4
6	Block reinforced with 50% polystyrene	F5
7	Block reinforced with 60% polystyrene	F6
8	Block reinforced with 70% polystyrene	F7
9	Block reinforced with 80% polystyrene	F8
10	Block reinforced with 90% polystyrene	F9
11	Block reinforced with 100% polystyrene	F10

mixed assay (content) of the PES.

The studied characteristics are as follows:

- density;
- the compressive strength and tensile strength by bending.

The notation F denotes blocks stabilized cement followed by a number which represents the percentage by volume of polystyrene added to 10.

Tables 1 and 2 show the values of different strengths for the manufacture of each type of sample.

2.3.2 Weight Loss Test

The withdrawal measures were accompanied by the weighing of 4 × 4 × 16 samples in order to determine their densities.

Measurements of weight variation were performed using an electromechanical balance to an accuracy of 0.1 g (Fig. 5).

2.3.3. Bending Tensile

The flexural tensile strength was determined using a three-point 10 kN bending machine and one 4 × 4 × 16 cm prismatic test in according with French standard NF P18-407 (NA 428).

The specimens were placed in the testing machines, as shown in Fig. 6.

After a perfect centering, the loading was the carried out with a constant speed of scalability. The machine is provided with a bending device is shown schematically whose principle in Fig. 7.

Denoting by F_f the failure of the test of load in bending, the moment of rupture is $F_f \times l/4$ and the corresponding flexural stress was determined by:

$$R_f = \frac{1.5 F_f l}{b^3} \tag{1}$$

2.4 Compression Test

The compression test is to break the test specimen between the two plates of a compression press. The press used is a compression machine with a capacity of 150 kN. The compression test on equivalent cubes 4 × 4 × 4 cm was made on the same compression machine. The half-prisms 4 × 4 × 16 specimens obtained after flexural strength were broken in compression, as shown in Fig. 8.

By appointing the breaking load of the compression cylinder F_c, the stress fracture at the corresponding compression was calculated by:

$$R_c(\mathrm{MPa}) = \frac{F_c(\mathrm{N})}{b^2(\mathrm{mm}^2)} \tag{2}$$

Expressing F_c(N) and considering the section specimens (40 mm × 40 mm), this resistance (MPa) is:

$$R_c(\mathrm{MPa}) = \frac{F_c(\mathrm{N})}{1{,}600} \tag{3}$$

Following the withdrawal of the clay after firing, the compression breaking stress, for cooked blocks, is calculated by the following formula:

$$R_c(\mathrm{MPa}) = \frac{F_c}{4b} \tag{4}$$

Table 2 Composition adopted for lightened with polystyrene block.

Items	Results										
Mixture volume (mL)	2,000										
Mixture content	Latérite/cement: 90%/10%										
Water (mL)	375										
PSE volume (mL)	0	200	400	600	800	1,000	1,200	1,400	1,600	1,800	2,000
Corresponding PES weight (g)	0	3.5	7	10.5	14	17.5	21	24.5	28	31.5	35
Designation	F	F1	F2	F3	F4	F5	F6	F7	F8	F9	F10

Fig. 6 The used bending machine.

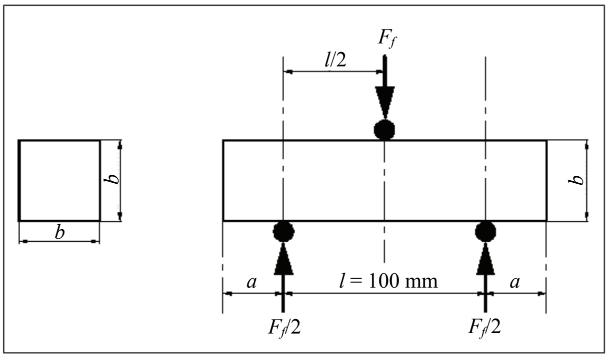

Fig. 7 Device tensile failure in bending.

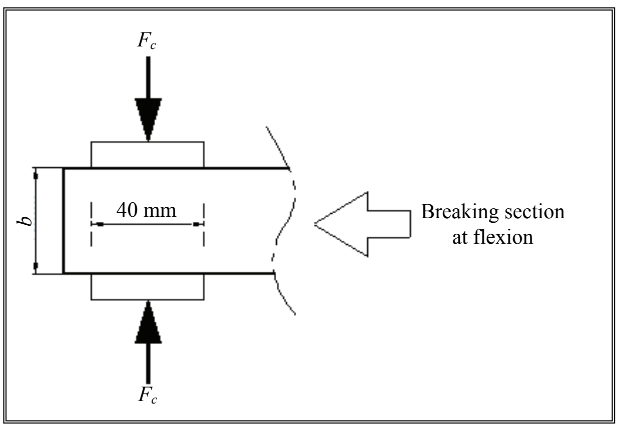

Fig. 8 Compression breaking device.

The results for each of the six half-prisms are rounded to 0.1 MPa, and then their average is calculated. If any of the results differs from 6 ± 10% of this average, it is discarded and the average is recalculated from the remaining five results. If again one of the five results deviates ±10% of this new medium, the series of six measures are dismissed as prescribed by the standard.

When the result is satisfactory, the obtained average is thus the resistance of the mortar to the considered age.

3. Results and Discussions

This section presents the different results obtained in this study and it aims to show the influence of the percentage of PSE on the bulk density, the compressive strength on cubic specimens and sample tensile strength.

3.1 Bulk Density ρ

The influence of the incorporation of the polystyrene beads on the density of the blocks was studied. All results obtained are summarized in Table 3. It is clear in Fig. 9 that the density of BTS eased decreases with increase in the percentage of PSE. For example, the density of the fired brick reference (F) is 1,896 kg/m^3, whereas the reinforced brick 100% PES (F10) is only 1,316 kg/m^3, which corresponds to a decrease of 31%. Ultra lightweight polystyrene aggregate is regarded as voids created within blocks explains this reduction in density.

The lightweight materials become very beneficial when the density reduction rate is at least equal to 15%. With stabilized earth blocks and lightweight, discounts up to 31% were obtained.

3.2 Influence of the PES on the Mechanical Performance

One of the important points to be considered in this

Table 3 Density polystyrene block of samples.

Designation	F	F1	F2	F3	F4	F5	F6	F7	F8	F9	F10
ρ (kg/m^3)	1,896	1,785	1,639	1,595	1,576	1,525	1,492	1,391	1,347	1,331	1,316
ρ/ρ_F (%)	100	94	86	84	83	80	79	73	70	70	69
Reduction (%)	0	6	14	16	17	20	21	27	30	30	31

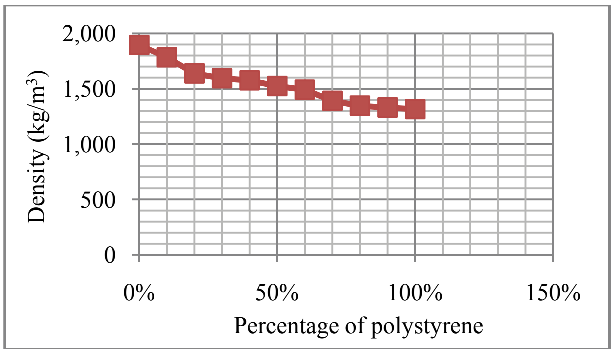

Fig. 9 Density of the tested samples.

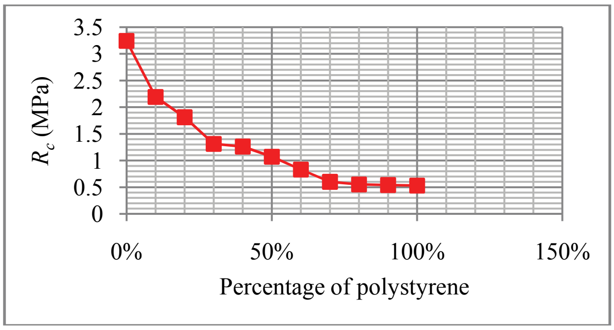

Fig. 10 Evolution of the compressive strength versus percent polystyrene beads.

research is indeed the mechanical performance. The strengthened polystyrene blocks were compared to control blocks to determine their influences depending on the dosages:

- cylinders prismatic 4 cm × 4 cm × 16 cm: for the testing of resistance to the three-point bending;
- half specimens broken in two parts during the bending test without changing the mechanical characteristics: for testing the resistance to compression.

The results of the companion measures are presented in the following.

3.3 Compressive Strength

The influence of the incorporation of the polystyrene beads on the resistance R_c of the compression blocks was studied. The obtained results are summarized in the Table 4 and represented by the curve.

Fig. 10 shows the development of resistance to compression of the blocks based on polystyrene rate.

In Fig. 10, a lower mechanical strength of the polystyrene blocks was observed, compared to control blocks when the polystyrene content increases. At contents ranging from 10% to 100%, the compressive strength is reduced from 6% to 68% relative to the control. These decreases on mechanical strength were observed by several authors (Chafi [5], Collins and Ravindrarajah [9]). Indeed, polystyrene aggregates create areas of weakness within the blocks and reduce the area of the resistant section of the test pieces.

3.4 Flexural Tensile Strength

All obtained results are summarized in Table 5.

The curve in Fig. 11 shows and confirms that the addition of polystyrene causes a reduction of the resistance of the blocks.

Whether three-point bending or compression occurs, the trend is the same: "The mechanical performance blocks with addition of PSE decrease with the content of PES".

The appearance of the bottom curve (cold) is due to the progression of the values given by the measuring machine. Indeed, values change 100 N into 100 N; Therefore, all values, between 0 and 100 and between 100 N and 200 N, respectively, are rounded to 100 N and 200 N. It is this fact which explains the shape of the curve obtained due to low resistance of the blocks.

Comparing Figs. 10 and 11, it is noted that the bending strength is less sensitive to the polystyrene content than the compressive strength. Chafi [5] obtained similar results on polystyrene reinforced mortar. To explain this difference in behavior between the influence of polystyrene on the strength of the mortar

Table 4 Results of the compressive strength on samples cut 4 × 4 × 4 cm

Designation	F	F1	F2	F3	F4	F5	F6	F7	F8	F9	F10
R_c (MPa)	3.24	2.19	1.81	1.31	1.26	1.07	0.83	0.60	0.55	0.54	0.53
Reduction (%)	0	32	44	60	61	67	74	81	83	83	84

Table 5 Results of the bending strength on prismatic specimens 4 × 4 × 16 cm.

Designation	F	F1	F2	F3	F4	F5	F6	F7	F8	F9	F10
R_c (MPa)	3.24	2.19	1.81	1.31	1.26	1.07	0.83	0.60	0.55	0.54	0.53
Reduction(%)	0	32	44	60	61	67	74	81	83	83	84

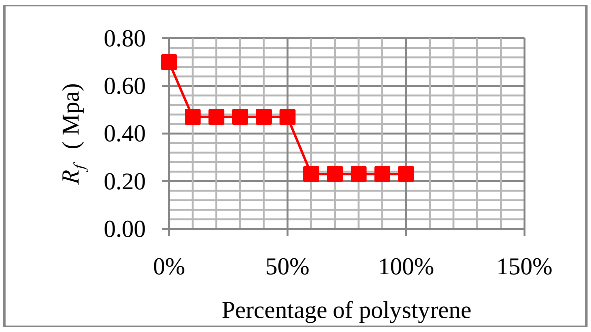

Fig. 11 Evolution of the flexural strength as a function of the percentage of polystyrene beads.

compressive and flexural strength, he is the link between the failure mode according to the mortar contains polystyrene or not; and found that the specimens containing polystyrene are not crushed into small particles, unlike those of the control. It has also made this observation during measurements. This means that there is a certain cohesion of the matrix due to adhesion between the cement paste and the beads. This same grip is useful to bending and helps keep higher proportions of resistance to bending in compression despite the presence of polystyrene.

4. Synthesis

The effects of the introduction of the polystyrene in the BTS are highlighted:

• A dropping resistor was expected since the polystyrene reduced resistant surface of a section. It is to manufacture blocks full of air pockets that have no resistance;

• Behaviors between compression and bending stresses are very different;

• By analogy with the resistance obtained during the compressive strength test, it is found that falls are identical to those of apparent densities, so there is a correlation between the two characteristics;

• The fall of the resistance to compression block is explained by the decrease in density due to charging of the internal structure of the latter.

5. Conclusions

The exploitation of experimental results has quantified most mechanical quantities and characteristics of developed samples. The experimental part of the study on the mechanical properties provides guidance for the choice of material for the thermal insulation of buildings, however, to consider other criteria for the final choice as behavior of these materials in contact with water. A first contribution concerns the development of new local composite materials for the building envelope.

After the experiment, the following conclusions were reached:

• The variation of these parameters is due to the nature of polystyrene dosing percentages in the composition;

• Depending on the percentage, increase in the polystyrene has been:

(1) a decrease in compressive strength;

(2) a decrease in the flexural resistance;

(3) a reduction in mass and density.

References

[1] Projet/PNUD/FEM/RAF-G32. 1999. *Reducing Greenhouse Gas Emissions by Improving the Energy Efficiency of Buildings in West Africa: Ivory Coast.* Senegal: Projet/PNUD/FEM/RAF-G32. (in French)

[2] Dreyfus, J. 1960. *Thermal Comfort in a Tropical*

Environment. Paris: Editions Eyrolles. (in French)

[3] Galdi, P. 1968. *Rural Housing in Senegal.* Dakar: Cheikh Anta Diop University. (in French)

[4] Sotehi, N. 2010. "Thermal Characteristics of Buildings and Walls of Improved Insulation." Ph.D. thesis, University Mentouri Constantine (Algeria). (in French)

[5] Chafi, N. 2005. *Fiber Reinforced Cement Matrix.* Magister thesis, Constantine University. (in French)

[6] Miled, K. 2005. "Size Effect in the Lightweight Concrete with Expanded Polystyrene." Ph.D. thesis, National School of Bridges and Roads. (in French)

[7] Fedeation Belge de La Brique. 2008. *Clay Masonry Manual.* Bruxelles: Fedeation Belge de La Brique. (in French)

[8] Rigassi, V. 1994. "Compressed Earth Blocks." In *Production Manual.* Vol. 1. Villefontaine: CRAterre (International Center for Earth Construction). (in French)

[9] Collins, J., and Ravindrarajah, S. 1998. *Temperature Development in Concrete with Expanded Polystyrene Beads.* Villefontaine: CRAterre.

Journal of Civil Engineering and Architecture 10 (2016) 72-80
doi: 10.17265/1934-7359/2016.01.008

Evaluation of Reinforced Concrete Structures with Views for Rehabilitation

Jackline de Assis Lopes S. Oliveira[1], Romildo Alves Berenguer[1], Lydia Barreto[1], Eliana Cristina Barreto Monteiro[1, 2] and Romilde Almeida de Oliveira[1]

1. Department of Civil Engineering, Catholic University of Pernambuco, Recife 51110-200, Brazil

2. Department of Civil Engineering, University of Pernambuco, Recife 51110-200, Brazil

Abstract: The increasing number of pathological occurrences is found in reinforced concrete structures, so does the demand for inspection and maintenance services in residential communities in the state of Pernambuco, which aim to detect damage to the structure in a timely manner to minimize repair costs, thus applying preventive maintenance in order to guarantee the estimated useful life of the project for the building. However, it is observed that the practice of periodic inspections is not yet part of the culture of a certain segment of the population that does not have economic means and knowledge of the importance of maintenance to ensure the integrity of the structure. It was used in this work an inspection script with use of tests and methodology to quantify damage and to check the state of degradation of two residential buildings with more than 20 years and built near the seafront where environmental aggression is strong. The deterioration found in each of the buildings has been differentiated due to different corrective maintenance performed at every building. The last maintenance, performed in Building A, was performed by corrective hand of unskilled labour guided by the community itself, which has no expertise in the field of civil engineering. In Building B, the situation is similar, compounded by the opinion of some tenants that there is no need for this routine, even the structure being in critical condition, as was confirmed with the application of the methodology employ. There should be a legislation that governs the execution of inspections and maintenance programs in addition to the existing technical standards. The methodologies presented suitable for checking the degree of degradation of the structures and performed tests confirmed the diagnosis obtained by visual inspection and quantification of damage.

Key words: Pathology, inspection, maintenance, lifespan, concrete.

1. Introduction

In the MRR (metropolitan region of Recife), several cases of disease and accidents with works of various types have occurred. These facts led to a serious social problem, by virtue of having created one of insecurity and apprehension framework for users of these buildings.

The reinforced concrete structures, even well designed, well executed and with the use of specified materials correctly, require preventive maintenance to achieve the expected lifetime, guaranteed by a durability with performance above the minimum acceptable limit. The current situation requires greater preparation for professionals and public awareness that the concrete structures are not designed for eternity.

In an attempt to increase the life of such structures, research institutions deepened studies on chemical reactions occurring during the hydration of cement, in view of the durability which is also directly connected to the constituents of the mixture (aggregates, cement and steel), the dosage (water/cement ratio, use of additives) and use of this material (density and healing). A maintenance program suited to the structure will increase the life and structural problems detected in its infancy and will have effects, and cost of repairs will lessen buildings.

2. Methodology

The methodology of the concrete deterioration

Corresponding author: Romildo Alves Berenguer, professor, research fields: concrete, corrosion and materials.

study developed by Swedish researcher Tuuti [1] classifies the evolution of corrosion process in two steps of initiation, where aggressive agents penetrate slowly through the concrete microstructure starting the damage and the step propagation, and the structures degradation rate is accelerated by the action of aggressive agents into the concrete, causing the appearance of cracks and loss of cover to the reinforcement and may compromise the stability of the building.

According to research carried out by Klein et al. [2], to works of art, Castro [3] found unfeasible in the proposal when applied to conventional structures. Thus, the methodology proposed by Castro [3] was based on principles contained in Klein's research [2], with adaptations and modifications necessary to quantify the evolution of damage over the life of the structure. There were still changes proposed by Lopes [4] and Boldo [5] and used by Lemos [6] in his dissertation, in order to better represent the damage to the structure. It is noteworthy that there was a concern not to distort the original configuration of the methodology proposed by Castro [3].

The methodology of the identification of pathological manifestations is found in reinforced concrete structures for residential buildings. Searches establish inspection and evaluation procedures of structure by determining the degree of deterioration of the structure and of their individual elements, in order to support maintenance plans of the structures over time.

Symbol meanings can be found as following:

CO_2: carbon dioxide;

SO_2: sulfur dioxide;

H_2S: gas hydrogen sulfide;

$Ca(OH)_2$: calcium hydroxide;

F_p: damage weighting factor;

F_i: damage intensity factor;

D: degree of damage;

M: amount of damage found on the element;

Gde: degree of deterioration of the element;

Gdf: degree of deterioration of the family of an element;

N: number of component elements family;

R_f: factor family relevant structural elements;

Gd: degree of deterioration of the structure;

K: number of families of elements present in the building;

VUE: estimated useful life;

VUR: life reference component.

3. Results (Case Studies)

3.1 Characterization of Respondents Environments

Inspected buildings are residential, aged between 20 and 30 years of built and located in the neighborhood Candeias, Jaboatão dos Guararapes, PE, in marine area of regions whose environmental aggressiveness is Class III, according to Ref. [7].

3.2 Description of the Analyzed Constructions

The first building, known as Building A, which has 20 years of built and a distance of 300 m from the seafront of Candeias, has three floors, type of apartments and the ground. Its facade is originally coated with gum and ground columns covered with tile, which is already part of the community intervention.

At a distance of 100 m from the seafront, the second studied building is located and has 25 years of built. It also consists of three floors and type of ground, used as a garage. This building, named Building B, has the facade coated with ceramic on three of its faces and the last one is only covered with plaster and paint.

3.3 Experiment Planning and Results

3.3.1 Environment Location

The inspected buildings contain three and seven floors, located in environmental aggression Class III, according to the rank [7]. Slabs, beams and reservoirs were inspected building. There were no authorizations for inspection of foundations in the two buildings. Scratch tests, carbonation depth and speed of the ultrasonic pulse on the ground floor (stilts) were performed, where there are the garages of the three buildings. It was difficult for the tests because it is not yet common practice in inspections, using difficulties of some equipment or availability.

3.3.2 Edification A (Visual Inspection)

In Building A, on visual inspection (Fig. 1), we observed detachment of the tablets on the facade, some cracks in the pavement edge beams at the level of infiltration stilts and the ceiling slab from the sanitary system facilities. Condo information was found that there were attempts to fix the leaks, but they did not succeed. Buildings regarding maintenance and condominium realize that information is held whenever it is necessary and possible financially to the tenants.

3.3.3 Carried-Out Tests (Edification A)

3.3.3.1 Test Speed of the Ultrasonic Pulse

In Table 1, the studied columns and their randomly-chosen results are listed, according to Ref. [8].

Despite the observed variation in the results obtained in this test (Fig. 2), the concrete quality is considered good according to the classification of Ref. [9].

3.3.3.2 Sclerometry Tests

Table 2 lists the columns and the results of sclerometry tests to Building A.

3.3.3.3 Carbonation Depth Test

The carbonation depth found in the tested columns of the building (Fig. 3) was small, compared with the result of the two buildings. Table 3 gives the depth of carbonation columns of Building A.

3.3.4 Deterioration Degree of Structure Elements

3.3.4.1 Columns

The building structure consists of 10 columns, in which damage was found in only three of them. With the identified damage, degree of deterioration of the element (the expression Gde_1 being developed by Castro [3] and Gde_2 by Lopes [4]) was calculated. Table 4 shows the conditions found during the inspection.

For this situation, it is observed that the degrees of deterioration of the elements are equal, both in use of

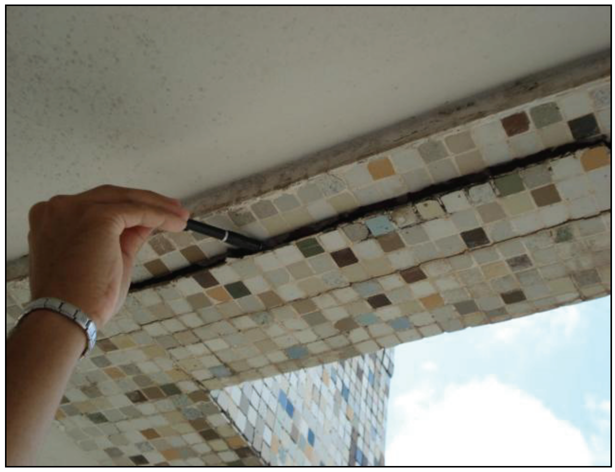

Fig. 1 Fissure in the edge beam of Building A.

Table 1 Speed test of the ultrasonic pulse in Building A.

Column	Speed *V* (m/s)	Concrete quality
P1	4,050	Durable
P2	3,850	High
P20	4,000	High

Fig. 2 Test speed of the ultrasonic pulse on Column P1 of Building A.

Table 2 Sclerometry test.

Column	Sclerometric index
P1	46
P2	36
P4	30

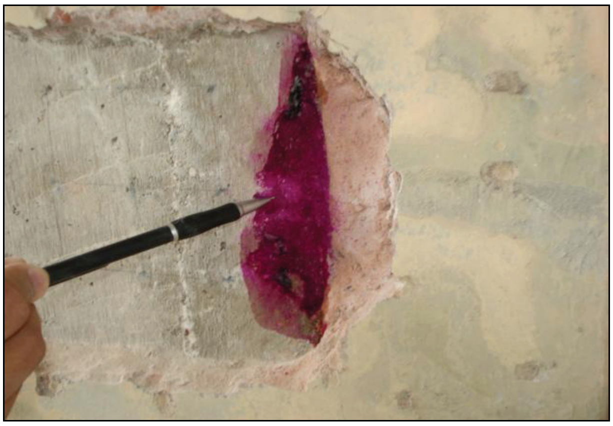

Fig. 3 Carbonation depth test of Column P20 of Building A.

Table 3 Carbonation depth test.

Column	Carbonation depth (cm)	Covering (cm)
P1	0	2
P5	0.1	1.8
P20	0	2

Table 4 Damage assessment and degree of deterioration of the column element.

Column	Damages	F_i	F_p	D	M	Gde_1	Gde_2
P3	Geometric deviation	2	8	6.4	1	6.4	6.4
P5	Segregation	1	6	2.4	1	2.4	2.4
P8	Exfoliation	1	8	3.2	1	3.2	3.2

Fig. 4 Detachment of reinforced concrete beam of Building A.

the formulation proposed by Castro [3] as the proposal by Lopes [4] and as analyzed columns which had only damage. And for the *Gdf*, zero was considered because in none of the columns damage was evidenced with $Gde \geq 15$, which would indicate spread of damage.

3.3.4.2 Beams

Despite showing damage in just two beams, it can be seen in Fig. 4 that intensity damages were considerably high, since equipment corrosion was observed (Table 5).

3.3.4.3 Slabs

As shown in Table 6, the damages found in slabs (Figs. 5 and 6) were punctual but in an advanced state.

3.3.4.4 Reservoir

In the visual inspection and by questioning the residents, there have been no damages to the reservoirs.

3.3.5 Degree of Deterioration of the Structure

Table 7 presents the degree of deterioration of the structure considering the deterioration of each element and the factor of structural importance.

Table 5 Damage assessment and degree of deterioration of the beam element.

Beams	Damages	F_i	F_p	D	M	Gde_1	Gde_2
Right side	Exfoliation	2	8	6.4	1	6.4	6.4
Staircase	Exfoliation	3	8	32	2	32	46.93
	Corrosion	3	7	8			

Table 6 Damage assessment and degree of deterioration of the slab element.

Damages	F_i	F_p	D	M	Gde_1	Gde_2
Disabled coverings	2	6	4.8	4	28.8	33.03
Corrosion	2	7	5.6			
Infiltration	3	6	24			
Efflorescence	2	5	4			

Fig. 5 Efflorescence on slab of Building A.

Fig. 6 Corrosion of slab reinforcement of Building A.

Table 7 Degree of deterioration of the structure of Building A.

Family	Gdf_1	Gdf_2	Gdf_3	F_r	K	Gd_1	Gd_2	Gd_3
Columns	-	-	-	5	2	31	40	40
Beams	32	47	47	4				
Slabs	29	33	33	4				
Lower Reservoir	-	-	-	3				

Gdf_1: calculation by the term used by Castro[3];
Gdf_2: calculation by the term used by Lopes [4];
Gdf_3: calculation by the term used by Boldo [5];
Gd_1: Gd calculation by the term used by Castro [3];
Gd_2: Gd calculation by the term used by Lopes [4];
Gd_3: Gd calculation by the term used by Boldo [5].

Fig. 7 Beam reinforcement corrosion with section loss in Building B.

3.3.6 Edification B (Visual Inspection)

Through visual inspection (Fig. 7), some conditions were observed in Building B that require immediate interventions, in order to minimize damage to the stability of the building. Infiltrations on stilts ceiling slab come from sanitary system facilities, corrosion of reinforcement comes in slabs, columns and beams in some cases at an advanced stage. There is also detachment of ceramic plates on the facade among other pathologies. It was also observed that the maintenance services and repairs are carried out improperly. It was found that part of the shareholders do not agree with the need for periodic maintenance.

3.3.7 Carried-Out Tests (Edification B)

3.3.7.1 Speed Test of the Ultrasonic Pulse

Table 8 shows that the inspected columns were randomly selected and their results are related to ultrasound testing.

Despite the observed variation in the results of this test, the quality of the concrete is considered good according to Ref. [9].

3.3.7.2 Sclerometry Test

Table 9 lists the columns and the results for the sclerometry test.

3.3.7.3 Carbonation Depth Test

Columns P4, P9, P13, P18 were tested, although the ultrasonic testings have characterized these concrete columns and durable high quality carbonated surface was found, as shown in Table 10.

Despite the variation found in coatings, we can see that work performance according to Ref. [10] in force

Table 8 Speed test of the ultrasonic pulse.

Column	Speed V (m/s)	Quality of concrete
P9	4,045	Durable
P13	3,600	High
P18	4,060	Durable
P20	3,950	High
P23	4,060	Durable
P22	3,670	High

Table 9 Sclerometry test.

Column	Sclerometric index
P4	45
P9	41
P13	23
P18	33
P20	36
P23	40
P22	15

Table 10 Carbonation depth test.

Column	Carbonation depth (cm)	Coverings (cm)
P4	2	2
P9	1.5	1.5
P13	> 2	2
P18	1.5	1.5

Fig. 8 Detachment column due to reinforcement corrosion.

at the time recommends coatings (least 1.5 cm) for reinforced concrete subjected to aggressive environments in Class III. And even with the recommended coatings, it can be seen that the carbonated thickness reaches the reinforcement (Fig. 8).

3.3.8 Quantification of Damage

3.3.8.1 Deterioration Degree of Structure Elements

(1) Columns

Table 11 presents the damage found in 22 of the 24 columns of Edification B. Analyzing the found data, it observes 41 kinds of damage to the columns.

(2) Beams

Table 12 shows the damages found in the beams of Building B (Fig. 9), where Gde_1 and Gde_2 are expressions used by Castro [3], Lopes [4] and Boldo [5], respectively.

(3) Slabs

During the inspection, infiltration of the slab from the sanitary system facilities was observed, where they are presented in Table 13.

(4) Lower Reservoir

To the found lower reservoir, the damages are listed in Table 14.

Table 11 Damage assessment and degree of deterioration of the column element.

Column	Damages	F_i	F_p	D	M	Gde_1	Gde_2
P1	Gap	2	10	8	1	8	8
P2	Gap	2	10	8	1	8	8
P3	Gap	2	10	8	2	32	38
	Exfoliation	3	8	32			
P4	Carbonation	2	7	5.6	1	5.6	5.6
P5	Exfoliation	2	8	6.4	1	6.4	6.4
P6	Segregation	2	6	4.8	3	32.8	35
	Corrosion	3	7	28			
	Coatings insufficient	2	6	4.8			
P7	Exfoliation	2	8	6.4	2	6.4	8
	Segregation	1	6	2.4			
P9	Carbonation	3	7	28	1	28	28
P10	Exfoliation	3	8	32	2	32	37
	Corrosion	2	7	5.6			
P13	Carbonation	2	7	5.6	2	5.6	7.9
	Gap	1	10	4			
P14	Exfoliation	3	8	32	1	32	32
P16	Gap	4	10	100	1	100	100
P17	Exfoliation	2	8	6.4	1	6.4	6.4
P18	Carbonation	3	7	28	1	28	28
P19	Exfoliation	3	8	32	2	32	47
	Corrosion	3	7	28			
P21	Exfoliation	3	8	32	1	32	32
P22	Gap	1	10	4	1	4	4
P23	Exfoliation	3	8	32	1	32	32
P24	Exfoliation	3	8	32	2	70	70
	Corrosion	4	7	70			

Gde_1: *Gde* calculation by the term used by Castro [3];
Gde_2: *Gde* calculation by the term used by Lopes [4] and Boldo [5].

Table 12 Damage assessment and degree of deterioration of the beam element.

Beams	Damages	F_i	F_p	D	M	Gde_1	Gde_2
Bottom	Deficient coating	2	6	4.8	4	82.8	94.79
	Exfoliation	3	8	32			
	Segregation	1	4	1.6			
	Corrosion	4	7	70			
Left side	Deficient coating	2	6	4,8	4	82.8	94.79
	Exfoliation	3	8	32			
	Segregation	1	4	1,6			
	Corrosion	4	7	70			
Right side	Exfoliation	2	8	6.4	3	104.8	108.8
	Cracks	4	10	100			
	Segregation	2	4	3.2			
Front	Deficient coating	3	6	24	2	24	28.54
	Corrosion	2	7	5.6			

Fig. 9 Stirrup of the exposed beam, with corrosion, in Building B.

Table 13 Damage assessment and degree of deterioration of the slab element

Damages	F_i	F_p	D	M	Gde_1	Gde_2
Coverings disabled	2	6	4.8	3	29.2	31.25
Corrosion	2	7	5.6			
Infiltration	3	6	24			

Table 14 Damage assessment and degree of deterioration of the reservoir element.

Damages	F_i	F_p	D	M	Gde_1	Gde_2
Waterproofing damage	2	8	6.4	2	8	11.55
Leak	2	10	8			

Table 15 Deterioration degree of structure of Building B.

Family	Gde_1	Gde_2	Gdf2	F_r	K	Gd_1	Gd_2	Gd_3
Columns	41	46	180	5	3	47	52	134
Beams	74	82	181	4				
Slabs	29	31	31	4				
Lower Reservoir	-	-	-	3				

3.3.9 Deterioration Degree of Structure Elements

In Table 15, the degree of deterioration of the structure of Building B is listed.

4. Results and Discussions

4.1 Visual Inspection

Although the recognition of the importance of maintaining the durability of reinforced concrete structures is growing, we observed the development of this research to give effect to the maintenance of buildings, and there is a need to create appropriate legislation.

By visual inspection, following the recommendations of the "checklist" developed by ABECE (Associação Brasileira de Engenharia e Consultoria Estrutural) [11], it was observed that the three structures are studied for wear at different points, the columns and the most deteriorated element of Building B, which has the columns coated with ceramic, thus providing greater physical protection to aggressive agents.

It was observed that damage, such as cracks, corrosion and leaks, performed more strongly in buildings, and the Building B was the most affected, with a critical situation. The Building A showed medium deterioration levels.

The last maintenance, performed on Building A, was corrective, performed by unskilled labor and driven by the condominium itself. In Building B, the situation is similar, compounded by the opinion of some tenants that there is no need for this routine, even the structure lying in critical condition, as was confirmed by the application of the methodology.

4.2 Tests

In an attempt to better characterize the structure, scratch tests, ultrasound and carbonation were used. In the sclerometry test, there was variability of the results, which were affected by phenomena, such as carbonation, roughness and moisture that existed in the tested parts.

Through the quality of the ultrasonic test of the concrete, buildings were classified into durable and high, these results being justified by the fact that such test pieces did not show pathology.

For the carbonation test, it was observed that the two buildings showed contamination by carbon dioxide, but only in the last Building B reached the rebar, allowing the development of corrosion of the same process.

4.2.1 Degree of Deterioration of Structures

It is possible to see variation in results between the degrees of damage of the structures of buildings. In Table 16, we observe the marked differences, despite being in areas of environmental aggression classes similar construction and having the same patterns. Also the need to conduct a greater number of tests and samples to set the parameters is considered.

For Gd = 30, using the methodology [3] found in Building A, it is considered that the structure has a medium level of deterioration, necessitating periodic observation and short-term intervention. Using the expression of Ref. [5], Gde = 40 was found, which falls into the same situation with short-term intervention recommendations, at most one year. Through inspection and analysis in Building B, Gd = 39 has been found, according to Ref. [3] and Gd = 125 according to the recommendations of Ref. [5]. For Gd = 39, the measure to be taken is the periodic observation with intervention in the medium term. And when Gd = 125, immediate intervention is needed to restore the building functionality.

The factor method [12] allows us to estimate the useful life of a component or component family. The starting point of factor method is the life of reference (VUR), equivalent to the lifespan of the project, which is the period in years, in which it is expected that a component or group of components can last. The method uses a set of seven factors that weigh the quality parameters related to the construction and use of the building. Each of these factors has a value of 0.8 to 1.2.

The service life is estimated by the following VUE (estimated useful life) equation:

$$VUE = VUR \times A \times B \times C \times D \times E \times F \times G \quad (1)$$

where:

Factor A: component quality;

Factor B: project level;

Factor C: project execution level;

Factor D: internal setting;

Factor E: external setting;

Factor F: terms of use;

Factor G: maintenance level.

4.2.2 Estimated Useful Life for Buildings A and B

For the accessible structural component, VUR = 50 shall be considered, for being the presumed value in Ref. [7] with the adopted safety factors. Table 17, used in all three cases of this work, contains the values adopted for the factors.

Therefore, the estimates of service life for Buildings A and B are resulted lower than the design life.

There is:

- Building A:

$$VUE = VUR \times 0.8 \times 1.0 \times 1.0 \times 1.0 \times 1.0 \times 1.0 \times 0.8 = 0.64 VUR \text{ (years)}$$

Considering VUR = 50 years for three cases, it is VUE = 32 years;

- Building B:

Table 16 The damage degree of comparison between the surveyed buildings.

Surveyed building	Gd_1	Gd_2	Gd_3
Building A	31	40	40
Building B	47	52	134

Table 17 The factors used in Buildings A and B.

Class of factors	Factor characteristics	Value factors	
		Building A	Building B
A	Component quality of reinforced concrete: fck = 15 MPa	0.8	0.8
B	Design level: normal	1.0	1.0
C	Labor execution level: concrete taken from the place without control	1.0	0.8
D	Aggressive internal environment influence of wastewater, high humidity	1.0	1.0
E	External environment: marine environment	1.0	0.8
F	Conditions of use: normal	1.0	1.0
G	Maintenance level: nonexistent	0.8	0.8

$$VUE = VUR \times 0.8 \times 1.0 \times 0.8 \times 1.0 \times 0.8 \times 1.0 \times 0.8 = 0.41\text{VUR (years)}$$

$$VUE = 21 \text{ years}$$

5. Final Considerations

The obtained results show the following conclusions:

- It can seen that the "evaluation" developed by ABECE [11] is perfectly functional and effectively serves as inspection checklist;
- The methodologies presented suitable for the verification of the degree of degradation of structures and the performed tests confirmed the diagnosis obtained by visual inspection and quantification of damages;
- There was a need to create an enlightening information of importance and execution of the maintenance program with language directed to the end user, emphasizing their importance;
- It is noted that the Building A showed the lowest degree of deterioration in the structure and the Building B had the greatest degree of deterioration, presenting critical condition. This could also be seen through the factor method.

References

[1] Tuuti, K. 1982. *Corrosion of Steel in Concrete.* Stockolm: Swedish Cement and Concrete Research Institute, 469.

[2] Klein, D., Gastal, F., Campanolo, J. L., and Son, L. C. S. 1991. "Criteria Adopted in the Survey and Evaluation of Works of Art." Presented at XXV South American Structural Engineering Conference, Porto Alegre, Brazil.

[3] Castro, E. K. 1994. "Development of Methodology for Maintenance of Reinforced Concrete Structures." Master thesis, University of Brasilia.

[4] Lopes, B. A. R. 1998. "System of Structural Maintenance for Large Inventories of Buildings: Study for Inclusion of Concrete Structure Component." Dissertation in Structures, University of Brasilia.

[5] Boldo, P. 2002. "Qantitative Assessment of Reinforced Concrete Structures of Buildings within the Brazilian Army." M.Sc. thesis, Department of Civil and Environmental Engineering, University of Brasilia.

[6] Lemos, S. P. P. 2006. "Degree of Damage Assessment of Underground Structures of Three Buildings Located in the Metropolitan Area of Recife, Pernambuco." M.Sc. thesis, Department of Civil Engineering, Catholic University of Pernambuco.

[7] ABNT (Associação Brasileira de Normas Técnicas). 2014. *Design of Concrete Structures—Procedure. NBR 6118.* Rio de Janeiro: ABNT.

[8] ABNT (Associação Brasileira de Normas Técnicas). 2013. *NBR 8802: Hardened Concrete—Determination of the Ultrasonic Wave Propagation Velocity*. Rio de Janeiro: ABNT.

[9] Rincón, O. T., Carruyo, C. A., Helene, P., and Diaz, I. 1998. "Manual Inspection, Evaluation and Diagnosis of Corrosion of Reinforced Concrete Structure." In *Last: Thematic Network XV. B Armor Durability.* Madrid: Ibero-American Science and Technology for Development.

[10] ABNT (Associação Brasileira de normas técnicas). 1978. *Design and Execution of Works of Reinforced Concrete (NB-1).* Rio de Janeiro: ABNT.

[11] ABECE (Associação Brasileira de Engenharia e Consultoria Estrutural). 2005. *Check List for Inspection of Buildings in Reinforced Concrete.* São Paulo: ABECE.

[12] Zarzar, F. C. J. 2007. "Method for Estimating the Life Span of Construction Elements, Based on the Method of Factors." Master thesis, Unicap (Catholic University of Pernambuco).

Journal of Civil Engineering and Architecture 10 (2016) 81-95
doi: 10.17265/1934-7359/2016.01.009

Restraint Usage Characteristics and Other Factors Associated with Safety of Children Involved in Motor Vehicle Crashes

Sunanda Dissanayake[1] and Niranga Amarasingha[2]

1. Department of Civil Engineering, Kansas State University, Manhattan KS 66506, USA

2. Department of Civil Engineering, Sri Lanka Institute of Information Technology, Malabe, Sri Lanka

Abstract: Involvement in road traffic crashes as vehicle occupants is a leading cause of death and serious injury among children. The objective of this study was to investigate crash severity factors and child safety restraint use characteristics in order to identify effective countermeasures to increase children's highway safety. Characteristics and percentages of restraint use among child passengers aged 4~13 years were examined using highway crash data from Kansas. The association between restraint use, injury severity and characteristics of children involved in crashes were investigated using OR (odds ratios) and a logistic regression model, which was used to identify risk factors. Results showed that children, who were unrestrained, were seated in the front seat, traveling with drunk drivers and on rural roads, and traveling during nighttime was more vulnerable to severe injury in the case of motor vehicle crashes. The most frequent contributing causes related to crashes involving children included driver's inattention while driving, failure to yield right-of-way, driving too fast, wet roads and animals in the road. Based on identified critical factors, general countermeasure ideas to improve children's traffic safety were suggested, including age-appropriate and size-appropriate seat belt restraints and having children seated in the rear seat. Parents and children must gain better education regarding these safety measures in order to increase child safety on the road.

Key words: Child safety, child restraint use, severity model, logistic regression model, crash data analysis.

1. Introduction

Motor vehicle crash involvement is the leading cause of death among children aged 4~13 years in the United States, according to the data reported by CDC (Centers for Disease Control and Prevention). From 2004 to 2007, a total of 3,809 fatalities due to injuries sustained in car crashes were reported among 4- to 7-year-old children and were the primary cause of death among this age group. According to CDC data, the leading cause of death among children aged 8~13 years was also traffic-related injuries, indicating a total of 5,234 fatalities. These motor vehicle crashes accounted for 51% of child deaths from unintentional injuries. Over the last few decades, the safety of child occupants in motor vehicle crashes has become a major concern. Despite efforts to improve child passenger safety, the continued improvement of children's traffic safety remains a national need.

Child restraints are expected to hold children in place and prevent them from being ejected from the vehicle or hitting the vehicle interior, while simultaneously avoiding dangerous levels of crash force on vulnerable areas of a child's body [1, 2]. Child restraint systems refer to the use of child safety seats restrained by seat lap belts as recommended by the *Federal Motor Vehicle Safety Standard* [2]. Children aged 4~7 years are restrained in the vehicle in booster seats. Proper restraining of children is the responsibility of parents or drivers since children do not have enough understanding of safety and typically are not aware of the risks associated with lack of safety

Corresponding author: Sunanda Dissanayake, Ph.D., P.E., professor, research fields: traffic engineering, highway safety, restraint usage and children's safety.

restraints. Older children might demonstrate a simpler understanding of why they wear seat belts, more so than the younger drivers. Typically, children are affected by parental influence and a desire to comply with the rules. Some children may express a desire not to wear their seatbelts and resist when parents tell them to buckle their safety belts. Hence, child passengers are different than other passengers, and it is important to give attention to this age group because this is when they begin to make independent decisions to wear their seat belts or not.

The main objective of this study was to investigate severity factors related with crashes involving children, with special focus on restraint usage, in order to identify effective countermeasures to increase children's highway safety. Objectives of this paper include the examination of various risk factors for children in crashes, such as failure to use restraint, riding with a drunk driver and child safety restraint usage characteristics. Seating position of the child passenger in the vehicle was also studied since seating position in the vehicle at a crash may contribute to injury risk. According to likelihood ratios of the developed model, potential actions that may improve safety of children involved in crashes are suggested.

2. Literature Review

Many researchers have evaluated the association between child restraint use and crash characteristics [1, 3]. The NOPUS (National Occupant Protection Use Survey), which collects detailed information regarding national-level shoulder belt and child restraint use levels as required by the NHTSA (National Highway Traffic Safety Administration), is often used by researchers to study child safety restraint characteristics of children under 12 years old. According to NOPUS data in 2009, observed seat belt restraint use among 4- to 7-year-old children in the US was 87%, which was slightly higher than 85% restraint use of children aged 8~12 years [4]. Child seat restraint system effectiveness has also been assessed using morbidity data taken from emergency departments or hospitals [1]. A few studies have been based on data from fatality databases, such as FARS (Fatality Analysis Reporting System) and state crash databases [4-6].

Agran et al. [7] investigated restraint use of children in fatal crashes in relation to vehicle and driver characteristics. Based on this study, restraint use of children was as low as 31% in older vehicles, 54% in rural areas and 23% between the hours of 3 a.m. and 6 a.m. The developed logistic regression models showed that restraint use declined with increasing number of occupants. As the age of children increased, the percentage of fatally injured children who were unrestrained also increased. Hence, child-occupant restraint use under all conditions of travel and all seating positions must be stressed by child-occupant protection counseling. Miller et al. [8] identified significant risk factors with the presence of a second adult in children-involved crashes involving a male driver, night driving, driving under the influence of alcohol, other moving or non-moving violations and the driver being unrestrained. Results showed that, as drivers got older, they were more likely to secure a baby in a child seat than ensure that the older children buckle up. Mature drivers in suburban areas were significantly more likely to restrain children than other drivers. A male driver, a young driver, a drunken driver and a nighttime trip each raised the likelihood of children being unrestrained when children were involved in crashes. The study pointed out that, other than programs promoting child safety and booster seats for the youngest children, few programs emphasize occupant restraint as the driver's responsibility.

Incidence rates of incapacitating injuries and risk ratios have been used to evaluate differences in injury risks to various regions of the body, based on restraint use among children involved in crashes [9]. Results indicated that use of child safety seats effectively reduces incidence rates of incapacitating injuries for children involved in frontal, side impact or rollover crashes. In near-side impacts, unrestrained children were 8 times more likely to sustain incapacitating injuries than restrained children. Valent et al. [10] evaluated differences in injury risks to various regions of the body according to restraint use by investigating crash ratios. Compared with unrestrained children, properly restrained children had significantly lower overall injury risk, indicating a risk ratio of 0.37. The results demonstrated that misused restraints were less effective in reducing injury risk compared with properly-used restraints. The study recommended that educational initiatives should focus on ensuring that parents know appropriate age-dependent restraint methods and how to use those restraints properly.

The double-pair comparison method was also used by Starnes [6] to examine restraint-use patterns among child occupants involved in crashes, in which a child was fatally injured. According to results, restraint use of fatally-injured child passengers and their drivers were strongly correlated. Child passengers were far more likely to be unrestrained if the driver was also unrestrained. Olsen et al. [11] used generalized estimating equations to estimate relative risk for child, driver and crash characteristics for restrained drivers as compared to unrestrained drivers. Restrained drivers with restrained children were less likely to exhibit risky behaviors, including intoxication, speeding, prior traffic violations and involvement in injury crashes. The study identified overall associations between driver restraint use and lower risk of child emergency department evaluations. Vehicle and crash characteristics were associated with more severe outcomes in children. The recommendation was made that mechanisms to increase safe-driving practices of drivers transporting child passengers could potentially decrease the number of child passenger injuries from crashes. Quinlan et al. [12] examined the characteristics of crashes involving child passenger death and injuries associated with drunken drivers and identified opportunities to prevent such crashes. Approximately 64% of fatal crashes occurred when a child was riding with a drunken driver. Of drivers involved in a crash in which a child passenger died, drunken drivers were more likely to have been previously convicted of driving while intoxicated or to have had their licenses suspended or revoked. The study also showed that a majority of drunken-driver-related child passenger deaths occurred when the child was unrestrained. The recommendation was made that further reduction of unacceptable risks of child passenger injury and death associated with alcohol-impaired drivers could be accomplished through legal, medical and educational interventions.

3. Data

This study used highway crash data from the KCARS (Kansas Crash Analysis and Reporting System) database, which is comprised of all police-reported crashes in Kansas above a certain property damage threshold ($1,000 for the data set considered here). Data on children involved in crashes from 2004 to 2008 traveling by a motorized vehicle covered under the *Kansas Child Passenger Safety Act*, such as an automobile, van, pick-up truck or sport utility vehicle, were extracted for consideration and analysis. Children between 4~13 years old traveling with adult drivers were selected as the focus group, based on restraint-use requirements in Kansas. Two different sub-age group categories were also considered for analysis as follows:

- children between 4 and 7 years, who are supposed to be restrained in booster seats unless weighing more than 80 pounds and taller than 57 in.;
- children between 8 and 13 years, who are supposed to be seat-belted.

The KCARS database includes details about restraint use for all vehicle occupants, including non-injured occupants. Records also contain information regarding crash circumstances, such as weather conditions at the time of the crash, road and light conditions, vehicle-related information and driver-related information. Occupant information consists of age, gender, exact position within the vehicle, use of safety restraint and injury severity among many others. The KCARS database covering five years contained 50,155 records of children aged 4~13 years involved in crashes.

4. Methods

This section describes the methodology adopted to identify important characteristics affecting child passengers involved in crashes. First, percentages of restraint use among child passengers involved in crashes in each age group were examined using KCARS data, and RR (relative risk) ratios of the older child sub-group were calculated in comparison to younger child passenger sub-group. Second, drivers were paired with each crash-involved child in the vehicle according to the double-pair comparison method because driver characteristics could be stronger predictors of child restraint use [12]. This method has been commonly used in child passenger safety literature if the driver and at least one child occupant are in a vehicle involved in a crash. Two occupants in the vehicle are referred to as subject occupant and control occupant. Subject occupant is the person whose characteristics are used to determine injury risk or restraint use. The control occupant standardizes the conditions to investigate restraint usage effectiveness of the subject occupant. In this study, the control occupant is the driver of the child involved in a crash, while the subject occupant is the child passenger. For example, a driver with two crash-involved children in the vehicle was included in two separate driver-passenger pairs, once for each child with the driver. Accordingly, different driver characteristics were determined for child passengers' restraint use and injury risk.

4.1 Logistic Regression Analysis

Logistic regression analysis was used to determine the relative effect of child restraint system usage when children are involved in crashes. Injury severity was selected as the dependent variable in a model investigating characteristics of restraint use. The dependent variable (injury severity) has several discrete categories. The dichotomous nature of the dependent variable facilitates the application of logistic analysis, for which the probability of injury against no-injury categories is estimated by the maximum likelihood method [13]. In the logistic model, a dependent variable is formulated by the following expression:

$$g(x) = \beta_0 + \beta_1 x_1 + \beta_2 x_2 + ... + \beta_j x_j + ... + \beta_p x_p \quad (1)$$

where:

$g(x)$ = independent variables formulated in the logistic model;

x_j = value of the jth independent variable;

β_j = corresponding coefficient of the jth independent variable;

p = number of independent variables.

With the independent variables, the conditional probability of a positive outcome is determined by:

$$\pi(x) = \frac{\exp\left(g(x)\right)}{1 + \exp\left(g(x)\right)} \quad (2)$$

where, $\pi(x)$ = conditional probability.

The maximum likelihood method is then employed to measure the associations by constructing the likelihood function as follows:

$$l(\beta) = \prod_{i=1}^{n} \pi(x_i)^{y_i} \left(1 - \pi(x_i)\right)^{1-y_i} \quad (3)$$

where:

$l(\beta)$ = likelihood function;

$\pi(x_i)$ = conditional probability of the dependent variable;

y_i = ith observed outcome, with the value of either 0 or 1 only;

i = 1, 2, 3,…, n, where n is the number of observations.

The log likelihood expression is considered to maximize the likelihood function in order to obtain the coefficients estimates:

$$LL(\beta) = \ln(l(\beta)) = \sum_{i=1}^{n}\left\{y_i \ln\left(\pi\left(x_i\right)\right)+\left(1-y_i\right)\ln\left(1-\pi\left(x_i\right)\right)\right\} \quad (4)$$

where:

$LL(\beta)$ = log likelihood function;

$l(\beta)$ = likelihood function;

$\pi(x_i)$ = conditional probability of the dependent variable;

y_i = ith observed outcome with the value of either 0 or 1 only;

i = 1, 2, 3,…, n, where n is the number of observations.

Maximization typically requires an iterative numerical method, which means that it involves successive approximations. Hence, the best estimate of β could be obtained by a numerical method using statistical software.

4.2 Goodness-of-Fit Measure

The goodness-of-fit of the predictive model could be assessed for significance and predictive power of the logistic regression model. To evaluate it, the change in deviance can be determined by comparing log likelihood functions between the unrestricted model and the restricted model, under the null hypothesis that coefficients for the predictive model are equal to 0, with the following expression [13]:

$$G = -2(LL(c) - LL(\theta)) \quad (5)$$

where:

$LL(c)$ = log likelihood function of the restricted model;

$LL(\theta)$ = log likelihood function of the unrestricted model;

G = goodness-of-fit value.

If G is significant at the 5% level, the null hypothesis would be rejected and the conclusion could be made that the proposed model generally fit well with the observed outcome.

The LR (likelihood ratio) test is the chi-square test where at least one of the predictors' regression coefficients is not equal to 0 in the model. The LR chi-square statistic can be calculated by:

$$LR = -2\log L(\text{null model}) - 2\log L(\text{fitted model}) \quad (6)$$

where:

L(null model) = intercept-only model;

L(fitted model) = intercept and covariates model.

The score chi-square test shows at least one of the predictors' regression coefficients is not equal to 0 in the model.

Another used goodness-of-fit measure is the AIC (Akaike information criterion), which is calculated as:

$$AIC = -2\log L + 2((k - 1) + s) \quad (7)$$

where:

L = likelihood of the model;

k = number of levels of the dependent variable;

s = number of predictors in the model.

The AIC is used for comparison of models from different samples or non-nested models. Ultimately, the model with the smallest AIC is considered the best. The SC (Schwarz criterion), which is also considered in evaluating goodness-of-fit, is defined as:

$$SC = -2\log L + ((k - 1) + s) \times \log(\Sigma f_i) \quad (8)$$

where:

L = likelihood of the model;

f_i = frequency values of the ith observation;

k = number of levels of the dependent variable;

s = number of predictors in the model.

Like AIC, SC penalizes for the number of predictors in the model, and the smallest SC is most desirable.

4.3 Multicollinearity

In some cases, logistic regression results may seem paradoxical, meaning the model fits the data well, even though no independent variables have a statistically-significant impact on predicting the dependent variable. In many situations, this occurs because of the correlation of two independent variables. Neither variable may contribute significantly to the model after the other one is included. However, model fit will be worse if both variables are removed from the model because the independent variables are collinear and the results show multicollinearity. The goal of traffic safety analysis is to understand how various independent variables impact the dependent variable; Hence, multicollinearity is a considerable problem [14]. One issue is that, even though the variable is important, model results show that it is not significant. The second problem is that the confidence intervals on model coefficients will be very wide. To assess multicollinearity, the correlation matrix of the independent variables can be investigated. If the element of correlation matrix has high value, model fit is affected by multicollinearity of the independent variable correspondent to that element. Also, each independent variable can be predicted from other independent variables. The model-fit statistics, such as individual R^2 value and a *VIF* (variance inflation factor), are high for any independent variable, and model fit is affected by multicollinearity.

4.4 Odds Ratios

To measure the strength of association between variables, OR (odds ratios) and 95% confidence intervals were calculated. The OR is a widely-used statistics in traffic safety studies to compare whether the probability of a certain event is the same for two groups [13]. An odds ratio greater than 1.00 indicates that the concerned attribute leads to a higher injury risk and vice versa. Univariate and multivariate techniques were used for analysis. Univariate techniques are those which utilize only a single independent variable, while multivariate techniques provide a linear combination of independent variables that satisfy statistical criteria.

5. Results

According to restraint-use percentages of children in crashes based on injury severity, restraint use was very low among fatally-injured child passengers, whereas restraint use was higher in the not-injured group. Age distribution of drivers for children involved in crashes indicates that a majority of children were traveling with 25- to 44-year-old drivers at the time of a crash. Results in Table 1 show that the straight-following road was the predominant crash type for children involved in crashes. Vehicle maneuver observation is important because it offers reasons for movements and actions that a driver may have performed, in case of a crash. Collision with a vehicle was the primary crash type; Non-collisions and overturning of vehicles occurred less frequently. A majority of crashes occurred during daytime hours and during weekdays, where children are more likely to be traveling. Majority of children were involved in crashes occurring in the afternoon and evening. In relation to most characteristics, calculated RR values of 8- to13-year-old children compared to 4- to 7-year-old children were above 1.00, as shown in Table 1. Those numbers also show that children aged 8~13 years had higher risk for injuries in crashes compared to children aged 4~7 years.

Table 2 shows child passenger and driver characteristics of crashes involving children, as well as older passenger and driver characteristics for other crashes. Unrestrained children had significantly higher rates of incapacitating injuries in side impacts than restrained children. Driver-injury-severity distribution indicates the driver was not injured in most crashes involving children. Gender distribution shows female drivers ride more frequently with children at the time of crashes. The proportion of female drivers was higher in crashes where children aged 4~7 years were involved than children aged 8~13 years. A considerable number of violations, such as failure to use the safety belt, alcohol involvement and lack of a valid license, can be observed among drivers riding with children involved in crashes. The gender of the child passenger was somewhat equally distributed among children involved in crashes. In addition, a considerable percentage of children aged 4~7 years who were supposed to be in booster seats were restrained by only seat belts. Approximately 93% of child passengers were restrained at the time of the crash. According to observational studies in Kansas, seat belt usage rate was approximately 77% in 2011, significantly less than the rate determined by crash data. Furthermore, the

Table 1 Vehicle-related and environmental-related characteristics for crashes involving children.

Characteristic	Children (4~7 years)		Children (8~13 years)		All children (4~13 years)		Child (8~13 years) passenger RR*
	Number	Percentage (%)	Number	Percentage (%)	Number	Percentage (%)	
Vehicle maneuver							
Straight-following road	12,987	60	17,367	60	30,354	61	1.15
Turn or changing lanes	2,947	14	4,304	15	7,251	14	0.94
Avoiding maneuver	552	3	703	2	1,255	3	1.32
Stopped, parking or backing	4,918	23	6,592	23	11,510	23	1.39
Other	119	1	128	0	247	0	2.10
Accident class							
Collision with a vehicle	16,505	73	21,923	75	38,428	74	1.13
Collision with pedestrian/animal	2,872	13	4,357	15	7,229	14	0.88
Collision with an object	2,872	13	1,989	7	4,861	9	1.40
Other non-collision and overturned	516	2	912	3	1,428	3	1.34
Light conditions							
Daylight	15,960	75	20,936	72	36,896	73	1.17
Not daylight	5,285	25	8,181	28	13,466	27	1.21
Weather conditions							
No adverse conditions	18,055	85	24,768	86	42,823	85	1.18
Rain	1,908	9	2,667	9	4,575	9	1.13
Adverse conditions	1,255	6	1,646	6	2,901	6	1.10
Time of crash							
5:00~9:00	2,343	11	3,209	11	5,552	11	1.12
9:00~13:00	4,015	19	4,492	16	8,507	17	1.12
13:00~17:00	6,759	32	9,120	32	15,879	32	1.16
17:00~21:00	6,417	30	9,188	32	15,605	32	1.13
21:00~5:00	1,685	8	2,912	10	4,597	9	1.24
Day of week							
Weekdays	15,402	73	19,858	69	35,260	70	1.19
Weekend	5,824	27	9,066	31	14,890	30	1.13

*RR of 8- to 13-year-old children compared to 4- to 7-year-old children;
Unknowns are not listed.

older-child group demonstrated greater risk than the younger-child group by showing RR values greater than 1.00, in all characteristics except ejection from the vehicle.

As indicated in Table 3, most 4- to 7-year-old children were involved in crashes occurring on urban collectors, while a higher proportion of crashes occurred at non-intersections on roadways where children aged 8~13 years were involved. Many crashes took place under no adverse weather conditions and a significant number of crashes occurred in adverse conditions. Crashes on dry roads and straight and level surfaces were the most prevalent crash conditions for children involved in crashes. In most cases, the vehicle was functional after the crash, thus reflecting the findings of many children-involved crashes in Kansas as belonging to the “not injured” category. The investigation of restraint use among children involved in crashes revealed that restraint use decreases with an increased number of occupants in the vehicle. Use of restraints was substantially lower in older vehicles and crashes that occurred during late night and early morning hours. Driver restraint use strongly influenced restraint use of children, such that children were more likely to be restrained in vehicles with restrained drivers. When the driver was restrained, 93% of children

Table 2 Child passenger and driver characteristics for crashes involving children.

Characteristic	Children (4~7 years)		Children (8~13 years)		All children (4~13 years)		Child (8~13 years) passenger RR*
	Number	Percentage (%)	Number	Percentage (%)	Number	Percentage (%)	
Child passenger injury severity							
Fatal injury	22	0	28	0	50	0	-
Disabled (incapacitating)	91	0	180	1	271	1	-
Injury, not incapacitating	786	4	1,358	5	2,144	4	-
Possible injury	1,200	6	1,771	6	2,971	6	-
Not injured	18,128	90	24,363	88	42,491	89	-
Child passenger gender							
Female	10,349	49	14,689	51	25,038	50	1.22
Male	10,877	51	14,448	50	25,325	50	1.11
Child passenger safety restraint							
Child/booster seat used	10,955	51	661	2	11,616	23	1.31
Seat belt used	8,965	42	25,938	90	34,903	70	1.07
None	709	3	1,246	4	1,955	4	1.19
Child ejection							
Ejected	36	0	122	0	158	0	1.11
Not ejected	19,934	99	27,376	99	47,310	99	1.15
Trapped	79	0	74	0	153	0	1.93
Driver injury severity							
Fatal injury	34	0	46	0	80	0	1.74
Disabled (incapacitating)	146	1	226	1	372	1	2.88
Injury, not incapacitating	1,077	5	1,570	6	2,647	5	1.39
Possible injury	1,548	8	2,008	7	3,556	7	1.12
Not injured	17,367	86	23,776	86	41,143	86	1.27
Driver gender							
Female	14,245	67	18,265	63	32,510	64	1.18
Male	7,025	33	10,901	37	17,926	36	1.17
License compliance							
Valid license	19,778	94	27,271	94	47,049	94	1.17
Not licensed or invalid license	1,295	6	1,660	6	2,955	6	1.31
Driver safety belt used	20,569	97	27,269	94	47,838	95	1.14
Alcohol related	140	1	185	1	325	1	1.35
Driver ejection							
Ejected	59	0	65	0	124	0	0.96
Not ejected	20,022	99	27,301	99	47,323	99	1.16
Trapped	48	0	136	0	184	0	1.19

*RR of 8- to 13-year-old-children compared to 4- to 7-year-old children;
Unknowns are not listed.

aged 4~7 years were restrained. When the driver was unrestrained, 56% of children passengers were restrained. In the older-child group, the percentage of unrestrained children increased whether they were traveling with unrestrained drivers or restrained drivers. In the older-child age group, 58% of children were not restrained when the driver was unrestrained, while 94% of children were restrained when riding with a restrained driver. Child restraint use was lower in rural areas compared to urban areas. Driver alcohol use was associated with lower restraint use, most likely indicative of high-risk drivers who are less likely to

Table 3 Road-related and vehicle-related characteristics for crashes involving children.

Characteristic	Children (4-7 years)		Children (8-13 years)		All children (4-13 years)		Child (8~13 years) passenger RR*
	Number	Percentage (%)	Number	Percentage (%)	Number	Percentage (%)	
Functional class							
Rural roads	1,318	6	4,178	14	5,496	11	1.21
Urban interstate	1,270	6	108	0	1,378	3	0.57
Urban arterial	111	1	9,515	33	9,626	19	1.15
Urban collector	7,503	35	1,892	7	9,395	19	1.19
Urban local street	3,865	18	3,574	12	7,439	15	1.11
Unknown	7,159	34	9,662	33	16,821	34	1.17
Crash location							
Non-intersection-on roadway	10,854	51	15,034	52	25,888	51	1.20
Intersection-on roadway	9,734	46	13,128	45	22,862	45	1.10
Off roadway	687	3	1,020	4	1,707	3	1.52
Road surface condition							
Dry	17,191	81	23,576	81	40,767	81	1.16
Wet	2,532	12	3,493	12	6,025	12	1.17
Debris	1,493	7	2,017	7	3,510	7	1.27
Work zone	605	0	780	0	1,385	0	1.25
Road surface character							
Straight and level	15,952	75	21,828	75	37,780	75	1.14
Straight not level	4,020	19	5,583	19	9,603	19	1.15
Curved	1,187	6	1,605	6	2,792	6	1.61
Vehicle damage							
None	537	3	727	3	1,264	3	1.32
Damage	6,036	29	8,251	28	14,287	28	1.22
Functional	8080	38	11,028	38	19,108	38	1.09
Disabling	5,597	26	7,649	26	13,246	26	1.16
Destroyed	918	4	1,387	5	2,305	5	1.37
Vehicle body type							
Automobile	9,100	43	12,523	43	21,623	43	1.10
Van	5,022	24	6,140	21	11,162	22	1.24
Pickup-truck	2,217	10	3,705	13	5,922	12	1.11
Sport utility vehicle	4,890	23	6,680	23	11,570	23	1.30
Other	48	0	106	0	154	0	0.76

*RR of 8- to 13-year-old-children compared to 4- to 7-year-old children;
Unknowns are not listed.

restrain children.

Approximately 94% of children were restrained by valid driver license holders, but only 83% of children were restrained by invalid license holders or drivers that were not licensed. Only 11% of crash-involved children were in the middle seating position of the rear seat, but almost 66% of children travelled in the rear seat. According to percentages of restrained children by seating position, children traveling in the front seat were less likely to be restrained than children traveling in the rear seats. Children who travelled in left and right rear-seating positions indicated a high percentage of restraint use. Restraint use among children involved in crashes decreased with increased age.

Table 4 shows the odds of univariate and multivariate analysis. Child passengers traveling with valid licensed and restrained drivers were lower in injury risk. Investigating odds of child-passenger-related

Table 4 Odds ratios for injury of children involved in crashes.

Characteristic		Univariate OR (odds ratio)	Multivariate Analysis		
			Odds ratio	95% confidence interval	
				Lower bound	Upper bound
Driver-related characteristics					
Male		0.994	0.993	0.904	1.091
Valid licensed		0.538	0.851	0.734	0.987
Safety belt used		0.174	0.621	0.541	0.712
Alcohol-related		5.035	1.932	1.292	2.889
Ejected		17.245	0.829	0.285	2.398
Child-related characteristics					
Child seat		0.682	0.293	0.243	0.354
Seat belt		0.640	0.334	0.286	0.390
Ejected		60.684	24.968	11.760	53.013
Rear seat		0.789	0.917	0.832	1.011
Environmental-related characteristics					
Not daylight		0.939	0.861	0.736	1.007
Weather	No adverse conditions	1.063	0.686	0.330	1.426
	Rain	0.998	0.792	0.368	1.629
	Adverse conditions	0.812	1.000	-	-
Time	5:00~9:00	1.006	0.946	0.824	1.086
	9:00~17:00	1.000	1.000	-	-
	17:00~21~00	0.971	0.993	0.888	1.109
	21:00~5:00	1.200	1.194	0.951	1.499
Week days		0.973	1.042	0.944	1.151
Road-related characteristics					
Rural roads		1.472	1.082	0.967	1.211
Location	Non-intersection-related	1.230	0.888	0.796	0.991
	Intersection-related	1.000	1.000	-	-
	Off roadway	3.339	1.012	0.807	1.268
Road surface condition	Dry	0.604	0.736	0.371	1.461
	Wet	0.608	0.865	0.426	1.755
	Debris	1.000	1.000	-	-
Surface character	Straight and level	0.875	0.888	0.796	0.991
	Straight not level	1.150	1.012	0.807	1.268
	Curved	1.000	1.000	-	-
Vehicle-related characteristics					
Vehicle damage	None	1.000	1.000	-	-
	Minor damage	0.709	0.775	0.310	1.934
	Function	1.107	1.152	0.463	2.865
	Disabling	5.347	4.720	1.902	11.717
	Destroyed	22.383	16.072	6.422	40.223
Vehicle	Automobile	0.489	0.821	0.232	2.902
	Van	0.262	0.546	0.154	1.937
	Pick-up truck, camper recreational vehicle	0.299	0.555	0.157	1.961
	Sport utility vehicles	1.000	1.000	-	-

variables, restrained children showed significantly lower risk than unrestrained. The odds ratio of rear seating was less than 1.00, indicating rear seating reduced injury risk for child passengers. An important risk factor was ejection, which may be due to failure to restrain. The odds ratios of environmental-related variables were not statistically significant at the 95% confidence interval. Injury risk on rural roads in which a child passenger was involved in crashes was higher than on urban roads in Kansas. Off-roadways showed a higher injury risk for children, and injury risk on dry roads was lower than wet roads when child passengers were involved in crashes. Also, riding on straight, level road surfaces was a significantly lower injury risk than travelling on curved or unleveled road surfaces. In the case of a crash, the child would be at a higher injury risk if the vehicle was disabled or destroyed, compared to a vehicle which did not sustain damage.

5.1 Logistic Regression Model

A logistic model was developed to further investigate child passenger injury and the dependent variable. Injury severity is defined as a binary variable depending on whether the child is injured or not injured. All other crash, vehicle, roadway, environment, driver and passenger attributes were used as independent variables. According to estimated coefficients in Table 5, male children were less likely to be injured when involved in crashes than female children. If the child was in a child seat, injury severity was less. Children using seat belts were less likely to suffer injuries when involved in crashes. If the child passenger was ejected or trapped, or if the vehicle was destroyed or disabled, the child had a high chance of injury. If the driver had a valid driving license, the vehicle was newer, and it did not get damaged, had minor damage, or was functional at the time of crash, child passengers were less likely to suffer injuries. Alcohol involvement of the driver, travelling on rural roads, travelling by automobile or pick-up trucks or travelling at high speeds showed high injury risk for child passengers.

5.2 Contributory Causes

Many factors combine to produce circumstances leading to a traffic crash; A single cause is rare. Contributing causes related to children involved in crashes are provided in Table 6. Inattention and failing to give enough time and attention to the driving task were the most frequent driver factors in child-involved crashes. When the contributory cause was distraction, reckless/careless/aggressive driving, alcohol involvement or restricted driver license, child-restraint use was significantly low. There were occasions when the driver had to react to unexpected events. Therefore, road conditions and surrounding conditions must be considered as primary factors, important for safe driving. Roadway-related contributory causes include wet, debris or icy roads as main factors. Child-restraint use was lower in rain, snow, smog or cloudy environmental contributory crashes. Tires and brakes were the most common vehicle-contributing causes for crashes involving children. Presence of one or more of these contributory causes does not prove that a child is being harmed or is at risk of harm, but it can alert to the possibility that a child may be at risk.

6. Countermeasures

The developed logistic regression model identified risk factors which increase injury severity. Safety-restraint use is one of the most highly significant variables that could reduce child-injury risk. Hence, age-appropriate and size-appropriate restraints can be used as an effective strategy for reducing injury severity of children involved in crashes and reducing costs associated with those crashes. Many efforts have been taken to increase age-appropriate and size-appropriate restraints for children. This analysis showed that many children are still transported without appropriate restraints. Therefore, continued efforts are needed to increase child-safety-restraint usage, especially in rural areas and during nighttime. Different strategies are necessary to increase child restraint use compared to adult seat belt use, as issues associated with increasing child restraint use are different than those for increasing adult seat belt use.

Table 5 Models fit statistics and maximum likelihood estimates.

Label	Parameter definition	Coefficient	*p*-value
Intercept	Intercept	−8.66	0.946
AGE	If 4~7 years, *AGE* = 1; 8~13 years, *AGE* = 0	−0.024	0.587
DRMALE	If driver is a male, *DRMALE* = 1, otherwise 0	−0.049	0.206
CHIMALE	If child is a male, *CHIMALE* = 1, otherwise 0	−0.199	< 0.0001*
SEAT	If front seating, *SEAT* = 1, otherwise 0	0.069	0.395
	If rear seating, *SEAT* = 1, otherwise 0	−0.026	0.716
VALID	If valid license, *VALID* = 1, otherwise 0	−0.124	0.045*
SEATB	If seat belt used, *SEATB* = 1, otherwise 0	−1.291	< 0.001*
	If child seat used, *SEATB* = 1, otherwise 0	−1.439	< 0.001*
AIRB	If airbag used, *AIRB* = 1, otherwise 0	1.219	< 0.001*
ALCO	If alcohol-related, *ALCO* = 1, otherwise 0	0.033	0.036*
DARK	If dark or night, *DARK* = 1, otherwise 0	0.074	0.243
WTHER	If good weather, *WTHER* = 1, otherwise 0	−0.062	0.83
	If rain, *WTHER* =1, otherwise 0	−0.553	0.851
	If adverse condition, *WTHER* = 1, otherwise 0	−0.212	0.475
TIME	If 5:00~9:00 a.m., *TIME* = 1, otherwise 0	−0.074	0.679
	If 9:00 a.m.~1:00 p.m., *TIME* = 1, otherwise 0	−0.104	0.555
	If 1:00~5:00 p.m., *TIME* = 1, otherwise 0	−0.043	0.803
	If 5:00~9:00 p.m., *TIME* = 1, otherwise 0	−0.04	0.813
	If 9:00 p.m.~1:00 a.m., *TIME* = 1, otherwise 0	−0.082	0.638
WEEK	If weekday, *WEEK* = 1, otherwise 0	−0.022	0.578
RDFUNC	If rural roads, *RDFUNC* = 1, otherwise 0	−0.095	0.108
	If urban interstate, *RDFUNC* = 1, otherwise 0	−0.208	< 0.001*
	If urban collector/local, *RDFUNC* = 1, otherwise 0	−0.219	0.001*
NEW	If vehicle made later than the year of 2000, *NEW* = 1, otherwise 0	−0.142	< 0.001*
SPD LIM	On-road speed limit	0.006	0.001*
Likelihood Ratio		7,337	< 0.001*
Score		9,016	< 0.001*
−2log*L*		23,170	-
CLASS	If non-collision or overturned, *CLASS* = 1, otherwise 0	9.967	0.938
	If collision with pedestrian or animal, *CLASS* = 1, otherwise 0	70.176	0.955
	If collision with vehicle=1, otherwise 0	0.591	0.94
	If collision with fixed object=1, otherwise 0	0.684	0.94
WZONE	If work zone, *WZONE* = 1, otherwise 0	−0.132	0.245
DAMEGE	If vehicle does not damage, *DAMEGE* = 1, otherwise 0	−0.601	0.029*
	If minor damage, *DAMEGE* = 1, otherwise 0	0.997	< 0.001*
	If driver and four passengers, *DAMEGE* = 1, otherwise 0	0.014	0.899
	If driver and five passengers, *DAMEGE* = 1, otherwise 0	−0.128	0.221
BODY	If automobile, *BODY* = 1, otherwise 0	0.35	< 0.001*
	If van, *BODY* = 1, otherwise 0	0.047	0.423
	If pick-up truck or camper rv, *BODY* = 1, otherwise 0	0.216	0.001*
MANEU	If straight-following road, *MANEU* = 1, otherwise 0	−0.544	0.002*
	If turn or changing lanes, *MANEU* = 1, otherwise 0	−0.67	< 0.001*
	If avoiding maneuver, *MANEU* = 1, otherwise 0	−0.579	0.003*
	If stopping, parking or backing, *MANEU* = 1, otherwise 0	−0.349	0.048*

(Table 5 continued)

EJECT	If child eject, *EJECT* = 1, otherwise 0	2.45	< 0.001*
	If child did not eject, *EJECT* = 1, otherwise 0	−0.841	< 0.001*
	If child trapped, *EJECT* = 1, otherwise 0	1.831	< 0.001*
ROADCHA	If straight and level, *ROADCHA* = 1, otherwise 0	−0.364	0.095
	If straight not level, *ROADCHA* = 1, otherwise 0	−0.303	0.171
	If curved, *ROADCHA* = 1, otherwise 0	−0.274	0.23
ROADWY	If off roadway, *ROADWY* = 1, otherwise 0	−0.26	0.905
	If non-intersection on roadway, *ROADWY* = 1, otherwise 0	−0.349	0.872
	If intersection on roadway, *ROADWY* = 1, otherwise 0	−0.085	0.969
AIC		23,286	-
SC		23,789	-

*Significant at 95% confidence level.

Table 6 Driver contributory factors for children involved in crashes.

Contributory causes		Number of children-involved crashes	Child restraint system used	
			Frequencies	Percentages (%)
Driver causes	Inattention	8,652	8,154	94
	Failed to yield right of way	3,999	3,786	95
	Too fast	2,492	2,268	91
	Improper turn/passing/backing/signal	2,203	2,113	96
	Followed too closely	2,027	1,939	96
	Disregard traffic signs or signal	1,291	1,204	93
	Distraction	746	663	89
	Avoidance or evasive action	708	651	92
	Reckless/careless/aggressive driving	332	245	74
	Under influence of alcohol/drugs	315	249	79
Road causes	Wet	32,702	30,829	94
	Debris or obstruction	886	860	97
	Icy or slushy	534	499	93
	Ruts, holes or bumps	167	163	98
Environmental causes	Animal	4,102	4,068	99
	Rain, snow, mist or drizzle	1,047	1,010	96
	Vision obstructed	407	386	95
	Strong winds	128	117	91
	Rain, snow, smog or cloudy	77	65	84
Vehicle causes	Tires	146	129	88
	Brakes	98	96	98
	Wheel(s)	63	58	92

6.1 Child Restraint Laws

Child restraint laws require children traveling in motor vehicles to be restrained in equipment appropriate for the child's age and size. Transitioning children from child seats to booster seats, instead of directly to seatbelts, provides more safety benefit for children at least through age of eight. NHTSA [15] stated that use of booster seats reduces injury risk of children in crashes by 45%, compared to use of vehicle safety belts only. Also, laws requiring children to use restraints whenever and wherever they sit in vehicles are needed. According to results of this study, children in the front seat are more vulnerable for injury when involved in crashes. Nevertheless, a significant proportion of children involved in crashes were sitting in front seats. Currently, children are strongly recommended to be restrained in the rear center seat. In order to increase child safety, legislation could be changed to require all children less than 8 years old be restrained in the rear seat.

6.2 Enforcement

More enforcement of child restraint laws for booster seat use for children aged 4~7 years is needed. Previous enforcement efforts increased correct use of booster seats and use of safety belts by older children. Therefore, law enforcement officers should continue to increase enforcement of child passenger restraint use laws. Highly-publicized, high-visibility enforcement of child restraint laws is one of the most effective countermeasures for increasing child restraint use, as reported by NHTSA [15]. Our findings suggest that driver characteristics play an important role in child passenger crashes. According to the developed model, avoiding alcohol-involved driving is an important factor in reducing child injury risk, which is also a factor in reducing crash involvement. Hence, enforcement against drunk driving is needed, especially at locations where high alcohol use is expected. Further results showed that driver restraint use is closely associated with child restraint use. Enforcement officers should pay more attention to increasing driver restraint use, thus increasing child passenger restraint use, reducing ejection at time of crash and reducing child injury risk. Enforcement activities should be more targeted and improved toward vulnerable drivers who do not have valid driving licenses and at more critical locations where high posted speed limits exist or in rural areas as identified from the developed model. Also, reckless, careless and aggressive driving should be reduced by enforcement activities because those drivers are less likely to buckle a child into proper restraints. Investigation of attitudinal or motivational factors to increase safety restraint use would be helpful in identifying critical areas for enforcement programs.

6.3 Publicity and Education

Restraint-use campaigns and education programs focusing on the negative impact of restraint non-use and addressing issues related to low habitual seat belt use by children are effective activities to increase child restraint use. According to NHTSA [15], community-wide information in addition to enhanced enforcement campaigns and child restraint distribution in conjunction with education programs are effective activities for increasing restraint use among children. Educational programs should focus on the main contributory causes that increase child passenger risk. Drivers should try to engage less in inattentive driving, failure to yield right-of-way, driving too fast, following too closely, distracted driving, disregarding traffic signs and signals, reckless, careless, aggressive driving and travel wet roads. In particular, parents should not allow to children to ride with an alcohol-impaired driver.

Education programs at schools are effective in improving safety restraint use by children aged 8~13 years [15]. Parents need to know that they are the most influential factor in child safety and children's use of safety restraints. Older children simply forget to fasten a seat belt or feel that seat belts are uncomfortable. In such situations, parents need to mention the importance of restraint and help them buckle up. Previous researchers revealed that some parents have limited knowledge on height and weight recommendations applicable to their children in regards to restraint use. Therefore, parental education programs are a good strategy to increase restraint use among children.

7. Conclusions

In order to identify risk factors associated with children aged 4~13 years who are involved in crashes, the logistic regression model was developed. The objective of this model was to study the effect of variables contributing to higher injury risk for children involved in crashes. Based on the model, restrained children traveling with a valid driver's license holder, in a newer vehicle or on urban roads, are at lower risk of increased severity. Traveling with a drunk driver, traveling in an automobile or pick-up truck or traveling at high speeds increases the possibility of an injury crash. The most frequent contributing causes related to crashes involving children in Kansas are inattention, failing to give time and attention to the driving task, driving too fast, wet roads and animals on the travel lanes. When a contributory cause is distraction, reckless/careless/aggressive driving, alcohol involvement or restricted driver's license, child restraint use was significantly low. Based on identified factors, improving child traffic safety requires many countermeasures, including age-appropriate and size-appropriate seat belt restraints and properly restraining children in the rear seat. Parents and children must gain better education regarding these critical factors which are necessary to increase child safety on the road. Enforcement efforts to increase correct use of child restraints should also be required.

Acknowledgments

This study was funded by the KDOT (Kansas Department of Transportation) and the authors acknowledge KDOT staff, especially engineers Pete Bodyk and Chris Bortz, for their help and support in providing data.

References

[1] Johnston, C., Rivara, F. P., and Soderberg, R. 1994. "Children in Car Crashes: Analysis of Data for Injury and Use of Restraints." *Pediatric* 93: 960-5.

[2] Glass, R. J., Segui-Gomez, M., and Graham, J. D. 2000. "Child Passenger Safety: Decision about Seating Location, Airbag Exposure and Restraint Use." *Risk Analysis* 20: 521-7.

[3] Moeller, S., Berger, L., Salvador, J. G., and Helitzer, D. 2002. "How Old Is That Child? Validating the Accuracy of Age Assignments in Observational Surveys of Vehicle Restraint Use." *Injury Prevention* 8: 248-51.

[4] Pickrell, T. M., and Ye, T. J. 2010. *Occupant Restraint Use in 2009: Results from the National Occupant Protection Use Survey Controlled Intersection Study.* Report No. DOT HS 811 414, National Highway Safety Administration, U.S. Department of Transportation.

[5] Braver, E. R., Whitfeild, R., and Ferguson, S. A. 1998. "Seating Positions and Children's Risk of Dying in Motor Vehicle Crashes." *Injury Prevention* 4: 181-7.

[6] Starnes, M. 2003. *The Relationship between Driver and Child Passenger Restraint Use among Fatally Injured Child Passengers Age 0~15.* Research Note DOT HS 809 558, National Highway Traffic Safety Administration, U.S. Department of Transportation.

[7] Agran, P. F., Anderson, C. L., and Winn, D. G. 1998. "Factors Associated with Restraint Use of Children in Fatal Crashes." *Pediatrics* 102 (3): E39.

[8] Miller, T. R., Spicer, R. S., and Lestina, D. C. 1998. "Who Is Driving When Unrestrained Children and Teenagers Are Hurt?." *Accident Analysis and Prevention* 30 (6): 839-49.

[9] Hanna, R. 2010. *Children Injured in Motor Vehicle Traffic Crashes. Publication DOT HS 811 325.* Washington, D.C.: NHTSA (National Highway Traffic Safety Administration), U.S. Department of Transportation.

[10] Valent, F., McGwin, G., Hardin, W., Johnston, C., Rue III, L. W. 2002. "Restraint Use and Injury Patterns among Children Involved in Motor Vehicle Collisions." *Journal of TRAUMA Injury, Infection and Critical Care* 52 (1): 745-51.

[11] Olsen, C. S., Cook, L. J., Keenan, H. T., and Olson, L. M. 2010. "Driver Seat Belt Use Indicates Decreased Risk for Child Passenger in a Motor Vehicle Crash." *Accident Analysis and Prevention* 42: 771-7.

[12] Quinlan, K. P., Brewer, R. D., Sleet, D. A., and Dellinger, A. M. 2000. "Characteristics of Child Passenger Deaths and Injuries Involving Drinking Drivers." *JAMA* 283 (17): 2249-52.

[13] Allison, P. D. 2001. *Logistic Regression Examples Using the SAS: Theory and Application*. 1st ed. Cary: SAS Institute Inc.

[14] Anderson, D. R., Sweeny, D. J., and Williams, T. A. 2005. *Statistics for Business and Economics.* Glendale: South-Western, A Division of Thomson Learning, Inc.

[15] NHTSA (National Highway Traffic Safety Administration). 2010. *Countermeasures that Work: A Highway Safety Countermeasure Guide for State Highway Safety Offices.* 5th ed. Washington, D.C.: NHTSA.

Journal of Civil Engineering and Architecture 10 (2016) 96-107
doi: 10.17265/1934-7359/2016.01.010

Railway Accident Prevention and Infrastructure Protection

El-Miloudi El-Koursi and Jean-Luc Bruyelle

IFSTTAR (French Institute of Science and Technology for Transport, Development and Networks), Villeneuve 59666, France

Abstract: Railway accident prevention and protection are a key part of a wider picture of transport safety. The rail sector thus needs to improve its knowledge of trespassing and suicide, including at level crossing, in order to work out suitable responses by analyzing measures already taken in various countries. Governments, the rail industry and road organizations have been implementing a variety of countermeasures for many years to improve railway safety. These actions are substantial and have resulted in a continuing decrease in the number and the severity of accidents. This paper presents existing suitable techniques that are used in the preventative measures targeted to reduce railway suicides, trespassing and level crossing user accidents. It describes them in terms of their capability to effectively reduce accidents, their cost-effectiveness and their integration within the railway transport system as a whole.

Key words: Railways, safety, infrastructure, level crossing, trespassing.

1. Introduction

The rail transport mode is made more effective and efficient by the fact that it connects the most populated areas at increasingly high speeds, providing social cohesion at local level and constituting an important factor in land use planning at the national, European and international levels. The rail sector thus needs to ensure its security against accidents and suicides occurring on its property in order to offer continued service and maximum reliability. An important means to achieve this goal is the analysis of the measures already taken in various countries to address these events. Responses cannot be easily transposed from one country to another as they take into account specific cultural and sociological phenomena; Furthermore, they depend on the socio-political organization of a country and the resultant allocation of responsibilities and competences. This paper describes general preventative measures targeted to reduce railway suicides and trespassing accidents, and it describes them in terms of their capability to effectively reduce accidents, their cost-effectiveness and their integration within the railway transport system as a whole.

A particular case is the level crossing, which is the interface between two very different transport modes. Moreover, accidents at level crossings are mostly linked to human errors committed by road users. It is thus difficult to define the responsibilities' borders in this case, and the approaches used to ensure safety are somewhat different from those used at other parts of the railway infrastructure [1-4].

The paper is organized as follows: (1) In Section 2, some relevant statistics on railway safety are presented and analyzed in order to identify the main trends; (2) In Section 3, the measures used to protect railway infrastructure and avoid accidents are presented and discussed; (3) Section 4 details the particular case of level crossings and the specific measures devoted to them; (4) Finally in Section 5, we conclude the study while exposing the main prospects of our work in this field.

2. Statistics Analysis

A significant source of information regarding

Corresponding author: El-Miloudi El-Koursi, Ph.D., research fields: railway and safety.

railway safety and accidents can be found at the European scale in the European Railway Agency's biennial reports on railway safety performance in the European Union [5], which gives an overview of both the global European situation and of the situation in the various participating countries. Other sources of information are the national authorities, as well as the RUs (railway undertakings) and IMs (infrastructure managers), who publish or allow access to more recent and/or more specific information. For instance, the investigation reports on specific accidents.

In this paper, we will mainly take into account the recent period, covering more specifically the 2010~2012 time-frame. More recent data are not fully available yet, so it is still too early to draw conclusions for the 2013~2014 period.

An important indicator of railway safety is the number of significant accidents, defined as any accident involving at least one rail vehicle in motion, resulting in at least one killed or seriously injured person, or in significant damage (i.e., equivalent to 150,000 euros or more) to stock, track other installations or environment, or extensive traffic disruption. Over the 2010~2012 period, the number of significant accidents has decreased from 2,294 to 2,088, a 9% drop. At the same time, the total number of fatalities also dropped by 9%, from 1,272 to 1,133 [5].

However, these figures are not homogeneously distributed among all the parts of the network or among all categories of victims. The most frequent accidents are accidents to persons (in which a person is hit by a railway vehicle in motion) followed by accidents at level crossings (in which a road user is hit by a railway vehicle in motion). In 2012, these two categories accounted for 58%, respectively 28% of the significant accidents, i.e., 86% of the accidents belonging to these two categories alone. The situation is the same if we consider the number of fatalities (Fig. 1), with 58% killed in accidents to persons and 33% at level crossings. More importantly, the longer-term trends depicted in Ref. [5] show that the accidents at level crossings are an exception to the generally decreasing number of fatalities, with a relative stability over the years since 2006. This resistance to mitigation measures, associated to the high number of both significant accidents and fatalities, has drawn considerable attention and effort from stakeholders and researchers to assess the existing measures, analyse the causes of their lack of effectiveness and propose new approaches to level crossing safety.

An important point, as regards fatalities on railways, is the predominance of suicides over accidents. The statistics in Europe show that suicides cause 4.6 times more fatalities than unauthorised person accidents. Moreover, the number of suicides is constantly raising (Fig. 2). This trend is particularly notable in some countries (UK, Sweden, Poland and Lithuania) where the number of suicides increased by 25% or more on a year-to-year basis. Statistics report suicides separately from accidents (in particular, they are not taken into account in Ref. [5] and Fig. 1), but obviously, the measures and policies aimed at improving railway safety have to take both these aspects into account.

3. Accidents to Persons: Trespassing and Suicides

The accidents implying persons out of level crossings, or "accidents to persons", mostly involve

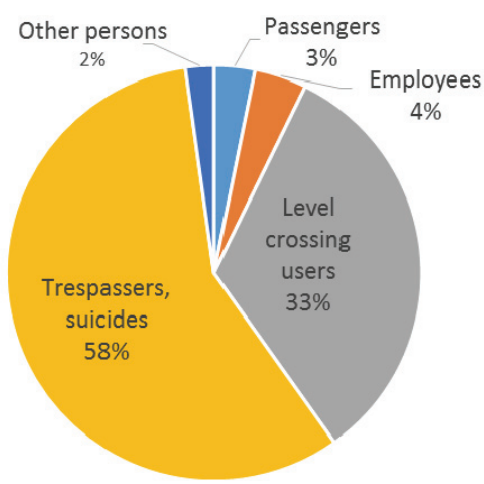

Fig. 1 Number of fatalities per victim category [5].

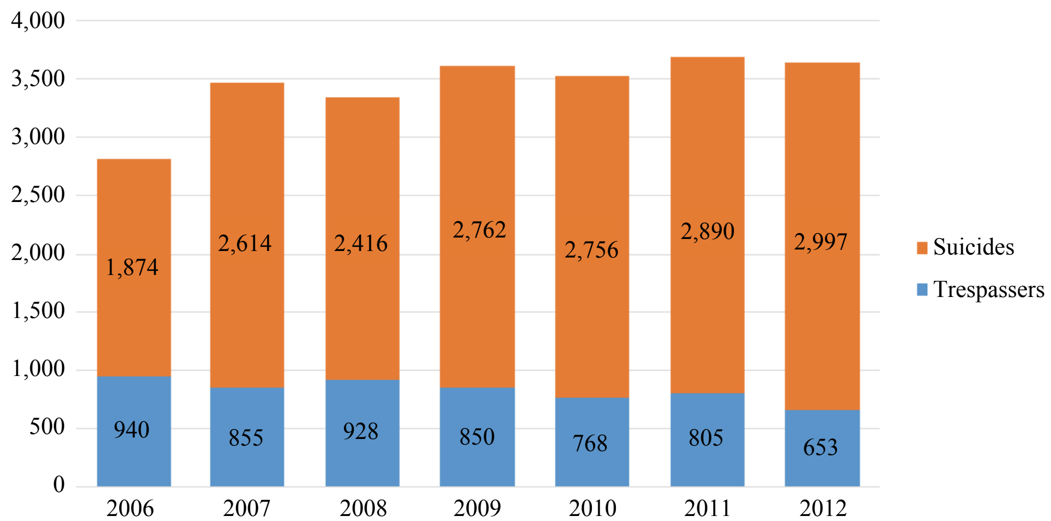

Fig. 2 comparison of unauthorized person fatalities and suicides [5].

unauthorized persons crossing or walking along the tracks, usually out of convenience. Another, much more common as seen above, cause of fatalities and significant accidents out of level crossings is the suicidal intent of persons entering the railway premises to voluntarily be hit by a train. This section aims at clarifying specific and common aspects of trespassing behaviours, with or without suicidal intent, in order to classify the measures aimed to either behaviour and assess their effectiveness.

Based on a review of the state of the art, the RESTRAIL project[1] has developed an explicit model to account for trespassing with suicidal intent, as well as trespassing with no intent of casualty. This model differentiates between suicidal intent and non-suicidal antecedents to the decision of entering into the track area [6, 7]. The steps afterwards are common to suicide and trespassing, although the attitudes and behaviours of trespassers in these steps are likely to differ depending on their intent.

The proposed model supports the analysis of the chain of events potentially leading to a collision. In the case of railway collisions, this chain is divided into two separate segments, one dealing with suicidal intent and the other with trespassing without suicidal intent, merging into a third common segment in the final stages leading to the collision.

The first motivation to enter the tracks refers to suicide-specific aspects and the associated countermeasures, such as the detection of suicidal intent near the tracks. These measures are dealing specifically with the intent of committing suicide and do not necessarily have any effect on trespassing with no intent of casualty. Another set of suicide-oriented measures aims at reducing the perceived attractiveness and availability of rail traffic as a mean of committing suicide.

The second motivation refers to trespassing behaviours with no intent of casualty, like shortcutting, loitering in railway premises, vandalism, etc. Some measures specifically target the various motivations to trespass: For example, measures targeting metal theft could result in a decrease of associated trespassing events. A second set of measures aims at increasing the knowledge of regulations and risks, as well as on other factors that might influence the decision to trespass. All these measures do not necessarily take the suicide into consideration, so their effects on the latter can be null or even negative. For example, developing measures to increase the knowledge of

[1] RESTRAIL (REduction of Suicides and Trespasses on RAILway property) is an FP7 project led by UIC, started in 2011 and ended in 2014. Details can be found on the website of the project: http://www.restrail.eu/.

risks could also increase the attractiveness of rail for persons willing to commit suicide.

A third possible antecedent is unintentional trespassing, i.e., situations in which the circumstances result in inadvertently entering the tracks. For example, absent or ambiguous signage, or the absence of lighting at night associated to an unprotected door opening to the tracks might result in unintentional trespassing. Falling or being pushed from the platform is another example of unintentional trespassing.

Finally, for the "common path" corresponding to the final steps before the collision, the associated measures at each step are likely to have a positive effect on both suicide and trespassing situations, although this effect can differ quantitatively and qualitatively. For example, a person attempting to commit suicide would stay on the tracks area whereas other types of trespassers would tend to leave the area once they understand the dangerousness of their act.

It is worth noting that one single measure may have an effect at different steps in the process. As an illustration, fences influence directly the accessibility to the tracks and, at the same time, they direct and support the correct behaviour. However, fences could also influence the perception of the availability of railway to commit suicide, at least in the considered area, which can also contribute to decreasing the number of suicides.

As one of the main consequence of our simplified model, measures dedicated to suicide and/or trespassing do not necessarily have an effect limited to one type of incident and can affect both types, either positively or negatively. Applying the model enables us to suggest the following a priori analyses:

Fig. 3 Trespassers using the rail tracks as a shortcut to the beach.

- The measures aiming to influence the decision to commit suicide on rail tracks influence the perceived attractiveness and availability railways as a mean for suicide and thus are specific to suicidal behaviour. They do not necessarily have a positive effect on trespassing and can even be counterproductive. For example, limiting or avoiding the report of information regarding suicide and other trespassing fatalities on rail could give the false impression that trespassing is not dangerous;
- The measures specifically designed to address the decision to trespass influence the knowledge of regulations and the awareness of risks and do not necessarily take the issues related to suicide into consideration. Therefore, their effect on the latter can be negative, for instance, by sending the message that crossing the tracks is fatal;
- The measures aiming to influence the first steps common to both suicide and trespassing (decision or act of entering the tracks), corresponding to constraints, guidance or support that avoid these behaviours. These measures aim to direct and support the correct behaviour (e.g., fencing, removal of paths across tracks or prohibitive signs) and to influence the access to tracks (e.g., landscaping). It is thus legitimate to think that these measures have a positive effect both on suicide and trespassing, although not with the same level of efficiency depending on the mechanism underlying the specific measure;
- The measures aiming to influence behaviours or the potential consequences once the person(s) being on the track area (potential and consequences of collision/electrocution) should mostly have a common positive effect on both suicide and trespassing. However, the measures could act differently on suicide and for trespassing due to the specific motives

and behaviours of persons at risk of suicide and trespassers once they are on the tracks. For example (Fig. 3), trespassers usually try to get off the tracks as quickly as possible when a train is approaching or when they have been spotted.

It is worth noting that some measures have potentially opposing effects. For example, campaigns to raise awareness of rail-related risks can influence positively the adoption of safe behaviours in the population, but they could also have a negative effect by increasing the attractiveness of rail as a means of suicide. Due to the current lack of evidence in the literature, the existence of such effects should be considered as potential rather than demonstrated. Three different cases can be distinguished:

- measures (potentially) having a positive impact on both suicide and trespassing prevention—this does not mean that the effect would be the same, however;
- measures (potentially) having a positive impact on one of the targets (suicide or trespassing) and a (potentially) negative impact on the other target, yielding a cross-over effect;
- measures (potentially) having a positive impact on one of the targets (suicide or trespassing) but no expected effect on the other target.

Measures dedicated to preventing suicide and trespassing accidents can be classified in several ways (Table 1). For example, they can be classified according to their nature, according to the targeted factor(s), according to their expected costs and benefits, and according to their acceptability. RESTRAIL has approached the various measures [6] with the distinctive notions of technical and soft measures, though no formal definition of them was initially available. The next sections present the definition we used and a way of extending these based on the notion of barriers commonly used in high risks industries [8, 9].

3.1.1 "Technical/Physical" Measures

Technical and physical measures correspond to physical or technological artefacts dedicated to the prevention of trespassing and/or suicides. Such measures typically include preventing entry to the site, monitoring the accesses by video surveillance or other sensors, enhancing the visibility or various ways to deter entry (vocal message, lighting, etc.). The technical measures related to trespassing have been classified into groups as follows:

- measures aiming at increasing the visibility of trains or trespassers;
- surveillance measures. Such measures can integrate the surveillance itself and other techniques, for instance, lighting or loudspeakers, in order to deter or influence the behaviour of possible trespassers;
- fencing and landscaping techniques used either in stations, to make the access to the tracks more difficult or to ease the crossing by safe means, e.g., tunnels or pathways and the associated signage;
- measures related to the design of stations and other locations to influence the movements of people.

3.1.2 "Soft" Measures

"Soft" measures encompass measures dedicated to influence knowledge and behaviours by actions, such as communication, training, calls for socially responsible behaviour, legal measures and sanctions. These measures typically include the design and placement of signage and posters [6, 10], mass media or local prevention campaigns [11, 12], intervention in schools and provision of educational materials, reward or punishment [12], attendance of station staff or security personnel. In the framework of the RESTRAIL project, the soft measures related to suicide and trespassing have been classified into groups as follows (Table 1):

- measures related to population education and communication to the public: education, media guidelines, campaigns, support to staff at risk, etc.;
- outreach support by trained staff;
- emergency information at stations, prohibitive signs, warning signs and posters;

Table 1 Technical and soft families of measures related to trespassing and suicide.

Families/forms of suitable identified measures	Trespassing	Suicide	Technical/soft
Increased visibility by lighting at railway crossings, tunnels and hotspots	T	S	Technical
Increasing visibility through removal of vegetation	T	S	Technical/soft
Surveillance to deter and prevent incidents: CCTV cameras (fixed or mobile)	T	S	Technical
Surveillance and light to influence behaviour	T	S	Technical/soft
Detection system combined with sound warnings	T	S	Technical/soft
Surveillance to deter (social measure)	T	S	Technical
Surveillance to deter (technical measure)	T	S	Technical
CCTV camera cameras/motion detectors, linked to (train) traffic stop warnings	T	S	Technical
Surveillance based on local intelligence (e.g., from police, health authorities)	-	S	Soft
Targeted campaigns (including shock campaigns)	T	S	Soft
Education and prevention in schools and outside of school	T	-	Soft
Mass media campaigns	T	S	Soft
Media guidelines	-	S	Soft
Staff Support (staff at risk of suicide)	-	S	Soft
Additional technologies for train drivers (e.g., spotlights, in-cab CCTV)	T	S	Technical
Emergency button at unstaffed stations	T	S	Technical
Training of staff—gatekeeper training	-	S	Soft
Training of staff—general awareness rising	T	S	Soft
Training of drivers/instructions to drivers	T	S	Soft
Outreach support by trained staff	-	S	Soft
Design of stations and other locations to influence the movements of people	T	S	Technical/soft
Design of stations and other locations—aesthetics (colours, lighting, music and other devices)	T	S	Technical/soft
Fences and barriers at specific parts of stations	T	S	Technical
Fences and barriers at locations outside stations where people take shortcuts across tracks	T	S	Technical
Design and landscaping of the railway environment	T	S	Technical/soft
Suicide pits at stations	-	S	Technical
Emergency information at stations (signs, posters, flyers, information on screens etc.)	T	S	Soft
Prohibitive signs	T	-	Soft
Warning signs and posters to address trespassing	T	-	Soft
Legal measures	T	S	Soft
Collaboration between organisations and agencies	T	S	Technical/soft
Risk assessment (e.g., of stations, special circumstances, at risk groups or individuals)	T	S	Technical/soft
Monitoring and learning from research and best practice	T	S	Soft
Local suicide and trespassing prevention plan	T	S	Soft

- surveillance based on local intelligence from police, health authorities, etc.;
- organisational and safety management measures: local or national collaboration, risk assessment, international best practices and research, prevention plans;
- legal measures.

4. Level Crossings

Fig. 4 shows the evolution of level crossing accidents and fatalities over the 2006~2012 period. With the exception of a peak in 2007, the trend is stable with an average of one person killed and close to one person seriously injured per day in Europe. In 2012, fatalities at level crossings represented 29% of the total railways fatalities, but only 1% of the road fatalities the same year [5].

The particular situation of level crossings, which are at the interface between road and railways, poses a particular problem as regards the management of accidents, which are considered a road-safety issue by the IMs even though they take a large share of the total

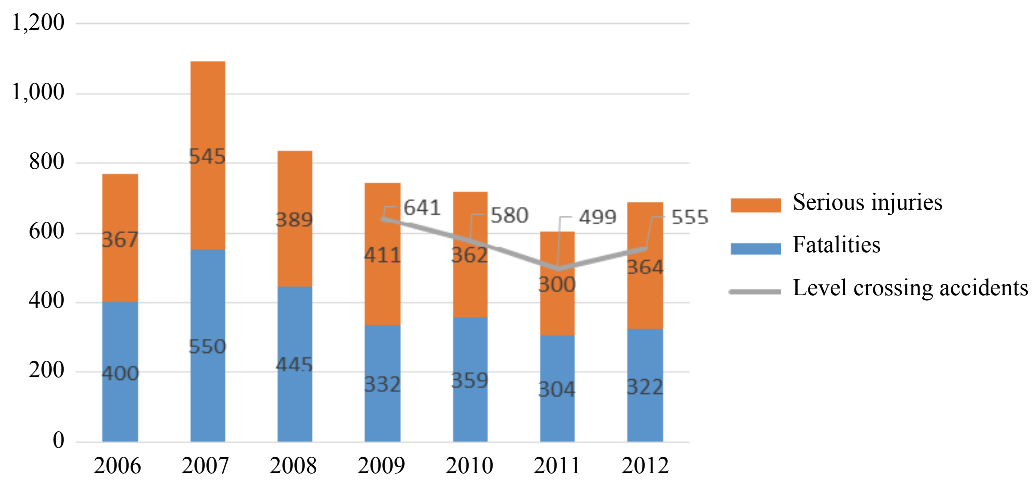

Fig. 4 Level crossing accidents and casualties [5].

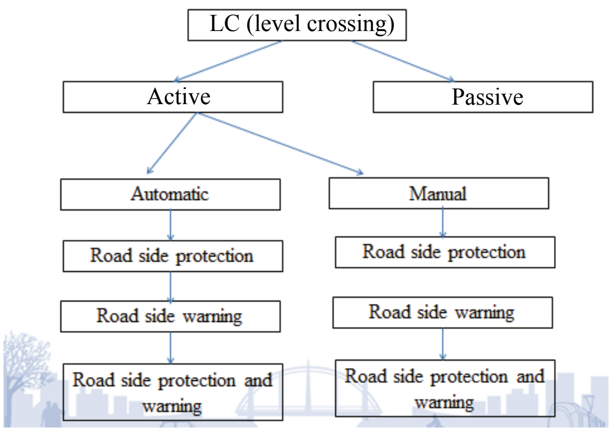

Fig. 5 Level crossings types as classified by ERA (European Railway Agency).

fatalities on railways. In contrast, they represent a minor problem for the authorities in charge of road safety. Another issue is that accidents on level crossings give rise to two separate investigations, one dealing only with the road side and the other focused exclusively on the railway side, which make system-oriented studies all the more difficult since both investigations use utterly different classifications and elements. Studying the safety of level crossings as an entity is, therefore, a difficult task for the researchers.

The European Commission produced in 2004, the Railway Safety Directive [13], in order to define common safety targets and to improve, where possible, the system safety levels. The directive stipulates that member states are duty-bound to conduct an independent investigation in order to improve rail safety and prevent accidents. In addition to serious accidents, the investigating body may conduct investigations into accidents and incidents which, in slightly different circumstances, might have led to more serious accidents, including technical failures in structural sub-sections or interoperability components of the trans-European high-speed or conventional rail system. The Railway Safety Directive requires the safety of railway transport to be defined according to the acceptable individual risks of level crossing users and expects the development of procedures and methods for risk evaluation and assessment. The CST (Common Safety Targets) define the minimum safety levels that must be reached by different parts of the railway system and by the system as a whole in each member state, expressed in risk acceptance criteria for individual and societal risks.

ERA [13] has classified the level crossings into two groups: active and passive (Fig. 5).

A passive level crossing is only equipped with permanent warning signs or any other protection equipment, and it has no form of warning system and/or protection system showing when it is unsafe for the user to traverse the crossing. On the contrary, an active level crossing is equipped with, e.g., lights or barriers, to change their configuration when the traffic conditions make crossing dangerous: The level crossing users are protected from, or warned of, the approaching train by the activation of devices when it is unsafe for the user to traverse the crossing. In the case of automatic active level crossings, these devices are activated by the approaching train. Manual active level crossings are activated by humans.

4.1 Using Advanced Technology to Improve Level Crossings Safety

The main focus of this section is to describe current and proposed approaches using emerging information technologies to improve the resolution of accident-prone situations on level crossings, which can also be adapted to address situations outside of level crossings to avoid accidents to persons. Such advanced technology can be used to:

- bring technological improvements to the level crossing safety infrastructure, such as the deployment of various types of sensors (audio, video, radar and lasers) for timely detection of potentially hazardous situations;
- use this knowledge to promote human awareness: Situations potentially leading to collisions are treated by sending information via radio networks to approaching railway and road users and prompting suitable behavior in order to avoid the accident. The use of fast, reliable and wireless links enables a seamless communication between the train, car drivers, the level crossing and the main control center.

On the road user side, human awareness can be improved by informing the vehicle drivers of the type of the danger level of the level crossing they are approaching—in particular, inform them of accidents/incidents at level crossings before they get there (Fig. 6). This information will give the road users important cues about the situation that they are going into, in the goal to promote situation awareness and allow early management of incidents, such as finding an alternative route to avoid a jammed level crossing. This information should be presented in a clear and concise way, using advanced technology, such as dynamic panels or short messages on the vehicle built-in displays, in order to avoid cognitive saturation which could in turn cause accidents, instead of avoiding them. A more advanced system could make use of the vehicle's GPS (global position system) to dynamically calculate and propose a new route avoiding the problem and preventing traffic jams.

On the railway side, the information can be sent to the driver's cab as a message that a problem is happening at the next level crossing, along with (if appropriate) the display of the video of the incident. The driver is then able to decide the appropriate action to take in order to avoid the incident. As in the case of road vehicles, caution must be paid to avoid cognitive saturation that might distract the drivers from their main task of driving the train.

It is also envisaged to send the same data (alert message and video/audio stream) to the control center for advanced management and decision making. An important point is to only trigger the sending of such alerts when they appear to become serious, i.e., when the risk of collision is elevated. It has been long established that unnecessarily warning of threats that constantly turn out to be unfounded quickly becomes a nuisance to the operators, and it is both ineffective and dangerous since an actual threat may not be taken

Fig. 6 Automatic detection of a car stopped on a level crossing.

seriously when it occurs. The robust filtering of such false alarms is not an easy task, and it is a topic of ongoing research.

4.1.1 Obstacle Detection at Level Crossings

Most of the level crossings are equipped with signalization, such as red light, automatic full/half barrier, notices, etc. They are not able to avoid all dangerous behaviors. Most of the collisions occurring at level crossings are due to drivers not seeing a train coming or believing that they can beat the train. That is why detection of trapped vehicles/pedestrians inside the barriers, in order to take appropriate action, may reduce the risk of collisions between trains and vehicles. Obstacle detection system seems to be a significant solution to improve level crossing safety and lower the number of fatalities.

An obstacle detection system on level crossing must fulfill the following requirements:

- improvement of the safety for both pedestrians and vehicles (car, truck, motorbike and bicycle);
- no or minimal delays for train and road users;
- accuracy for safety and productivity reasons;
- reasonable condition in terms of costs to install, operate and maintain.

We will first summarize the existing technologies used for object detection at level crossing. Then we will present a test case, based on video imaging and evaluated in life situation.

4.1.2 Current Detection Technologies

The detection of a vehicle/pedestrian or other obstacles on the level crossing, when a train is approaching, requires the installation of a detector. Several technologies are capable of doing this, such as optical or sonic sensor, inductive loop, radar and video imaging.

The choice of the appropriate detector can hardly depend on external factors, e.g., environmental conditions or the size of object to detect. Several types of detectors, conventional or newer can be used according to the detection task and operational constraints [14].

4.1.3 Conventional Detection Systems

The conventional obstacle detection has been used to prevent crashes between trains and vehicles:

(1) Optical beam: Optical emitters are placed on one part of the crossing, each which emits a directed optical beam having a defined field of emission. If the beams are interrupted, it means that an object is located on the level crossing. Optical beam detectors are easy to replace but they have many important disadvantages: high cost, need for several detectors along the crossing, need to stop the traffic for installation and unusableness in heavy snow;

(2) Sonic detector: The ultrasonic method relies on differences in ultrasonic reflection time. They transmit pulses of ultrasonic energy towards the roadways, which are reflected back quicker when a vehicle passes through. Sonic detectors can detect both stopped and moving vehicles, but they are expensive to purchase and to install and extremely sensitive to the environmental conditions—in particular, they are inaccurate in congested conditions;

(3) Inductive loop: It is probably the most common vehicle detection technology. A wire is embedded under the roadway, generating a magnetic flux around it. A metal-made vehicle passing over the wire cuts the flux, which is detected by the change in inductance. Inductive loops have many advantages: ease of installation and insensitivity to the environmental conditions. But they are costly to install and service, and the traffic must be delayed. Also, they cannot detect pedestrians or bicycles.

4.1.4 Newer Detection Systems

Two newer detection systems are introduced as following:

(1) Radar: Microwaves are sent from a transmitter based at the side of the roadway and reflected back to a receiving antenna with a different frequency according to the speed of the reflecting object (Doppler effect). The advantages are easy installation and immunity to electromagnetic interference. However, these sensors are difficult to maintain;

(2) Video imaging: Video surveillance is one of the newest technologies on level crossings. A camera is placed above the intersection, looking down. The video image is sent by radio to the train driver who can see early whether the intersection is clear and stops on time if not [15, 16].

4.1.5 Automatic Video Detection

This section is mainly concerned with the timely detection of events that could result in collisions on level crossings. The main purpose of the tools is to detect them when they first happen and it is still time to react and prevent the collision. Examples of such events include a car stopped on the tracks, an object fallen on the tracks or a vehicle unsuccessfully trying to egress a level crossing.

The main aim of automatic video detection is to develop cost-effective and integrated technical solutions able to support pro-active surveillance procedures on a railway network.

Indeed, CCTV (close circuit television) at level crossings can be used for various purposes:

- Off-line use: The perception system is used to produce statistics related to the use of the level crossing and the users' behaviors, automatically detect and identify the abnormal behaviors. This also allows the stakeholders to have quick access to a video sequences and to have a better understanding of the behaviors that led to dangerous situations;
- On-line use: The objective is to identify potentially dangerous situations, such as the presence or approach of objects (pedestrians, motor-cycles, vehicles or other obstacles which could be in the way). In this method, the objective consists in detecting and anticipating a critical situation.

4.2 Level Crossing Advanced Driver Information System

Communications between railway stations and railway network elements are vital for uninterrupted and safe operation of railways. Nowadays, data communications provide cost-effective solutions for the data communications and telecommunications needs of the railway industry.

The goal of this section is to compare current situations regarding wireless communications in railway and road exploitation, i.e., CBTC (communication-based train control) and C2I (car-to-infrastructure) communications. On the railway side, CBTC systems, also known as PTC (positive train control) systems, provide positive train separation, speed enforcement and road worker protection using wireless communications to exchange control information. On the road side, based on WLAN (wireless local area network) communications, VANET (vehicular ad-hoc networks) provide distributed real-time communication of traffic hazards and road conditions among vehicles in radio line of sight. These wireless communication systems could then be used to reduce road-rail collisions by communicating information to road vehicles regarding the train movements and the condition of the level crossings.

4.2.1 Train Wireless Communication System

Instead of dedicated telecommunication systems used in the older systems, railway wireless communication systems are now more and more using telecommunication industry existing products, upgraded if necessary. Using such an approach, railway industry takes full advantage of the R&D investment of the telecommunication industry, cost effective, if compared to the huge telecommunication mass market. Moreover, railway industry takes also benefit of all the telecommunication standards evolutions.

In the telecommunication industry, the first WLAN was introduced in order to substitute for existing conventional wire networks inside buildings. After its initial success, this first objective has been extended to a wide variety of wireless networks that can be named WxAN. They represent different usable levels of compromise between high bit rates and mobility. As such, they are complementary to the cellular network that allows worldwide mobility but a restricted bit rate.

4.2.2 Car Wireless Driver Information System

As stated before, in a CBTC system, the Railway Local Control Centre and the Main Control Centre are interconnected by bi-directional data communication links which may be wired or wireless. This is not yet the current situation on the road side where only a lateral visual signalization exists, and no distant repetition of the level crossing signaling information is performed inside the vehicles. This situation could evolve in a near future.

In fact, improving traffic efficiency, reducing congestion on roads and reducing accidents, as well as damage cost, are challenging tasks in most regions of the world. To put the problem into context, annual damage cost caused by accidents in the EU (European Union) alone is approximately 100 billion euros. This can be potentially minimized by using new information and communication technologies. Among these technologies, C2C (car-to-car) and C2I communications are good candidates to improve the current situation. In this way, connecting vehicles between them or with the infrastructure by a wireless radio link enables a new range of applications and the improvement of existing applications [17].

Using centimetric waves, C2I communications are expected to be operated using omnidirectional and semi directional antennas radiating in a horizontal plane and concentrating energy at low angles over the road surface.

Such a level crossing to vehicle wireless communication could, therefore, provide the repetition of the level crossing signalling information inside the vehicles along a significant communication range. At a mean speed of 60 km/h, this represents receiving driver warning information 30 s before arriving in the level crossing area.

5. Conclusions

The rail sector needs to ensure its safety against accidents occurring on its property in order to offer continued service and maximum reliability. An important means to achieve this goal is the analysis of the measures already taken in various countries to address these events. This paper describes general preventative measures targeted to reduce railway suicides and trespassing accidents including at level crossings, and it describes them in terms of their capability to effectively reduce accidents, their cost-effectiveness and their integration within the railway transport system as a whole. It discusses the existing countermeasures for reducing suicides, preventing trespasses and mitigating the consequences on rail operations.

References

[1] Bruyelle, J. L., O'Neill, C., El-Koursi, E. M., Hamelin, F., Sartori, N., and Khoudour, L. 2014. "Improving the Resilience of Metro Vehicle and Passengers for an Effective Emergency Response to Terrorist Attacks." *Safety Science (Elsevier)* 62: 37-45. doi: 10.1016/j.ssci.2013.07.022.

[2] Fakhfakh, N., Khoudour, L., El-Koursi, E. M., Bruyelle, J. L., Dufaux, A., and Jacot, J. 2011. "3D Objects Localization Using Fuzzy Approach and Hierarchical Belief Propagation: Application at Level Crossings." *EURASIP Journal on Image and Video Processing, Special Issue Advanced Video-Based Surveillance, Hindawi* 2011: 1-15. doi: 10.1155/2011/548604.

[3] Ghazel, M., and El-Koursi, E. M. 2014. "Two-Half-Barrier Level Crossings Versus Four-Half-Barrier Level Crossings: A Comparative Risk Analysis Study." *IEEE Transactions on Intelligent Transportation Systems* 15 (3): 1123-33. doi: 10.1109/TITS.2013.2294874.

[4] Khoudour, L., El-Koursi, E. M., Velastin, S., Buch, N., Lim-Thiebot, S., and Fontaine, F. 2011. "An Approach for Protecting a Critical Transport Infrastructure." In *Proceedings of the Institution of Mechanical Engineers, Part F: Journal of Rail and Rapid Transit, Professional Engineering Publishing,* 383-93.

[5] ERA (European Railway Agency). 2014. "Railway Safety Performance in the European Union." ERA. Accessed June 18, 2014. http://www.era.europa.eu/Document-Register/Documents/SPR2014.pdf.

[6] Silla, A., Kallberg, V. P., Rådbo, H., Whalley, S., and Ryan, B. 2012. "Summary and Conclusion of D1.1: Data Concerning Railway Suicides and Trespassing Accidents." RESTRAIL. Accessed June 18, 2014.

http://restrail.eu/IMG/pdf/restrail-d1-1-281212-summary_and_conclusion.pdf.

[7] Rådbo, H., Svedung, I., and Andersson, R. 2008. "Suicide Prevention in Railway Systems: Application of a Barrier Approach." *Safety Science* 46: 729-37.

[8] Haddon, W. 1995. "Energy Damage and the 10 Countermeasure Strategies. 1973." *Injury Prevention: Journal of the International Society for Child and Adolescent Injury Prevention* 1 (1): 40-4.

[9] Hollnagel, E. 2004. *Barriers and Accident Prevention*. Farnham: Ashgate Publishing, Ltd.

[10] RSSB (Rail Safety and Standard Board). 2006. *T555 Improving the Content and Placement of Anti-trespass Signs*. Final Report No. T555, Halcrow Group Limited in Partnership with Human Engineering Limited.

[11] Lobb, B., Harre, N., and Suddendorf, T. 2001. "An Evaluation of a Suburban Railway Pedestrian Crossing Safety Programme." *Accident Analysis and Prevention* 33: 157-65.

[12] Lobb, B., Harré, N., and Nicola, T. 2003. "An Evaluation of Four Types of Railway Pedestrian Crossing Safety Intervention." *Accident Analysis and Prevention* 35 (4): 487-94. doi: 10.1016/s0001-4575(02)00026-x.

[13] Railway Safety Directive. 2004. "Directive 2004/49/ec of 29 April 2004 on Safety on the Community's Railways and Amending Council Directive 95/18/ec on the Licensing of Railway Undertakings and Directive 2001/14/ec on the Allocation of Railway Infrastructure Capacity and the Levying of Charges for the Use of Railway Infrastructure and Safety Certification." *Official Journal of the European Union* L220: 16-39.

[14] Little, A. D. 2006. *Obstacle Detection at Level Crossing*. Research Report T522, RSSB (Rail Safety and Standard Board).

[15] Foresti, G. L. 1998. "A Real-Time System for Video Surveillance of Unattended Outdoor Environments." *IEEE Transactions on Circuits and System for Video Technology* 8 (6): 697-704.

[16] Ohta, M. 2005. "Level Crossing Obstacle Detection System Using Stereo Cameras." *QR of RTRI* 46 (2): 110-17.

[17] The e-Safety Working Group Communications. 2007. *Final Report and Recommendations of the Communications Working Group*. Brussels: The e-Safety Working Group Communications.

Journal of Civil Engineering and Architecture 10 (2016) 108-121
doi: 10.17265/1934-7359/2016.01.011

Tenure of Urban Land: Structure, Form and Transformation in Ribeirão Preto, Brazil

Ivone Salgado and Dirceu Piccinato Junior

CEATEC (Center for Exact Sciences, Environment and Technology), Pontifical Catholic University of Campinas, Campinas 13 090 610, Brazil

Abstract: The purpose of this study is to explore the urban morphological aspects of cities governed by the juridical regime of emphyteusis, a recurrent situation in the northeastern part of the state of São Paulo, Brazil, with special attention to the city of Ribeirão Preto. The concession of lands to the Catholic Church was a recurring practice in Brazil during the colonial and imperial periods, when the cities were being established. As these lands were intended for the formation of patrimonial goods to show the devotion of the residents to a Catholic saint, the lands were not allowed to be commercialized. The tenure reveals a relation in which there is an owner—the landlord—who has direct control of the urban land. This owner allows another—the leaseholder—the useful domain of the land, thus giving the latter the right to use the land, the obligation to pay an annual tax and the responsibility to give the owner a percentage of the sales generated from the land. In 1845, farmers donated a tract of land to be used to glorify São Sebastião. This land is now the city of Ribeirão Preto, and it is this conjuncture that defined the structure and the transformation of the original urban form of the current city.

Key words: Tenure, emphyteusis, urban land, Catholic Church, urban morphology, concession of lands.

1. Introduction

As the city is a complex object that manifests various phenomena and interactions, various social sciences have converged in the study of urban forms. The urban form is the result of a range of factors, elements, junctions and conflicts that are more than the sum of their parts. In this way, the complexity and organization of the urban system make the city a specific object to be understood by the cross confrontations of the questions and answers of the human sciences [1].

The term "urban morphology" is not restricted to a single science but rather to numerous sciences, including sociology, anthropology, history, geography, architecture and urban planning, among others, when consistent with a new perspective, thus pointing to new ideas and new understandings. Studying the various aspects of urban form, Kropft [2] showed that the diversity and complexity of cities reflect a variety of ways to understand them, which, consequently, have resulted in the elaboration of different research methods and approaches to study the morphology of cities.

In short, the term "urban morphology" refers to the study of the physical form of a city. However, considering that the city is a socially diverse entity, every society seeks to reproduce exterior forms, whether permanent or not. This means that these forms obey a given socio-political order of the group which creates them and that they respond to a functional and effective sociability that also regulates the use of the city space and the resources contained within that space, thus defining their own models of appropriation of the city [3]. Thereafter, the full character of a social process in configuring the urban form can be considered in the studies of urban morphology.

With respect to certain aspects of urban form, Kropft [2] pointed to its definition, which has its

Corresponding author: Ivone Salgado, Ph.D., professor, research fields: urban history, urban form and history of town planning.

parameters as the work *Good City Form* by Lynch [4], in which Lynch identified six distinct aspects. The first refers to the physical form; The second condenses the use, activities and movement of the form; The third addresses control; The fourth relates to perception; The fifth presents the process of continuity or change; The sixth refers to the flow of materials and information. These are the main aspects that must be observed when conducting a critical analysis of urban morphology.

Kropft [2] discussed urban form in the context of a relatively recent time with the aim of establishing a better understanding of the urban configuration. When we look to Brazil in an attempt to list the aspects that outline the urban form of Brazilian cities, the study of urban morphology, according to this methodology, should consider the local social, cultural, geographical and historical contexts of the cities.

According to Vasconcelos [5], when examining the morphology and various aspects of the urban form of Brazilian cities, it was possible to identify modeling agents that were jointly present in the urban setting. However, during the subdivision of this examination into a case-by-case study, it was possible to identify the presence of, if not most, at least one agent that was common to all cities. Five modeling agents were identified. The first was the State, especially at the upper level, i.e., the Portuguese Crown, which played a key role in the implementation of the first towns and cities in Brazil as the Portuguese Crown sought to manage its colony through orders sent directly by the metropolis. The second agent was the Church, whose decisive role was tantamount to that of the state with respect to the structure of Brazilian cities. The Church in Brazil was founded on the patronage system following an agreement between the Vatican and the Portuguese Crown. The Church counted on the presence of the secular clergy, which, as the highest order of the Church, included bishops, archbishops, ecclesiastical courts and seminaries, and the regular clergy, which comprised religious male and female orders. The third agent was the lay orders, which were Catholic institutions that were relatively independent of the official Church and were formed by volunteers of laymen and laywomen. The fourth agent referred to economic agents or external economic agents, who were land owners and domestic economic agents, such as traders, financiers, slave traders and craftsmen. The fifth agent involved the population and social movements. The population was composed of employees, especially staff, masters of letters, surgeons, as well as the poor, the freed and the slaves (until the year of 1888 when slavery was abolished in Brazil). The social movements were extremely important to the national history due to the various uprisings and rebellions articulated by dissident social groups.

The present case study highlights the role of the Church as the authorizing agent of urban form. The morphological urban aspects of cities, governed by the juridical regime of emphyteusis, which is recurrent in the northeastern part of the state of São Paulo, Brazil, are explored with special attention to the city of Ribeirão Preto.

2. Urban Morphology: Some Considerations

In recent studies, the understanding of urban morphology presents diverse perspectives of methodological approaches from the assessing of the physical forms of the city and the listings of the fundamental elements, streets, lots and buildings [6] to the describing and prescribing of the urban forms according to a multidimensional, systematic, exploratory and quantitative environment [7]. Studies of multidisciplinary discussions about urban morphology have resulted in the acceptance of the relevancy of the social sciences and humanities with respect to the construction of urban form [8]. In some studies, as noted by Kim [9] regarding the urban form of South Korea, it is possible to observe a particular focus on the formal aspects of cities and towns wherein the parameters of analysis are the history and the influence of European morphology in the country. A variety of models of urban forms are examined through a cultural perspective in which the construction of the form is the result of theory and practice, and thus the representations of a particular culture and the historical conditions of the form are described [10].

These various methodological approaches to study urban morphology point to the fact that the analysis and understanding are configured according to the interdisciplinary relations of science, with different views, as well as specific economic, cultural and social conditions of a country or a city. In this sense, this work intends, similarly to Ehlers [10], to discuss the structure, shape and transformation of the urban form of the city according to the social and political articulations in the representation of the its physical form.

As the urban environment is subject to multiple readings, the instruments of analysis draw attention to the phenomena involved in the production of the space. This suggests that the numerous meanings associated with the city and its architecture correspond to numerous conflicts and agreements that helped, directly or indirectly, in the configuration of the urban form.

Lamas [11] noted that the morphological study does not address the urbanization process, i.e., the social phenomena and the economic and other engines of urbanization. Rather, according to the Lamas [11], these "engines" converge in the morphology and in the explanation of the production of form, but they are not the objects of study. However, the study of urban morphology is a cumulative process in which every temporal dimension identifies a result and a possibility, and therefore, it is a continuous movement. Accordingly, we question whether every urban formation is also a social formation in that the latter necessarily spatializes itself [3].

The field of morphologic study is characterized in its entirety as a place of transformation produced by man or as a place of architectural and urban intervention. This means, "man lives in an environmental continuity, and urban or territorial forms are constituted by the composition of different spatial units and morphological elements" [11].

The morphological elements are directly related to urban size and can be identified by the form. Thus, the analysis of this form requires movement and pathways. Lamas [11] identified these elements as the soil, the buildings, the lot (land parcel), the block, the architecture, the layout (the street) and the square, among others that define and explain the urban landscape and its structure.

In general trends of urban formations in colonial Brazil, social confluences were evident in the donation of a strip of land for the establishment of patrimonial goods, and it was on such land assets that the vast majority of Brazilian cities were developed. The city of Ribeirão Preto is no exception to this, as the strip of land on which Ribeirão Preto exists was granted to a saint of Catholic devotion, thereby establishing its religious heritage. Thus, it is possible to identify the concept of urban form, one that is produced by social connections and/or political conflicts on a pre-defined area—the soil.

3. Formation of the Religious Heritage of Ribeirão Preto

The formation of cities in Brazil, according to some researchers, should not be analyzed in a systematic, gradual or regimented way but must be considered in light of two standards—"parsimonious and generalizing" [12]—or in the observing of general trends in the configuration of the Brazilian urban form [13]. This situation is explained by the fact that the formation of cities was determined by the prevailing political and economic interests of the important men of the locality [14]. One element, the religious heritage, was common in the formation of urban space in Brazil during the colonial period (1500~1822), imperial period (1822~1889) and part of the first republic (1889~1930).

This religious heritage emerged in Brazil in a discrete way. It constituted a tract of land that allowed for the construction of the chapel and for the external space, as recommended by the *First Constitutions of the Archbishop of Bahia* for the formation of houses to shelter the small sesmeiros. This gave rise to what would be the future urban core. The sesmeiro was the person to whom the sesmaria was granted, and the sesmaria was a Portuguese legal principle that regulated the distribution of land for cultivation in colonial Brazil. "On one hand, it occupied a predetermined ground and planted the desired temple; On the other hand, it propitiated the agglomeration of houses and businesses" [12].

The territorial plots tended to be large during the colonization of Brazil, which hindered the full use of these plots because of the high costs and charges. Thus, many of the settlers ended up not having access to land, while those who had the resources could acquire lands. This resulted in the poorer settlers forming large contingencies or "clusters" that then became owners of large tracts of land.

In the formation of the city of Ribeirão Preto, Lages [15] reported that the religious heritage of the city was dedicated to São Sebastião and that the strip of land was donated by many owners in the years 1852, 1853 and 1856 (Table 1). The relevance of this nonproprietary population was important for the productive sector, which is why the religious heritage arose tentatively, but effectively, in the context of the formation of urban form.

As land extensions were granted by one or more landowners, the disadvantaged workers began to settle in the area. However, the granting of this strip of land did not directly benefit this group of individuals but, rather, benefitted the Catholic saint of devotion, as the administrative care of this patrimony was the compulsory responsibility of the Church [16]. With respect to Ribeirão Preto, it was possible to identify the boundaries of the religious heritage of the city through the information about the blocks that were properly listed together within the Archdiocese of Ribeirão Preto and the 1st and 2nd notary real estate registry (Fig. 1).

At the time of the transcription of the donation, it was common for the donor or donors to request a specific religious endowment as compensation for the act, such as a mass after death, a select burial site, etc. [17].

The administration of this heritage was under the care of the Church Factory, which constituted an entity formed by the religious. The rich men of the town were jealous of the goods of the parish and of the disposing of lands donated in urban form that were assigned under the jurisprudence of the long lease institute or the tenure of those interested in maintaining the balance of land. The term "Factory" comes from the factory manufacturing idea of the Church—its construction, beautification and purchase of ornaments. Thus, it was where issues related to the tenure of the resources of urban land were to be addressed [17].

Once established as the patrimony of holy devotion, local people gathered to build the first building—the chapel. This could not be built just anywhere, according to the *First Constitutions of the Archbishop of Bahia*, but must be built on a "high and decent place,

Table 1 List of donors of land for the development of the patrimonial goods of São Sebastião of Ribeirão Preto.

Donors	Farm	Extension (acre)	Date
João Alves da Silva and Ana Delfina Bezerra	Retiro	30	December 19, 1852
Severiano João da Silva and Gertrudes Maria Teodora	Retiro	12	March 16, 1853
José Borges da Costa and Maria Felizardo	Retiro	9	March 20, 1853
Inácio Bruno da Costa and Maria Izidora de Jesus	Retiro	9	April 19, 1853
José Borges da Costa and Maria Felizarda	Retiro	12	March 20, 1853
José Alves da Silva and Pulcina Maria de Jesus	Barra do Retiro	2	March 18, 1856

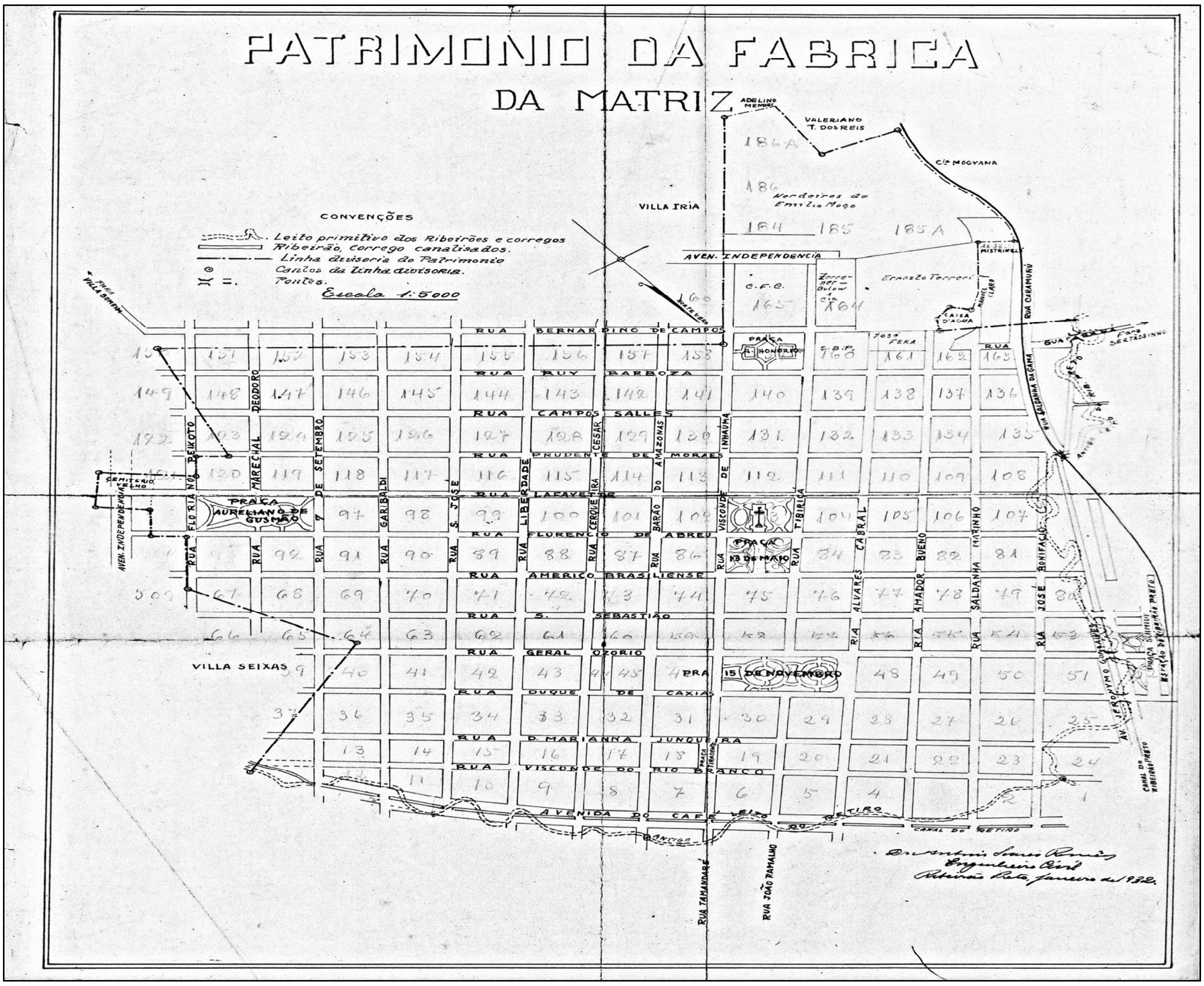

Fig. 1 Patrimonial goods of the Mother Church of São Sebastião of Ribeirão Preto, 1932. The limits of the patrimonial lands in the urban form where the city was originated are highlighted, and it is possible to observe the blocks slightly listed (*Public Archives and History of Ribeirao Preto*).

free from humidity, private homes and other walls in a distance in which the processions could walk by without impediments…" [18]. At this time, the religious building and its urban status were defined as a chapel.

With the increase in population, the inhabitants of the chapel could ask the ecclesiastical and civil institutions for the elevation of its urban condition to a parish. While the elevation in status from a chapel to a parish took into account demographic and economic criteria, it was the political interests that prevailed [14].

In this new urban condition, the criteria for the location of the Mother Church were not necessarily the same as those for the first chapel. Rather, the criteria could be changed to better meet the interest of the local residents as it was the case in Ribeirão Preto. The modest chapel underwent several reforms to become the main church, a prestigious place where religious events were conducted and citizens meetings were often held.

Once attaining a certain level of power and strength, the parish could ask the civil and religious powers for a promotion in status from parish to village. With such an elevation in status, came "…political autonomy, the status of a municipality" [12]. Under this new title, it became the responsibility of the village to define itself, as it was now a territory comprising chapels, parishes and neighborhoods and, as such, was under the control of a city council. It was now also up to the village to identify and define a park—a smaller geographical area to be divided into plots that would integrate the assets of the city council. “This could divide them into ‘grounds’ (lots) and grant them, upon payment of annual pension, to the residents who asked for them to build their homes” [13].

With respect to religious heritage, “property” of the Saint, which was managed by the Church, was superimposed on a new demarcation—the park, which constituted public land. A conflict, however, arose between the civil and religious powers about land ownership, a situation that was resolved by the overlapping of civil power over religious power in most Brazilian cities. However, in other cities in the northeastern part of the state of São Paulo, the conflict still remains today [19]. The city of Ribeirão Preto is a case in point.

Thus, in the composition of the Brazilian urban landscape, religious buildings outlined the structure and defined its form. The presence, poise, refinement and, especially, the privileged position in which were placed the religious buildings made them the ordering agents in the urban form of both small and large agglomerations [20]. What is observed is the result of the pragmatism and constructive need that initially demanded a simplification of procedures, tracts and architecture. Accordingly, these principles can be considered as a condition for the innovation and transformation of urban form [21].

The title of city was usually only assigned to those villages that performed important religious, political or military roles. Thus, the term was not attributed only to the bishopric seats but also to towns on the coast and in border areas that incorporated high squares [13]. The difference between towns and cities was, therefore, judicial in character and not necessarily hierarchical [16].

4. The Institute of Long Lease

The institute of tenure or long lease of land is a legal instrument that was formulated in ancient Greece and later assimilated into the Roman Empire to legitimize the use and retention of workers on the ground. During the Middle Ages, Portugal included this instrument in its set of laws. The first reference was in the *Afonsina Ordinances* (1500~1514), it was then instituted again in the *Manuelina Ordinances* (1514~1603) and finally in the *Filipina Ordinances* (1603~1916). The latter prevailed in Brazilian lands until the year 1916 when it was enacted in first civil code, which recognized the right of long lease. This code remained until 2002, when a new civil code was formulated, but little change about tenure was introduced in the new code. For this study, the civil code of 1916 was used as a source of analysis because it recognized tenure as a right, and it remained in effect until the beginning of the XXI century.

The long lease or tenure is a way to divide the property of a perpetual contract as holder of the long lease gives others the powers of use, enjoyment and disposition, and only transfers them to third parties with his approval.

The long lease can only occur in uncultivated lands or in lands intended for building as stated in article 680 of the civil code. Therefore, it is not possible to establish long lease on the mobile natural goods of the land, on buildings already constructed or on plots already colonized. In this sense, the economic purpose of the long lease is to encourage the use of uncultivated or unbuilt lands.

The institute of tenure or long lease is a territorial alienation contract that divides the ownership of a property into two domain types—the direct domain (imminent) and the indirect domain (useful). This means that there are necessarily two people—the direct landlord who owns the property and the copyholder who acquires real rights. The first is the holder of the domain, while the second has the rights of possession, use and disposal, although these rights are subject to certain limitations for the benefit of the direct landlord [22].

According to Amorin [23], in Brazil, the lands tenured by private personnel have as their landlord the

Church, its religious orders and the religious institutions established by them. Additionally, there is still the imperial family (urban land in the city of Petrópolis, RJ) and some hundreds of individuals who make up the following assemblages: 60% are tenured lands held by the Church; 30% are public lands; 3% remain the property of the former royal family; The remaining 7% belong to private individuals. The significant percentage of tenured lands held by the Church shows how common the use of ecclesiastical power was in the formation and of urban form.

Peculiar to the long lease is the payment of an annual pension, the value of which was a small, symbolic amount. In many cities, this practice was abolished, unlike that of the laudêmio.

The laudêmio was a compensation that was to be paid directly to the landlord for not having exercised the right of a purchase option. It is the obligation of the seller, not the buyer, to pay the laudêmio. It is important to clarify that in the buying and selling process what was being negotiated was the right to use the land, not the right to own it.

In Ribeirão Preto, when a resident of heritage land wanted to sell the property, he would transfer to the new owner only the right to use the land because it was the Church that held ownership of the land.

The laudêmio was prepaid, the deed of sale was not tilled and the letter of auction was not issued without having resolved the mentioned tribute. The value of laudêmio was 2.5% of the total value.

The tenure of urban land in Brazil has long been one of the agents of the configuration of urban form. Many churches, such as that of Ribeirão Preto, maintain on file the books of tenured lands wherein the clerics wrote down the granting of urban land and the payment of taxes (forum or board and the laudêmio). Such records directly contribute to the identification and establishment of the structure, the shape and the urban transformations of the city. These are historical documentary sources that decode and crystallize urban morphology.

5. Ribeirão Preto and Its Morphological Conditions

During the 16th, 17th, 18th and 19th centuries, occupying unoccupied and uncultivated lands became a normal behavior among those who wanted to settle. Thus, it could be considered, according to Lima [24], as a "legitimate way of acquiring domain at first, and after in replacing the distorted system of land grants, sesmarias". In this way, the many squatters living throughout the Brazilian lands during the Empire (XIX century), already occupied but were not yet integrated into the agrarian export economy. A recurring output for these men, who had no titles, was the foundation of a chapel with a saint of devotion. The granting of land to the Church for the establishment of a religious heritage was a way of regularizing possession of the land.

Under such conjecture, Lages [15] and Garcia [25] agree with the view that the donation of lands to integrate the heritage of São Sebastião of Ribeirão Preto, the saint of devotion of the locals, was beyond the religious context, that is, the residents had a strategy to legitimize and regulate the possession of the land possession

According to Lages [15], Garcia [25] and Costa [26], there were two attempts to donate to the formation of the heritage that failed because of the lack of documents proving the legitimacy of the land. The first attempt occurred in 1845 and the second in March 1852. It was not until July 1852 that Ribeirão Preto was divided into the lands of two farms - Retiro and Barra do Retiro (Table 1).

Once, the patrimony and granting of the lands for the development of the urban form of Ribeirão Preto in the land of São Sebastião was constituted, it was essential to nominate a vestryman, who would oversee the patrimonial lands and manage the parish goods. While Costa [26] referenced *Manuel de Nazareth Azevedo*, *Manuel Fernandes do Nascimento* was an important figure dating back to the first donations as he was the witness and signer for those donors who could not read and not write.

According to Garcia [25], from 1859, the responsibility of caring for the territory, tracing the first streets and building a chapel in honor of the patron saint was entrusted to *Manuel Fernandes do Nascimento*. However, Garcia [25] noted that there is no document that effectively proves that the tracing and the division of lots of the urban territory were actually carried out by *Manuel Fernandes do Nascimento*.

Lages [15], Costa [26] and Laureano [27] claimed that even before the final regularization of the third and final donation, the residents of the Retiro farm had built a temporary chapel. This small chapel was located in front of the current Rio Branco Palace, where today stands City Hall.

The courtyard opened to build this modest church and comprised the Viscount Inhaúma, General Osório, Cerqueira Cesar and Duque de Caxias blocks, and the chapel was located on the block made up of Barão do Amazonas, General Osório, Cerqueira Cesar and Duque de Caxias streets (Fig. 2).

According to Laureano [27], it was around this chapel that "emerged the first roads and the first buildings, still primitive, of a village". Lages [15] added that, at this time (in 1857), according to an analysis of the packet of voters of the Historical Archives of the state of São Paulo, there were 23 residents who, according to their annual income, were eligible to vote. However, the number of residents was certainly much greater, though at this time, slaves and women could not vote.

In the 1860s, the population of the farms near the village of São Sebastião of Ribeirao Preto grew considerably, while the core of the local population remained modest. However, Costa [26] identified, in the person of the vestryman Manuel Fernandes, the strong desire to build a new house of worship.

In August 1859, Manuel Fernandes forwarded a request to the Diocesan Bishop D. Antônio José de Melo, to place a baptismal font in the chapel. Supported by the local population, the Bishop authorized the construction of the baptismal providing it was located in a "decent" place. In 1861, the resident Maria Felizarda made a large donation in honor of São Sebastião. This donation possibly instigated the vestryman of the building of a new parish church to increase the speed in which the region was developing. In 1862, permission to build a new chapel on the left side of the stream of Palmeiras was granted by the Bishop of São Paulo, a location that guaranteed diocesan provisions and patrimony

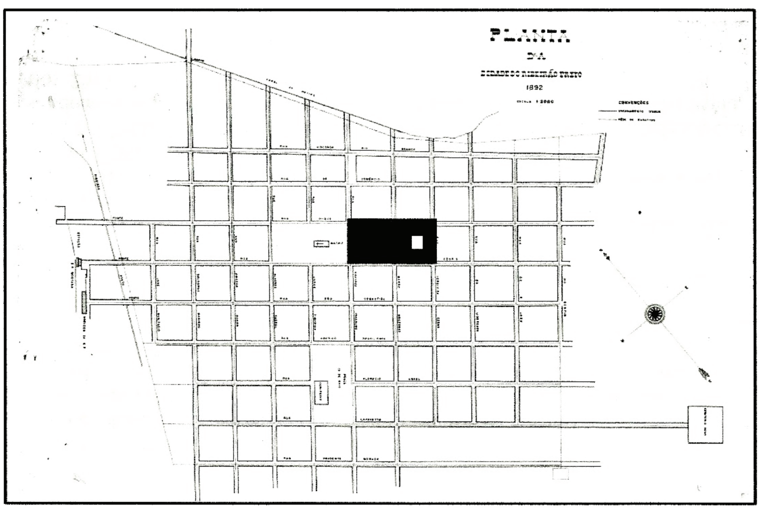

Fig. 2 One interpretation, referring to the block highlighted by the black rectangle where the first chapel in Ribeirão Preto was located, in the center in white on the City Plan, is credited to the Engineer Olímpio Antunes. It was built in 1892 as part of the studies for the implantation of sewage and supply networks (*Public Archives and History of Ribeirão Preto*).

legalized by the court.

Interests and disputes among residents of Barra do Retiro led the priest Manuel Euzébio de Araújo, under the guidance of the priest Jeremias José Nogueira, to demarcate a new location for the construction of the new church. The place was chosen in the patrimonial area of São Sebastião do Ribeirão Preto, where the 15 de Novembro Square is currently located. According to Laureano [27], while "buildings were erected, the population of the village gradually increased, to the point of having 3,000 or even 4,000 inhabitants as others assert" (Fig. 3). The plots of land granted within the patrimony were placed under the institute of long lease in accordance with the descriptive request of land from the City Council, which was documented in August 1882.

The role of the vestryman as a street architect and as the organizer of the orthogonal layout of the original urban form of Ribeirão Preto was of great importance. Proof of this importance was substantiated with the murder of the vestryman Manuel Fernandes do Nascimento on February 10, 1867 by a wealthy merchant, Manuel Soares de Castilho, because the vestryman had determined, without the merchant's consent, to run a street through his backyard.

The rapid growth of the town was considerable. On July 2, 1870, the President of the Province of São Paulo, Dr. Antônio Cândido da Rocha, elevated Ribeirão Preto to the category of parish through *Provincial Law 51*. On July 16, 1870, the Vicar of São Paulo, Monsignor Dr. Joaquim Manoel Gonçalves de Andrade, signed the decree creating the Parish of São Sebastião do Ribeirão Preto, and confirming as the first vicar priest Joseph Philidory Torres.

The *Provincial Law 67* of April 12, 1871 elevated the parish to a village, whose territory was then dismembered from the town of São Simão. Its first board was elected on February 22, 1874 and installed on June 4 of the same year.

In 1883, the tracks of the Mogiana Railroad Company reached the village of Ribeirão Preto. From this moment on, the economic, social and cultural contexts had a major impact on the future of this area. The Church no longer defined the morphology of the village, but instead, the Mogiana Railroad Company and the railway station built on the right side of the heritage lands next to the stream of Ribeirão Preto,

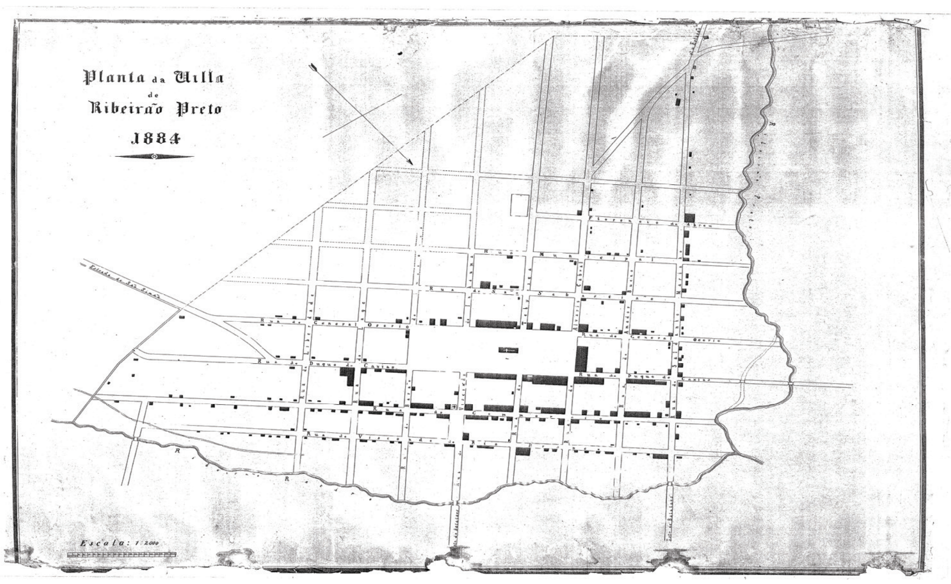

Fig. 3 The village plan of Ribeirão Preto, 1884.
The urban structure has, as a guiding point, the Church, which is located in the center of a large open space. Around the church and nearby are the first buildings on tenured plots (*Public and Historical Archives of Ribeirão Preto*).

currently channeled because of the construction of Jerônimo Gonçalves Avenue, began to dominate the land and its morphology. During the transition between the 1870s and 1880s, Ribeirão Preto joined the pioneer front of coffee production, which had as a condition the private ownership of the land. As the land turned into capital, the social relations were regulated by the commodity. "These relations do not end in the personal contact sphere anymore. The functioning of the market is the regulator of wealth and poverty" [15].

The interest was no longer proximity to the Church, but rather the proximity to the market and to the railway station. The railway station was the place of the loading and unloading of goods and the place of arrival and departure of people, thus it became a new meeting point, a place where ideas, ideals and culture were discussed and created. In the Books of Tenure of the Archdiocesan Curia of Ribeirão Preto, we observed the continual applications for tenured plots that were located next to the Mogiana rails and controlled by the Church (Fig. 4).

In addition to the rise of coffee barons, there was also a new class of immigrant settlers who came to Brazil to replace slave labor. The concept of market capitalization of production is well illustrated in this context, as shown in Fig. 4, where it is possible to identify a latent occupation in the region.

Ribeirão Preto played an important role in the national and international scene as a major producer of coffee. The major local landowners, general population and small groups of religious people organized a construction committee to raise funds for the construction of a new main church in a new location beginning in 1900. This commission was formed by priest Joaquim Antônio de Siqueira as the president and Francisco Schmidt, the owner of one of the largest coffee producing areas, as vice-president as

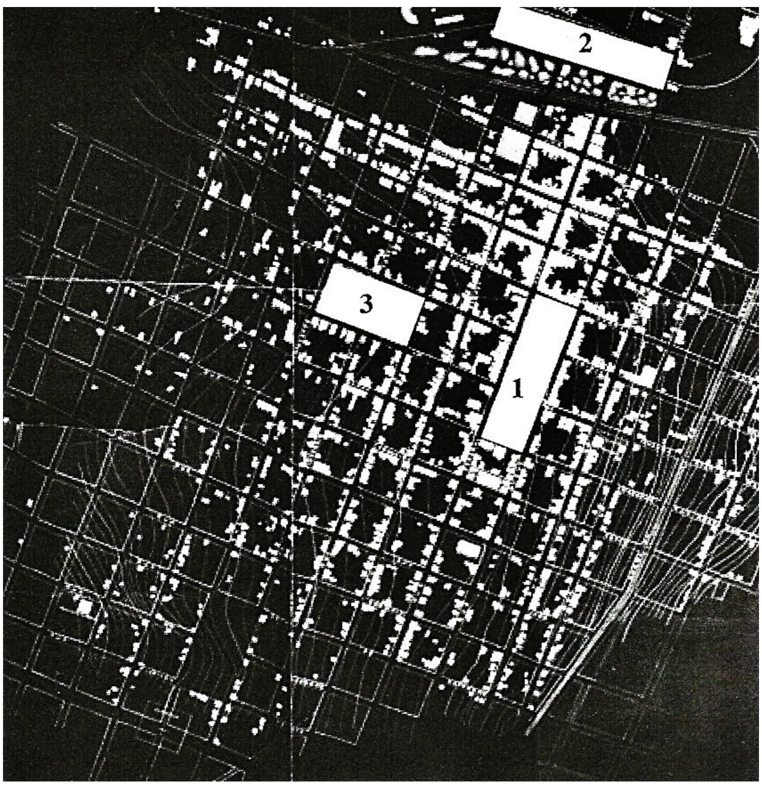

Fig. 4 Detail of the City Plan of Ribeirão Preto as organized by the office of the Light Company, 1911~1914.
In this detail of the religious heritage, it is possible to identify the three places: (1) the old square of the main church; (2) at the top of the plan, the buildings of the Mogiana Company, and in the nearby blocks, the occupation of the tenured lands; (3) at the left side at the top, 13 de Maio Square, where now stands the Cathedral (*Public and Historical Archives Ribeirão Preto*).

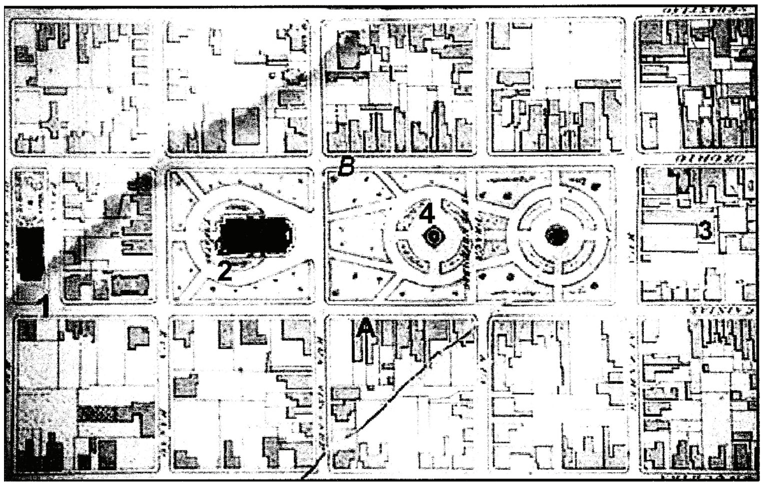

Fig. 5 Detail of the city plan of Ribeirão Preto.
In the 1930s, the ancient Main Church Square, where Praça XV de Novembro is located today, is highlighted, and it is possible to see the settings of the tenured plots of land and buildings thereon. Standing out in the Rio Branco Palace: (1) is the Carlos Gomes Theatre (now demolished); (2) the Central Hotel (now demolished); (3) the location of the former Main Church; (4) the Duque de Caxias street (A) and General Osório Street (B) (*Public and Historical Archives of Ribeirão Preto*).

well as other important members of the city of Ribeirão Preto.

Furthering the studies of the urban morphological structure of Ribeirão Preto through the development of the tenured land, it is possible to observe, according to surveys found in the books of tenure of the Archdiocese of Ribeirão Preto, certain irregularities in the dimensions of the land. According to a book on tenured lands from 1929, which transcribes the tenured lands since the 1870s, a wide range was identified. Examples of such irregularities include measurements of areas 17.20 m wide by 23.70 m long; 7.00 m wide by 23.00 m long; 11.00 m wide by 23.00 m long; 9.80 m wide by 27.00 m long; 20.50 m wide by 44.10 m long; and 11.40 m wide by 24.45 m long, as well as other plots of land that did not have the geometric shape of a rectangle (Fig. 5).

According to Garcia [25], the granting of lots within the religious heritage of Ribeirão Preto was integrated within the process of the formation of the city, which is common in any urban form where ecclesiastical heritage was responsible for officiating the distribution of the lands. Garcia [24] added that this process in Ribeirão Preto was further linked to the creation of a land market. Therefore, the original land structure of the city had undergone changes in form, a fact that was not restricted to drawings or factors, but rather to the modeling agents who, through social articulations, made their greatest contribution to the morphological constitution of Ribeirão Preto.

6. Conclusions

Urban science can not be analyzed and understood from a single academic perspective. Urban science comprises interdisciplinary research from the social sciences, humanities and exact sciences. The present study of urban morphology does not attempt to analyze a city's physical form solely by form but by the interactions, relationships and tensions between the modeling agents, especially the Church, which was largely responsible for the structure, shape and transformation of Brazilian cities.

The formation of religious heritage in Brazil and the tenure of Brazillian lands was a tentative but determined procedure in configuring urban forms in many cities. Long leases, which aimed to bring residents together for work, became a modeling agent for cities.

This case study crystallizes the conjuncture of parsimonious rules for founding cities in Brazil. Tensions began with land grants for forming religious heritage, the original urban area of the city, discussions on the first chapel location, and changes in location in land granted to residents by the Church. Long lease, a law that grants only the right to use urban land to the purchaser, was the recurrent land distribution system in the city of Ribeirão Preto. In this system, the property remains the responsibility of the Church.

The city of Ribeirão Preto is an example of the reminiscent appeal to the institute of long lease in urban formation and the crystallization of the context of Brazilian colonization.

In Brazilian colonial cities (1500~1822), religious heritage was a common element in configuring urban form. Starting from the imperial period (1822~1889), new rules were imposed to distribute urban land to form private ownership in a capitalist economy. However, in places where the power of the clergy overlapped with civil power, the heritage of some Brazilian cities remained with the Church.

In the Republican period (1889~1930), the Church continued to manage urban land in some Brazilian cities. In many cities belonging to the Bishopric of Ribeirão Preto, the Church maintains power in regulating urban land. In this region, many cities, including Ribeirão Preto, have their central urban area regulated by the Church.

This central area of Ribeirão Preto has the same religious heritage that was established between 1852 and 1856. The initial Ribeirão Preto settlement was founded in 1870. In this area of donated land, the residents do not own the property on which they live and pay for the Church, which owns the urban land. This land remains under tenure, as during the colonial period.

In the nineteenth century, when ownership urban land changed, taking possession of unoccupied and uncultivated land became a priority among individuals who sought to settle in the city. In Ribeirão Preto and cities in its metropolitan region, which is under the religious administration of the Bishopric of Ribeirão Preto, inhabitants of the urban center adopted a strategy to legitimize and regularize land tenure.

The present study illustrates the strategies of residents for occupying urban land. Although these lands are regulated by the Church, many residents have sought to appropriate this urban territory, even if they are required to pay the courts and do not have ownership of the land or building, only tenure. The most avid residents requested that the Church concede several lots to the same family using children and other relatives to regularize this request. Because ownership implies use of the property, the same person cannot request more lots. This strategy was used to accumulate properties and was typical in capitalist cities.

The vestryman, a Church employee, formed the streets, distributed lots and administered the religious patrimony of the Church. This case study in Ribeirão Preto reveals the importance of the vestryman as head of urban layout and in deciding the locations of new streets. In the beginning of this process, the area surrounding the Church was privileged.

When the railroad arrived in Ribeirão Preto in 1883, the city became part of a pioneering front for coffee export. New blocks and streets were defined around the train station by the vestryman. This new urban area initiated growing interest from residents to obtain lots donated by the Church. The train station halls attracted new urban land and became a site not only for loading and unloading goods but also as a new meeting point to circulate ideas, ideals and culture.

The institute of long lease has existed in Brazil since the colonial period, but the Civil Code of 1916 and the latest in 2002 abolished long lease for new properties. However, despite these codes, the maintenance of tenure of urban land, especially in areas of religious heritage, such as in Ribeirão Preto, is still administered by the Church, which keeps the land as a vested right. Thus, the urban land of a city of one million inhabitants, the center of a modern agro-industrial economy, is administered by the Church, similar to the colonial period. This case study sought to demonstrate how archaic land structures survive in modern cities. This phenomenon has not yet been evaluated in other Brazilian cities [19, 28, 29].

Acknowledgments

The authors wish to thank the FAPESP (Research Founding Agency of São Paulo State), the CNPq (Brazilian Research Council) and the CAPES (Brazilian Coordination for the Education Improvement of Higher Level) for the financial support.

References

[1] Lepetit, B. 2001. *To a New Urban History.* São Paulo: University of Sao Paulo Publisher. (in Portuguese)

[2] Kropft, K. 2009. "Aspects of Urban Form." *Journal of the International Seminar on Urban Form* 13: 105-20.

[3] Moraes, A. C. R. 2005. *Territory and History in Brazil.* São Paulo: Annablume. (in Portuguese)

[4] Lynch, K. 1981. *Good City Form.* Cambridge: MIT (Massachusetts Institute of Technology) Press.

[5] Vanconcelos, P. A. 2009. *Modelers Agents of the Colonial Cities in L. Pessotti; NP Ribeiro, Colonial Urbanism: Towns and Cities of Portuguese.* Rio de Janeiro: Matrix Press, 10-25. (in Portuguese)

[6] Oliveira, V. 2013. "Morpho: A Methodology for Assessing Urban Form." *Journal of the International Seminar on Urban Form* 17: 21-33.

[7] Gil, J., Beirão, J. N., Montenegro, N., and Duarte, J. P. 2012. "On the Discovery of Urban Typologies: Data Mining the Many Dimensions of Urban Form." *Journal of the International Seminar on Urban Form* 16: 27-40.

[8] Whitehand, J. W. R. 2012. "Issues in Urban Morphology." *Journal of the International Seminar on Urban Form* 16: 55-65.

[9] Kim, K. J. 2012. "The Study of Urban Form in South Korea." *Journal of the International Seminar on Urban Form* 16: 149-64.

[10] Ehlers, E. 2011. "City Models in Theory and Practice: A Cross-Cultural Perspective." *Journal of the International Seminar on Urban Form* 15: 97-119.

[11] Lamas, J. M. R. 2010. *Urban Morphology and Design of the City.* Lisbon: Foundation Calouste Gulbenkian. (in Portuguese)

[12] Marx, M. 1991. *City in Brazil: Land of Who?.* São Paulo: Nobel: University Press. (in Portuguese)

[13] Fonseca, C. D. 2011. *Camps and Villages D'el King, Space and Power in the Eighteenth Century Minas.* Belo Horizonte: UFMG (Universidade Federal de Minas Gerais). (in Portuguese)

[14] Derntl, M. F. 2013. *Method and Art: Urbanization and Territorial Formation in the Province of Sao Paulo, 1765~1811.* Sao Paulo: Alameda Press. (in Portuguese)

[15] Lages, J. A. 1996. *From Figueira to Barra of Retiro—The Settlement of the Region by Incoming Miners in the First Half of the Nineteenth Century.* Ribeirao Preto: VCA Publishing and Printing. (in Portuguese)

[16] Abreu, M. A. 2006. "The Appropriation of Land in Colonial Brazil." In *IE de Castro (et al.) Geographic Explorations.* Rio de Janeiro: Bertrand Brazil. (in Portuguese)

[17] Ghirardello, N. 2010. *The Formation of the Religious Heritage in the Sao Paulo: Urban Expansion Process 1850~1900.* São Paulo: UNESP (Universidade Estadual Paulista). (in Portuguese)

[18] Vide, D. S. M. 1853. *First Constitutions of the Archbishopric of Bahia.* Sao Paulo: Typographia Press. (in Portuguese)

[19] Piccinato Jr., D., and Salgado, I. 2012. "Urban Land: The Relationship of Religious and Public Institutions in Control of the Original Land Heritage of the City of Buritizal/SP." *Notebooks PROARQ (UFRJ)* 18: 35-47. (in Portuguese)

[20] Marx, M. 1980. *Brazilian City.* São Paulo: Melhoramentos and São Paulo University Press. (in Portuguese)

[21] Teixeira, M. C. 2011. *Brazilian Urban Models of Portuguese Cities in L. Pessoti; NP Ribeiro, Construction of the Portuguese City in America.* Rio de Janeiro: PoD Publishing Company. (in Portuguese)

[22] Monteiro, W. B. 1953. *Civil Law Course: Property Law.* São Paulo: Saraiva. (in Portuguese)

[23] Amorim, E. C. 1986. *Theory and Practice of Long Lease.* Rio de Janeiro: Forense Press. (in Portuguese)

[24] Lima, R. C. 1990. *Small Territorial History of Brazil: Allotments and Vacant Lands.* Sao Paulo: State Department of Culture. (in Portuguese)

[25] Garcia, V. E. 2013. "The Holy? Or Who... Ribeirão Preto: Genesis of Merchandise City." Ph.D. thesis, Architecture and Urbanism Institute, University of São Paulo. (in Portuguese)

[26] Costa, O. E. 1955. *History of Ribeirão Preto.* São Paulo: Foundation Collection History Magazine. São Paulo. (in Portuguese)

[27] Laureano, J. 1973. *Subsidies for the Religious History of Ribeirão Preto.* Ribeirão Preto: Metropolitan Curia of Ribeirão Preto. (in Portuguese)

[28] Piccinato Jr., D., and Salgado, I. 2014. "Urban Conflict: The Difficult Relation between the Church and the Municipality in the Management of the Urban Land in

Brazil." In *Proceedings of the 16th International Planning History Society Conference,* 890-903.

[29] Piccinato Jr., D. 2012. "Urban Land, Land Heritage: An Historical Analysis of Land Ownership in the Urban Setting in the Northeast of São Paulo (1800~1930)." Master thesis, School of Architecture and Urban Planning, Pontifical Catholic University of Campinas. (in Portuguese)

Journal of Civil Engineering and Architecture 10 (2016) 122-130
doi: 10.17265/1934-7359/2016.01.012

Node of International Flows or the Other Face of El Eulma

Mohamed Gherbi [1], Badia-Belabed Sahraoui[2] and Paul Boino[3]

1. Department of Architecture, Faculty of Science and Technology, University of Tebessa, Tebessa 12002, Algeria

2. Faculty of Architecture, University of Constantine 3, Ali Mendjeli 25016, Algeria

3. Institute of Urbanism of Lyon, University of Lyon 2, Berthelot 69007, France

Abstract: El Eulma has become an important node of transnational informal trade. It maintains strong relationships with international market places since the period where the "Trabendo" have seen a wide development in Algeria. On the national and regional level, the city of El Eulma is the main element of the network of informal merchant areas known by "Doubaï" markets. The most important areas are located in the central and eastern of Algeria. This dual membership was conferred to it because of the strong presence of import companies and the existence of discrete and dynamic networks well-organized, formed of false importers. This article focuses on commercial trajectories, the forms of networks and their developments and tries to know the logic. From these trajectories, how the merchant places could be formed in Algeria, as was the case for El Eulma.

Key words: Trabendo, international nodes of informal trade, "Doubaï" markets of Algeria, discrete networks of globalization from below, silk road.

1. Introduction

The transnational and cross-border informal trade has grown following after the gradual withdrawal of the state and the reduction of its monopoly, especially in the foreign trade sector in favor of private importers. This was made in the framework of the market economy but encouraged by the political instability that had known in Algeria at the time, combined with the unsafe situation after 1990 and the weakness of the state.

This situation has inevitably led to the emergence of informal markets specialized in specific trade segments which the most important were named "Doubaï" markets. They are located in central and eastern Algeria like Algiers (El Hamiz), Setif (El Eulma), Mila (Tadjenanent and Aïn M'lila) and Oum El Bouaghi (Aïn El Fakroun).

The informal market in Algeria was structured around the phenomenon known by the "Trabendo".[1] This latter has been apparently imposed as a strength and main pillar of the Algerian economy, and characterized the transitional period from a planned economy to a market economy. Qualified as "underground", [2] clandestine and illegal, the "Trabendo" has become a national expression since 1988, related to the informal in the sense of the "resourcefulness".[3] It was a normal practice in the daily life and well organized, responding to a

Corresponding author: Mohamed Gherbi, lecturer, research fields: architecture, sustainable urban design, heritage protection, urbanism, informal trade and cities, land use and management of quality in higher education.

[1]The "Trabendo" was born during the economic crisis of the end of 1980s and beginning of 1990s. It is the deformation of the Spanish term "Contrabando" (smuggling), and was borrowed by the retailers of the Algerian western during 1970s and 1980s. The "Haraguas" imported illegal goods from Melia, Tangier via Oujda in Morocco, and passed them through Maghnia in Tlemcen, a border town located in the west of Algeria.

[2]The expression used by Tarrius [1].

[3] The "resourcefulness" is related to the meaning of the temporary work. It includes the all types of trafficking: the resale of imported goods on the street, the real estate market, the medical domain (dental or pharmaceutical), etc. The resourcefulness has infringed the monopoly territory of the state and has started to compete it. It was reinforced by the crisis which had heavily reduced the number of workers in 1997, that is why many dealers of different ages are versed in the trafficking.

particular codified system.

The "Trabendo" is organized in fact, almost in the same way as the official economy. It has its own national and international networks of smugglers and information, and its supply markets around the world because the imported goods have multiple origins.

On the other side, the "Trabendo" seems to forge close ties with politicians in the power that significantly affect the economic policy. It has in fact benefited the monopoly in the import, the credits and the banking facilities [2].

In this logic, the migration movements have appeared actively in well-organized networks that partly resemble to those of the official economy. However, they do not benefit any subsidies [2], because most of them are versed in smuggling like the case for cross-border networks [3]. As a real case of these networks, there were the "Haraguas",[4] where most of whom are wealthy but often illiterate, without any level of education [4]. They import of counterfeit goods and/or often with false official statements, and use all allowed and not allowed means to escape the taxation and custom taxes.[5]

The "suitcase trade" or "caba"[6] was the most used tool at the time, before the introduction of import and export authorizations. It was exercised by "Trabendistes" or small importers of "globalization from below",[7] who occasionally or professionally during their travels, visited often various European and Arab countries in the Middle East and the gulf. They used trade roads opened by sailors, students, migrants and pilgrims, and met the traders from the ex-Soviet bloc and from Africa and Asia [10].

[4]The "Haraguas" is a term that refers to the smugglers active in the informal. They take advantage of the inadequacy of the administration to override all the legal procedures of the monitoring and verification in the country borders. They are illegal importers or smugglers but different from illegal immigrants who are also part of this category.

[5]It happened, for instance, for an invoice of €10,000, only the 5% of its true value is declared, corresponding to the sum of €2,000.

[6]It is a word of Algerian slang which means the bag or suitcase.

[7]The expression is borrowed from Portes [5], Tarrius [6], Thorez [7] and Pliez [8], [9].

The Algerian networks have known a considerable development and dynamism that result from the development of Marseilles' underground activities which their involvement has affected other Mediterranean countries [11].

So following the supply chains in the journey taken by the young Algerian importers of "globalization from below", the relayed spaces emerge from either side of the Mediterranean. They concern cities like Marseille, Naples, Istanbul, Oran, Algiers, Annaba, Tunis, Tripoli, Damascus, etc. Through the informal ways, trade exchanges take place between the two sides. But after the official introduction of the private practice of import-export in Algeria in 1990,[8] the goods start to come from "Dubaï" in the Emirates, and transit Marseille[9] or the Italian city (Naples) to reach El Eulma for instance. These practices have encouraged the emergence of a wealthy social layer from the year 2000, which was renamed later: the "new multibillionaires" or "s'hab Echkara".[10]

2. The New Wealthy Class in Algeria

According to the Ministry of Trade in 2004, Algeria had around 40,000 billionaires. But they are passed to 46,000 in 2009 according to the statement and analysis of financial experts [13], with an increase of 13%, dividing them into two categories. The first contains 30,000 billionaires coming from wealthy families who exercise export since colonial times, while the second category includes from 16,000 to 20,000 billionaires constituting nearly 40% of the informal fund. The estimated index of their total wealth, in the absence of accurate statistics, is situated between 2 and 50 until 60 billion Algerian dinars (€600,000,000).[11]

[8]This period was known by the great "Trabendo" or the era of semi-informal import of containers [12].

[9]When the French authorities have tightened controls at ports, particularly Marseille, the imported goods were directed to some Italian port cities.

[10]It is an Algerian term in plural that means the holders of bags full of money.

[11]*Ibid*.

The origin of the fortune of the second category seems to come from the informal and illegal trade, and contains billionaires who have got rich from the corruption and embezzlement of public funds, where most of them are prosecuted by the courts. However, according to some financial experts, the number of billionaires had reached 50,000 or more during the year 2013. This figure seems far exceed the statistics provided by the NWW (New World Wealth),[12] in 2012 in the framework of the formal economy. In its recent study, this office confirms that Algeria has 35 billionaires and 4,100 millionaires[13] in 2012 where the number of dollar millionaires could reach 5,600 in 2020 if the average growth rate remained at 4.1% [14] of the period of 2012~2020.

The city of El Eulma concentrates a lot of these billionaires where the number of importers has become more of 1,000, in which most of them are active in the informal markets whereas the huge financial flows that transit this city remain unreported. El Eulma will generate trans-regional flows and be in competition with big cities where some of them have lost their monopoly of supply of markets.

At this scale, El Eulma is considered as the cornerstone of east wholesale markets that surround, by the intensity of trade that has with them. That intensity is based on the couple specialization-monopolization which seems to be well structured, making any distribution of goods throughout the national territory, is obliged to pass through El Eulma.

3. “Doubaï” Markets of the Algerian Eastern

In the east and the central of Algeria, a dynamic network of places, spaces and roads of informal trade of import is formed in the large, medium and small cities. The size of the city in this logic has no importance because the “Doubaï” markets are based on other issues and criteria different from the planning of cities. They have transformed their cities into places of high traffic of goods and accelerated significant changes of their function and urban organization.

From the observations, it appears that the existing “Doubaï” markets relay located in the east of Algeria have the role of complementarity with El Eulma by the specialization in one or two commercial segments. They position according to the channels of distribution organized at large scale as major merchant places (Fig. 1). That is why El Eulma is identified as the business segments in particular the hardware, furniture, mobile phones and computers, Tadjenanet, meanwhile, remains active in the import of wood and Aïn M'lila in the sale of vehicle parts. For their part, Sidi Mabrouk, which is located in Constantine, and Aïn El Fakroun to Oum El Bouaghi, specialize in cheap clothes, while Bir El Ater in the wilaya of Tebessa is known by the thrift store [15].

The organization at this scale has permitted the maintaining of exchanges between these poles as long as possible, but the massive and continuous arrival of imported goods or those locally produced, to El Eulma and the speed of distribution to the four corners of the country and the neighboring countries such as Tunisia, testify the importance and how El Eulma takes its place in the region.

4. Global Discrete Networks in El Eulma and Their Strategies

The geography of transnational trade road which was drawn before 1990 connected in fact, El Eulma to Egyptian cities by the illegal import of the stationery, hardware and furniture, especially from 1988 to 1990. El Eulma was also linked to Libyan cities, particularly Tripoli by informal import of mobile phones, cigarettes

[12] The NWW (New World Wealth) is a consulting cabinet based in Britain that defines the millionaire in his study as an individual with net assets of more than $1,000,000 (over 100 million AD (Algerian dinars)). It is based on surveys and data including those provided by transnational institutions like the World Bank and WTO (World Trade Organization).

[13] More than half, nearly 2,300 millionaires counted, are in the capital Algiers. On the other hand, the NWW considers that 4,100 millionaires accumulate a total of $5,000,000,000, equivalent to 430 billion AD.

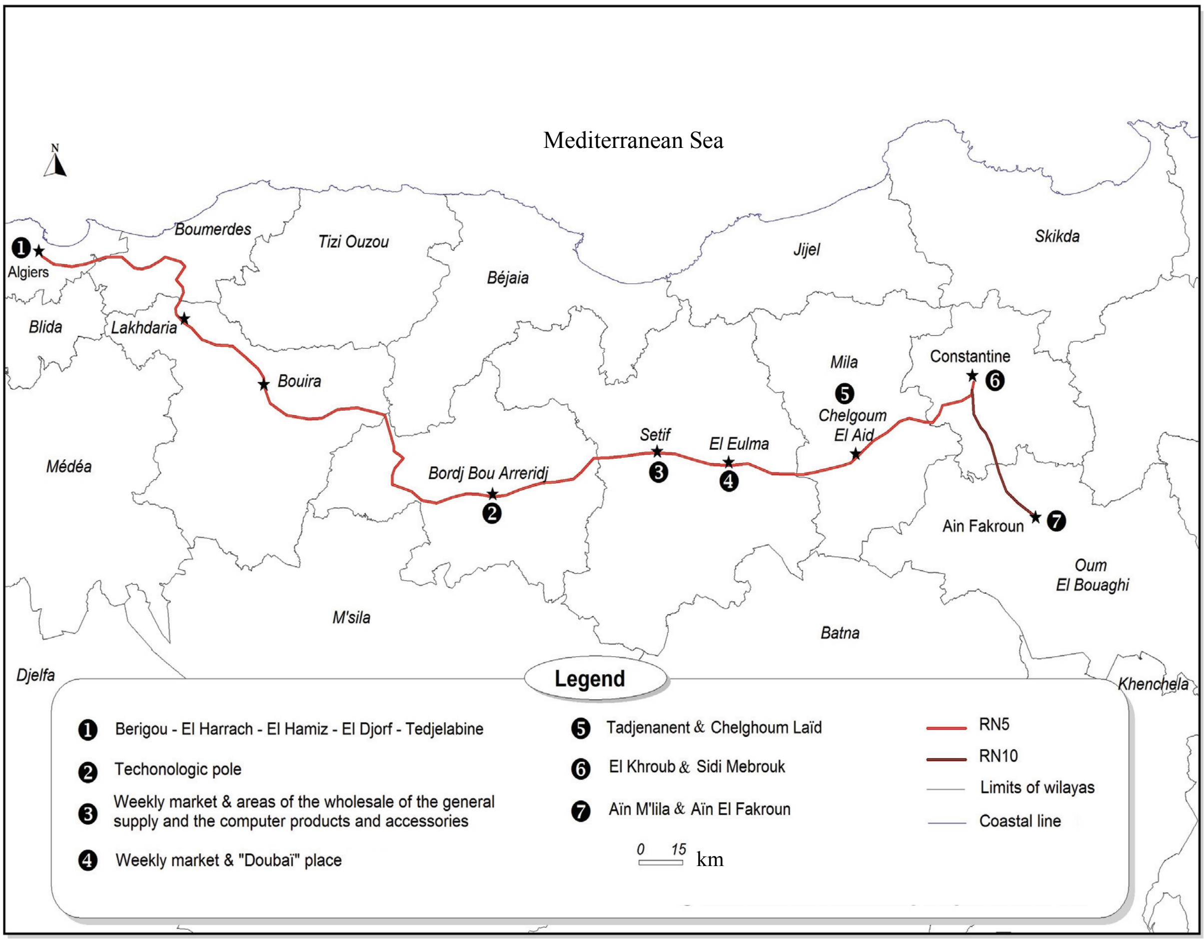

Fig. 1 Markets of national and regional importance near of the RN5 (national road).
Source: Gherbi, M. 2011. Tourism's base map of Algeria, INCT (National Institute of Cartography and Remote Sensing), 1997 ed.

and clothing, especially jeans. The transfer of goods was affected via the terrestrial borders in the east of the country,[14] by the traders and/or smugglers of Tebessa and Sufis, playing the role of intermediate smugglers.[15]

The products arrived in El Eulma, came generally from important places, known for their low prices and the mass and variety of products, such as Selloum in the Egyptian-Libyan border and the markets of the capital Tripolis and those of Ben Gardane located in the Tunisian-Libyan border [7, 9, 16].

A discreet organization has thus grafted in the territory of each country.[16] This discontinuous spacial device arrives to form a dynamic link that ensures the illegal distribution to other countries in the south such as ex-Sudan, Mali and Niger. The smugglers and dealers store their goods in hidden warehouses and expect the easing of control procedures applied at the borders, to move them.

Once the export-import has become authorized to the private investor by granting him the commercial register, some "Mâalims"[17] of El Eulma specialized

[14]The Algerian-Libyan borders but also via Tunisia.
[15]It should be recalled that Algerian smugglers use the land border axis in the east of Algeria, formed by El Taref, Souk Ahras, Tebessa and Oued Souf, in cooperation with their Tunisian and Libyan similars. They take the uncontrolled paths and trails by the security authorities of the three countries to pass the goods.

[16]Pliez and Boubakri have identified and analyzed the roads of transit of goods used in the smuggling into the territory of Libya and Tunisia, which all lead to the east border of Algeria. It is a real sieve where El Eulma is well ingrained in these roads [15].
[17]It is an Algerian term in plural which means the big bosses or the notables of the city.

in the sale of furniture, for instance, have realized that Egypt was only the interface of the re-export of such goods, and that Indonesia is the place of origin of manufacture. They have since the beginning of 1993, taken the new commercial circuit leading to the cities of this country, looking for contacts with producers and for the acquisition of exclusive rights to certain brands, at the lowest possible price. And since then, the containers full of furniture arrive to the ports of Algiers and then are moving towards El Eulma with often false statements and without invoices.

Parallel to this network, another network was formed between El Eulma and some cities of Turkey and especially Istanbul during 1995~1996, where a large informal trading was recorded for multiple trades which confirm the traders met in the investigations carried out in “Doubaï” place of El Eulma.

The strategy of this network, because of the lack of political visibility of the state at this period for import and export, consisted in that two traders travel both for a group of traders who work with them and trust them. These dealers were selected on the basis of their knowledge in Turkey and their experience in the workings and circuitry of the informal import. They have an average financial capital formed from their own fund and the fund of their colleagues (cash money).[18]

Once in Turkey, these both traders will quickly find privileged interlocutors from whom they will pass their commands, but after having done a rapid check of goods prices in the market. They negotiate prices and buy variety of product batches other than the hardware (fabrics, household appliances, batteries, shoes, etc.) to put them in containers to be transported by the sea road.

The private forwarders, usually the Kurds, register the goods and ship them. They have a better knowledge of the Arabic language, which permit them to deal with customers, mostly from the Middle East countries such as the Syrians and also the traders of Maghreb, especially the Algerians and Tunisians.

In the beginning of the official exercise of import to El Eulma and in the atmosphere devoid of confidence, the traders and importers avoided taking the risks and invested in the import only with modest capital. In that way, if the goods, for a reason as for another, is destroyed during their shipment or seized by customs or police suddenly uncooperative during checks, which from time to time become hard, the costs of this loss will be shared between all merchants concerned by this delivery.

Once out of the ports of Algiers, the trucks and trailers carry the containers via the RN5 (national road) and cross all the roadblocks deployed by the national gendarmerie and customs, or the services of the national security at the entrances and exits of the cities.[19] Just arrived at El Eulma, the traders start to share and store the goods in their warehouses. Some merchants sell their products with lower prices and entrust much of the goods to a network of resellers who distribute it to the four corners of the country. This method facilitates them to repay all their stay expenses in Turkey, and recover quickly their profits.

The technic of purchase of diversified products was adopted by importers traders of El Eulma even in the imports of “Dubaï” in the Emirates, considering the possible arrival on the market, of similar products in large quantities. Also the import of a single type of goods may risk making too slow the rotation of their stock because of the particularity of the Algerian market.

4.1 Direction to “Dubaï” in the Emirates

The pace of the development of commercial

[18]The financial assistance from the state to traders was not operational because the procedures were not applied because of the economic and security situation of the country.

[19]The shipments arriving at the names of some traders and importers undergo, from their entry into ports until their final delivery to El Eulma, a minimum of control. In some cases, they are exempt from all types of controls and checks because of their owners whom have relationships with certain of high officials of the Algerian state.

networks in El Eulma has experienced a fast pace since the end of 1996 and beginning of 1997, due to the practice of the merchant road to “Dubaï” in the Emirates as a new destination of supply for their imports. This road begins seriously to compete the road to Istanbul in Turkey for three following reasons:

(1) The goods off food, ordered and imported to El Eulma were not all made in Turkey;

(2) Most of goods come from “Dubaï”;

(3) The Turkish forwarders were just intermediates because they concluded with the Iranian forwarders installed in “Dubaï” in the Emirates, the transit terms and reshipment of the commands of their Algerian customers, especially the Eulmis.

The road to “Dubaï” in Emirates has allowed the traders of El Eulma to make profits and savings in time and money. At first, orders of the first import companies in El Eulma[20] were treated by the Iranian forwarders.[21] However, the multiplicity of flows of goods due to the transactions between El Eulma and “Dubaï” has been accompanied by the opening of companies of cargo transits by the Eulmis installed in “Dubaï” that will process all orders to El Eulma.

This change will give to El Eulma, a strong reputation and a new identity and will transform its “Doubaï” district to a powerful merchant place. It was founded by these importers-traders based in El Eulma, exceeding 1,000 importers.

The orientation towards “Dubaï” in the Emirates is dictated by several factors. The most important are the absence of border controls, the strong flexibility in the administrative procedures and the considerable reduction of the customs duty to 4% of the value reported [17]. These new conditions have rendered the traders using fraudulent introduction of most products from “Dubaï”, and have made that the selling price of a product imported to El Eulma, equal to two or three times cheaper than the local product or the national sold. For instance, a midsize refrigerator of two doors with a freezer, imported in 2011 was sold to 20,000 Algerian dinars per unit (retail price), which is near of €150,[22] whereas that produced in Algeria, cost 33,000 AD equivalent to €250. In this case, the imported product permits to the Algerian customer to save 13,000 AD (€100).[23]

4.2 Reinvention of the Silk Road

After several trips to “Doubaï” in the Emirates, the merchants and traders of Eulmis have realized that “Doubaï”, is in fact only a center for the global transit of goods flow re-exported from the Southeast Asia: South Korea, Malaysia[24] and China. They have discovered that 95% of the goods entering to El Eulma routed from the ports of “Hong Kong”[25] via “Doubaï”, and are manufactured in a small Chinese town located at 300 km to the east—“Yiwu”, classified as one of the greatest Chinese centers of the hardware [19] which is also the most present in El Eulma.

When China was closed to the world, the merchants of “Dubaï” in the Emirates passed their commands of the products from the Chinese manufacturers and resold them to the countries of the world. But since the GDP (gross domestic product)[26] of China has

[20]In theory, the trade registers established in order to benefit several advantages, as the exemption and reductions of taxes are related to the activity of import-export. However, only few of the beneficiaries really exercise the import-export, because in most of the cases observed, their activity is only limited to the import.

[21]According to the interviewed merchants, the fees of services of some Iranian forwarders who have rich knowledge of the mechanisms of workings of administrative procedures in Emirates are very competitive.

[22]According to the rate applied in the parallel market of currency. The currency exchange has known an exponential growth compared to the value of the Algerian dinar. The proof is that, use 2008~2011 as an example, Euro was worth 133 AD (Algerian dinars) but in 2014, it increased to 156 AD and is arrived to more of 160 AD. It should be recalled that Algerian dinars has lost 20% of its value according to the statement of the governor of the Central Bank of Algeria presented to the National People’s Congress and the Senate.

[23]The results of surveys conducted in 2006~2011.

[24]The furniture is imported from Malaysia.

[25]It contains the third biggest port in the world where tens of thousands of containers depart from this port [18].

[26]In 2010, the gross domestic product of China, in a nominal term, has amounted to $5.8786 trillion compared to $5.4742 trillion for Japan, but the GDP/inhabit., stays 10 times lower in China than in Japan [20].

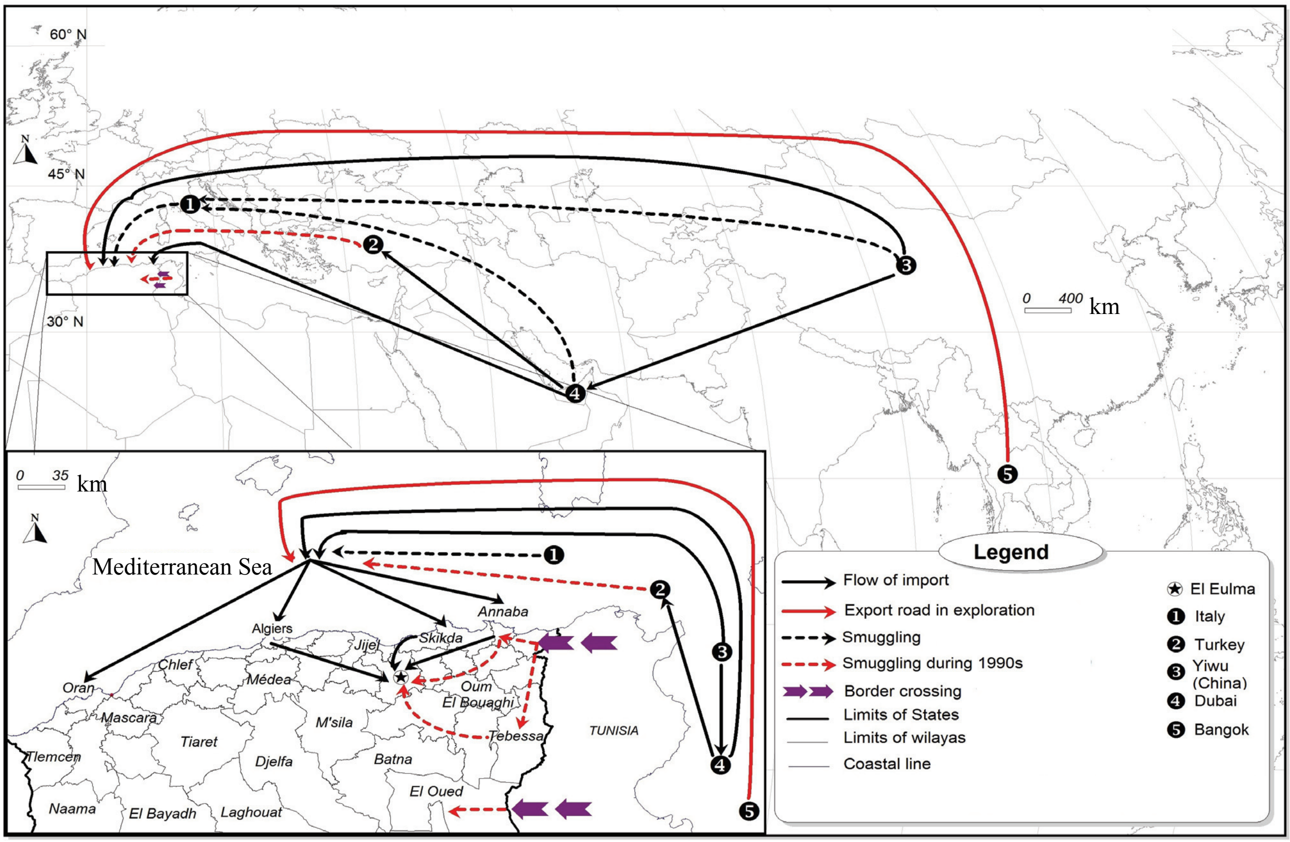

Fig. 2 Merchant places and new roads undertaken by the Eulmis importers.
Source: Gherbi, M. 2010. Based on world map and map of administrative of Algeria, 1984.

increased significantly and a mass of multinationals have installed after its opening to the world, China has known a development in all sectors of the economy never seen before, due to the abundance of the skilled but cheaper workforce.

China exports today the majority of its production to all five continents. It was ranked as the second powerful economy in the world in 2010 behind the United States of America. The place was occupied by Japan since 1968. An evolution promises the throne of China in 2025 according to the estimates by the World Bank and various financial institutions,[27] with the possibility of marginalization of Europe in 2020, if the rate of its current growth is maintained over a decade as advocated by some strategists [21].

It was obvious therefore that the traders-importers of El Eulma fly to that country and specifically to Yiwu in the end of 1990s.[28]

Having the names of some suppliers and the address of the Arab district[29] for their stay,[30] they visit alone or in small groups to Yiwu during the periods of universal exhibitions,[31] and conclude their business at the lower cost and without intermediates.

[27] *Ibid*.

[28] They are less interested in the important Chinese cities like Beijing or Shanghai, but they know Yiwu and the "exotic" district well, concentrating the Arab and Muslim communities.

[29] This district is appeared in Binwang, near the first exhibition center, in the end of 1990s. It is known for the trade with the Arab and Muslim countries but currently, it is closed for urban renovation. It has taken the name "Exotic Street" in reference to the name of its main street. Morphologically, the district is formed of several islands and five parallel streets, lined with shops. It is cosmopolitan due to the presence of Uighurs, Huis, Kazakhs, Arabs, Africans and Turks. This district contains restaurants and one of them is managed by one Eulmi who takes care of the passing Algerians traders [22].

[30] The restaurant of this Eulmi was closed because of the urban renewal in the district suffered, therefore the Algerians who come, are often found in the snack and in the two Chinese hotels, located near the "Exotic street" [22].

[31] Yiwu organizes every year about 83 universal exhibitions.

At Yiwu, they walk with local translators, often young Chinese women to finish their orders on site.[32]

Many foreigners living in Yiwu, opened their representations as traders. They organize the delivery of orders to their country of origin. Approximately twenty offices belonging to the Algerians exist in the Arab district. They treat large orders towards Algeria and recruit local workforces and those coming from Algeria.

The presence of the Algerian community starts to become visible in the city and is now in competition with the Egyptian, Syrian, Lebanese and Turkish communities [22]. For the Eulmis importers and at present, they are exploring new trade routes bringing them to far places such as Bangkok in Thailand, Indonesia and India, looking for goods with lower prices than proposed by their traditional suppliers (Fig. 2).

5. Conclusions

The experience acquired over these years and the relationships with wholesalers or the forwarders of the scapegoat composed of Marseille, Naples, Istanbul and "Dubaï", have opened a door to the importers-traders of El Eulma. The possibilities of investment allow the traders to conquer the new international trade places grafted on the old roads in the countries of the Southeast Asian, especially China. These importers are working for broadening their relationships and increasing their sites of supply without going through the intermediates.

By following the roads undertaken by the importers of El Eula, the figure of the discontinuous commercial discrete networks is reconstituted and the actors that animate are identified. This pattern has shown its success in its adaptation and its organization inside the country and has crossed the national borders and the boundaries of the international agreements. It has permitted to better taken of the trajectories and forms of structuring networks and to better understand the logic of how, from these roads, could be formed in Algeria the merchant places like the case of El Eulma, with national radiation and international connections.

[32]They command lower quality products because of the weak purchasing power in Algeria.

References

[1] Tarrius, A., and Missaoui, L. 1995. *Arabs of France in the World Economy from Below*. Avignon: Monde en Cours Collection, 220.

[2] Battegay, A. 2005. "Dubaï: the Trading Economy and Migratory Crossroad. Study of Functioning." In *Worlds in Movements, Migrants and Migration to the Middle East at Nearby of XXI Century,* edited by Jaber, H., and Metral, F. Karthala: French Institute of the Near East, Direction of Contemporary Studies DGCID (MAE)-CNRS (FRE 2895).

[3] Peraldi, M. 2001. *Cabas and Containers. Informal Trading Activities and Cross-border Migrants' Networks*. Paris: Maisonneuve & Larose, 361.

[4] Boumaza, Z. 2003. "Trabendo, a Mode of Informality in Algeria of Years 1980~1990." In *Transversal Modernities: Citizenship, Politic and Religions,* edited by Kouvouama, A., and Germod, C. D. Brazaville: Paari Editions, 107-11.

[5] Portes, A. 1999. "Globalization from Below, Emergence of Transnational Communities." In *Proceeding of Social Science Research,* 15-25.

[6] Tarrius, A. 2002. *Globalization from Below: New Nomads of the Underground Economy*. Le Muveran: Voix & Regards Collection, 169.

[7] Thorez, J. 2008. "Bazaars and Trade Roads to Central Asia—Post-soviet Transformation and Globalization from Below." *Revue Européenne des Migrations Internationales* 3 (24): 167-89.

[8] Pliez, O. 2007. "The Chinese Jeans in the Streets of Cairo, or the Discrete Spaces of Globalization." M@ppemonde 88. Accessed February 19, 2008. http://mappemonde.mgm.fr/num16/articles/art07404.html.

[9] Pliez, O. 2010. "The Silk Roads Lead to Yiwu (China). Contractors and Muslim Migrants in a Chinese Economic Area." *L'Espace Géographique* 2 (39): 132-45. Accessed June 20, 2011. http://www.cairn.info/revue-espace-geographique-2010-2-p-132.htm.

[10] Battegay, A. 2000. "Dubaï, the New Merchant Place." Presented at the 2000 Seminar of the Mediterranean Sociology Laboratory, Aix-en-Provence, France.

[11] Marchal, R., Adelkhah, F., and Hanafi, S. 2001. *Dubai, the Global City*. Paris: National Center for Scientific Research, 131.

[12] Cote, M. 2001. "New Territorialities in Algeria." In *Where Is Going Algeria?,* edited by Mahiou, A., and

Henry, J. R. Paris: Iremam Editions, 257-72.

[13] Bachouche, N., and Benyehia, H. 2009. "46,000 Billionaires in Algeria." *Echorouk* 08/05. Echorouk. Accessed July 19, 2010. http://www.echoroukonline.com/fra/index.php?news=4754.

[14] Grim, N. 2013. "According to a Study of New World Wealth, in 2012, Algeria Had 35 Billionaires and 4,100 Millionaires in Dollar." El Watan, 09/03. Accessed October 18, 2013. http://www.elwatan.com/pdf/telecharger2.php?pdfpf=/archives/edition.php&pdfg=%2Fpdf%2Ftelecharger.php%3Fdir%3DJOURNAL%26file%3D20130903.pdf&ed=2013-09-03.

[15] Gherbi, M. 2010. "Doubaï in El Eulma, from a Residential District to an Important Place of Trading." In *Transversal Days, Organized by LISST (Interdisciplinary Laboratory Solidarities, Societies, Territories) (Cas-Cers-Cieu)*. Toulouse: Le Mirail University.

[16] Boubakri, H. and Mbarek, W. 2009. "Places, Actors and Networks of the Informal Economy at the Tunisian-Libyan Border." In *Rural Development, Environment and Territorial Interests: Cross Views Moroccan Oriental and Tunisian South-Eastern,* edited by Bonte, P., Elloumi, M., Guillaume, H., and Mahdi, M. Tunis: Cérès Editions, 343-62.

[17] Lavergne, M. 2002. "Dubai or Incomplete Metropolization, a Relay Pole of the Economy of the World." *Les cahiers de la Méditerranée* 64: 257-96.

[18] Dusci, S. 2009. "The Exclusive Survey: The New Mercenaries of the Anti-counterfeiting Fight." In *Emission Broadcasted.* French TV Channel M6, September 27. Accessed October 10, 2009. http://www.m6replay.fr/#/info/enquete-exclusive/2530.

[19] Jianguo, S. 2005. "Made in Taiwan. The Chinese Goods in Algeria." Xinhua News Agency. Accessed March 9, 2006. http://www.french.xinhuanet.com/french/2005-06/29/content_133081.htm.

[20] Le Monde.fr. 2011. "China Has Become the Second World Economy." Le Monde.fr. Accessed May 5, 2011. http://www.lemonde.fr/economie/article/2011/02/14/la-chine-est-devenue-la-deuxieme-economie-mondiale_1479580_3234.html#xtor=AL-32280184.

[21] Mebtoul, A. 2012. "Which Prospects for the Algerian-Chinese Cooperation?" Liberté, 07/11. Accessed December 14, 2012. http://www.liberte-algerie.com/6146.pdf.

[22] Belguidoum, S. 2014. "The Dynamism of New Merchant Places of the Algerian Eastern: An Urban Reconfiguration and New Social Data." HAL-SHS (Sciences de l'Homme et de la Société). Accessed March 4, 2014. https://halshs.archives-ouvertes.fr/halshs-00936444.

Journal of Civil Engineering and Architecture
Volume 10, Number 1, January 2016
David Publishing Company
616 Corporate Way, Suite 2-4876, Valley Cottage, NY 10989, USA
Tel: 1-323-984-7526, 323-410-1082; Fax: 1-323-984-7374, 323-908-0457
http://www.davidpublisher.com, www.davidpublisher.org
civil@davidpublishing.com, civil@davidpublishing.org, civil_davidpublishing@yahoo.com

ISSN 1934-7359
01
9 771934 735160